Université Fédérale
Toulouse Midi-Pyrénées

THÈSE

En vue de l'obtention du

DOCTORAT DE L'UNIVERSITÉ DE TOULOUSE

Délivré par :

Université Toulouse 3 Paul Sabatier (UT3 Paul Sabatier)

Présentée et soutenue par :
Chao WANG

le mardi 16 décembre 2014

Titre :

Modélisation et prédiction des assemblages de phytoplancton à l'aval de la rivière des Perles, en Chine

---

École doctorale et discipline ou spécialité :

ED SEVAB : Écologie, biodiversité et évolution

Unité de recherche :

Laboratoire Évolution et Diversité Biologique (UPS, France)

Directeur/trice(s) de Thèse :

Prof. Sovan LEK (Université de Paul Sabatier, Toulouse, France)

Jury :

Prof. Helena Guasch (University of Girona, Spain) Rapporteur
Prof. Lirong Song (Institute of Hydrobiology, China) Rapporteur
Prof. Michèle Tackx (University Paul Sabatier, France) Examinateur
Chercheur Alain Dauta (CNRS, Toulouse) Examinateur
Research Scientist Christophe Baehr (CNRS, Météo France) Examinateur
Research Scientist Fangmin Shuai (Pearl River Fisheries Research Institute, China) Examinateur

THESE

En vue de l'obtention du

DOCTORAT DE L'UNIVERSITÉ DE TOULOUSE

Délivré par:

UNIVERSITE TOULOUSE 3 PAUL SABATIER (UT3 PAUL SABATIER)

Présentée et soutenue par:

CHAO WANG

Modélisation et prédiction des assemblages de phytoplancton à l'aval de la rivière des Perles, en Chine

Directeur(s) de Thèse:

Prof. Sovan LEK (Université de Paul Sabatier, Toulouse, France)

Jury

Prof. Helena Guasch (University of Girona, Spain) Rapporteur

Prof. Lirong Song (Institute of Hydrobiology, China) Rapporteur

Prof. Michèle Tackx (University Paul Sabatier, France) Examinateur

Chercheur Alain Dauta (CNRS, Toulouse) Examinateur

Research Scientist Christophe Baehr (CNRS, Météo France)

Examinateur

Research Scientist Fangmin Shuai (Pearl River Fisheries Research

Institute, China) Examinateur

Table of Contents

Part Ⅱ: Publications

[1] Chao Wang, Xinhui Li, Zini Lai, Yanyi Zeng, Yuan Gao, Qianfu Liu, Wanling Yang, Sovan Lek. Temporal and spatial pattern of *Scenedesmus* in the river web of the Pearl River Delta, China. *Acta Ecologica Sinica*, 2014, 34(7): 1800-1811. (in Chinese with English abstract)

[2] Chao Wang, Xinhui Li, Zini Lai, Yuefei Li, Alain Dauta, Sovan Lek. Patterning and predicting phytoplankton assemblages in a large subtropical river. *Fundamental and Applied Limnology*, 2014, 185(3-4): 263-279.

[3] Chao Wang, Christophe Baehr, Zini Lai, Yuan Gao, Sovan Lek, Xinhui Li, 2014. Exploring temporal trend of morphological variability of a dominant diatom in response to environmental factors in a large subtropical river. *Ecological Informatics*, 2014, accepted, DOI:10.1016/j.ecoinf.2014.11.002.

[4] Chao Wang, Xinhui Li, Xiangxiu Wang, Zini Lai, Qianfu Liu, Wanling Yang, Sovan Lek. Spatial-temporal pattern and prediction of phytoplankton assemblages in a subtropical river delta system. 2014 (completed)

ACKNOWLEDGEMENTS

I would not have been able to finish my dissertation without the help and support of all the kind people around me, but to only some of whom it is possible to give particular thanks here.

My first and sincere appreciation goes to Prof. Sovan LEK, my respected supervisor for all I have learned and gained from him and for his continuous help and support in all stages of this thesis. Actually, Prof. Sovan LEK gave me a good model to be as a diligent, amiable, humorous and modest international scientist, and also as a life expert. I was deeply impressed with his quick response to my email for any questions, even in late evening and early morning, which stimulated me to work hard! Through this one year's study following him, I will rethink and redesign my research and life in the future. Great appreciation should be given to him again for providing me the chance to study abroad and open my eyesight!

My greatest and deepest gratitude goes also to Prof. Xinhui LI and Prof. Zini LAI, my two leaders of the lab in the Pearl River Fisheries Research Institute (PRFRI), China, who have struggled to help me to get the scholarship and opportunity to study abroad. They often sent email to care about my life and studying during my stay in Toulouse, which gave me warmth and courage to finish my study!

I would like to express my great appreciations to Associate Prof. Sithan LEK-ANG who take care my life during my stay in Toulouse, thanks a million for her frequent invitation and sharing her delicious food with us. She and Prof. Sovan LEK entertained me so much that I felt having a new home in Toulouse!

Special thanks go to Prof. Alain DAUTA for advising to improve my manuscript and to discuss replying to review comments one by one; to Prof. Christophe BAEHR for teaching me wavelet analysis; to Prof. Michèle Tackx for giving professional comments on my manuscript; to Dr. Loïc TUDESQUE for discussing with me and giving advices on bibliometrics analysis; to Prof. Sébastien BROSSE for allowing me stay in his office to finish my PhD thesis during the late period of the study, which

guarantee a quiet environment and ensure my efficient work; to beautiful Dr. Isabelle MARECHAUX for helping me whenever I met difficulties for language barrier. Without all of your help, I could not continue my research work and life so smoothly in EDB.

My greatest appreciation and friendship goes to my closest friends and colleagues both in “Laboratory of Fishery Resources and Environmental Conservation” at PRFRI, China (they are Pang Shixun, Li Yuefei, Yang Wanling, Gao Yuan, Zeng Yanyi, Liu Qianfu, Li Jie, Yang Jiping, Zhu Shuli, Zhao Li’na, Li Lin, Wu Zhi, Zhang Weizhen, Chen Fangcan, Yu Hongliang) and “SEVAB” at UPS, France (Dr. Liu Yang, Dr. Zhao Tian, Dr. Yao Jingmei, Dr. Shuai Fangmin, Dr. Guo Chuanbo, Dr. Ratha Sor). Special thanks should owe to Dr. Liu Yang, my closest friend in Toulouse, who gave me a lot of help not only in statistical methods but also in life. I felt so lucky to meet such a good friend I always want. I am really lucky that I can work with these two big families!

I would like to thank the student Wang Xiangxiu from Chongqing University (China), since she helped me a lot during the first half year. I hope her study and life in Tongji University (China) goes well! My great friendship also goes to two beautiful girls: Dr. Jiang Qianhong and Dr. Xie Xiaomin. We were just like old friends when we met for the first time!

I also want to thanks this city Toulouse and this country France, since it is really my lucky place! This is the second time for me to visit here, but it is the first time to stay here for so long time. Actually, I have my own interesting experiences and stories in this city. Its amity, beauty, quietness, and cleanness leave me a deep impression.

Last but not least, I would like to express my great appreciations to my mother, who always care about my growth and encourage me to move on, it is really not easy to cultivate me after my father’s death. I sincerely thank my beloved wife who accompany with me to overcome difficulties I met, regardless of success or failure. I must thank myself, since I bear too much pressure from the beginning of application to the last defense. It really needs courage and confidence to leave my family and country to study here, and to complete the thesis and get the PhD degree in just one

year. I am sure that the life of my family will be better and better.

I was concerned that I might forget to mention lots of you in this short acknowledgement, but please accept my faithfully wishes, to all of you!

The research was financially supported by Guangxi Province Natural Science Foundation of Key Projects (2013GXNSFEA053003) and Public Sector (agriculture) Special Scientific Research Projects (201303056-5). We are grateful to the Pearl River Fisheries Research Institute (PRFRI), Chinese Academy of Fishery Science (CAFS) and Lab Fishery Environment Conservation of PRFRI for their financial support of my study abroad.

Faithfully yours

Chao WANG

15/10/2014

Résumé

Les écosystèmes aquatiques sont soumis à des pressions croissantes dues aux changements climatiques et aux activités anthropiques. Les rivières sont considérées comme la voie la plus importante pour la circulation de l'énergie, de la matière et des organismes. Le phytoplancton constitue le niveau de base de la chaîne alimentaire aquatique, et en liaison avec son cycle de vie, il a en plus une réponse rapide à des facteurs environnementaux qui régulent l'activité biologique et la qualité de l'eau. Les phytoplanctons ont été étudiés essentiellement en milieux lentiques tels que les lacs et les réservoirs, mais encore peu d'études ont été menées en écosystèmes lotiques. La rivière des Perles est le plus grand fleuve de plaine de Chine du Sud, mais les études pertinentes ont été interrompues au cours des trois dernières décennies. Ainsi, dans la présente étude, nous cherchons à mettre en évidence les patrons d'assemblages de phytoplancton de ce grand fleuve, par des approches de modélisation.

Premièrement, nous faisons la synthèse des tendances scientifiques des études phytoplanctoniques entre 1991 et 2013 à l'aide d'une analyse bibliométrique. Le nombre de publications annuelles sur les phytoplanctons a montré une croissance rapide au cours des deux dernières décennies, sa contribution au total des articles scientifiques est toujours restée en dessous de 10%. Dans le cadre du développement rapide de la recherche scientifique, les publications dépendantes (en termes d'écosystèmes multi-aquatiques et des collaborations internationales) montrent une tendance à la hausse. Les variations de mots clés associés à des régions de recherche sont principalement impactées par les zones géographiques adjacentes aux différents pays, qui sont généralement les top-contributeurs. Les tendances des variations des mots-clés relatifs aux méthodes de recherche, le contenu de la recherche et des facteurs environnementaux indiquent que les études de phytoplancton menées à grande échelle et à long terme sont en significative augmentation, tandis que les études traditionnelles et à l'échelle locale sont en décroissance.

Deuxièmement, les caractéristiques temporelles des assemblages de

phytoplancton ont été analysées dans la partie avale de la rivière des Perles, grâce à un échantillonnage de séries chronologiques quotidien pendant toute l'année 2009. Les conditions excessives d'éléments nutritifs conduisent à une dominance de diatomées dans la communauté de phytoplancton. Alors que les algues vertes contribuent plutôt à la diversité spécifique. En utilisant la carte d'auto-organisation (SOM), des échantillons de phytoplancton ont été classés en quatre groupes sur la base de similitudes d'espèces. Ces groupes étaient bien différenciés par la richesse spécifique, la biomasse et les espèces indicatrices. En outre, le modèle LDA montre que ces groupes peuvent être facilement prédits par des facteurs environnementaux tels que la température de l'eau, le débit et la précipitation. Concernant les éléments nutritifs, seul le phosphate pourrait avoir un impact sur les assemblages de phytoplancton. Le score global de prédiction des assemblages était de 64,2%.

Troisièmement, la distribution spatiale du phytoplancton a été analysée dans le delta de la rivière de Perle, en s'appuyant sur un échantillonnage saisonnier en 2012. La richesse en teneur d'éléments nutritifs et l'excellence des échanges d'eau ont abouti à une communauté de phytoplancton dominée par la diversité des Bacillariophyceae et Chlorophyceae et la biomasse de Bacillariophyceae. Par utilisation des méthodes d'ordination NMDS et la classification hiérarchique, les échantillons de phytoplancton ont pu être groupés en 5 clusters. Ces groupes étaient nettement différents, en termes de richesse spécifique, de biomasse et des espèces indicatrices, mais les différences entre les groupes ne sont significatives que dans la dimension spatiale. Le modèle prédictif LDA a indiqué que la répartition spatiale des assemblages de communautés de phytoplancton pourrait facilement être différenciée par des variables associées à la qualité de l'eau (TP, Si, Do et transparence). Le score global de prédiction des assemblages était de 75%.

Enfin, la variabilité morphologique des espèces de diatomées prédominantes, *Aulacoseira granulata* (Ehrenberg) Simonsen, a été étudiée dans la partie avale de la rivière des Perles. On observe une grande cohérence entre les paramètres morphologiques, en particulier la taille de la cellule. En outre, les angles de phases des ondelettes-croisées illustrent bien que le diamètre des cellules est le paramètre le

plus sensible aux variations de l'environnement et que par là les variations de taille des cellules et des filaments pourraient y être liées. La température de l'eau a des impacts sur les taux d'occurrence des algues et la taille au cours de la période printemps-hiver. Le cycle de vie des algues pourrait être affecté par le débit, tout comme la longueur de filament, dans la sélection de chaînes avec la flottabilité optimale. Les réponses de la taille des algues à des nutriments, en particulier la silicate, l'azote total et le phosphate, ont été associées avec le début et à la fin d'un cycle de vie. Ces corrélations entre la taille et les nutriments ont été démontrées à la fois par l'analyse par ondelettes et par la RDA. En outre, les valeurs extrêmement élevées à la fin de l'année ont été expliquées comme le recrutement d'algues au niveau du benthos.

Notre présente étude dessine les tendances scientifiques du monde entier dans les études de phytoplancton en utilisant l'analyse bibliométrique, en démontrant les tendances temporelles et spatiales des assemblages de phytoplancton en réponse à des environnements dans un grand fleuve tropical en Chine. Nos résultats ont contribué ainsi à la compréhension de la dynamique du phytoplancton dans les écosystèmes d'eau douce, ainsi que dans les grands fleuves du monde entier.

Mots-clés: phytoplancton, rivière, Rivière des Perles, Chine, modèle, analyses bibliometriques, patron temporel et spatial, prédiction, variabilité morphologique

Abstract

Freshwater ecosystems throughout the world are experiencing increasing pressures from both climate changes and anthropogenic activities. Rivers, the typical lotic freshwater ecosystems, are regarded as important pathways for the flow of energy, matter, and organisms through the landscape. Phytoplankton constitutes the base level of the aquatic food web, and it has quick response to environmental factors that regulate biological activity and water quality. Studies on phytoplankton have been extensive in lentic fresh-waters such as lakes and reservoirs, but still less in lotic ecosystems. The Pearl River is the largest lowland river of South China, but relevant studies were interrupted during the last three decades. Consequently in the present study, we contribute to highlight the patterns of the phytoplankton assemblages of this large river, with the approach of several ecological modeling.

Firstly, we summarize the scientific trends in phytoplankton studies between 1991 and 2013 based on bibliometric analysis. Although the annual publication output of phytoplankton demonstrated a rapid linear increasing tendency during the last two decades, its contribution to total scientific articles always kept below 10%. Under the background of fast scientific research development, dependent publications (in terms of multi-aquatic ecosystems and international collaborations) indicate linear increasing trend. The variations of keywords associated with research regions are mostly impacted by the geographic adjacent countries, which are generally the top contributors. Variation trends of all the keywords relating to research methods, research contents and environmental factors indicate that phytoplankton studies carried out in large scale and long term are in significant ascending trend, while traditional and local scale studies are in descending trend.

Secondly, temporal patterns of phytoplankton assemblages were analyzed within the downstream region of the Pearl River (China), through time-series sampling during the whole of 2009. The excessive nutrient conditions resulted in a diatom dominant phytoplankton community. While green algae only contributed more in

species diversity. Phytoplankton samples were classified into four clusters using a self-organizing map (SOM) based on species similarities. These clusters were clearly different, with respect to species richness, biomass and indicators. Moreover, the LDA predicting model indicated that these clusters could easily be differentiated by physical factors such as water temperature, discharge and precipitation. As for nutrients, only phosphate could have an occasional impact on phytoplankton assemblages. The global score for predicting the assemblages was 64.2%.

Thirdly, spatial patterns of phytoplankton were analyzed within the Pearl River delta system (China), through seasonal sampling during 2012. The excessive nutrient conditions and well water exchanges resulted in a phytoplankton community that Bacillariophyceae and Chlorophyceae dominated in diversity and Bacillariophyceae dominated in biomass. Phytoplankton samples were revealed by the ordination method using a NMDS and five groups were determined by using hclust. These groups were clearly different, with respect to species richness, biomass and indicators, but differences between the patterning groups were only significant in spatial dimension. The LDA predicting model indicated that the spatial patterns of phytoplankton community assemblages could easily be differentiated by variables (TP, Si, DO and transparency) associated with water quality. The global score for predicting the assemblages was 75%.

Lastly, the morphological variability of the predominant diatom species, *Aulacoseira granulata* (Ehrenberg) Simonsen, was observed within the downstream region of the Pearl River (China). High coherence between morphological parameters, especially cell size, was confirmed. Moreover, phase angles in wavelet figures also illustrated that cell diameter was the most sensitive parameter to environmental variations and through this way cell and filament size variations could be related. Water temperature impacted algal occurrence rates and size values during the spring-winter period. Algal life cycle could be affected by discharge, as well as filament length by allowing for selection of chains with optimum buoyancy. The responses of algae sizes to nutrients, especially silicate, total nitrogen and phosphate, were associated with the start and end of a life cycle. These correlations between size

and nutrients were supported by both wavelet analysis and RDA. Moreover, the extremely high values at the end of the year were explained as algal recruitment from benthos.

Our present study have introduced the worldwide scientific trends in phytoplankton studies using bibliometric analysis, demonstrated the temporal and spatial patterns of phytoplankton assemblages in response to environments within the downstream region of a large subtropical river in China. Our results will benefit the understanding of phytoplankton dynamics in freshwater ecosystems, as well as the large rivers all over the world.

Key words: phytoplankton, river, the Pearl River, China, model, bibliometric analysis, temporal and spatial patterns, predicting, morphological variability

Part I: Synthesis

1. Introduction

1.1 General scientific trends in phytoplankton studies

This is an era of information explosion, and around 6000 new research articles come out every day. Therefore, it is actually difficult for researchers to catch up with the scientific development, even in a specific research field. Especially for beginners, who are getting acquainted with their new research topic, the difficulties to understand both the background and the frontier of their own research field are substantial. Phytoplankton is a collective of photosynthetic microorganisms, adapted to live partly or continuously in open waters, and a major primary producer of organic carbon in both marine and inland waters (Reynolds, 2006). Phytoplankton research and its literature as such are of basic importance in all studies related to trophic and biogeochemical functioning of aquatic ecosystems.

Bibliometric analysis is a common research method which has already been widely applied for the scientific production and research trends in many disciplines of science (Keiser & Utzinger 2005, Li et al. 2009, Zhang et al. 2013, Liao & Huang 2014). The Science Citation Index (SCI), from the Institute for Scientific Information (ISI) Web of Science databases is the most frequently used database to obtain a broad review on a scientific field (Bayer & Folger 1966, Ho 2014). Carneiro et al.'s (2008) article in *Limnology*, titled "Trends in the scientific literature on phytoplankton", mainly summarized the information associated with affiliations (journals, countries and regions) and applications (citation and impact factor) of phytoplankton publications. But the research trends are still unknown, thus a deeper understanding in this is anticipated. This method has been used in many disciplines of science and engineering to measure scientific progress, and is a common research instrument for systematic analysis (Van Raan 2005). The analysis results could help to illustrate the global trends of phytoplankton research and potentially give some guidance to scholars for developing and deepening their respective researches.

From 1991 to 2013, the total publication output on phytoplankton was 39150, and the annual publication output demonstrated a rapid linear increasing tendency in the last two decades, from only about 800 in 1991 to 2600 in 2013, actually more than 3 folds increase during the last 20 years (Fig. 1). But the proportion of phytoplankton publications in total scientific articles always remained below 0.1%, with a light fluctuation between 0.07~0.09%.

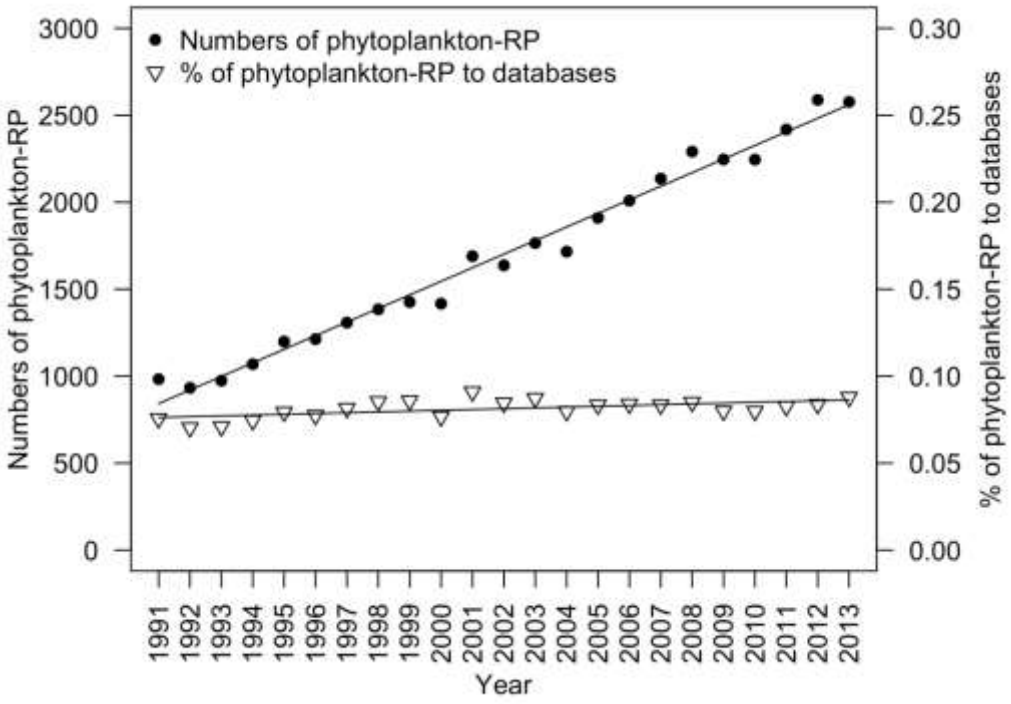

Figure 1 Temporal trend of the number of phytoplankton research papers and its proportion in total databases

Temporal variations of the relative proportions of phytoplankton research papers in six major aquatic ecosystems and others (including those in other aquatic ecosystems and those in other research fields) were shown in Fig. 2. The results indicated that the six aquatic systems contributed a large part (> 80%) of total phytoplankton publications, and the temporal variations of their sum values showed a slight increasing trend during the last 20 years. However, the relative proportion of different aquatic systems maintained steady, and publications in marine systems contributed the largest part (around 50%), while the sum proportion of freshwater

areas fluctuated around 25%. Publications in the river ecosystems showed a slight increasing trend.

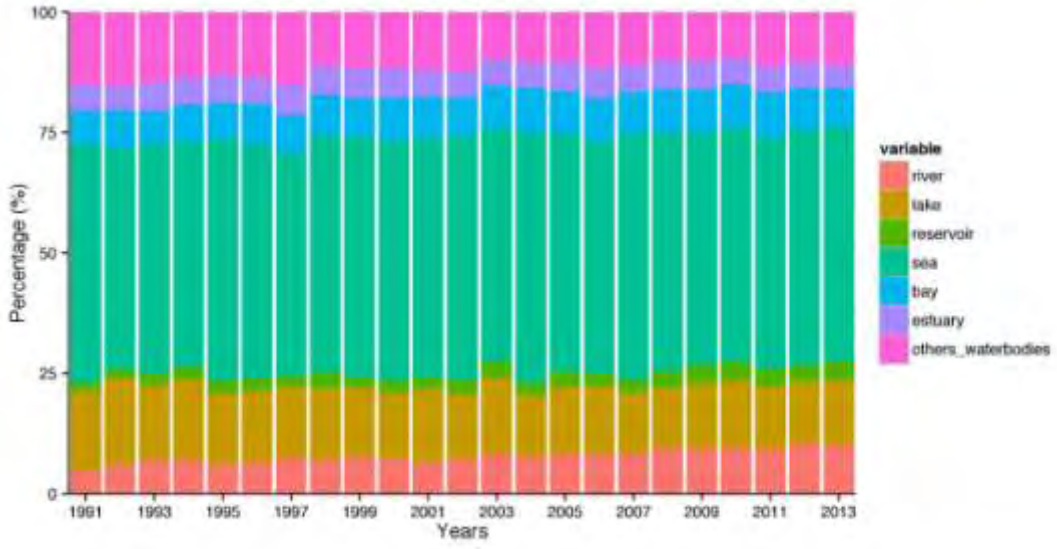

Figure 2 Temporal trend of relative contributions of phytoplankton articles in different types of aquatic systems

Considering aquatic ecosystems, 15401 articles were published in the single-aquatic system category and 16346 articles were published in multi-aquatic system category. While both categories represent a comparable number of articles, the linear positive ascending trend (around 15% increase) of publications in multi-aquatic ecosystems (Fig. 3) implied that publications in single-aquatic system (independent research) were previously more dominant, but gradually overtaken by publications in multi-aquatic systems during the last 20 years.

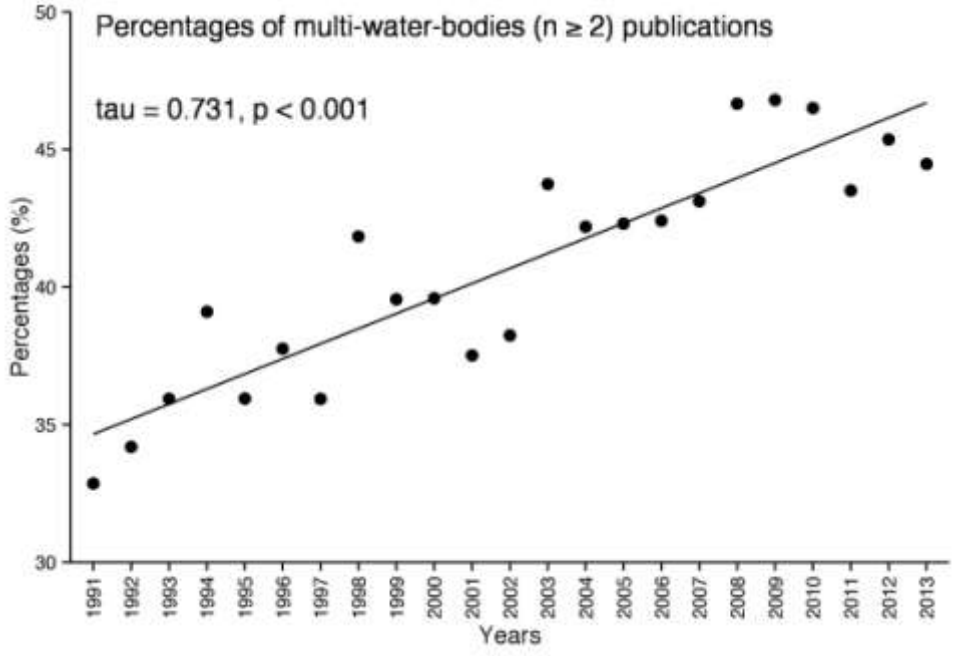

Figure 3 Temporal trends of percentages of phytoplankton articles referring to ≥ 2 aquatic ecosystems in total phytoplankton articles.

1.2 Phytoplankton studies in the river ecosystem, with reference to the Pearl River

Freshwater ecosystems throughout the world are experiencing increasing pressures from both climate changes and anthropogenic activities. Such pressures generally lead to variations in temperature, light availability, hydrologic conditions and nutrient contents of the water bodies (Devercelli 2010, Hamilton et al. 2012, Larroudé et al. 2013). Rivers, the typical lotic freshwater ecosystems, are also regarded as important pathways for the flow of energy, matter, and organisms through the landscape (Karadžić et al. 2013). Large rivers, from headwaters to estuaries, represent a continuum of interdependent ecosystems, so studying each section of the river will be base to understand the whole aquatic ecosystem (Gamier et al., 1995).

Phytoplankton constitute the base level of the aquatic food web, and species composition and variation can efficiently respond to environmental factors that regulate biological activity and water quality (Reavie et al. 2010, Hamilton et al. 2011, 2012). Studies on phytoplankton have been extensive in lentic fresh-waters such as lakes and reservoirs, where long residence times and low flow velocities allow

sufficient time for growth and reproduction (Sabater et al. 2008, Torremorell et al. 2009, Elliott 2012, Fornarelli et al. 2013). However, relevant studies in lotic ecosystems (such as streams and rivers) are still less studied (Kiss 1987, Piirsoo et al. 2008, Wu et al. 2011, Sipkay et al. 2012) compared with lentic systems. Spatial and temporal patterns of phytoplankton communities in large rivers are driven by a mixture of physical, chemical and biological factors, which vary seasonally and their relative weight depends on river typologies (Rossetti et al. 2009, Tavernini et al. 2011). The response of phytoplankton to environmental factors has become a central topic of current research (Wu et al. 2011). The identification of key factors that control phytoplankton in a particular water body is essential for choosing an appropriate management strategy for the maintenance of a desired ecosystem (Peretyatko et al. 2007). However, as environmental drivers co-act simultaneously, it is not easy to identify which has the most important impact on the river community. Fortunately, more and more ecological models have been applied to phytoplankton studies in such lotic aquatic systems for this purpose (Billen et al. 1994, Thebault & Qotbi 1999, Jeong et al. 2006, Sipkay et al. 2012). Self Organizing Maps (SOMs) are capable of evaluating large and dense datasets, and have been applied successfully to phytoplankton studies for the classification and rapid discrimination function (V árb író et al. 2007, Aymerich et al. 2009). To date, the discussion is still open: what are the main controlling factors of river phytoplankton? Are the factors physical (Devercelli 2010, Salmaso & Zignin 2010, Domingues et al. 2012) or chemical (Dodds 2006, Torremorell et al. 2009), or a combination of both? Therefore, further studies are still required, notably those reporting on classic large rivers in the world and advanced ecological models may provide new approaches to answer the above questions.

The Pearl River Delta, characterized by a prosperous economy and dense human population, has always been an important center of southern China for politics, economics and culture. The Pearl River, the original river of this region, is the largest lowland river of South China. The oldest data for phytoplankton in the river basin are from the beginning of 1980s, when a general survey on aquatic organisms and water

environments was carried out through the cooperation between several regional research organizations (Lu 1990). Moreover, only a simple primary dataset was collected during the investigations, and the minimal identification unit of phytoplankton composition was only specific to genus; temporal and spatial distributing patterns were still unclear. After this basic investigation, studies on phytoplankton ecology in the river basin were interrupted for the following thirty years. During recent years, relevant studies on phytoplankton were mainly carried out in Guangzhou segment (Lei et al. 2007, Zhang et al. 2011) and published in Chinese local journals. The author also reported the basic temporal and spatial patterns of phytoplankton in the main stream (Wang et al. 2013a) and the delta system (Wang et al. 2013b). However, studies in the Pearl River Estuary (Huang et al. 2004, Zhao et al. 2008, Shen et al. 2011) have always been paid more attention. Therefore, further understanding on phytoplankton patterns and predictions in the Pearl River, especially the main stream, is still anticipated, introducing more advanced statistical methods with the goal of finally providing more effective management guidelines for government.

1.3 Potential indicating role of a dominant diatom

Diatoms are known as the most important group of phytoplankton assemblages in lotic river ecosystems (Reynolds 2006). The genus *Aulacoseira* contains a group of centric diatoms with chain colonies composed of cylindrical frustules united by shortened linking spines (Tremarin et al. 2012). Population dynamics and new species records of this genus were often reported in various aquatic ecosystems (Hötzel & Croome 1996, Wang et al. 2009, Usoltseva & Tsoy 2010, Horn et al. 2011, Poister et al. 2012) due to its high taxonomic compositions and obvious high density. Moreover, morphological studies of this genus always generated interest because changes in cell size and hence in filament dimension were often observed and reported in natural waters (Davey 1987, Babanazarova et al. 1996, Turkia & Lepistö 1999, O'Farrell et al. 2001, Manoylov et al. 2009, Poister et al. 2012), and these morphological features could potentially be used as indicators when their correlations with environments

were built up, as the response of morphological changes was more rapid than possible observations of changes in population dynamics (Gibson et al. 2003). In addition, the rigid silica cell wall of members of this genus permits only two main possibilities for adaptation: varying either length or diameter; thus the process of morphological changes could be observed (Jewson et al. 2010).

Aulacoseira granulata, a cosmopolitan species of this genus, has an international distribution due to its adaptive capacity and tolerance of a wide range of environmental conditions. Generally, *A. granulata* is regarded as a good indicator species to eutrophic water conditions (Nogueira 2000, Kamenir et al. 2004, Lepistö et al. 2006), since it can easily form predominant populations and even become blooms (Miyajima et al. 1994, Nakano et al. 1996) in eutrophic waters under suitable conditions (e.g. high temperature). The author has also reported that *A. granulata* is predominant in the downstream of the Pearl River (Wang et al. 2009, 2012, 2013), which is known as a hyper-eutrophic river system. Except for population abundance, morphological variability of *A. granulata* was also found closely related to environmental variations, especially sensitive to nutrient concentrations (Stoermer et al. 1981, Davey 1987, Gómez et al. 1995, Turkia & Lepistö 1999). Relevant studies on the correlations between its morphology and environments have been carried out more in lentic water bodies such as lakes (Stoermer et al. 1981, Davey 1987, Turkia & Lepistö 1999, Manoylov et al. 2009) and reservoirs (Reynolds et al. 1986, Gómez et al. 1995), in which strong stratification occurred. Generally, the eutrophic status and specific nutrient availability of the studied water system explained a significant proportion of the observed morphological results (Gómez et al. 1995, Turkia & Lepistö 1999, O'Farrell et al. 2001). In rivers, conditions are different: the lotic flows and oligotrophic status may enhance the importance of physical and hydrological factors in impacting morphological changes, especially in filament size selectivity. In such lotic systems, exploring temporal trend of morphological variability of *A. granulata*, based on frequent sampling, might help finding more elaborate and accurate correlations between this diatom species and environments.

The author has observed the diverse morphological variability of *A. granulata* (Fig. 4-7), and significant differences are found existing under different nutritional levels. This interesting research point has been funded by the National Natural Science Foundation of China (41403071) in the following three years (2015~2017).

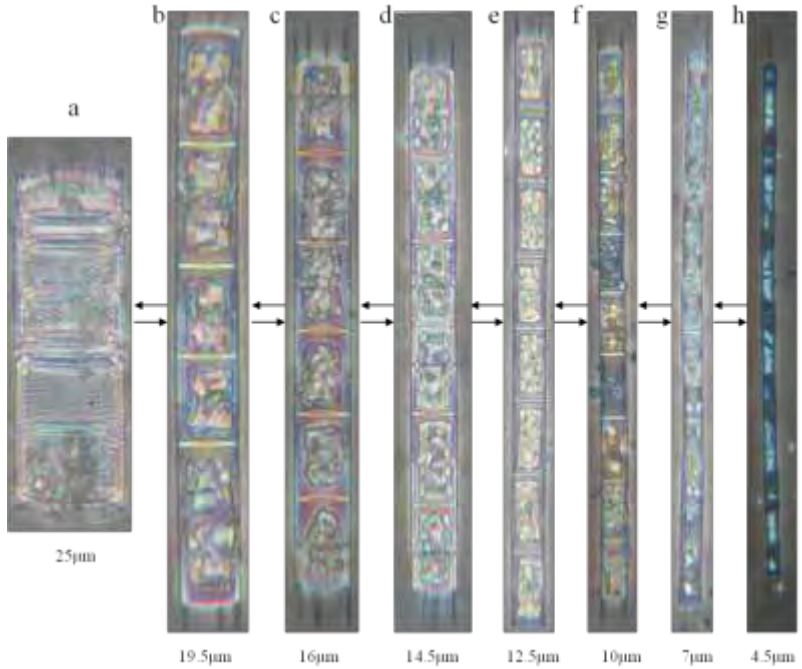

Figure 4 Morphological variability in linear forms

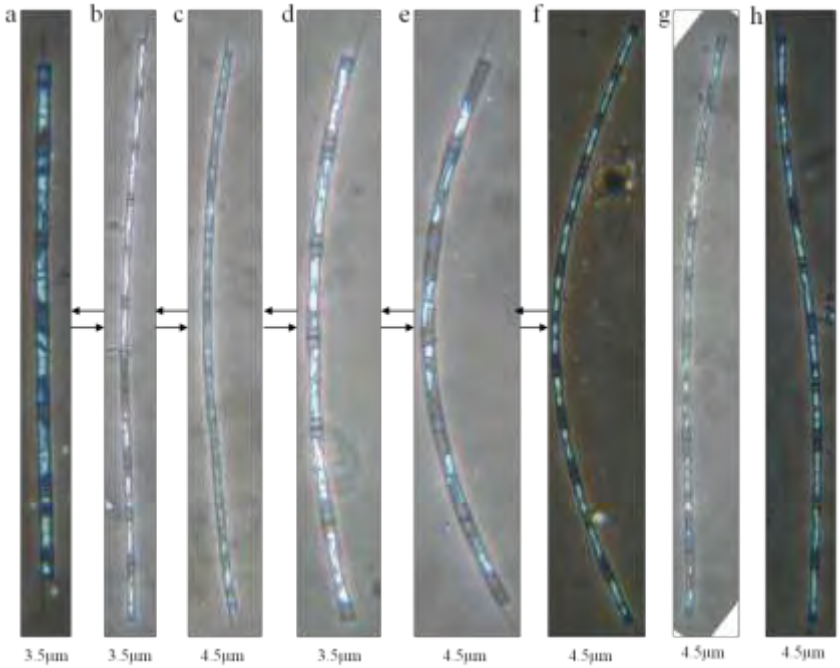

Figure 5 Morphological variability in narrow forms

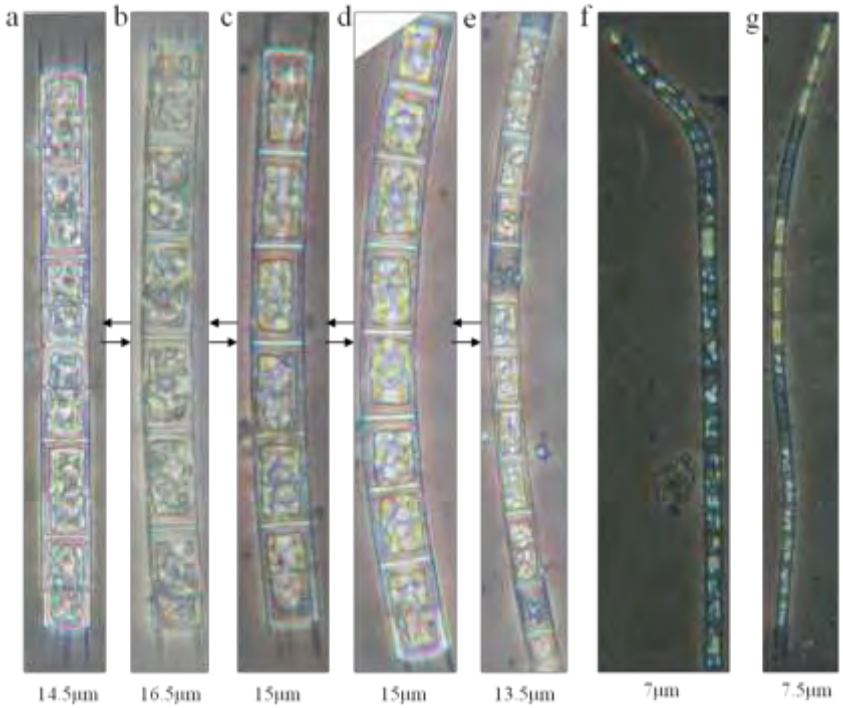

Figure 6 Morphological variability from linear to curved forms

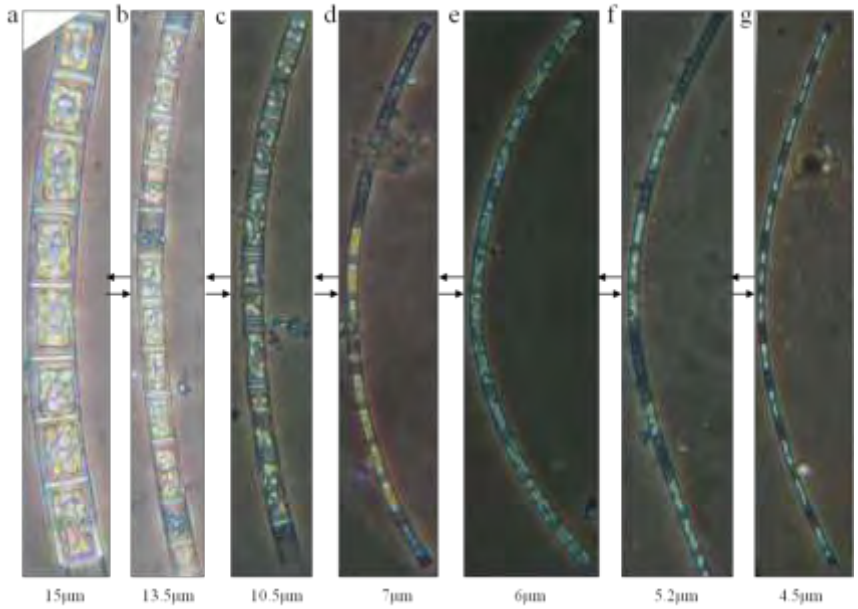

Figure 7 Morphological variability in curved forms

1.4 Specific objectives

The Pearl River is the largest river of South China, and it also represents a classic large subtropical river in the world. Phytoplankton is the primary producer of this large lotic ecosystem, and it generally shows quick response to environmental

variations. However, very few efforts aimed at the phytoplankton assemblage patterns of this large river during the last three decades. Consequently, in the present study, we focused on the pattern and predicting of phytoplankton assemblages at the downstream of the Pearl River ecosystem, which was closely associated with human beings activities.

Specifically, the present study mostly aims to 1) introducing the general scientific trends in phytoplankton studies with bibliometric analysis; 2) patterning and predicting the annual variations of phytoplankton assemblages of the Pearl River; 3) demonstrating the spatial pattern and prediction of phytoplankton assemblages in the Pearl River delta system; 4) exploring the potential indicating role of a dominant diatom species through morphological variability at the downstream of the Pearl River.

2. Materials and Methods

2.1 Study area

2.1.1 Study area in the mainstream of the Pearl River

The Pearl River, with a length of 2,320 km, a catchment area of 450,000 km^2, and a moderate annual discharge of 10,000 m^3 s^{-1}, is the third longest river in China. This large river consists of three major tributaries: West River, North River and East River, and the West River (2129 km), running through Guangdong province and Guangxi province, is the largest tributary. Our fixed long-term sampling site (23°2′40″N，112°27′5″E) is located at the downstream of the West River (Fig. 8), near the wharf of the Zhaoqing Fishery Administration, which is about 160 km upper from the Pearl River Estuary. The depth of the sampling site is between the lowest and highest water levels and ranges from 3 to 5 meters.

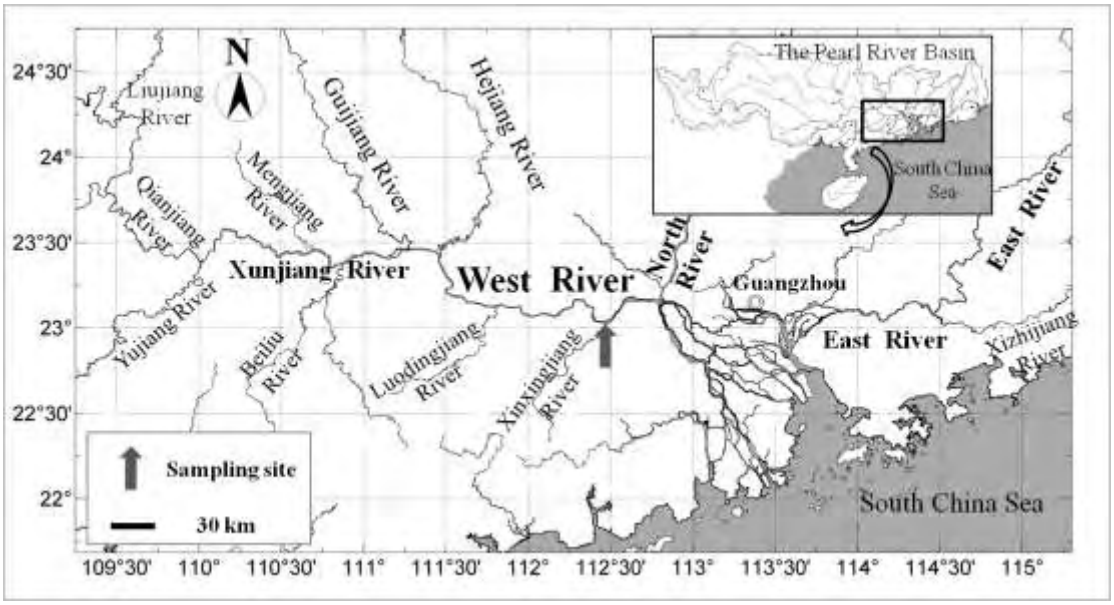

Figure 8 The downstream river network of the Pearl River, including river tributaries and the sampling site.

2.1.2 Study area in the Pearl River delta system

The three large tributaries of the Pearl River join together and form the Pearl River Delta before their entering to the South China Sea (Yang et al., 2010). Fig. 9 shows a general layout of the PRD basin: the basin location, the main river sources

and tributaries, and the 13 spatial sampling sites. The area of PRD (21°40'–23°N, 112°–113°20'E) is about 9,750 km^2, and it is dominated by a sub-tropical monsoon climate with abundant precipitation. The annual mean precipitation is 1,470 mm and most rains occur in April–September. The topography of the PRD has mixed features of crisscross river-network, channels, shoals and river mouths (gates). A total of 13 sampling sites are set up, covering the important positions of the river network, including Qingqi (QQ), Zuotan (ZT), Waihai (WH), Xinwei (XW), Xiaolan (XL), Xiaotang (XT), Beijiao (BJ), Lanhe (LH), Hengli (HL), Chencun (CC), Zhujiangqiao (ZJQ), Lianhuashan (LHS) and Shiqiao (SQ). Among of them, QQ, ZT, WH and XW are located along the main channel of West River, finally flowing through Modao mouth and entering into the estuary. ZJQ and LHS are located along the other side of the delta, of which ZJQ is in Guangzhou channel and LHS is in East River side. Other sites are located in inner part of the delta.

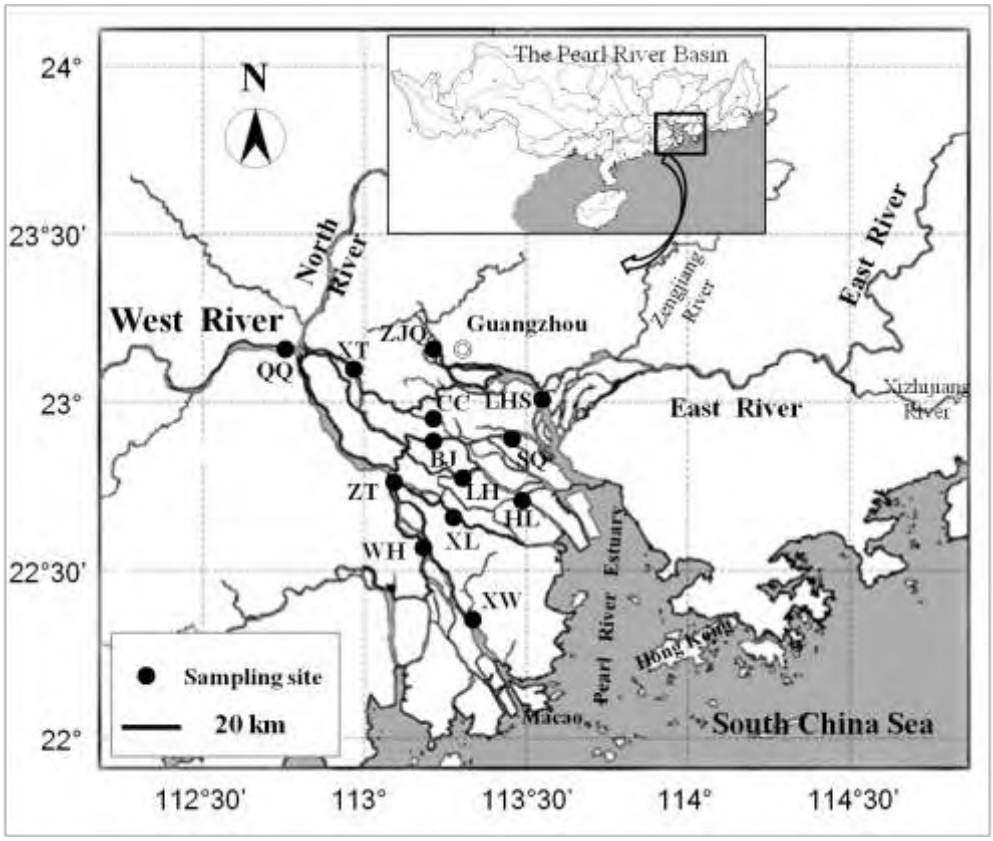

Figure 9 The river network system of the Pearl River Delta, including three main tributaries of the Pearl River and sampling sites. QQ—Qingqi, ZT—Zuotan, WH—Waihai, XW—Xinwei, XL—Xiaolan, XT—Xiaotang, BJ—Beijiao, LH—Lanhe, HL—Hengli, CC—Chencun, ZJQ—Zhujiangqiao, LHS—Lianhuashan.

2.2 Data collection

2.2.1 Bibliometric analysis dataset

Any articles containing the keyword "phytoplankton" in title, abstract and keywords fields, published between 1991 and 2013, were queried from all citation indexes on Web of Science (Thomson Reuters). A XML file containing titles, keywords, abstracts, years of publication, authors' names, and authors' affiliations, cited times and cited reference counts was exported. The search query was constructed as below: (TITLE-ABSTRACT-KEYWORDS: "phytoplankton").

2.2.2 Phytoplankton assemblages dataset

The main stream

Phytoplankton samples were collected at 8:00 am every 5 days for each month of 2009. For each phytoplankton sample, 1 L of water was collected from 0.5 m below the surface using a 5 L HQM-1 sampler. The sample was put into a polyethylene bottle and fixed immediately with formaldehyde solution (5%). A phytoplankton sample was fixed and concentrated by sedimentation to 100 ml. All the algae were counted using a 1-ml Sedgewick-Rafte counting frame (inverted microscope Nikon Eclipse TS100). A second phytoplankton sample was assigned for diatom identification and enumeration. This sample was concentrated and treated with dilute HCl and H_2O_2, and at least 400 valves were counted. The systematic grouping of phytoplankton was done following the manual of Van den Hoek et al. (1995).

Phytoplankton biomass was calculated from the biovolume of each species, assuming unit specific gravity, by geometrical approximation according to Hillebrand et al. (1999). Median values of both species richness and biomass were used to represent the population dynamics of each group or cluster.

The Pearl River delta

Phytoplankton samples were collected seasonally (March, May, August and December) during 2012, and the investigation of each season was managed in successive 2 to 3 days. Phytoplankton samples collection, measurement, identification and calculations were dealt with in the same way as that in the main stream.

2.2.3 Morphological parameters of *Aulacoseira granulata*

Qualitative subsurface phytoplankton samples were collected at 8:00 am every 5 days each month. For each qualitative sample, 9–10 L of water was collected from subsurface and passed through a 20 μm nylon mesh. The retained particles were then washed into a preweighed glass bottle using 100–200 mL of water. Aliquots of the qualitative samples were cleaned by conventional methods (Patrick & Reimer 1966) and subsequently used to prepare permanent slides. The valve diameter and mantle height were measured for a minimum of 100 cells per sample, and the results represented cell diameter and cell length respectively. Moreover, the cell volume was calculated from diameter and mantle height by applying geometric formulae. In each sample, the number of cells per colony was recorded for a minimum of 100 colonies to determine the average filament length of *A. granulata*.

2.2.4 Environmental variables dataset

The main stream

An additional water sample of 250 ml was filtered *in situ*, and taken back to the laboratory for nutrient analysis (including phosphate, silicate, total nitrogen, nitrate nitrogen, nitrite nitrogen and ammonia nitrogen) using an injection water quality analyzer (Skalar-SA1100) or a spectrophotometer (Shimadzu UV-2501PC). Water temperature was recorded using an automatic water temperature recorder (HOBO water temp Pro V2) at a frequency of once per hour at the sampling site. Water discharge was collected from the website: http://xxfb.hydroinfo.gov.cn, and precipitation data was collected from the website: http://weatheronline.co.uk/weather.

The Pearl River delta

Water temperature, salinity, pH value and dissolved oxygen (DO) was determined in situ with a portable instrument (YSI6600-02). Transparency was determined using black and white transparent plate. An additional water sample of 250 ml was filtered *in situ*, and taken back to the laboratory for nutrient analysis (phosphate, silicate, total nitrogen, nitrate, nitrite and ammonia) using water flow injection analyzer (Skalar-SA1100) and spectrophotometer (Shimadzu UV-2501PC).

2.3 Model techniques

2.3.1 Self-organizing map (SOM)

Phytoplankton species assemblages were classified using a self-organizing map (SOM), which is one of the most well-known neural networks with unsupervised learning rules. In this study, the temporal variation pattern of phytoplankton species was described by the SOM model: a total of 69 species with more than 10% occurrence rate was analyzed. Sampling dates with similar species composition and structure were classified into the same neuron or into neighboring neurons, according to the degree of dissimilarity. A total of 90 neurons (virtual units) was the output of the SOM, which was arranged into a 10 × 9 hexagonal lattice to provide better visualization. The map size was set according to $5 \times (\text{number of samples})^{1/2}$ (Vesanto 2000), and then based on the minimum best values of quantization and topographic errors. The cells of the map were then subdivided into different groups according to the similarity of the weight vectors of the neurons using Ward's linkage method. The group numbers were mainly based on the degree of dissimilarity of each SOM cell in the hierarchical clustering. The unified distance matrix (U-matrix; Ultsch 1993) and Davies-Bouldin index (Davies & Bouldin 1979) were also applied to reinforce the group definition. All these analyses were carried out with Matlab software (Mathworks Inc 2001) using the SOM toolbox (Alhoniemi et al. 2000).

To assess the effectiveness of the hierarchical clustering on the SOM units, the cophenetic correlation coefficient (Sneath & Sokal 1973) was calculated using R software (Ihaka & Gentleman 1996). The contributions of each input component with respect to cluster structures were obtained from weight vectors of the SOM and then visualized by boxplot (He et al. 2011). We used the Kruskall-Wallis test to compare differences of species richness among clusters in the R software. After the Kruskall-Wallis test, multiple comparison tests were also carried out in the R software using the 'pgirmess' package (Giraudoux 2006).

2.3.2 Linear Discriminant Analysis (LDA)

Linear Discriminant Analysis (LDA) is a method used in statistics, pattern

recognition to find a linear combination of features which characterizes or separates two or more classes of objects or events. LDA explicitly attempts to model the difference between the classes of data. Here, LDA was conducted to determine which environment variables discriminate between the groups previously defined by the hierarchical clustering. Standardized coefficients for each variable in each discriminated function represent the contribution of the respective variable to the discrimination between clusters. A random Monte Carlo test with 1000 permutations was used to reveal the significance of environmental variables among clusters.

2.3.3 Non-metric multidimensional scaling (NMDS)

Non-metric multidimensional scaling (NMDS) was used to evaluate among-sites separation (Kruskal & Wish, 1978), which does not rely on (primarily Euclidean) distances like other ordination techniques but uses rank orders, and thus it is an extremely flexible ordination method that can accommodate a variety of different kinds of data and is especially well suited to data that are discontinuous, non-normal, on arbitrary or otherwise questionable scales. "Ordination stress" is a measure of departure from monotonicity in the relationship between the dissimilarity (distance) in the original *p*-dimensional space and distance in the reduced *k*-dimensional ordination space (Wu et al., 2011). In this analysis, we used Bray-Curtis similarity as the distance measure.

2.3.4 IndVal method

To identify indicator species, the IndVal method (Dufrêne & Legendre 1997) was used to define the most characteristic species of each group. These indicator species were found mostly in a single group of the typology and present in the majority of the sites belonging to that group, for summarizing the assemblage patterns (He et al. 2011). Based on the fidelity and the specificity of species for each cluster, INDVAL 2.0 was used to identify indicator species. The formula is as following: $IndVal_{ij} = A_{ij} \times B_{ij} \times 100$, where $A_{ij} = Nbiomass_{ij} / Nbiomass_i$, $B_{ij} = Nsample_{ij} / Nsample_j$, and *i* means species *i*, *j* means cluster *j*. Only significant and greater than 25 IndVal have been taken into account. In this way, it implies that a characteristic species occurs in

at least 50% of one site's group, and that its relative abundance in that group reaches at least 50%.

2.3.5 Wavelet analysis

The signals contained in data set often reflect the results of the superimposition of different natural mechanisms. These mechanisms may have different time characteristics and different patterns (Bliss 1970). Most of them are periodic and correspond to cyclic phenomena. The Fourier transform is a mathematical tool used to analyze the different cycles or frequencies embedded in a time series (Hornberger & Wiberg 2006). But calculating processes of some natural mechanisms are irrelevant with a Fourier analysis. Therefore we have to use more powerful techniques taking into account the time series characteristics. For instance we may use methods considering the possibility of patterns different from the harmonics. Moreover, we may also use methods reflecting the shape, the time characteristics of the embedded phenomena and their time localization. The Wavelet Analysis has been designed during the 80's in order to analyze local signals or non-cyclic patterns (Morlet et al. 1982, Mallat 1989). The wavelets can also be used to extract information from many different types of time-series data such as audio signals and images.

In order to introduce the wavelet analysis method, we have to explain the concept of scale for data series and the concept of localization (see Fig. 10). We assume that the signal may be not only composed of periodic harmonics, but also composed of a sequence of structures (a structure is a specific pattern, like steps or transitory signals for instance) with different characteristic time lengths. The scale structure refers to the time length of the phenomenon (see Fig. 10). Then the whole time series may be seen as the superimposition of all the structures existing at the different scales (Daubechies 1990). To proceed to the wavelet analysis, a dilatation/contraction of a specific pattern (called mother wavelet) is performed (see Fig. 10), meanwhile a comparison with a part of the series is also performed. These local comparisons are equivalent with local correlations using a special inner product. This method is able to analyze any type of time series, regular or not, continuous or

not, periodic or not. The more adaptive to the time series the wavelet is, the better the analysis will be. Thus this tool is very suitable for analyzing natural and geophysical data series.

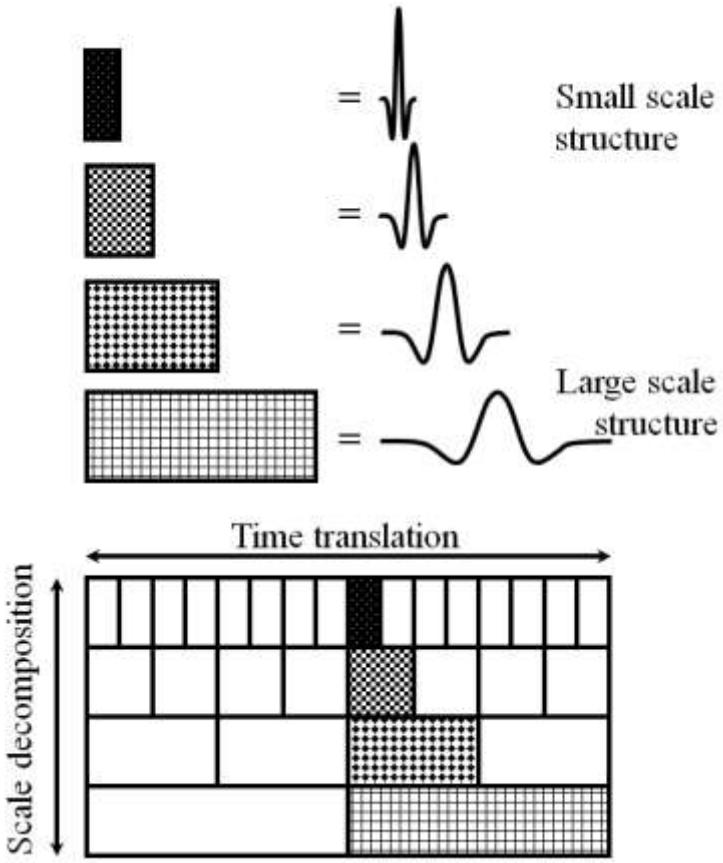

Figure 10. The different parts of the time series are compared with a wavelet . The wavelet pattern is dilated or contracted according to the scale of analyze and translated in time.

From the mathematical point of view, considering the time $t \in [1, T]$, where $T > 0$ and a mother wavelet $\Psi(t)$ satisfying the admissibility conditions (Daubechies 1992), we define the wavelet $\Psi_{m,n}$ for the m-th scale and the n-th time by the equation: $\Psi_{m,n}(t) = \frac{1}{\sqrt{m}} \Psi(\frac{t-n}{m})$, $m \in \mathbb{R}^+, n \in [1, T]$. Considering now a time series or a signal $f(t)$, the wavelet coefficient for the m-th scale and the n-th time is given by the equation: $W_{m,n}(f) = \int_1^T f(t)\, \Psi^*_{m,n}(t) dt$, where $.^*$ denotes the complex conjugate. The scale factor m may be seen as a dilation of the function f while the number n is the time translation. As said previously, the wavelet coefficients provide local (in time) correlations between the data and the wavelet with

respect to analyzed scale.

Using the wavelet concept, it is possible to define the analog of a cross-correlation with a time series and a scale point. This is the purpose of the Coherency estimation using the Cross-Wavelet analysis. The cross-wavelet has an equivalent in frequency domain with the Fourier cross-spectrum and reflects the Wiener-Khintchine theorem. If two series present some common structures, the high values of the cross-wavelet coefficients are locally highlighting these structures. To the contrary when the two series have no relation the cross-wavelet analysis gives back weak coefficients.

Mathematically, let be a first time series $f(t)$ and a second $g(t)$ both defined in the interval $[1, T]$. One may define the cross-wavelet $W_{m,n}(f,g)$ by the wavelet coefficients inner product: $W_{m,n}(f,g) = < W_{m,n}(f), W^*_{m,n}(g) >$ (Maraun & Kurths 2004, Grinsted et al. 2004). Thus a cross-wavelet coefficient is a complex number with an absolute value and an argument (or phase angle). By definition, the cross-wavelet coefficients are un-normalized coefficients. To be relied to the cross-correlation, the cross-wavelet coefficients have to be normalized. These new figures are called Coherency (Maraun & Kurths 2004). The coherency is the ratio of the energy of $W_{m,n}(f,g)$ by the product of the energy of $W_{m,n}(f)$ and $W_{m,n}(g)$. More precisely using a normalized smoothing operator $<>$ in scale and in time, the wavelet coherency is given by the equation: $R_{m,n}(f,g) = \frac{|<W_{m,n}(f,g)>|}{(|<W_{m,n}(f)>||<W_{m,n}(g)>|)^{1/2}}$. The coherency is 1 if the two series f and g are linearly dependant around the time n and on a scale m. A zero value means no local cross-correlation. The coherency is therefore an excellent tool to qualify the relationship between two parameters. In the sequel we perform analyzes between biological characteristic of algae and environmental parameters in order to highlight their possible links. The wavelet coherency phase angle $\phi_{m,n}(f,g)$ is the argument of the coefficient: $W_{m,n}(f,g)$, which could be computed using the following equation: $\phi_{m,n}(f,g) = \text{atan}\left(\frac{\Im(<W_{m,n}(f,g)>)}{\Re(<W_{m,n}(f,g)>)}\right)$, where for a complex number$z \in \mathbb{C}$, $\Re(z)$ is its

real part, and $\Im(z)$ is its imaginary part.

The phase angle is a common way to illustrate the difference between two waves, for instance when they reach their maximum. A null phase angle means that the two waves are in phase (↑), i.e. they reach their maximum at the same time. The phase angle is –π when the waves are anti-phased (↓), i.e. the first is reaching its maximum while the second is at its minimum. The phase angle is π/2 when the first series leads the second (→) and is –π/2 when the second series leads the first (←). The phase angle may be also seen as the phase difference between the two series (the shape of the time lag between the series). Therefore the wavelet analysis is a well-adapted tool to study data series with local structures or with sparse occurrence like hydrological quantities or physiological parameters. In our work instead of use the direct coefficient, we choose to examine the Wavelet Power Spectrum (WPS). WPS is defined as $2^j|W_{m,n}(f)|^2$, where j is the scale level. This technical choice provides easier graphical examination among hydrologic changes and physiological parameters. In the sequel the Morlet Wavelet Transform will be used (with the mother wavelet for the parameter k given by $\Psi_k(t) = \pi^{-\frac{1}{4}} e^{-ikt} e^{-\frac{|t^2|}{2}}$) and we selected the 95% confidence interval for wavelet power as significance criteria. The coherency and phase angle are evaluated to bear out the first analyses and complete the diagnoses.

2.3.6 Redundancy analysis (RDA)

Morphological parameters responding to environmental factors were also identified by redundancy analysis (RDA) using the software package R 3.0.2 (http://www.r-project.org). To analyze the influence of these environmental factors on morphological parameters of *A. granulata*, RDA was performed using the R add-on package 'vegan'. A forward selection of environmental factors was applied to avoid using collinear environmental factors in the same constrained ordination model. Only those parameters contributing significantly ($p < 0.05$ via 1000 times permutation tests) to morphological variations were added to the model.

3. Results

3.1 Scientific trends of phytoplankton research

At the country level, a majority of 27946 articles were published in the single-country category versus 11204 articles in the multi-country category. However, the linear positive ascending trend (around 20% increases) of publications in the multi-country category (Fig. 11) implied an increase of international collaborations for publications on phytoplankton research.

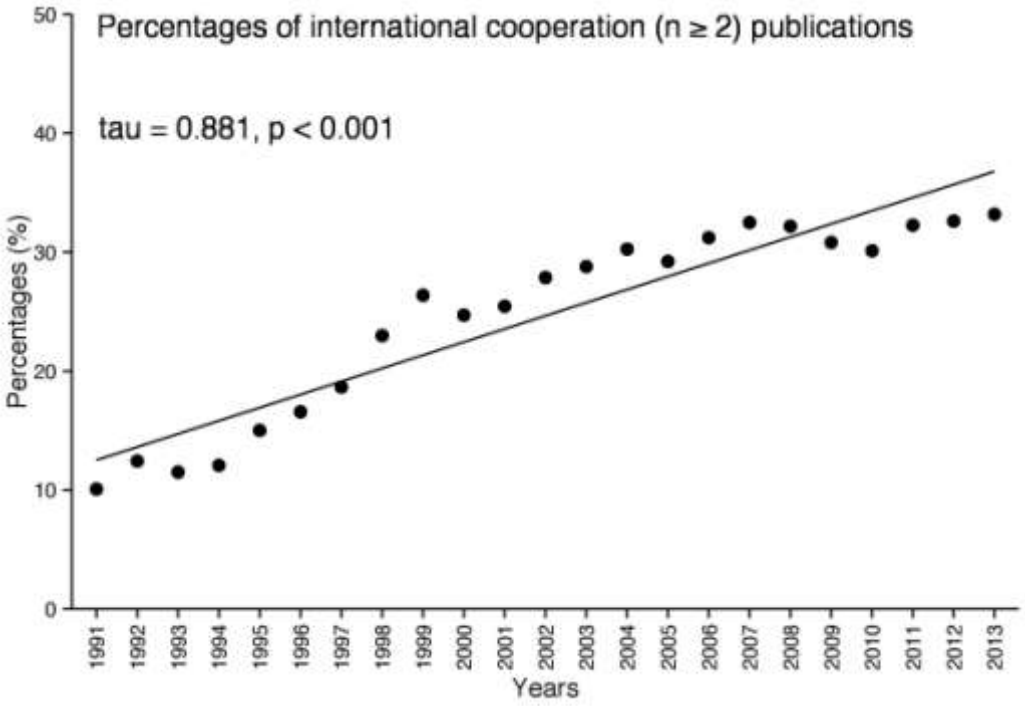

Figure 11 Temporal trend of percentages of phytoplankton articles based on cooperation between ≥ 2 countries in total phytoplankton articles.

The top 20 countries contributing most to phytoplankton publications and their collaboration relationships were visualized in Figure 12. The size of nodes stand for the specific country's degree of contributions and the thickness of links stand for the strength of correlation. In this study, The United States contributed most and took the central positions in the international collaboration network (Fig. 12). Britain, Germany, France and Canada were also principal collaborators and major productive

countries in the network. These countries showed stronger international collaborations than others. The strongest correlation was established between the USA and Canada.

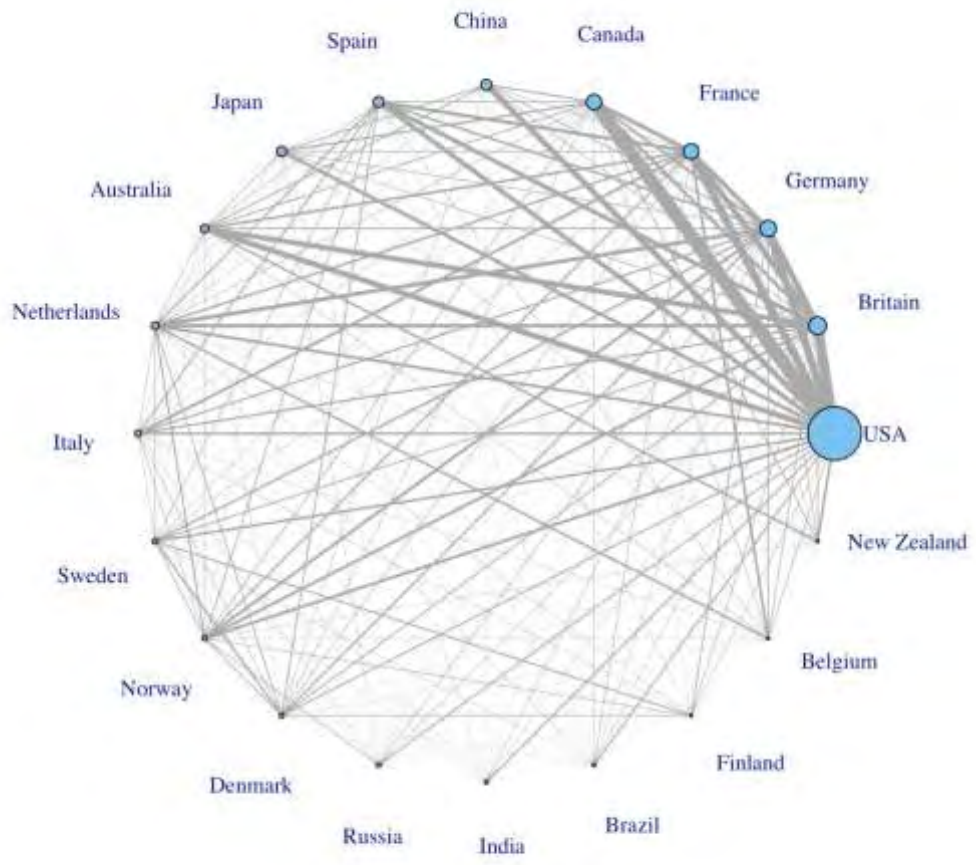

Figure 12 Top 20 countries for phytoplankton articles publications and cooperation correlations.

The top 50 keywords with ascending trend and their temporal trends are shown in Figure 13. All the above keywords could be classified into four categories: research regions, research methods, research contents and environments. The keywords belonging to research regions included “baltic sea”, “atlantic ocean”, “north atlantic oscillation”, “gulf of mexico”, “brazil”, “east China sea”, “arctic ocean”, “south China sea” and “shallow lake”. The keywords belonging to research methods included “stable isotope”, “remote sensing”, “algorithm”, “stoichiometric”, “seawif”, “ecosystem model”, “classification” and “in situ”. The keywords belonging to phytoplankton research contents included 26 words, and they could be further

classified into five sub-categories. The first sub-category was associated with bloom, including "phytoplankton bloom", "harm algal bloom", "algal bloom" and "cyanobacteria bloom". The second sub-category was associated with diversity, including "diversity", "biodiversity" and "species richness". The third sub-category was associated with temporal variations, including "interannual variable", "time series", "long term change" and "seasonal dynamics". The fourth sub-category was associated with ecosystem, including "marine ecosystem" and "aquatic ecosystem". The fifth sub-category was associated with other topics, including "sensitivity", "picophytoplankton", "trophic cascade", "community composition", "microcystin", "evolution", "*microcystis aeruginosa*", "submerged macrophyte", "regime shift" and "ocean acidification". The keywords belonging to environments included "climate change", "water quality", "phosphorus limit", "atmospheric corrosion", "sea surface temperature", "iron fertilization", "dissolved oxygen" and "hypoxia".

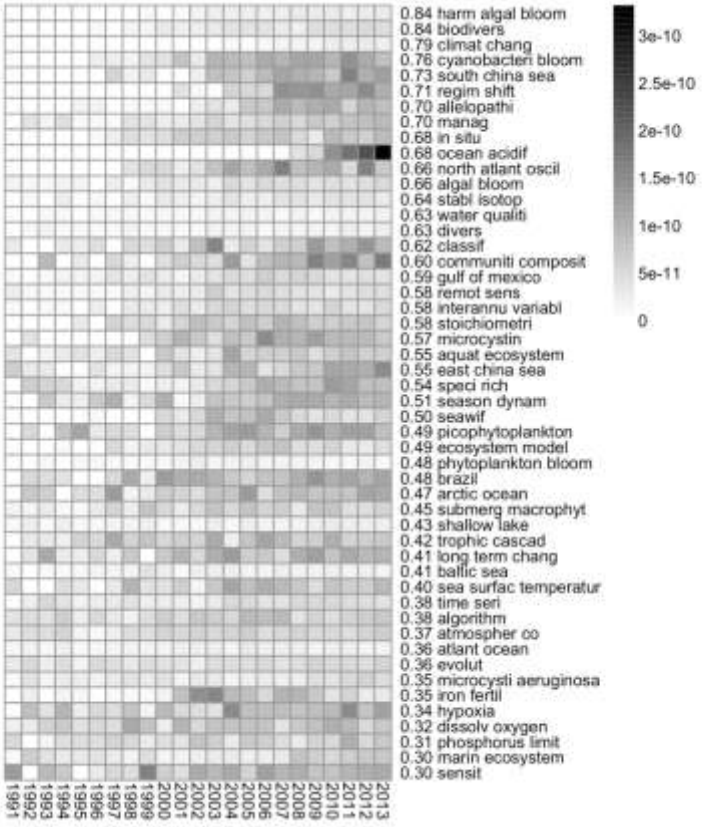

Figure 13 Top 50 key words with ascending trend in phytoplankton articles. The values of each keyword represent the ascending trend coefficient, and the scale at the right is the Mann-Kendal trend test result.

The top 50 keywords with descending trend and their temporal trends are shown in Figure 14. All the above keywords could also be classified into four categories: research regions, research methods, research contents and environments. The keywords belonging to research regions included “seawater”, “north atlantic”, “chesapeak bay”, “sargasso sea”, “north sea”, “marine”, “ocean”, “water”, “sediment”, “lake”, “sea”, “freshwater” and “estuarine”. The keywords belonging to research methods only included “model”. The keywords belonging to research contents included 29 words, and they could be further classified into five sub-categories. The first sub-category was associated with algae, including “alga”, “bacteria”, “plankton”, “diatom”, “chlorophyll”, “marine phytoplankton”, “spring bloom”, “bacterioplankton” and “microalga”. The second sub-category was associated with growth, including “growth”, “phytoplankton growth”, “growth rate” and “rate”. The third sub-category was associated with phytoplankton production, including “organic matter”, “production”, “primary production”, “carbon” and “dissolved organic carbon”. The fourth sub-category was associated with phytoplankton community, including “community”, “biomass”, “dynamic”, “pattern”, “abundance” and “population”. The fifth sub-category was associated with other topics, including “limit”, “fish”, “zooplankton”, “photosynthesis” and “ecosystem”. The keywords belonging to environments included “iron”, “nutrient limit”, “nutrient”, “phosphorus”, “nitrogen”, “temperature” and “light”.

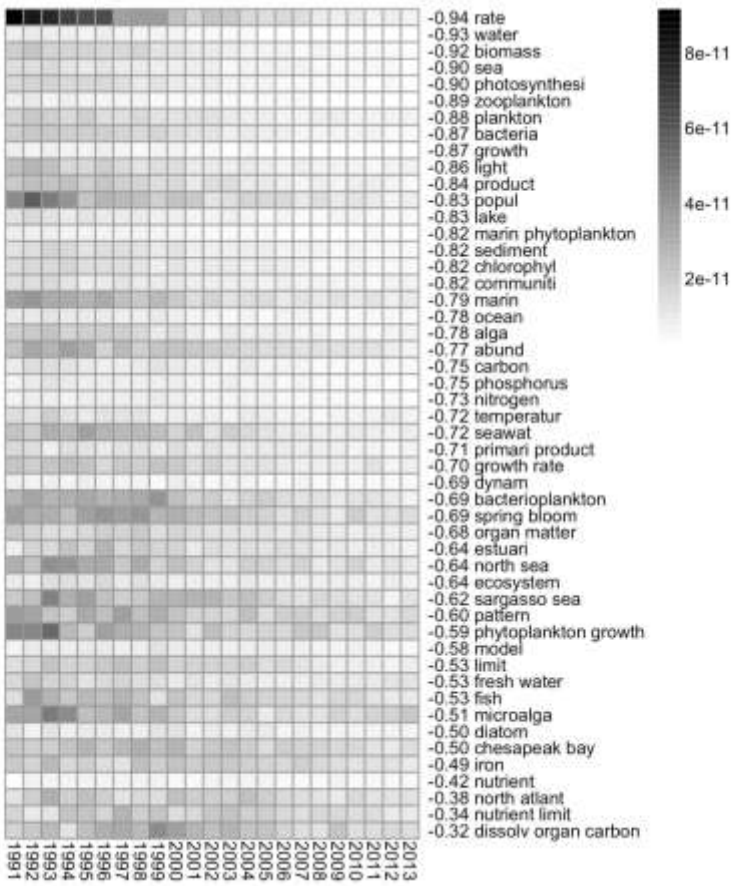

Figure 14 Top 50 key words with descending trend in phytoplankton articles. The values of each keyword represent the descending trend coefficient, and the scale at the right is the Mann-Kendal trend test result.

The top 20 high-frequency keywords and their correlations were visualized in Figure 15. The size of nodes stands for the proportion to the occurrence frequency. The lines depicted the connection relationship between two keywords and the thickness of links stands for the strength of correlation. In this study, “growth” had the highest occurrence frequency, and “water”, “zooplankton” and “marine phytoplankton” also had high occurrence frequency, but they did not form a strong correlation centre. The strongest correlation was established between the words “nitrogen” and “phosphorus”, and the correlations between other keywords were not so strong.

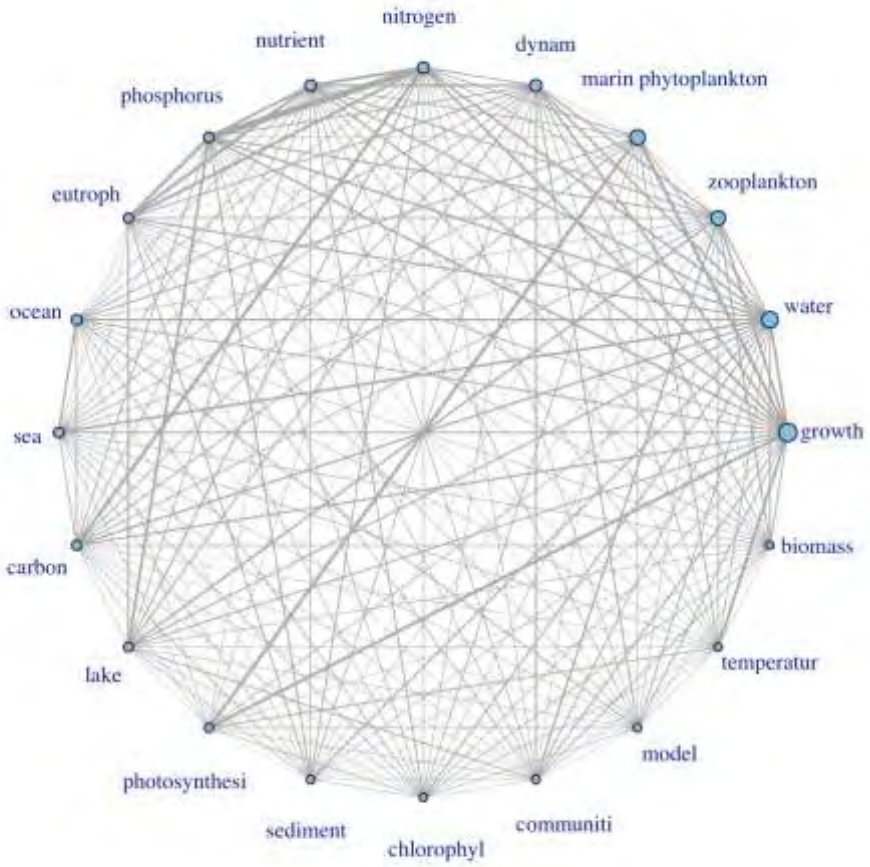

Figure 15 Top 20 key words in phytoplankton articles and correlations.

3.2 Temporal pattern of phytoplankton assemblages in the main stream

3.2.1 Environmental factors

Temporal variations of nine environmental factors are shown in Fig. 16. Water temperature increased continually from the beginning of the year and peaked on September 10th, and then decreased continually to the end of the year (Fig. 16a). The values ranged from 6.4 to 31.4 ℃, with a median value of 24.4 ℃. There was rain in all seasons except for winter (January and February). Precipitation was relatively low but frequent in summer (flood season) compared with other seasons, while heavy rain could occur occasionally in drought winters (Fig. 16b). In winter, discharge was very low, with values under 3000 m^3 s^{-1}. It increased gradually to floods (June to August) with values no less than 5000 m^3 s^{-1} (Fig. 16c). The concentration of phosphate fluctuated under 0.5 mg L^{-1} before November, but it increased dramatically after that and peaked on December 25th (Fig. 16d). The concentration of silicate fluctuated around 3.5 mg L^{-1} before May, and then increased continuously to the end of the year (Fig. 16e). The concentration of total nitrogen showed large fluctuations before May, but remained steadily around 1.70 mg L^{-1} after that period (Fig. 16f). The concentration of nitrate had a similar trend as total nitrogen before May, and then it showed a weak decreasing trend to the end of the year (Fig. 16g). The concentration of nitrite fluctuated dramatically during most times of the year except in May and June (Fig. 16h). The concentration of ammonia increased gradually from the beginning of the year and remained around 0.67 mg L^{-1} from mid March, with only four high values appearing on March 10th, June 30th, September 30th and December 30th, respectively (Fig. 16i).

Figure 16 Temporal variations in the environmental factors (a. water temperature; b. precipitation; c. discharge; d. phosphate; e. silicate; f. total nitrogen; g. nitrate; h. nitrite; i. ammonia).

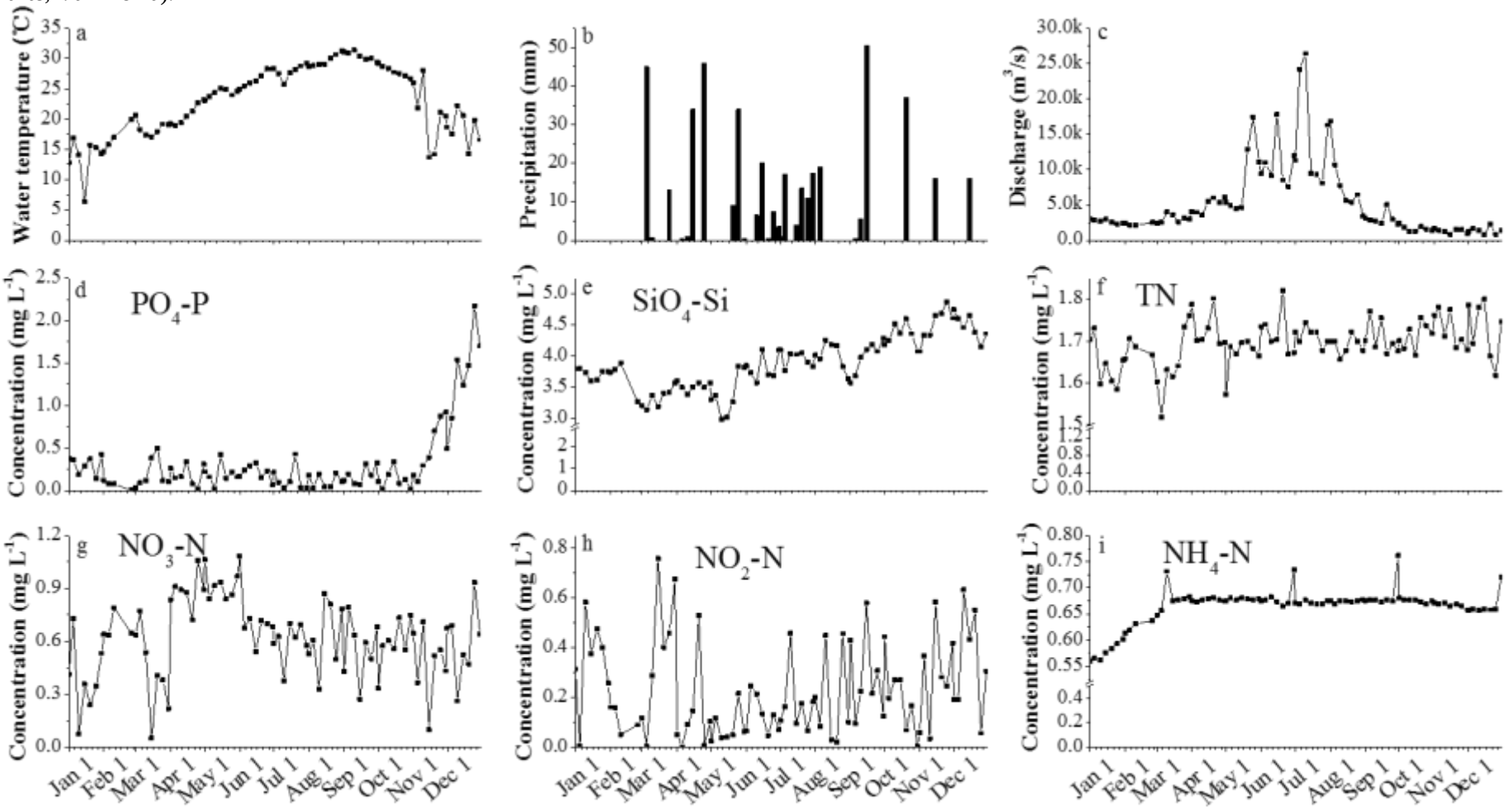

3.2.2 Phytoplankton composition

A total of 245 algal taxa (including varieties and forms) were identified. Seven phytoplankton phylum groups – Bacillariophyceae, Chlorophyceae, Euglenophyceae, Cyanobacteria, Dinophyceae, Chrysophyceae and Xanthophyceae – were represented. The highest richness was 104 taxa for Bacillariophyceae, contributing 42.4% of the total species numbers; the second was Chlorophyceae (85 taxa, 34.7%); third was 31 taxa for Euglenophyceae (12.7%); and the fourth was 18 taxa for Cyanobacteria (7.3%). Of the Bacillariophyceae, *Navicula* had the highest richness of 14 species, and the following were *Aulacoseira* (*Melosira*) (10 taxa), *Nitzschia* (9 taxa), *Cymbella* (8 taxa), *Synedra* (8 taxa). Of the Chlorophyceae, *Scenedesmus* had the highest richness with 17 species, and *Pediastrum* had 8 species. *Euglena* of the Euglenophyceae had 17 species.

Latin names and abbreviations of the 107 taxa whose occurrence rate was greater than 5% are listed in Table 1. We can see from Fig. 17 that a single species shows an apparently high proportion of the biomass (> 80%), and even the second rank species is lower than 5%, which means almost a 20-fold difference (Fig. 17a). The two species are *Aulacoseira granulata* var. *granulata* and *Melosira varians* respectively. According to occurrence frequency rank (Fig. 17b), four species are very common (occurrence rate > 70%), and one even beyond 80%. The sequence of the four species is *A. granulata* var. *granulata* > *M. varians* > *Closterium acutum* var. *variabile* > *Cyclotella meneghiniana*. Two other species were also common (occurrence rate between 50% and 70%): *Cyclotella comta* and *Desmodesmus armatus*. The other 13 species were moderately common (occurrence rate between 25% and 50%). Eighty-eight species were scarce (occurrence rate < 25%), and among them, thirty-eight species were very scarce (occurrence rate < 10%). Above all, *A. granulata* var. *granulata* is the single predominant species of the phytoplankton assemblages.

Table 1 List of 107 taxa with an occurrence rate over 5% in all samples

Group	Species name	Abbreviation	Occurrence rate (%)
Bacillariophyceae	*Amphora ovalis*	Amov	9.9
	Amphora sp.	Amsp	22.2
	Aulacoseira ambigua	Auam	19.8
	Aulacoseira distans	Audi	27.2
	Aulacoseira granulata var. *curvata*	Augc	12.3
	Aulacoseira granulata var. *granulata*	Augg	82.7
	Aulacoseira granulata var. *angustissima*	Auga	35.8
	Aulacoseira granulata var. *angustissima f. spiralis*	Augas	6.2
	Aulacoseira italica	Auit	13.6
	Bacillaria paxillifera	Bapa	23.5
	Belonastrum berolinensis	Bebe	30.9
	Caloneis sp.	Casp	23.5
	Carinasigma rectum	Care	14.8
	Cocconeis sp.	Cosp	18.5
	Craticula cuspidata	Crcu	8.6
	Cyclotella bodanica	Cybo	16
	Cyclotella comta	Cyco	63
	Cyclotella meneghiniana	Cyme	74.1
	Cymbella affinis	Cyaf	22.2
	Cymbella cistula	Cyci	9.9
	Cymbella sp.	Cysp	17.3
	Cymbella tumida	Cytu	12.3
	Fragilaria crotonensis	Frcr	7.4
	Fragilaria hinganensis	Frhi	11.1
	Fragilaria hinganensis var. *longissima*	Frhl	19.8
	Fragilaria sp.	Frsp	12.3
	Gomphonema sp.	Gosp	8.6
	Gyrosigma sp.	Gysp	14.8
	Halamphora coffeaeformis	Haco	8.6
	Hantzschia sp.	Hasp	7.4
	Licmophora abbreviata	Liab	46.9
	Melosira varians	Meva	75.3
	Navicula dicephala	Nadi	17.3
	Navicula lanceolata	Nala	11.1
	Navicula sp.	Nasp	44.4
	Navicula subminuscula	Nasu	21
	Navicula transitans	Natr	9.9
	Nitzschia acicularis	Niac	17.3
	Nitzschia lorenziana var. *subtilis*	Nils	9.9
	Nitzschia palea	Nipa	33.3
	Nitzschia panduriformis	Nipan	24.7
	Nitzschia sigmoidea	Nisi	6.2
	Pinnularia microstauron	Pimi	6.2
	Pleurosigma sp.	Plsp1	18.5
	Pseudostaurosira brevistriata	Psbr	6.2
	Surirella minuta	Sumi	16
	Surirella robusta	Suro	8.6
	Synedra sp.	Sysp	22.2
	Synedra ulna	Syul	30.9
	Tabellaria sp.	Tasp	7.4
	Tabularia fasciculata	Tafa	14.8

	Thalassiosira sp.	Thsp	24.7
	Ulnaria acus	Ulac	7.4
	Ulnaria contracta	Ulco	6.2
	Ulnaria delicatissima var. *angustissima*	Ulaa	12.3
Chlorophyceae	*Actinastrum hantzschii*	Acha	14.8
	Acutodesmus acuminatus	Acac	9.9
	Acutodesmus dimorphus	Acdi	25.9
	Ankyra ancora	Anan	14.8
	Chlamydocapsa planctonica	Chpl	7.4
	Closterium acutum var. *variabile*	Clav	75.3
	Closterium praelongum	Clpr	11.1
	Cosmarium sp.	Cosp1	6.2
	Crucigenia fenestrata	Crfe	18.5
	Crucigenia lauterbornei	Crla	9.9
	Desmodesmus armatus	Dear	71.6
	Desmodesmus denticulatus	Dede	12.3
	Desmodesmus perforatus	Depe	9.9
	Dictyosphaeria cavernosa	Dica	28.4
	Micractinium pusillum	Mipu	14.8
	Monactinus simplex	Mosi	11.1
	Monoraphidium arcuatum	Moar	12.3
	Monoraphidium griffithii	Mogr	18.5
	Monoraphidium komarkovae	Moko	12.3
	Monoraphidium mirabile	Momi	42
	Palmella mucosa	Pamu	9.9
	Pediastrum simplex var. *duodenarium*	Pesd	16
	Pediastrum tetras var. *tetraodon*	Pett	6.2
	Planktosphaeria sp.	Plsp	12.3
	Quadrigula chodatii	Quch	11.1
	Radiococcus planktonicus	Rapl	14.8
	Scenedesmus armatus var. *boglariensis f. bicaudatus*	Scabb	25.9
	Scenedesmus biguga	Scbi	11.1
	Scenedesmus communis	Scco	18.5
	Schroederia nitzschioides	Scni	19.8
	Sphaerocystis schroeteri	Spsc	9.9
	Staurastrum gracile	Stgr	6.2
	Westella botryoides	Webo	8.6
Cyanobacteria	*Aphanocapsa sp.*	Apsp	6.2
	Arthrospira platensis	Arpl	9.9
	Merismopedia glauca	Megl	6.2
	Merismopedia tenuissima	Mete	12.3
	Microcystis sp.	Misp	8.6
	Oscillatoria fraca	Osfr	29.6
	Oscillatoria limosa	Osli	9.9
	Oscillatoria subbrevis	Ossu	30.9
	Phormidium chlorinum	Phch	16
	Raphidiopsis curvata	Racu	8.6
Euglenophyceae	*Euglena cylindrica*	Eucy	11.1
	Euglena gracilis	Eugr	6.2
	Euglena mutabilis	Eumu	8.6
	Euglena sp.	Eusp	11.1
	Lepocinclis acus	Leac	6.2
	Phacus circulatus	Phci	6.2
	Trachelomonas sp.	Trsp	22.2

Dinophyceae	*Peridinium umbonatum*	Peum	6.2
	Peridinium sp.	Pesp	14.8

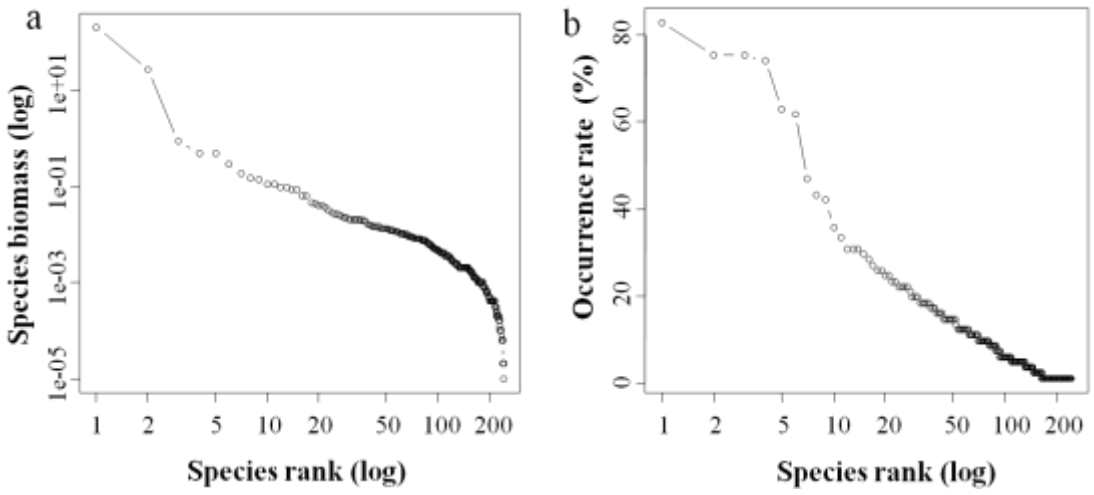

Figure 17 The rank of biomass and occurrence rate for all phytoplankton species (a. biomass; b. occurrence rate).

3.2.3 The species assemblage analysis

The samples in terms of 81 sampling days were projected onto the 10 × 9 SOM map cells according to the similarity of their species composition (Fig. 18b). Based on the phytoplankton composition and similarity of different cells, two clusters of communities, I and II, were primarily identified. The cluster II was then subdivided into two smaller sub-clusters, IIa and IIb (IIb was further subdivided into two sub-clusters IIb1 and IIb2) (Fig. 18a). In all, four clusters were defined on the SOM. No further subdivisions were considered in the present study. The cophenetic correlation coefficient (r = 0.81) indicated that the hierarchical clustering of different cells was stable. Cluster IIb2 had the highest with 43 samples, which covered all the 12 months of the year, and most samples of this cluster belonged to the cold season. For example, all the samples from January to March could be found there. Cluster IIa had the second highest with 21 samples, which covered all the months from April to December but June. The last four months contributed more than half of the total. Cluster IIb1 had 13 samples, which covered all the months from June to September, and most samples of June and July contributed to this cluster. Cluster I was the lowest with 4 samples, with continual time series from August 20th to September 1st.

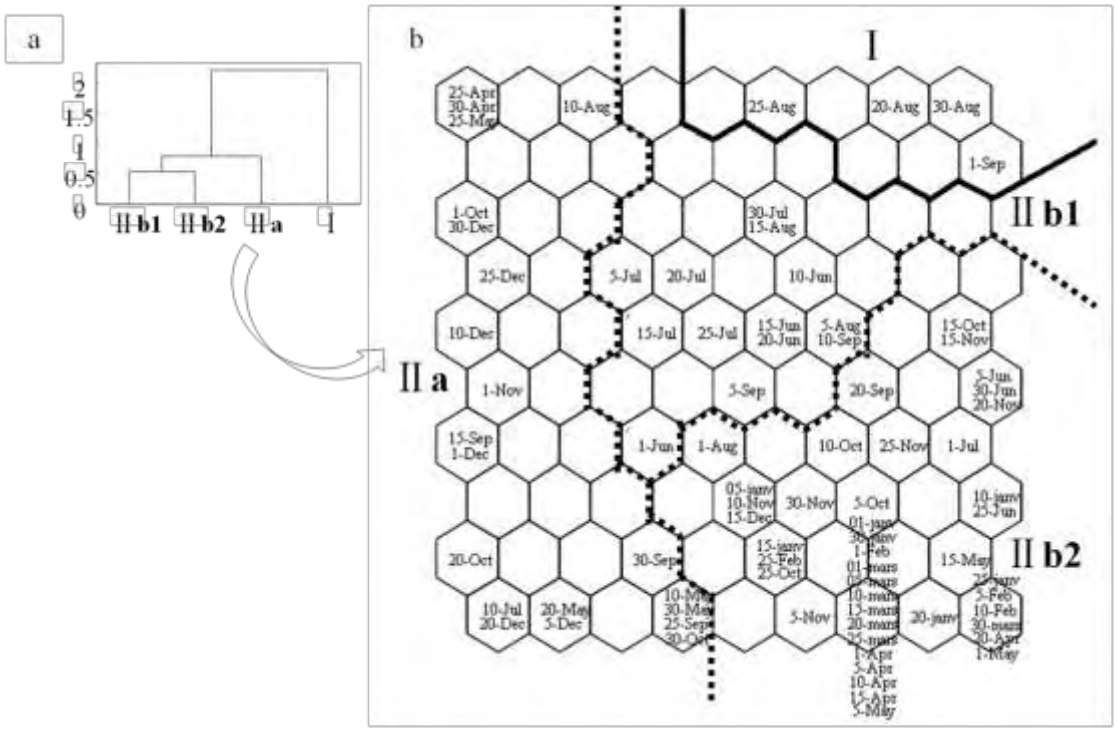

Figure 18 Relationship between each cluster and distribution of the sampling days on the SOM (The similarity of neighboring cells can be grouped in clusters (bold line) and sub-clusters (dashed line) using a U-matrix algorithm).

Box-plots of phytoplankton species richness and biomass with the percentage of different groups of each cluster are shown in Fig. 19: the values varied and differed significantly among clusters (the Kruskall-Wallis test, $p < 0.001$). Cluster I showed the maximum median values among all clusters in both species richness and biomass. The other three clusters had very close median values in biomass, but they had obvious different median values in species richness. Cluster IIb2 showed the minimum median values in both species richness and biomass (Fig. 19a1, b1).

The most significant feature for the percentage of different groups in each cluster was that diatoms contributed the most in terms of both species richness and biomass. However, green algae, the second contributor, showed an obvious difference in species richness and biomass composition. They contributed more in species richness, and the percentages in cluster I and IIb1 were obviously higher than that in the other two clusters (Fig. 19a2, b2).

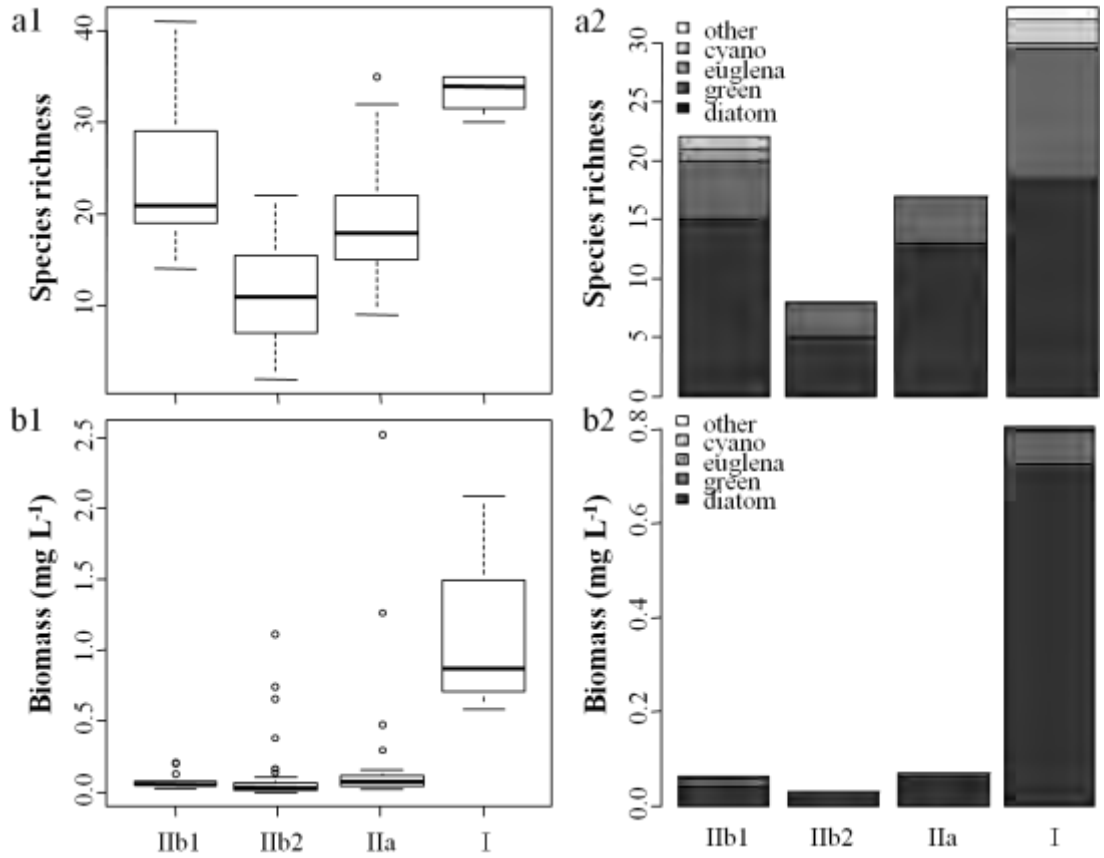

Figure 19 Box plot of phytoplankton species richness and biomass of each cluster (a1. species richness; a2. percentage of different groups to species richness in terms of median values; b1. biomass; b2. percentage of different groups to biomass in terms of median values).

Fig. 20 showed the occurrence probability of individual species in each cluster, and the results show apparent differences among clusters. Cluster I was most diverse in contributing species with relatively higher occurrence probabilities in terms of median values. The occurrence probabilities of most taxa in this cluster were below 20%. The median values of nine taxa, of which seven were diatoms (including four tychoplankton and three euplankton), varied in the range of 40-60%. Another group of nineteen taxa, mainly composed of diatoms (including five tychoplankton and three euplankton) and green algae (all nine taxa were euplankton), were in the range of 20-40%. The other three clusters had apparently low occurrence probabilities in contributing species, and the median values of most species were below 20%. The three highest probable occurrence diatoms (*Navicula dicephala*，*Caloneis sp.* and *Cocconeis sp.*) of cluster IIa were in the range of 20-40%, and they all belonged to tychoplankton. In cluster IIb1, the median value of *Amphora sp.* was greater than 40%, while the other three species: *F. hinganensis* var. *longissima*, *Navicula sp.* and *Oscillatoria subbrevis*, were in the range of 20-40% with all these taxa belonging to

tychoplankton. In cluster IIb2, the median values of all species were below 20%, and only *Aulacoseira distans* and *Navicula sp.* were a little higher than the others.

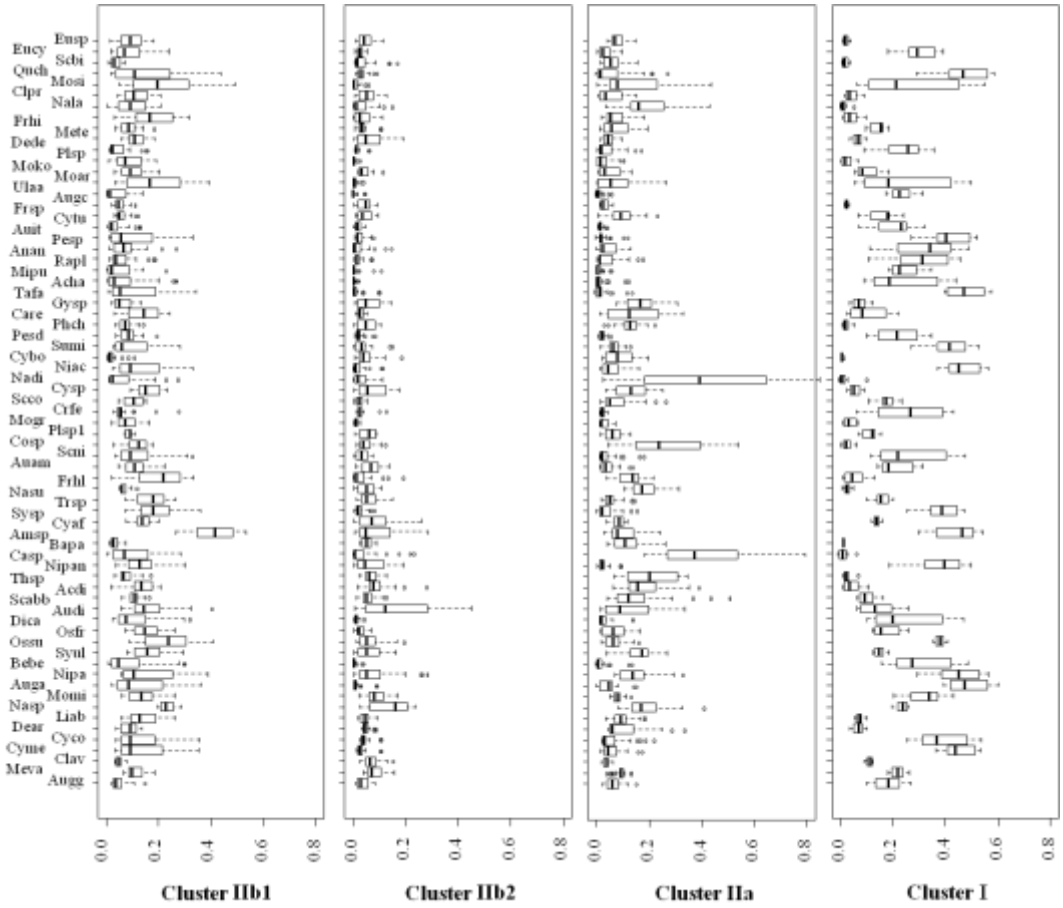

Figure 20 Box-plots showing the occurrence probability (%) of each species (see full-names in Table 1) in each of four clusters. Values were obtained from the weight of virtual vectors of the trained SOM.

Based on both IndVal (indicator value > 25) and SOM code book values, i.e. the high occurrence probability in each SOM cluster, a total of 29 indicator species were determined in different hierarchical levels (Table 2). The number of indicator species composition varied significantly among clusters, and increased along the sequence IIb2, IIb1, IIa and I (0, 2, 3 and 24, respectively). The indicator species of cluster I had significantly higher IndVal and occurrence probabilities than those of cluster IIa and IIb1, which suggested that the second dichotomy (cluster I) had a strong ecological significance. Indicator species were found with a low occurrence frequency, especially those that had extremely high indicator values.

Cluster I contained the most diverse indicator species, including twelve diatoms, of which five were euplankton and seven were tychoplankton; nine green algae, of which eight were euplankton and one was tychoplankton; one tychoplanktonic

cyanobacteria, one euplanktonic *Euglena* and one euplanktonic dinoflagellate. Three diatoms (*M. varians*, *C. meneghiniana* and *C. comta*), which had an apparently high occurrence frequency (> 60%) in the whole year, were also good indicator species of this cluster. The indicator species cluster IIa was composed of three diatoms, and the indicator sequence in importance was *Caloneis sp.*, *Navicula dicephala* and *Cocconeis sp.*, and all of them were tychoplankton. The indicator species of cluster IIb1 included two tychoplanktonic diatoms: *Amphora sp.* and *Fragilaria hinganensis* var. *longissima*, and both were pennate diatoms. The cluster IIb2 had no indicator species.

Table 2 Indicators of each cluster based on IndVal (indicator value) and SOM (occurrence probability in each cluster, see Fig. 20). Only species that are significant in both criteria should be accepted. X means significant, Y means accepted.

Cluster	Indicator species	Indicator value (%)	IndVal	SOM	Indicator
I	Augc	99	X	X	Y
	Mipu	98	X	X	Y
	Acha	97	X		
	Tafa	96	X	X	Y
	Bebe	94	X	X	Y
	Auga	89	X	X	Y
	Niac	85	X	X	Y
	Sumi	83	X	X	Y
	Cyme	82	X	X	Y
	Cyco	78	X	X	Y
	Nipan	74	X	X	Y
	Augg	70	X		
	Pesp	68	X	X	Y
	Scse	65	X	X	Y
	Crfe	63	X	X	Y
	Pesd	59	X	X	Y
	Quch	58	X	X	Y
	Dica	58	X		
	Ossu	57	X	X	Y
	Momi	56	X	X	Y
	Sysp	54	X	X	Y
	Meva	54	X	X	Y
	Nipa	48	X	X	Y
	Rapl	43	X	X	Y
	Plsp	42	X	X	Y
	Eucy	41	X	X	Y
	Anan	36	X	X	Y
	Osfr	33	X		
IIa	Casp	62	X	X	Y
	Nadi	54	X	X	Y
	Cosp	32	X	X	Y
IIb1	Frhl	51	X	X	Y
	Moko	45	X		
	Amsp	42	X	X	Y
	Trsp	34	X		
	Frhi	29	X		

3.2.4 The prediction of phytoplankton assemblages from environmental factors

The most influential factors predicting the four clusters I, IIa, IIb1 and IIb2 (Fig. 21) were identified by discriminant function analysis and principal component analysis. Three discriminant functions were generated and the random Monte Carlo permutation test showed that they were highly significant ($p < 0.001$). These axes (F1, F2 and F3) accounted for 59, 22 and 18% of the between-cluster variability, respectively. All the four community clusters overlapped each other to some extent, and cluster IIa overlapped more with three other clusters. Since F2 and F3 contributed approximately equal proportions to the results, two dimensional figures based on F1 × F2 and F1 × F3, were shown respectively, with a corresponding distribution of water quality parameters. In this respect, the correlations could be exhibited adequately.

The nine environmental factors used were able to predict the community clusters and types of phytoplankton species assemblage patterns (i.e. global score of prediction) at 64.2% accuracy, and the prediction success rate for clusters I, IIa, IIb1 and IIb2 were 50, 48, 62 and 74%, respectively.

Cluster IIb1 and IIb2 were ordered along the first axis F1 (i.e. horizontal axis) of the analysis based on both F1 × F2 (Fig. 21a1, a2) and F1 × F3 (Fig. 21b1, b2) figures, and the gradients of water temperature, discharge and precipitation were loaded along this axis and were important controlling variables. Meanwhile, phosphate was along the second axis F2 (i.e. vertical axis) and was an important controlling variable to cluster IIa, based on the F1 × F3 figure. Cluster I was ordered between the horizontal and vertical axes (Fig. 21a1, b1) and its linkage with environmental variables was unclear (Fig. 21a2, b2).

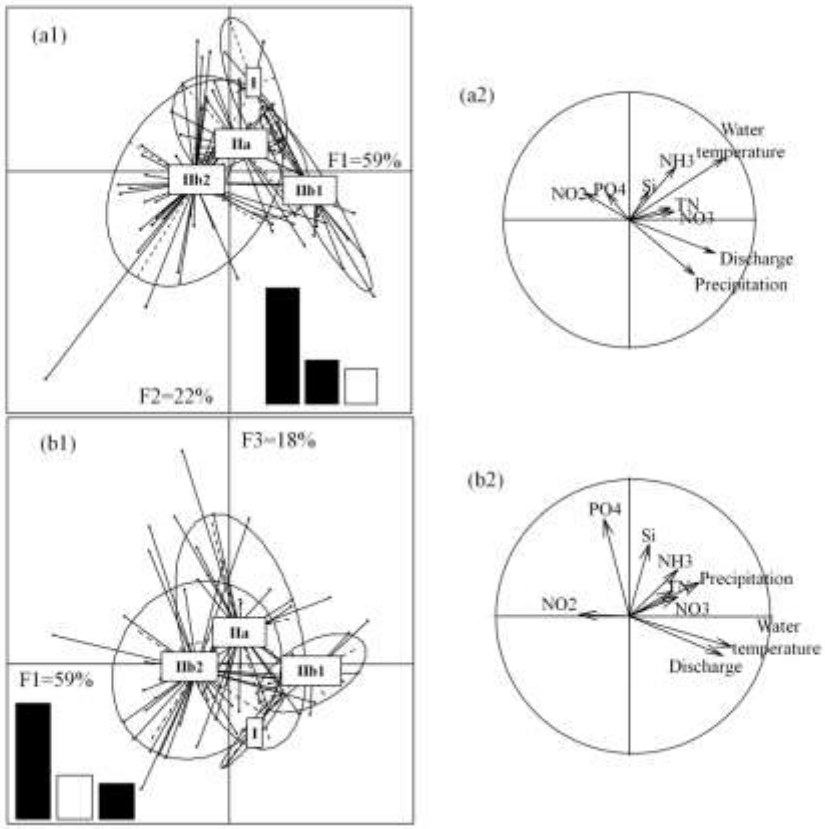

Figure 21 Results from the LDA analysis showing: (a1) the distribution and overlap of clusters in F1 and F2 dimensions; (a2) the distribution of water quality parameters corresponding to F1 and F2; (b1) the distribution and overlap of clusters in F1 and F3 dimensions; (b2) the distribution of water quality parameters corresponding to F1 and F3. The three bar plots in a1 represent F1, F2 and F3 in sequence.

3.3 Spatial-temporal pattern of phytoplankton assemblages in the river delta system

3.3.1 Environmental factors

Means (± SD) of main environmental factors at all sites were listed in table 3. Among all sampling sites, the two sites (ZJQ and LHS) nearing Guangzhou were apparently different from others. These two sites had apparently higher values of water temperature, salinity and nutrients, but apparently lower values of transparency and DO. Moreover, pH values of them were also lower than other sites.

Table 3 Means (±SD) of main environmental factors at all sites in the river network of PRD

Station	Longitude and latitude	Water temperature (℃)	Salinity	pH	Transparency (cm)	Dissolved oxygen (mg/L)	Total nitrogen (mg/L)	Total phosphate (mg/L)	Silicate (mg/L)
QQ	112°47'11.0"E 23°10'14.5"N	20.7 ±6.9	0.15 ±0.07	7.89 ±0.52	55 ±21	6.3 ±1.4	3.06 ±0.64	0.18 ±0.02	3.39 ±0.41
ZT	113°03'26.0"E 22°48'46.6"N	22.1 ±8.1	0.14 ±0.06	7.88 ±0.52	56 ±31	7.5 ±1.6	3.74 ±2.56	0.13 ±0.03	3.85 ±0.41
WH	113°09'20.3"E 22°36'14.5"N	22.2 ±8.5	0.14 ±0.07	7.92 ±0.35	44 ±20	8.0 ±1.4	2.43 ±0.14	0.15 ±0.05	3.91 ±0.33
XW	113°16'41.5"E 22°22'45.6"N	21.4 ±7.0	0.15 ±0.07	7.92 ±0.38	53 ±14	7.4 ±1.9	3.69 ±2.39	0.20 ±0.09	3.95 ±0.51
XL	113°17'17.9"E 22°38'13.8"N	21.6 ±7.7	0.14 ±0.06	7.83 ±0.23	54 ±21	7.3 ±2.0	2.54 ±0.51	0.12 ±0.03	3.78 ±0.36
XT	112°57'51.1"E 23°05'27.4"N	21.3 ±8.1	0.12 ±0.06	7.87 ±0.43	43 ±30	6.9 ±1.0	3.09 ±0.77	0.19 ±0.10	4.20 ±0.24
BJ	113°11'54.5"E 22°54'04.1"N	21.4 ±7.9	0.13 ±0.06	7.75 ±0.51	46 ±27	7.1 ±2.1	4.69 ±3.32	0.15 ±0.05	4.29 ±0.71
LH	113°19'53.4"E 22°49'15.2"N	21.5 ±7.5	0.13 ±0.07	7.88 ±0.40	46 ±25	6.8 ±1.4	2.82 ±0.46	0.15 ±0.06	4.67 ±0.55
HL	113°29'02.2"E 22°44'05.4"N	21.5 ±6.9	0.14 ±0.09	7.70 ±0.27	48 ±17	6.9 ±1.7	3.18 ±0.18	0.16 ±0.06	3.54 ±0.40
CC	113°14'55.7"E 22°58'15.1"N	21.4 ±8.6	0.13 ±0.07	7.84 ±0.47	48 ±30	6.0 ±1.1	2.76 ±0.45	0.16 ±0.05	5.02 ±1.57
ZJQ	113°13'16.5"E 23°08'12.6"N	22.8 ±8.6	0.31 ±0.20	7.49 ±0.44	28 ±6	1.0 ±0.4	7.06 ±0.49	0.56 ±0.17	5.63 ±1.21
LHS	113°30'37.0"E 23°00'58.0"N	24.3 ±8.0	1.53 ±2.55	7.51 ±0.30	25 ±4	4.2 ±1.2	4.58 ±1.04	0.28 ±0.07	5.04 ±0.86
SQ	113°24'49.0"E 22°55'24.2"N	22.3 ±8.0	0.16 ±0.12	7.95 ±0.44	44 ±8	5.6 ±0.8	3.00 ±0.70	0.21 ±0.06	4.44 ±0.38
All dates and sites		21.9 ±6.9	0.26 ±0.73	7.80 ±0.39	45 ±21	6.2 ±2.2	3.59 ±1.75	0.20 ±0.13	4.29 ±0.89

3.3.2 Phytoplankton composition

A total of 383 algal taxa (including varieties and forms) were identified, of them seven phyla – Bacillariophyceae, Chlorophyceae, Euglenophyceae, Cyanobacteria, Dinophyceae, Chrysophyceae and Cryptophyceae – were represented. The highest richness was 160 taxa for Bacillariophyceae, contributing 41.8% of the total species numbers; and the second was Chlorophyceae (112 taxa, 29.2%); third was 84 taxa for Euglenophyceae (21.9%); and the fourth was 20 taxa for Cyanobacteria (5.2%). Of the Bacillariophyceae, *Navicula* had the highest richness of 19 species, and the following were *Gomphonema* (15 taxa), *Aulacoseira* (*Melosira*) (14 taxa), *Nitzschia* (12 taxa), *Cymbella* (12 taxa), *Synedra* (8 taxa). Of the Chlorophyceae, *Scenedesmus* had the highest richness with 24 species, and *Pediastrum* and *Crucigenia* had 8 and 7 species respectively. *Euglena* of the Euglenophyceae had 29 species.

Scientific names and abbreviations of the 123 taxa whose occurrence rate is greater than 10% are listed in Table 4, with corresponding tolerance range (+ median value) of important factors for each species. The species rank of biomass and occurrence rate for all phytoplankton species is shown in Fig. 22. According to biomass rank (Fig. 22a), one species (*Aulacoseira granulata* var. *granulata*) shows an apparently high biomass, contributing 51.7% to total assemblages. The following secondary level contains three species, i.e. *Amphiprora alata*, *Cyclotella meneghiniana* and *Dictyosphaeria cavernosa*, which contributes 7.5%, 6.8% and 5.5% to total assemblages respectively. This means that the first and second ranking levels keep 7 to 10-fold difference. According to occurrence rate rank (Fig. 22b), three species are extremely common (occurrence rate > 90%), and the sequence of them is *A. granulata* var. *granulata* (98%) > *C. meneghiniana* (96%) > *Scenedesmus armatus* (94%). Five other species are very common (occurrence rate between 70% and 90%), and the sequence is *Scenedesmus dimorphus* (83%) > *S. armatus* var. *boglariensis f. bicaudatus* (79%) > *Nitzschia palea* (73%) = *Synedra acus* (73%) = *Synedra berolinensis* (73%). There are still other 14 species are common (occurrence rate between 50% and 70%), and 45 species are moderately common (occurrence rate between 25% and 50%). Most species are very scarce (occurrence rate < 10%), with proportion of 67.9% in total species number. Based on biomass and occurrence rank, *A. granulata* and *C. meneghiniana* are the most important species of phytoplankton assemblages in the studied area.

Table 4 List of 123 taxa whose occurrence rate over 10% in all samples, and corresponding tolerance range (+ median value) of environmental factors: WT (℃), TN (mg/L), TP (mg/L), Si (mg/L).

Group	Species name	Abbreviation	Occurrence rate (%)	WT	TN	TP	Si
Bacillariophyceae	*Acanthoceras zachariasii*	Acza	12	15.9 - 30.5 (29.6)	2.12 - 3.37 (2.78)	0.11 - 0.29 (0.24)	3.55 - 4.88 (4.54)
	Amphora ovalis	Aovs	21	13.3 - 29.9 (14.2)	2.31 - 6.42 (3.44)	0.12 - 0.47 (0.15)	2.92 - 5.32 (4.17)
	A. ovalis var. *gracilis*	Agrs	13	13.5 - 14.2 (14.0)	2.31 - 4.07 (2.99)	0.12 - 0.15 (0.12)	3.15 - 7.28 (3.54)
	Asterionella formosa	Afoa	13	13.5 - 28.1 (14.5)	2.21 - 7.58 (3.28)	0.10 - 0.23 (0.12)	3.15 - 5.66 (3.95)
	Aulacoseira distans	Adis	29	13.3 - 18.3 (14.2)	2.31 - 7.58 (3.44)	0.10 - 0.82 (0.15)	2.92 - 7.28 (4.42)
	A. distans var. *alpigena*	Aala	38	14.1 - 32.0 (17.0)	2.37 - 7.58 (2.96)	0.09 - 0.49 (0.19)	3.38 - 6.04 (4.53)
	A. granulata var. *angustissima*	Aana	69	13.5 - 32.0 (26.5)	2.12 - 9.64 (3.15)	0.10 - 0.82 (0.17)	3.38 - 7.28 (4.17)
	A. granulata var. *angustissima f. spiralis*	Asps	13	13.5 - 29.6 (15.8)	2.60 - 7.58 (3.37)	0.11 - 0.82 (0.24)	3.38 - 7.14 (4.24)
	A. granulata var. *curvata*	Acua	50	13.3 - 32.0 (27.4)	2.12 - 7.58 (3.37)	0.10 - 0.82 (0.22)	2.92 - 7.14 (4.42)
	A. granulata var. *granulata*	Agra	98	13.3 - 32.0 (23.4)	1.99 - 9.64 (2.96)	0.09 - 0.82 (0.16)	2.92 - 7.28 (4.15)
	A. islandica	Aisa	12	13.9 - 14.3 (14.1)	2.31 - 4.07 (2.59)	0.10 - 0.15 (0.12)	3.15 - 5.32 (3.54)
	A. italica f. curvata	Acur	23	13.5 - 29.8 (14.2)	2.31 - 7.27 (2.99)	0.10 - 0.82 (0.12)	3.15 - 7.28 (4.17)
	A. italica	Aita	35	13.9 - 29.7 (15.8)	2.21 - 9.64 (2.90)	0.10 - 0.82 (0.14)	3.15 - 7.28 (4.17)
	A. italica var. *tenuissima*	Aten	69	13.5 - 32.0 (17.0)	1.99 - 7.58 (2.90)	0.09 - 0.49 (0.15)	3.15 - 7.28 (4.17)
	Bacillaria paxillifera	Bapa	31	13.3 - 29.4	1.99 - 5.23	0.10 - 0.23	2.92 - 7.28

				(14.3)	(2.83)	(0.13)	(4.28)
	Belonastrum berolinensis	Bebe	73	13.5 - 32.0 (18.3)	2.12 - 7.58 (2.99)	0.09 - 0.82 (0.17)	3.15 - 7.14 (4.28)
	Caloneis macedonica	Cmaa	12	13.3 - 29.8 (23.4)	2.23 - 4.02 (2.99)	0.12 - 0.35 (0.14)	2.92 - 5.32 (3.54)
	Carinasigma rectum	Care	12	14.1 - 32.0 (15.9)	2.12 - 3.49 (2.99)	0.09 - 0.38 (0.12)	3.65 - 5.32 (4.44)
	Cocconeis sp.	Cocs	33	13.5 - 29.4 (16.3)	1.99 - 9.64 (2.60)	0.10 - 0.19 (0.12)	3.15 - 5.32 (3.95)
	Craticula cuspidata	Crcu	19	13.5 - 29.9 (26.6)	2.21 - 7.58 (2.48)	0.10 - 0.35 (0.13)	3.40 - 4.53 (3.65)
	Cyclotella comta	Ccoa	65	13.3 - 32.0 (23.4)	1.99 - 7.58 (3.14)	0.09 - 0.82 (0.18)	2.92 - 7.28 (4.24)
	C. meneghiniana	Cmea	96	13.3 - 32.0 (23.4)	1.99 - 9.64 (2.94)	0.09 - 0.82 (0.16)	2.92 - 7.28 (4.21)
	Cylindrotheca closterium	Cycl	33	14.5 - 32.0 (29.0)	2.36 - 7.58 (3.15)	0.11 - 0.47 (0.23)	3.38 - 6.04 (4.42)
	Cymbella affinis	Cafs	27	13.5 - 29.9 (14.2)	2.31 - 7.27 (2.94)	0.10 - 0.82 (0.13)	3.15 - 7.28 (4.09)
	C. tumida	Ctua	29	13.9 - 29.9 (14.9)	2.21 - 4.07 (2.64)	0.10 - 0.18 (0.13)	3.15 - 7.28 (4.09)
	Fragilaria hinganensis var. *longissima*	Floa	12	13.9 - 29.8 (14.2)	2.59 - 4.07 (2.99)	0.12 - 0.35 (0.13)	3.53 - 5.32 (4.53)
	Gomphonema augur	Gaur	27	13.9 - 29.9 (26.5)	2.21 - 9.64 (2.59)	0.09 - 0.32 (0.16)	3.53 - 7.28 (4.06)
	G. subclavatum	Gsum	12	15.4 - 29.7 (28.6)	2.48 - 3.36 (2.96)	0.10 - 0.25 (0.22)	3.38 - 4.92 (4.28)
	Hantzschia amphioxys	Hams	12	13.5 - 16.6 (14.0)	2.90 - 5.23 (3.49)	0.12 - 0.23 (0.15)	3.15 - 7.28 (4.44)
	H. sp.	Hasp	12	14.9 - 29.0 (16.6)	2.36 - 7.26 (2.94)	0.10 - 0.23 (0.17)	3.56 - 4.92 (4.86)
	Licmophora abbreviata	Laba	27	13.3 - 29.7 (14.2)	2.31 - 4.07 (2.73)	0.10 - 0.22 (0.12)	2.92 - 7.28 (3.65)

	Melosira juergensii var. bothnica	Mboa	17	13.9 - 29.6 (14.9)	2.31 - 4.07 (2.81)	0.09 - 0.24 (0.13)	3.15 - 4.92 (4.15)
	M. varians	Mvas	56	13.3 - 32.0 (15.8)	2.21 - 7.58 (3.15)	0.09 - 0.82 (0.18)	2.92 - 7.28 (4.28)
	Navicula dicephala	Ndic	46	13.3 - 32.0 (16.6)	2.21 - 9.64 (2.90)	0.10 - 0.38 (0.15)	2.92 - 7.28 (4.08)
	N. lanceolata	Nlaa	27	14.0 - 29.9 (16.6)	2.21 - 7.26 (2.62)	0.10 - 0.47 (0.13)	3.15 - 4.92 (3.95)
	N. subminuscula	Nsua	37	13.5 - 30.3 (25.9)	2.23 - 9.64 (2.94)	0.11 - 0.47 (0.15)	3.38 - 4.57 (4.08)
	N. transitans	Ntrs	12	13.3 - 27.7 (14.3)	2.31 - 4.02 (2.59)	0.12 - 0.32 (0.18)	2.92 - 4.44 (3.93)
	Nitzschia acicularis	Nacs	12	15.1 - 29.9 (28.6)	2.50 - 7.58 (5.23)	0.18 - 0.47 (0.35)	3.38 - 6.04 (4.53)
	N. lorenziana	Nloa	25	13.9 - 30.2 (16.3)	2.12 - 4.07 (2.96)	0.09 - 0.35 (0.14)	3.15 - 7.28 (4.28)
	N. palea	Npaa	73	13.3 - 32.0 (17.0)	2.23 - 9.64 (3.06)	0.10 - 0.82 (0.16)	2.92 - 7.28 (4.35)
	Pinnularia sp.	Pisp	12	13.9 - 25.9 (14.3)	2.31 - 7.58 (3.49)	0.12 - 0.47 (0.15)	3.54 - 7.28 (4.44)
	Psammodictyon panduriforme	Pspa	21	15.9 - 32.0 (27.4)	2.12 - 5.26 (3.10)	0.09 - 0.38 (0.22)	3.63 - 5.86 (4.35)
	Stephanodiscus sp.	Stsp	48	13.5 - 32.0 (15.9)	2.31 - 7.58 (2.96)	0.10 - 0.82 (0.13)	3.15 - 7.28 (4.21)
	Synedra ulna	Sula	19	13.9 - 30.5 (28.3)	1.99 - 7.26 (3.15)	0.10 - 0.47 (0.23)	3.56 - 5.66 (4.48)
	Tabellaria sp.	Tasp	15	15.4 - 29.9 (26.6)	2.21 - 7.26 (2.50)	0.12 - 0.23 (0.14)	3.56 - 5.86 (3.63)
	Tabularia fasciculata	Tafa	54	14.0 - 32.0 (26.5)	2.12 - 9.64 (3.10)	0.09 - 0.82 (0.18)	3.15 - 7.14 (4.32)
	Ulnaria acus	Ulac	73	13.5 - 32.0 (25.9)	2.12 - 9.64 (2.99)	0.10 - 0.82 (0.16)	3.38 - 7.14 (4.15)
	U. contracta	Ulco	15	13.5 - 29.8	2.52 - 7.58	0.10 - 0.35	3.15 - 5.32

				(15.4)	(3.36)	(0.13)	(4.17)
	Urosolenia sp.	Ursp	13	14.9 - 32.0 (29.8)	2.12 - 6.97 (3.15)	0.12 - 0.49 (0.24)	3.65 - 4.85 (4.53)
Chlorophyceae	*Actinastrum hantzschii*	Ahai	48	14.0 - 32.0 (28.1)	2.12 - 9.64 (3.18)	0.10 - 0.82 (0.19)	3.15 - 7.14 (4.24)
	Acutodesmus acuminatus	Acac	42	14.3 - 32.0 (25.7)	2.12 - 7.58 (2.94)	0.09 - 0.49 (0.19)	3.47 - 6.04 (4.24)
	A. dimorphus	Acdi	83	13.3 - 32.0 (23.4)	1.99 - 9.64 (2.96)	0.09 - 0.82 (0.17)	2.92 - 7.14 (4.15)
	A. obliquus	Acob	58	13.5 - 32.0 (26.5)	2.21 - 9.64 (2.96)	0.09 - 0.82 (0.16)	3.22 - 7.14 (4.08)
	Ankistrodesmus falcatus	Afas	31	14.1 - 30.5 (17.0)	2.12 - 6.42 (2.62)	0.09 - 0.47 (0.14)	3.38 - 5.32 (4.35)
	Ankistrodesmus gracilis	Angr	15	15.1 - 32.0 (27.7)	1.99 - 9.64 (3.10)	0.10 - 0.49 (0.16)	3.61 - 6.04 (3.93)
	Closterium acutum var. *variabile*	Cvae	37	14.0 - 32.0 (25.9)	2.37 - 9.64 (3.49)	0.10 - 0.82 (0.18)	3.15 - 7.14 (4.35)
	C. parvulum	Cpam	21	14.1 - 32.0 (26.5)	2.36 - 9.64 (6.42)	0.12 - 0.82 (0.23)	3.56 - 7.14 (4.57)
	Cosmarium tinctum	Ctim	12	13.3 - 16.6 (14.3)	2.99 - 7.27 (4.02)	0.12 - 0.82 (0.21)	2.92 - 7.14 (5.32)
	Crucigenia fenestrata	Cfea	44	13.3 - 32.0 (26.2)	2.12 - 9.64 (3.44)	0.10 - 0.82 (0.19)	2.92 - 7.14 (4.48)
	C. lauterbornei	Clai	29	14.1 - 32.0 (26.5)	1.99 - 9.64 (4.77)	0.10 - 0.82 (0.23)	3.54 - 7.14 (4.57)
	C. quadrata	Crqu	33	14.1 - 32.0 (27.7)	2.21 - 7.58 (2.96)	0.10 - 0.82 (0.22)	3.47 - 7.14 (4.48)
	C. tetrapedia	Ctea	65	13.3 - 32.0 (25.9)	1.99 - 9.64 (2.94)	0.09 - 0.82 (0.17)	2.92 - 7.14 (4.15)
	Crucigeniella apiculata	Crap	33	25.7 - 32.0 (29.1)	1.99 - 9.64 (3.14)	0.12 - 0.49 (0.18)	3.47 - 4.85 (3.93)
	C. rectangularis	Crre	40	14.9 - 32.0 (27.4)	2.12 - 7.58 (2.96)	0.09 - 0.49 (0.18)	3.22 - 6.04 (4.32)

	Desmodesmus armatus	Dear	94	13.3 - 32.0 (25.7)	1.99 - 9.64 (2.96)	0.09 - 0.82 (0.16)	2.92 - 7.14 (4.09)
	D. communis	Deco	23	15.8 - 32.0 (28.1)	2.23 - 9.64 (4.77)	0.10 - 0.82 (0.22)	3.47 - 7.14 (4.53)
	D. denticulatus	Dede	19	14.9 - 32.0 (29.0)	2.38 - 9.64 (3.15)	0.12 - 0.49 (0.23)	3.47 - 4.85 (4.28)
	D. granulatus	Degr	25	13.5 - 29.4 (26.5)	2.23 - 9.64 (3.20)	0.10 - 0.47 (0.15)	3.40 - 6.04 (4.06)
	D. opoliensis	Deop	54	14.5 - 32.0 (27.4)	1.99 - 9.64 (3.14)	0.10 - 0.82 (0.18)	3.22 - 7.14 (4.21)
	D. opoliensis var. carinatus	Deoc	13	16.6 - 29.6 (27.3)	1.99 - 9.64 (3.37)	0.13 - 0.24 (0.16)	3.47 - 4.86 (3.66)
	Dictyosphaeria cavernosa	Dcaa	42	14.9 - 32.0 (27.3)	1.99 - 9.64 (3.14)	0.11 - 0.49 (0.17)	3.22 - 6.04 (4.06)
	Enallax acutiformis	Enac	21	14.9 - 30.5 (28.9)	1.99 - 3.36 (2.48)	0.09 - 0.29 (0.16)	3.38 - 4.56 (3.65)
	Hyaloraphidium rectum	Hrem	63	14.1 - 32.0 (25.9)	1.99 - 9.64 (2.96)	0.09 - 0.82 (0.17)	3.22 - 7.14 (4.44)
	Lacunastrum gracillimum	Lagr	17	14.3 - 30.2 (27.4)	2.12 - 7.26 (3.18)	0.12 - 0.47 (0.16)	3.56 - 4.56 (4.21)
	Micractinium pusillum	Mpum	46	13.5 - 32.0 (26.5)	2.12 - 9.64 (3.15)	0.10 - 0.82 (0.18)	3.22 - 7.14 (4.24)
	Monactinus simplex	Mosi	12	16.3 - 32.0 (29.0)	2.62 - 7.26 (3.36)	0.10 - 0.49 (0.23)	3.38 - 4.92 (3.63)
	Monoraphidium arcuatum	Marm	35	13.3 - 32.0 (25.7)	2.21 - 9.64 (3.49)	0.10 - 0.82 (0.19)	2.92 - 7.14 (4.44)
	M. griffithii	Mogr	29	13.5 - 32.0 (16.3)	2.36 - 7.58 (3.06)	0.10 - 0.82 (0.18)	3.15 - 7.28 (4.85)
	M. komarkovae	Mkoe	58	13.3 - 32.0 (27.4)	2.12 - 9.64 (3.18)	0.10 - 0.82 (0.19)	2.92 - 7.14 (4.21)
	M. mirabile	Momi	31	13.5 - 30.5 (26.2)	2.12 - 7.58 (2.96)	0.10 - 0.82 (0.14)	3.40 - 7.14 (4.17)
	Oocystis lacustis	Olas	12	13.3 - 29.8	3.10 - 7.58	0.21 - 0.82	2.92 - 7.14

				(28.3)	(6.42)	(0.47)	(4.84)
	Palmella miniata	Pmia	12	25.9 - 29.9 (29.0)	2.50 - 7.26 (3.14)	0.14 - 0.35 (0.18)	3.54 - 4.53 (3.56)
	P. mucosa	Pmua	65	14.0 - 32.0 (27.4)	1.99 - 9.64 (3.06)	0.10 - 0.49 (0.18)	3.15 - 6.04 (4.08)
	Pediastrum duplex	Pdux	23	14.9 - 29.4 (26.5)	2.21 - 9.64 (5.23)	0.10 - 0.82 (0.16)	3.55 - 7.14 (4.48)
	P. duplex var. *duodenarium*	Pdum	27	14.9 - 32.0 (26.2)	2.31 - 9.64 (3.72)	0.10 - 0.49 (0.16)	3.63 - 6.04 (4.48)
	Quadrigula chodatii	Qchi	29	13.5 - 32.0 (18.3)	2.44 - 9.64 (3.72)	0.11 - 0.82 (0.23)	3.40 - 7.14 (4.54)
	Radiococcus planktonicus	Rpls	35	13.5 - 32.0 (17.5)	2.38 - 9.64 (3.10)	0.11 - 0.82 (0.16)	3.40 - 7.14 (4.44)
	Scenedesmus arcuatus	Sars	33	14.1 - 32.0 (28.1)	2.23 - 9.64 (3.06)	0.10 - 0.49 (0.16)	3.47 - 6.04 (4.06)
	S. armatus var. boglariensis	Sbog	17	13.5 - 32.0 (16.3)	2.23 - 7.58 (3.06)	0.10 - 0.82 (0.29)	3.40 - 7.14 (4.54)
	S. armatus var. boglariensis f. bicaudatus	Sbis	79	14.1 - 32.0 (26.6)	1.99 - 9.64 (2.96)	0.09 - 0.82 (0.17)	3.22 - 7.14 (4.21)
	S. biguga	Sbia	33	13.3 - 32.0 (25.7)	1.99 - 7.58 (2.99)	0.10 - 0.49 (0.21)	2.92 - 5.66 (4.15)
	S. javaensis	Sjas	17	14.1 - 32.0 (27.4)	2.12 - 6.97 (3.18)	0.10 - 0.49 (0.19)	3.55 - 5.66 (4.57)
	Schroederia nitzschioides	Snis	12	14.3 - 29.8 (23.4)	2.64 - 7.58 (3.10)	0.10 - 0.35 (0.18)	3.22 - 4.84 (4.15)
	S. setigera	Ssea	12	14.1 - 30.5 (28.1)	2.23 - 7.58 (2.99)	0.10 - 0.29 (0.14)	3.56 - 5.32 (3.82)
	Spondylosium pygmaeum	Spym	31	14.9 - 32.0 (26.5)	2.12 - 9.64 (3.18)	0.10 - 0.49 (0.19)	3.38 - 6.04 (4.56)
	Stauridium tetras	Stte	27	14.3 - 32.0 (28.1)	2.44 - 9.64 (4.77)	0.10 - 0.49 (0.23)	3.65 - 6.04 (4.54)
	Tetraedron bifurcatum	Tbim	12	15.1 - 30.5 (28.3)	2.44 - 9.64 (4.77)	0.16 - 0.47 (0.29)	4.06 - 6.04 (4.48)

	T. minimum	Tmim	15	14.0 - 32.0 (23.4)	2.12 - 6.97 (2.90)	0.12 - 0.49 (0.16)	3.22 - 7.28 (4.15)
	T. trigonum	Ttrm	31	14.1 - 32.0 (28.3)	2.12 - 9.64 (3.10)	0.12 - 0.49 (0.24)	3.54 - 6.04 (4.48)
	Tetrastrum elegans	Tels	48	14.1 - 32.0 (26.5)	2.12 - 9.64 (2.94)	0.09 - 0.49 (0.16)	3.47 - 6.04 (4.44)
	T. punctatum	Tpum	15	13.5 - 29.4 (16.5)	2.23 - 9.64 (3.49)	0.09 - 0.82 (0.18)	3.40 - 7.14 (4.35)
	Westella botryoides	Wbos	17	15.1 - 32.0 (18.3)	2.52 - 7.58 (5.26)	0.12 - 0.82 (0.38)	4.08 - 7.14 (4.85)
Euglenophyceae	*Euglena cylindrica*	Ecya	37	16.6 - 32.0 (28.3)	2.21 - 9.64 (3.15)	0.10 - 0.49 (0.22)	3.22 - 5.86 (4.21)
	E. ehrenbergii	Eehi	13	15.1 - 32.0 (29.0)	3.06 - 7.58 (6.42)	0.22 - 0.49 (0.38)	3.56 - 6.04 (4.84)
	E. gracilis	Egrs	38	14.0 - 32.0 (27.4)	2.12 - 7.27 (2.83)	0.09 - 0.82 (0.18)	3.15 - 7.14 (4.09)
	E. mutabilis	Emus	13	16.6 - 32.0 (29.6)	2.44 - 6.97 (3.10)	0.16 - 0.49 (0.24)	3.86 - 4.86 (4.57)
	E. pisciformis	Epis	21	14.1 - 32.0 (28.9)	2.23 - 7.58 (3.10)	0.10 - 0.49 (0.18)	3.38 - 4.86 (3.82)
	Lepocinclis acus	Leac	37	13.5 - 32.0 (28.3)	2.21 - 7.58 (3.15)	0.12 - 0.82 (0.23)	3.22 - 7.14 (4.08)
	L. oxyuris	Leox	29	13.5 - 32.0 (27.7)	2.21 - 6.97 (2.78)	0.11 - 0.49 (0.17)	3.22 - 4.88 (4.15)
	Phacus triquetra	Ptrr	19	14.1 - 32.0 (29.0)	2.44 - 9.64 (4.77)	0.12 - 0.49 (0.29)	3.22 - 5.32 (4.53)
	Trachelomonas scabra	Tsca	17	13.5 - 30.2 (27.4)	2.12 - 9.64 (3.44)	0.10 - 0.47 (0.16)	3.22 - 4.56 (3.82)
Cyanophyceae	*Anabaenopsis sp.*	Ansp	12	15.1 - 30.5 (28.3)	2.44 - 7.58 (4.77)	0.10 - 0.47 (0.29)	3.82 - 6.04 (4.48)
	Arthrospira platensis	Apls	19	14.1 - 32.0 (29.6)	2.31 - 7.58 (2.62)	0.10 - 0.49 (0.18)	3.54 - 4.92 (4.24)
	Merismopedia cantonensis	Mcas	19	13.3 - 32.0	2.31 - 9.64	0.13 - 0.49	2.92 - 4.85

				(26.5)	(3.10)	(0.23)	(4.35)
	M. tenuissima	Mtea	52	14.9 - 32.0 (28.6)	1.99 - 9.64 (3.06)	0.10 - 0.49 (0.18)	3.22 - 6.04 (3.86)
	Oscillatoria fraca	Ofra	31	14.3 - 32.0 (29.1)	2.44 - 9.64 (3.20)	0.10 - 0.49 (0.22)	3.54 - 5.66 (4.42)
	O. limosa	Olia	12	14.0 - 14.3 (14.2)	2.31 - 3.49 (2.99)	0.12 - 0.18 (0.13)	3.15 - 7.28 (4.44)
	O. subbrevis	Osus	21	14.0 - 32.0 (18.3)	2.23 - 5.26 (2.94)	0.12 - 0.38 (0.22)	3.15 - 7.28 (4.35)
	Phormidium chlorinum	Phch	50	14.1 - 32.0 (27.4)	1.99 - 9.64 (2.96)	0.11 - 0.49 (0.16)	3.38 - 6.04 (4.15)
	Raphidiopsis sinensia	Rsia	21	14.9 - 32.0 (29.0)	2.50 - 9.64 (3.20)	0.10 - 0.38 (0.18)	3.54 - 4.86 (4.06)
Dinophyceae	*Gonyaulax sp.*	Gosp	15	13.5 - 30.3 (28.1)	2.36 - 7.58 (3.44)	0.10 - 0.47 (0.17)	3.40 - 4.84 (3.82)
	Prorocentrum cordatum	Prco	19	16.1 - 32.0 (28.1)	1.99 - 7.58 (2.44)	0.10 - 0.49 (0.14)	3.47 - 4.85 (3.82)
Chrysophyceae	*Dinobryon sertularia*	Dsea	19	15.1 - 32.0 (27.4)	1.99 - 9.64 (3.72)	0.12 - 0.49 (0.24)	3.65 - 6.04 (4.54)

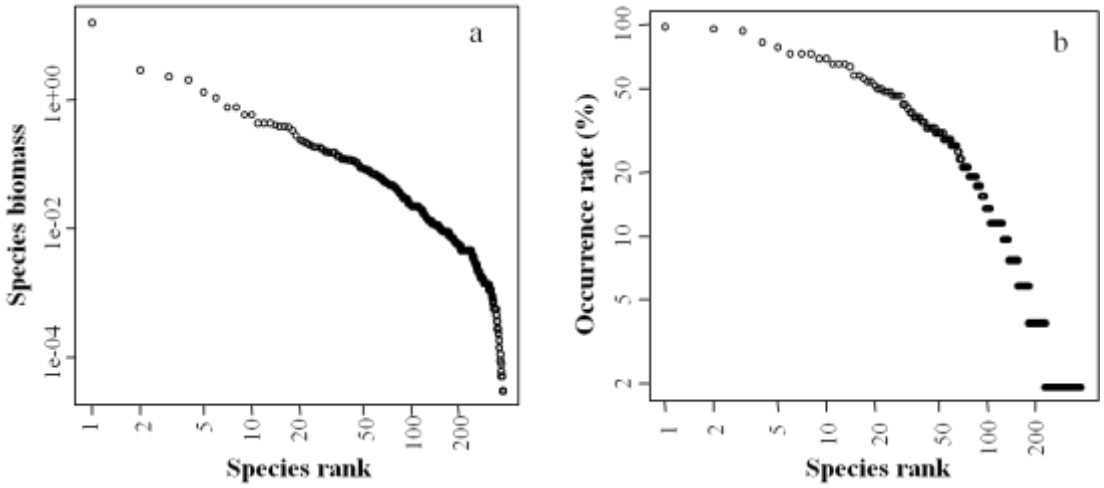

Figure 22 The rank of biomass and occurrence rate for phytoplankton species as function of the decreasing of the species rank, both horizontal and vertical axes are log-transformed (a. biomass; b. occurrence rate).

3.3.3 Phytoplankton species assemblage analysis

The ordination of the phytoplankton samples of PRD was obtained by mean of NMDS, and results indicated that most of the samples distributed in the same direction and only a small group in opposite direction. Similarities between samples were analyzed using the cluster analysis method, and similar samples were connected together with lines and groups were identified by distinct symbols and different colors (Fig. 23). Five groups (G1 to G5) were finally identified. G2, composed of all samples of the two urban sites ZJQ and LHS, was clearly differentiated from other groups with high values of water temperature, salinity and nutrients, but apparently lower values of transparency, pH and DO. G4, located between G2 and other three groups, was composed of samples of five inner sites. This group could also be differentiated from others. The other three groups (G1, 3, 5) distributed closely, and they could be differentiated mainly through seasonal differences. G3 was mainly composed of samples of summer (May and August), and its samples covered all rural sites. G1 was mainly composed of samples of winter (March), and its samples covered most of the rural sites. G5 was mainly composed of samples of December, and its samples covered most of the rural sites.

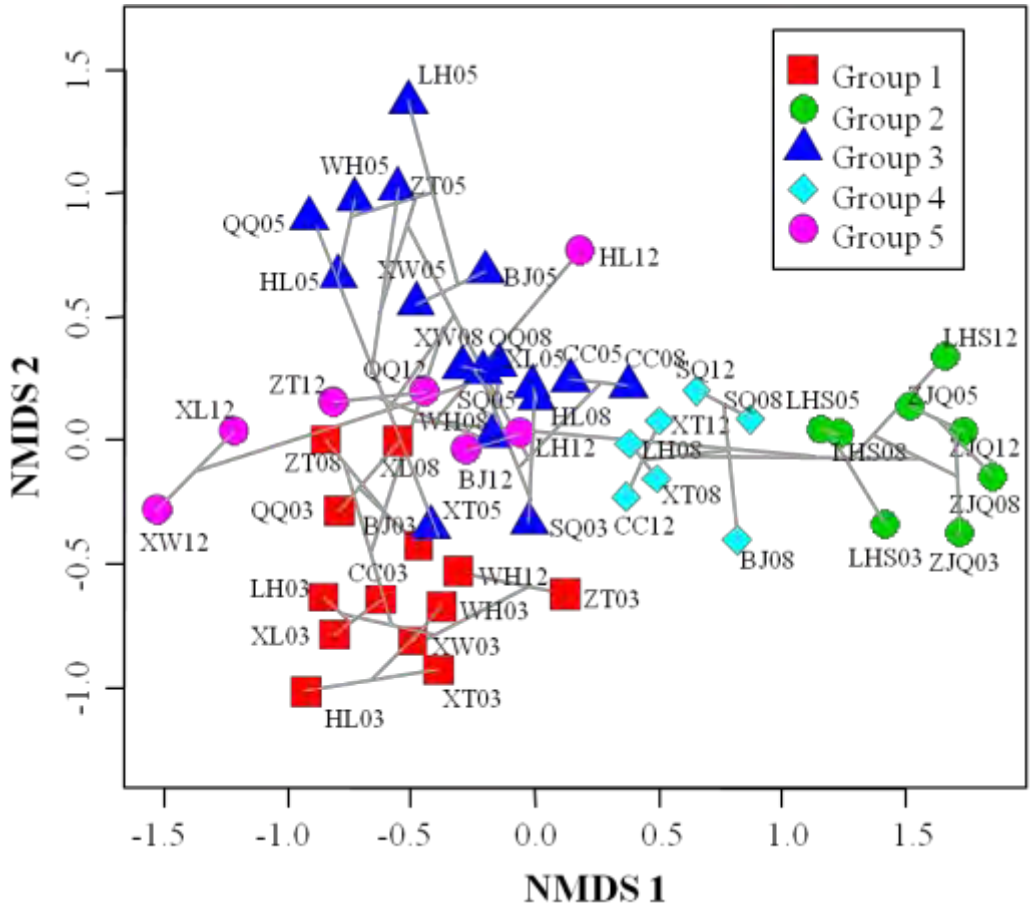

Figure 23 Ordination of phytoplankton samples in the two-dimensional non-metric multidimensional scaling (NMDS) configurations. Based on log (n + 1) transformed biomass values of taxa, five groups are extracted through ward clustering of Bray-Curtis dissimilarity matrix. And then, the NMDS result is combined and the dendrogram is added. Sample locations are coded with symbols denoting the groups they represent.

Phytoplankton species richness and biomass with the percentage of different phyla of each group are shown in Fig. 24: the values varied and differed significantly among groups (the Kruskall-Wallis test, $p < 0.001$). G2 shows the maximum median values and G4 ranks the second among all five groups in both biomass and species richness. The other three groups have very close median values in biomass, but they are also obviously different in species richness. G1 has the minimum median values in biomass and G5 shows the minimum median values in species richness (Fig. 24a1, b1).

The percentage of different phyla in each group indicated that diatom and green algae dominated in species richness and diatom in biomass (Fig. 24a2, b2). Compared to biomass proportion of different phyla in five groups that absolutely dominated by diatom, the species richness proportion of them was more apparently different between each group. G1 was diatom dominated in species richness, and its proportion

was higher than 70%, and green algae contributed less than 20%. G5 showed considerable equal proportion of diatom and green algae in species richness, and sum value reached around 90%. While all the other three groups showed that green algae dominated in species richness, although diatom contributed around 30% and other phyla also contributed more than 10%. Although diatom absolutely dominated in biomass of each group, the considerable proportion (> 10%) of green algae could also be found in G2, 3, 4.

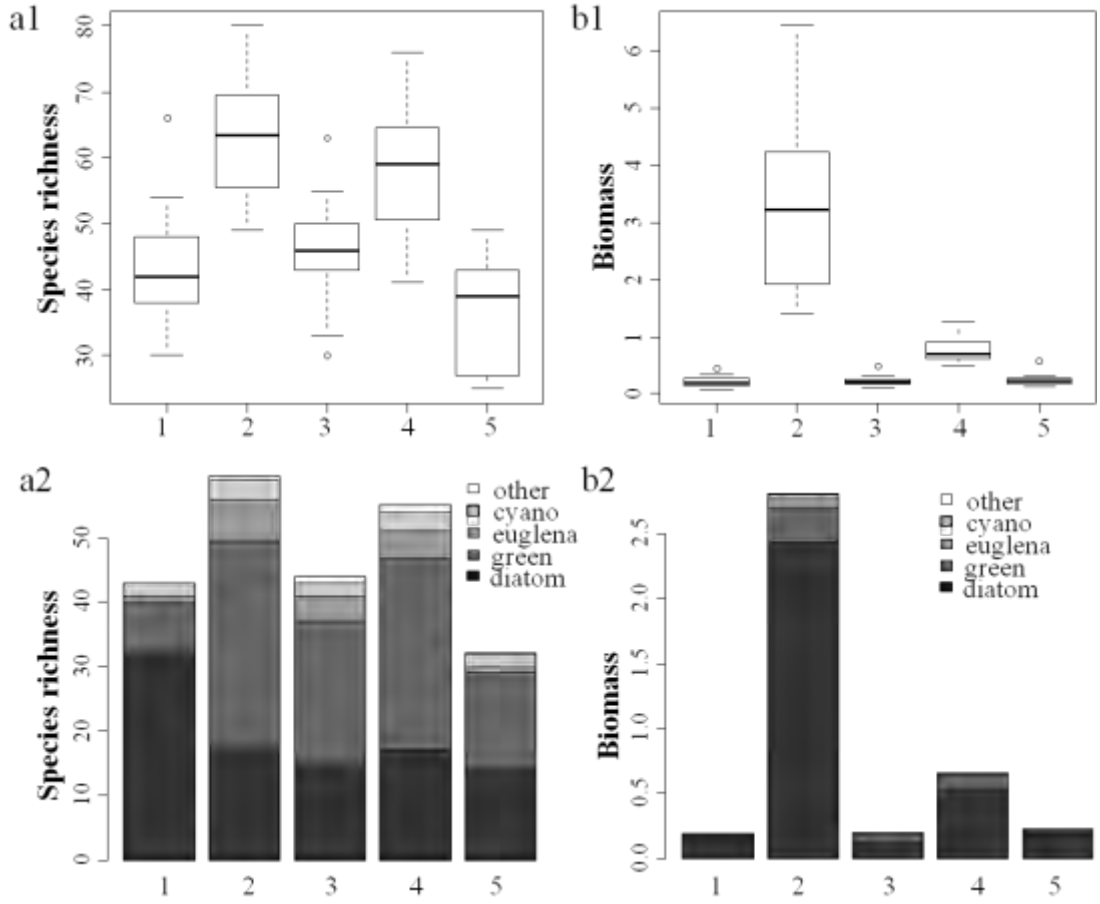

Figure 24 Variation of species richness and biomass of phytoplankton in each group of community (a1. species richness; a2. percentage of different groups to species richness in terms of median values; b1. biomass; b2. percentage of different groups to biomass in terms of median values).

3.3.4 Indicator species

Based on IndVal (indicator value > 25), a total of 56 indicator species were determined in different groups (Table 5). The number of indicator species varied significantly among groups, and increased along the sequence G3, G5, G4, G1, G2 (0, 3, 6, 12 and 35 indicator species, respectively). Indicator species were found with low occurrence frequency especially those that had extremely high indicator values.

G2, representing urban sites, contains the most diverse indicator species. Most of

them are true plankton, including 7 diatoms, 24 green algae, 2 true *Euglena* and 2 cyanobacteria. Three species (Agra, Cmea and Sarm), with extremely high occurrence frequency (> 90%), are also good indicator species of this group. G1, representing a period of cold winter in most rural sites, whose indicator species are composed of 11 diatoms and 1 blue alga, and most of them are tychoplankton. G4, representing some inner sites, whose indicator species include 3 tychoplanktonic diatoms, 1 planktonic and 1 tychoplanktonic green alga, and 1 true planktonic *Euglena*. G5, representing a period of winter in some rural sites, whose indicator species included 2 diatoms and 1 *Euglena*, and all of them are true plankton.

Table 5 Indicator species of each group based on IndVal (indicator value), with *p* values. The species, not included in table 4, were given the full name.

Group	Indicator species	Indicator value (%)	*P* value
1	Laba	75	0.001
1	Mvas	59	0.002
1	Cafs	57	0.001
1	Agrs	54	0.001
1	Aisa	46	0.005
1	Acur	43	0.011
1	Aovs	43	0.008
1	Bapa	42	0.026
1	Adis	40	0.01
1	*Fragilaria capucina*	31	0.017
1	*Fragilaria crotonensis*	31	0.01
1	Olia	29	0.042
2	Wbos	99	0.001
2	Acua	90	0.001
2	Cmea	84	0.002
2	Cvae	76	0.002
2	Qchi	76	0.001
2	Aana	74	0.001
2	Agra	73	0.001
2	Acdi	73	0.003
2	Cfea	71	0.003
2	Hrem	70	0.001
2	Cpam	70	0.001
2	Stsp	69	0.002
2	Leac	69	0.001
2	Mogr	69	0.001
2	Sbis	68	0.002
2	Ahai	63	0.019
2	Dear	59	0.007
2	Deop	58	0.001
2	Acac	57	0.002
2	Ccoa	54	0.004
2	Ttrm	52	0.019

2	Crqu	52	0.004
2	Mkoe	51	0.046
2	Sbia	51	0.022
2	Crre	50	0.046
2	Stte	48	0.008
2	Eehi	48	0.003
2	Sbog	38	0.008
2	Pdux	38	0.01
2	*Closterium intermedium*	37	0.014
2	Mcas	35	0.028
2	*Mesotaenium macrococcum*	34	0.013
2	Olas	34	0.045
2	*Anabaena flos-aquae*	29	0.016
2	Nacs	29	0.042
4	Tafa	50	0.034
4	Ursp	42	0.004
4	Egrs	35	0.033
4	Snis	35	0.005
4	*Staurastrum gracile*	32	0.011
4	*Cymatopleura solea* var. *subconstricta*	29	0.035
5	Aten	58	0.003
5	Aala	48	0.002
5	*Phacus tortifolius*	43	0.005

3.3.5 The prediction of phytoplankton assemblages from environmental factors

Five significant environmental variables were selected from 16 variables through constrained redundancy analysis (RDA), i.e. water temperature, dissolved oxygen, transparency, silicate and total phosphorus. The prediction analysis of how these five phytoplankton groups could be differentiated by the significant environmental variables was determined by discriminant function analysis (Fig. 25). Three discriminant functions were generated, and the random Monte Carlo permutation test showed that they were highly significant ($p < 0.001$). These axes (F1, F2 and F3) accounted for 47, 29 and 24% of the between-cluster variability, respectively. Since F2 and F3 contributed approximately equal proportions to the results, two dimensional figures based on F1 × F2 and F1 × F3, were shown respectively, with corresponding distribution of water quality parameters. In this respect, the correlations could be exhibited adequately.

The five environmental factors used were able to predict the phytoplankton assemblage groups and types of phytoplankton species assemblage patterns (i.e. global score of prediction) at 75% accuracy, and the prediction success rate for G1, G2, G3, G4 and G5 were 69, 88, 94, 0 and 100% respectively.

G2 was clearly separated from the other four groups which assembled and overlapped with each other to some extent. G1 and G2 were ordered along the first axis F1 (i.e. horizontal axis) in opposite directions based on both F1 × F2 (Fig. 25a1, a2) and F1 × F3 (Fig. 25b1, b2) figures. And the gradients of total phosphate, silicate, dissolved oxygen and transparency were loaded along this axis and were important controlling variables to G1 and G2 (Fig. 25a1, a2). Meanwhile water temperature was along the second axis F2 (i.e. vertical axis) and was an important controlling variable to G3 and G5, based on F1 × F2 figure. Moreover, silicate, DO and transparency were also factors influencing G3 and G5 based on F1 × F3 figure. G4 was ordered around the center, and its linkage with environmental variables was unclear.

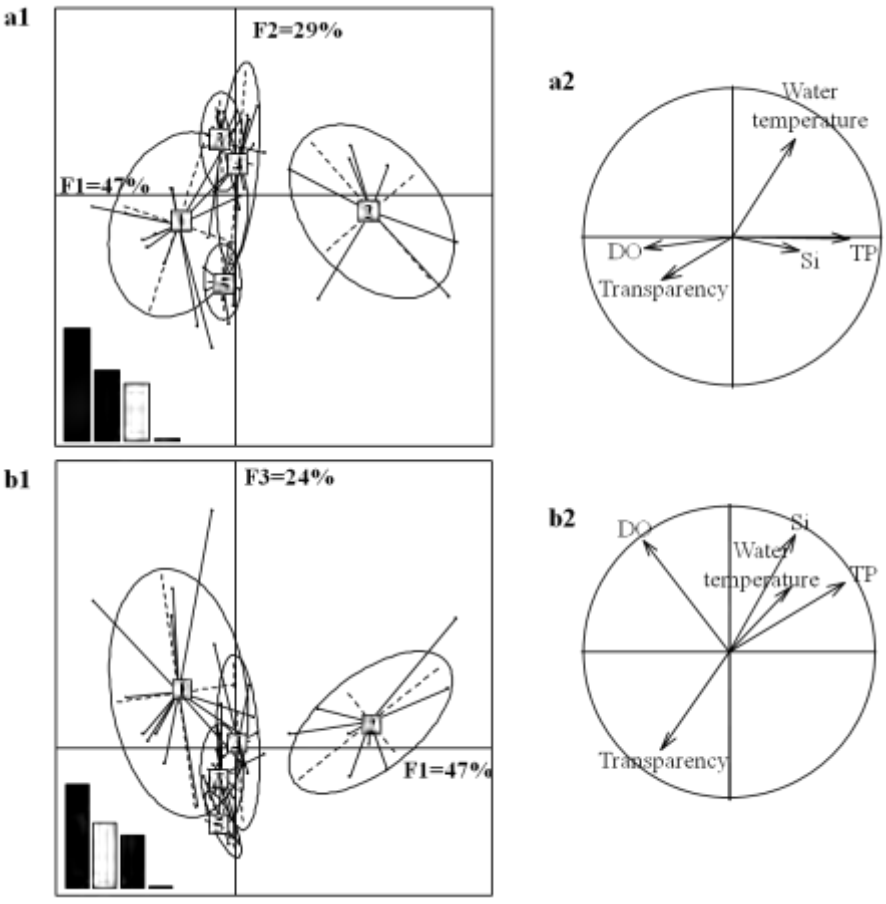

Figure 25 Results from the Linear Discriminent Analysis (LDA) and Principal Component Analysis (PCA) showing: (a1) the distribution and overlap of groups of community in F1 and F2 dimensions; (a2) the correlation circle of water quality parameters corresponding to F1 and F2; (b1) the distribution and overlap of groups in F1 and F3 dimensions; (b2) the correlation circle of water quality parameters corresponding to F1 and F3. The three bar plots in a1 and b1 represent Eigen values of the contributed axes.

3.4 Morphological variability of *A. granulata* in the main stream

3.4.1 Annual variation pattern of morphological parameters of *A. granulata*

The annual variations of cell size parameters and filament length (in terms of number of cells per filament) are shown in Fig. 26. The mean cell diameter ranged from 5 ± 0 to 17.25 ± 2.22 μm, with an average of 9.25 ± 1.45 μm. The highest value appeared on November 15th, and the lowest value appeared on January 30th. The annual variation pattern of cell diameter showed four distinct periods. The first period lasted from January to April, characterized by low values and light fluctuations, with values mainly ranging from 6 to 9 μm. The second period was from early May to early July, which started with two narrow consecutive ascending-descending cycles and then decreased continually until early July. The third period lasted from mid July to mid October, which was characterized by two wider consecutive ascending-descending cycles; with the small cycle lasting one month and the big cycle lasting two months. The fourth period was from October 15th to December 20th, characterized by extremely high values mainly in the range of 10 to 16 μm, and the maximum value of this period was 17.25 ± 2.22 μm on November 15th (Fig. 26a).

The mean cell length ranged from 11.25 ± 3.75 to 17.75 ± 6.5 μm, with an average of 14.03 ± 1.12 μm. The highest value appeared on December 1st, and the lowest value appeared on May 25th. The annual variation pattern showed two distinct periods. The first period was from January 1st to August 10th, characterized by fluctuations under 15 μm, mainly in the range of 11 to 15 μm. The second period was from August 15th to December 20th, characterized by an apparent ascending trend which peaked and then dropped, and the mean values ranged primarily from 13 to 17 μm (Fig. 26b).

The mean cell volume ranged from 235.50 ± 0 to 4131.77 ± 1820.86 μm^3, with an average of 1145.37 ± 424.40 μm^3. The highest value appeared on November 30th, and the lowest value appeared on January 30th. The annual variation pattern was almost the same as that of cell diameter, but only one big cycle was significant during the corresponding two mid periods (Fig. 26c).

The mean filament length (number of cells per filament) ranged from 1.16 ± 0.37 to 67.80 ± 48.80 cells, with an average of 12.64 ± 9.28 cells. The highest value appeared on November 10th, and the lowest value appeared on September 5th. The

annual variation pattern showed two distinct periods. The first period was from the beginning of the year to mid October, with low filament length, mainly fluctuating under 10 cells. The second period was from October 20th to December 20th, with high filament length, and mean values mainly ranging from 20 to 70 cells (Fig. 26d).

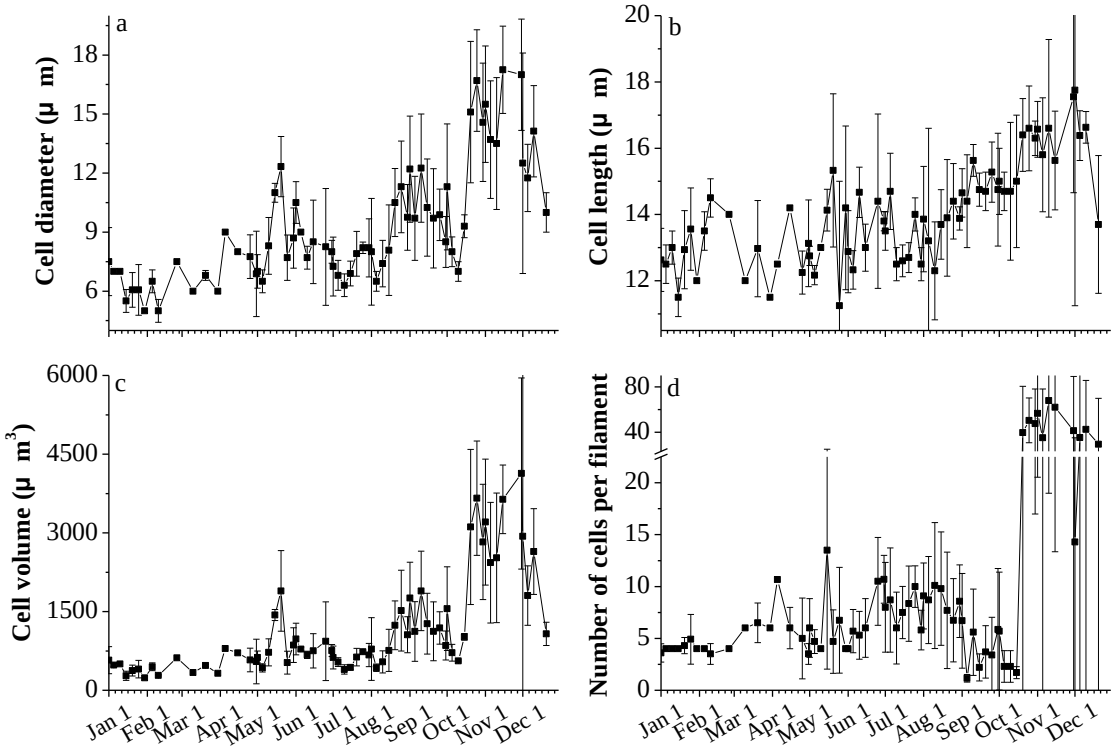

Figure 26. Annual variation pattern of cell and filament dimensions (Means ± SD). a. Cell diameter; b. Cell length; c. Cell volume; d. Filament length. Only values of the 67 samples that *A. granulata* positioned are shown in the figure.

3.4.2 Cross wavelet analysis on morphological parameters

The relationship between cell diameter and cell length with cross wavelet analysis is shown in Fig. 27. The horizontal axis indicates the study period; and the vertical axis is the scale number for the wavelet analysis. The areas blocked by the black lines indicate the 95% confidence interval.

Fig. 27a showed that full coherence existed between cell diameter and cell length with the scale number of 0 to 8, except for a period from April to May around scale 3, and a period from mid July to late October with the scale number of 0 to 6, but light coherence was also found between late August and late September nearing scale 0. Arrows pinpoint left-to-right directions in the highest coherence area, which meant that cell diameter varied before cell length during this period. Fig. 27b represents the cross wavelet coefficients and confirms the reading of the coherence in Fig. 27a.

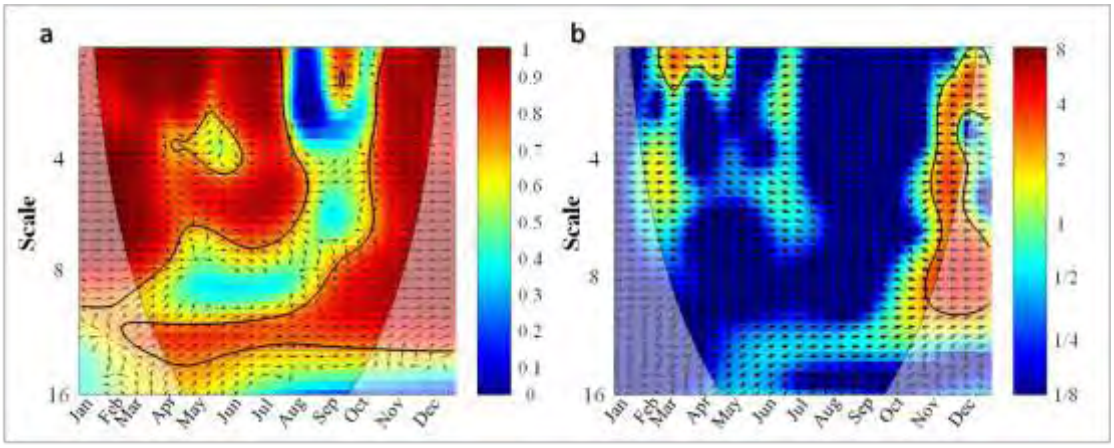

Figure 27. Cross wavelet analysis of relationships between cell diameter and cell length (a. coherence; b. cross wavelet coefficients). The 5% significance level against red noise is shown as a thick contour. The relative phase relationship is shown as arrows (before-phase pointing right, after-phase pointing left, in-phase pointing up, and anti-phase pointing down). The horizontal axis represents the 81 sampling days, and the vertical axis represents analysis scale. Coefficients in terms of different colors are shown in right column of each figure.

Full coherence between the cell diameter and filament length was shown in Fig. 28a with the scale number of 0 to 6, except for a period from late April to early June in scale range of 0 to 4, and a period from early July to early October in scale range of 0 to 6. Most arrows of high coherence area were in direction of left to right, meaning that cell diameter varied before filament length during this period (Fig. 28a). Fig. 28b confirms the reading of the coherence in Fig. 28a.

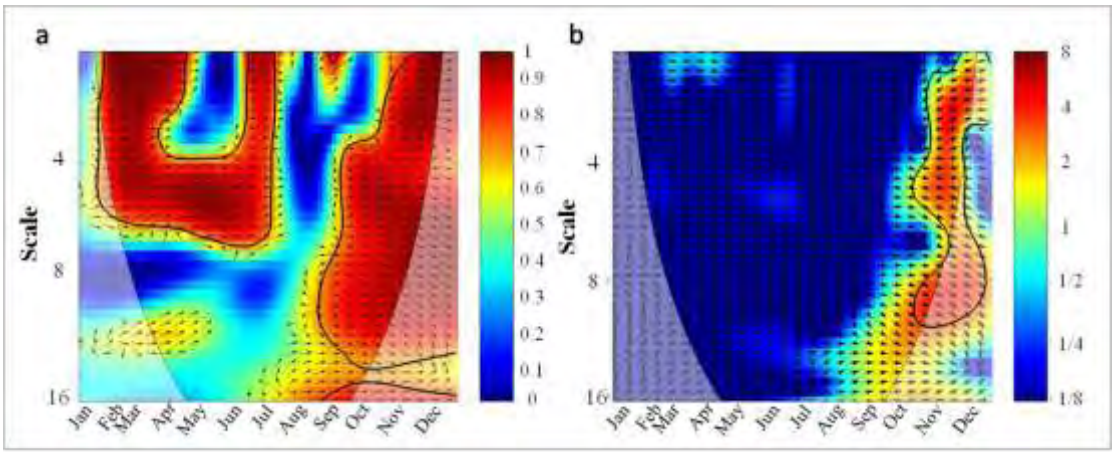

Figure 28. Cross wavelet analysis of relationships between cell diameter and filament length (a. coherence; b. cross wavelet coefficients). The 5% significance level against red noise is shown as a thick contour. The relative phase relationship is shown as arrows (before-phase pointing right, after-phase pointing left, in-phase pointing up, and anti-phase pointing down). The horizontal axis represents the 81 sampling days, and the vertical axis represents analysis scale. Coefficients in terms of different colors are shown in right column of each figure.

3.4.3 Cross wavelet analysis of correlations between morphological parameters and environmental factors

Relationship between cell diameter and environmental factors

In figures 29a to 29i, a full coherence was highlighted by wavelet analysis between the variable cell diameter and environmental factors. Table 6 gave the details including period, analyzing scale and the possible link between the variables. Full coherence with water temperature occurred in three periods with different scales, and phase angles indicated the moderate before-in-phase in spring, in-phase for one period of autumn, and before-phase for the rest of autumn (Fig. 29a, Table 6). The full coherence period with discharge occurred in flood season through spring and summer, and phase angles indicated the anti-phase (Fig. 29b, Table 6). While the full coherence period with precipitation occurred in spring and the coherence was in-phase (Fig. 29c, Table 6). Full coherence with phosphate was confirmed in four periods, two of which appeared at the beginning and the end of the year, and the other two appeared in spring and autumn respectively. Phase angles of the fourth period exhibited definite after-phase coherence, while the first and third period exhibited moderate after-in-phase, and the second period exhibited moderate before-anti-phase (Fig. 29d, Table 6). Full coherence with silicate appeared in winter, summer and autumn, and corresponding relationship was before-in-phase, before-anti-phase and after-phase respectively (Fig. 29e, Table 6). Four full coherence periods with total nitrogen occurred in all seasons except spring, and phase angles indicated the relationship was before-phase in winter, after-phase in summer, moderate after-anti-phase for the first autumn period, and before-anti phase for the second autumn period (Fig. 29f, Table 6). All four full coherence periods with nitrate nitrogen occurred in summer and autumn, and the relationship was moderate before-in-phase in summer, after-phase for both the first and fourth autumn period, and in-phase for the second autumn period (Fig. 29g, Table 6). Full coherence with nitrite nitrogen were confirmed in four periods covering all seasons except winter, and the relationship was after-anti-phase in spring, before-in-phase in the first autumn period, before-phase in the second autumn period, and anti-phase in the last period (Fig. 29h, Table 6). Only two full coherence periods between cell diameter and ammonia nitrogen were confirmed, which occurred in summer and autumn, and the opposite phase angles indicated the before-phase in summer and after-phase in autumn (Fig. 29i, Table 6).

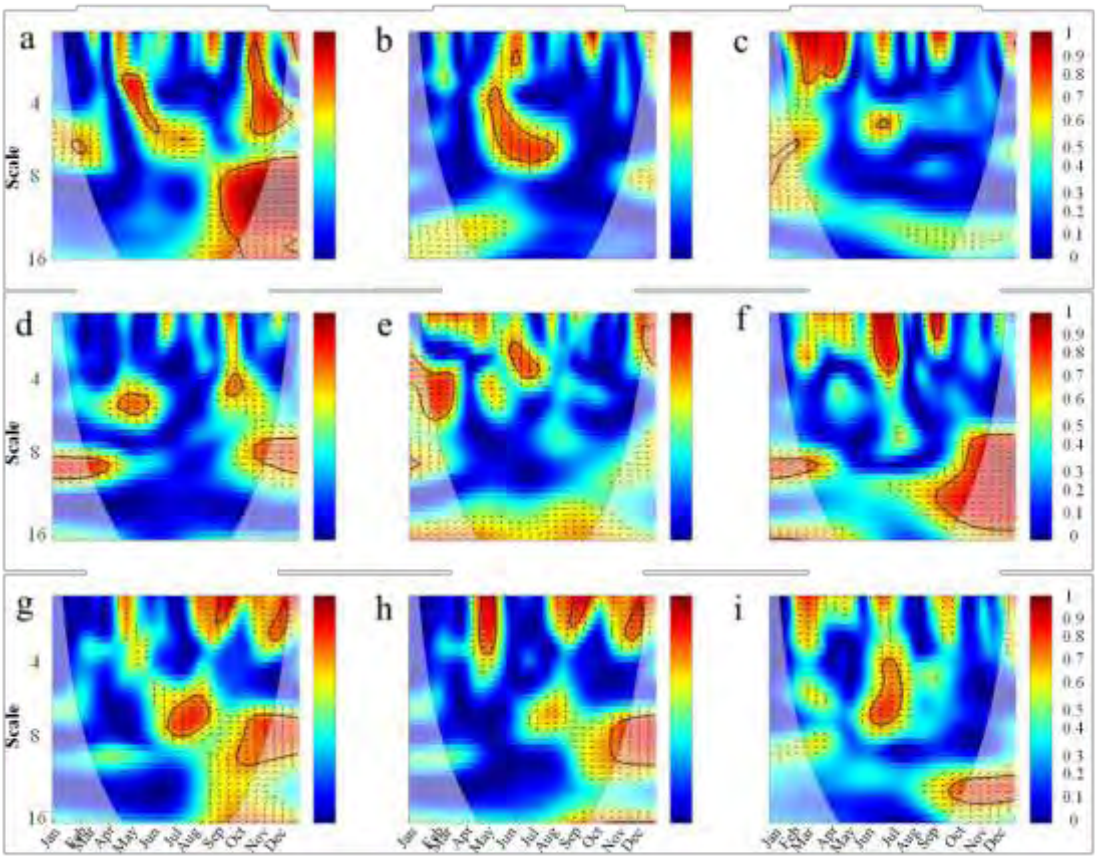

Figure 29. Cross wavelet analysis of relationships between cell diameter and environmental factors (a. water temperature; b. discharge; c. precipitation; d. phosphate; e. silicate; f. total nitrogen; g. nitrate nitrogen; h. nitrite nitrogen; i. ammonia nitrogen). The 5% significance level against red noise is shown as a thick contour. The relative phase relationship is shown as arrows (before-phase pointing right, after-phase pointing left, in-phase pointing up, and anti-phase pointing down). The horizontal axis represents the 81 sampling days, and the vertical axis represents analysis scale. Coefficients in terms of different colors are shown in right column of each figure.

Relationships between filament length and environmental factors

From figures 30a to 30i, a full coherence was highlighted by the wavelet analysis between the variable filament length and environmental factors. Table 6 also gave details including the temporal distribution and the possible link between the variables. Full coherence with water temperature occurred in three periods covering all seasons except spring, and phase angles indicated the before-phase in winter, in-phase for the first autumn period, and moderate before-in-phase for the second autumn period (Fig. 30a, Table 6). The full coherence period with discharge covered spring and summer, and phase angles indicated the moderate after-anti-phase (Fig. 30b, Table 6). While the full coherence with precipitation occurred in spring, and phase angles indicated in-phase (Fig. 30c, Table 6). Both the two full coherence periods with phosphate appeared in spring, with different scales, and phase angles indicated the moderate before-anti-phase and before-phase respectively (Fig. 30d, Table 6). Full coherence

with silicate appeared in four periods covering all seasons except spring, and the relationships were moderate before-in-phase in winter, anti-phase in summer, and after-phase in both the two autumn periods (Fig. 30e, Table 6). Full coherence with total nitrogen occurred in three periods covering summer and autumn, and phase angles indicated after-phase in both the summer periods, and before-phase in the autumn period (Fig. 30f, Table 6). Both the full coherence periods with nitrate nitrogen appeared in autumn and the relationships were moderate after-in-phase and before-in-phase (Fig. 30g, Table 6). Full coherence with nitrite nitrogen was also confirmed in two autumn periods, and the relationships were moderate before-anti-phase and after-anti-phase (Fig. 30h, Table 6). Two full coherence periods with ammonia nitrogen occurred in winter and summer, and with the same correlation: before-phase (Fig. 30i, Table 6).

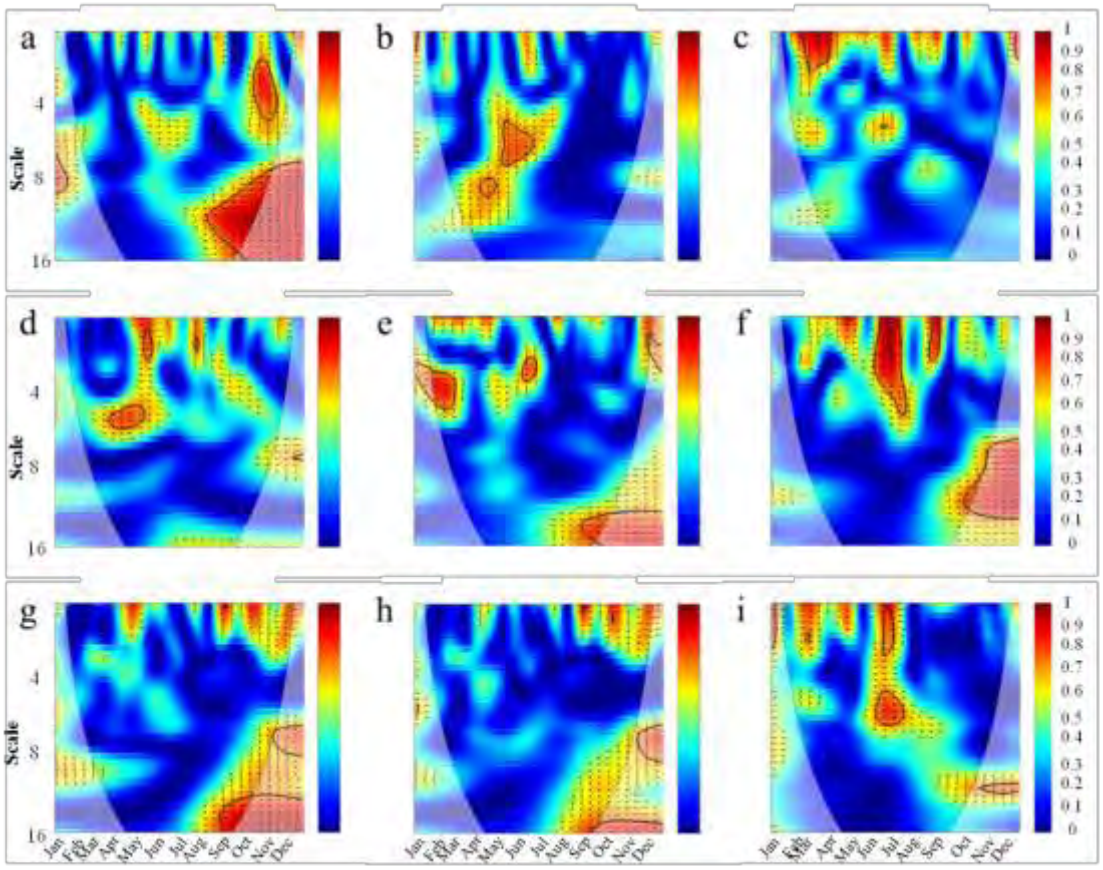

Figure 30. Cross wavelet analysis of relationships between filament length and environmental factors (a. water temperature; b. discharge; c. precipitation; d. phosphate; e. silicate; f. total nitrogen; g. nitrate nitrogen; h. nitrite nitrogen; i. ammonia nitrogen). The 5% significance level against red noise is shown as a thick contour. The relative phase relationship is shown as arrows (before-phase pointing right, after-phase pointing left, in-phase pointing up, and anti-phase pointing down). The horizontal axis represents the 81 sampling days, and the vertical axis represents analysis scale. Coefficients in terms of different colors are shown in right column of each figure.

Table 6 Summary of information (including period, analyzing scale and phase angle) on full coherence between morphological parameters (cell diameter and filament length) and environmental factors based on figure 29, 30. All the periods in significant correlations with each environmental factor are shown in the table.

Environmental factors	Cell diameter			Filament length		
	Period	Analyzing scale	Phase angle	Period	Analyzing scale	Phase angle
Water temperature	15/04-10/06	3-5	↗	01/01-15/01	Around 8	→
	15/10-15/12	1-5	↑	10/10-20/11	2-5	↑
	05/09-30/12	7-16	→	15/08-30/12	7-16	↗
Discharge	05/05-10/08	3-7	↓	10/05-30/06	Around 6	↙
Precipitation	10/02-25/04	0-3	↑	25/02-10/04	0-2	↑
Phosphate	01/01-01/04	Around 8	↖	30/03-20/05	Around 5	↘
	15/04-30/05	Around 5	↘	20/05-01/06	Around 1	→
	20/09-05/10	Around 4	↖			
	25/10-30/12	Around 8	←			
Silicate	01/01-15/03	2-6	↗	01/01-05/03	2-5	↗
	01/06-15/07	Around 3	↘	15/06-05/07	Around 3	↓
	10/12-30/12	1-3	←	05/12-30/12	Around 2	←
				05/09-30/12	13-16	←
Total nitrogen	01/01-25/03	Around 8	→	01/06-15/07	0-5	←
	01/06-10/07	0-3	←	25/08-01/09	0-2	←
	30/08-15/09	0-1	↙	10/10-30/12	7-14	→
	05/09-30/12	7-15	↘			
Nitrate nitrogen	25/06-20/08	6-8	↗	20/11-30/12	Around 7	↖
	05/09-30/09	Around 1	←	30/08-30/12	13-16	↗
	01/10-30/12	7-9	↑			
	20/11-15/12	Around 2	←			
Nitrite nitrogen	20/04-15/05	0-3	↙	20/11-30/12	7-9	↘
	30/08-30/09	Around 1	↗	15/09-30/12	Around 16	↙
	20/11-10/12	Around 2	→			
	30/10-30/12	7-11	↓			
Ammonia nitrogen	30/05-15/07	3-6	→	01/01-10/01	0-2	→
	30/09-30/12	Around 13	←	05/06-15/07	Around 6	→

3.4.4 Canonical correlations between morphological parameters and environmental factors

Constrained RDA with environmental factors resulted in five significant variables, which explained 53.4% of the variation in morphological parameters of *A. granulata* (Fig. 31). The ANOVA test on the RDA model indicated that the reduced model could reflect the correlations between morphology and selected variables well (p = 0.001), and test on all canonical axes indicated that axis RDA1 (p = 0.001) had a significant influence on the correlations. The eigenvalue of the axis RDA1 was 0.659,

and it explained 97.48% of the total variance in morphology variation. Silicate (p = 0.001), total nitrogen (p = 0.001), discharge (p = 0.002), phosphate (p = 0.002) and ammonia nitrogen (p = 0.01) were the main factors that jointly influenced the morphological parameters, and their coordinates on RDA1 were 0.82, 0.55, -0.54, 0.48 and 0.37 respectively. All nutrients exhibited a positive effect on morphological parameters especially cell diameter, cell volume and filament length, while discharge exhibited a negative effect. Correlation between cell diameter and cell length was greater than with any other two parameters (Fig. 31).

Using the K-means classification method, sample dates were divided into four clusters based on the weighted orthonormal site scores of the RDA model. The sum of squares within errors of cluster 1 to 4 were 0.06, 0.22, 0.21 and 0.08 respectively, indicating that differences between samples within cluster 2 and 3 were bigger than any other two clusters. Four clusters along the dotted line corresponded to the succession in time series, when they were combined with the correlations between morphology and environments, we could find that the positive relationship between morphological parameters and nutrients mainly occurred from middle August to the end of the year, while the negative relationship between morphological parameters and discharge mainly appeared in flood period (Fig. 31).

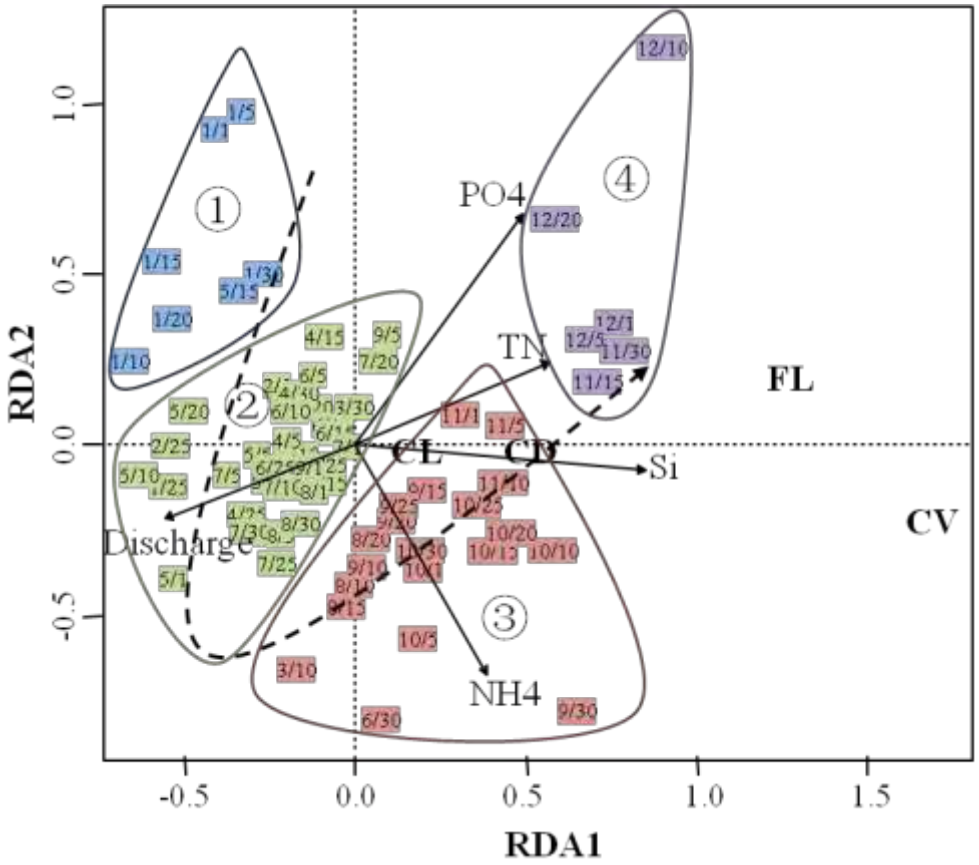

Figure 31. Redundancy analysis (RDA) of the effect of environmental factors on morphological parameters, with date sample clusters positioned on the ordination diagram. Only those environmental factors which significantly ($p < 0.05$ by 1000 times permutation tests) explain the variation in morphological parameters is shown. Regular lines with arrows represent environmental factors, bold characters represent morphological parameters. Four clusters (from K-means classification) along the dashed arrow line show the time-series gradient among dates and clusters. Abbreviations: CD: cell diameter; CL: cell length; CV: cell volume; FL: filament length; PO4-phosphate; Si-silicate; TN-total nitrogen; NH4-ammonia nitrogen.

4. Discussion

4.1 Bibliometric analysis of phytoplankton research trends

4.1.1 Research trend based on publications

Although the number of phytoplankton publications showed a linear increasing trend during the last 20 years, its proportion in total databases remained a steady low value, which seemed also a common phenomenon in other research fields (Ohniwa et al. 2010, Wen & Huang 2012, Ma et al. 2013, Niu et al. 2014). And increasing trend of publications on phytoplankton could also be found when considering the sum of six classic aquatic ecosystems (river, lake, reservoir, sea, bay and estuary), but their relative contributions remained steady, only the proportion of river showed a slight increasing trend. Since the classic lotic aquatic ecosystem was thought as an important link between other aquatic ecosystems, rivers have been paid more and more attention and have been found linking frequently with other aquatic ecosystems during the last two decades (Talling & Prowse 2010, Li et al. 2013, Battauz et al. 2014, Yu et al. 2014), also anticipated in the future. While rivers are classically considered as phytoplankton-poor systems (Vannote et al., 1980), the presence of phytoplankton within rivers in considerable abundance is being evidenced lately (Améziane et al., 2003; Tekwani et al., 2013, Abonyi et al., 2014).

Our results indicated that dependent research publications with reference to studied regions equaled to independent research among the six major aquatic ecosystems. Independent research was generally the basic and important way to collect the primary dataset, but publications became more dependent when considering multi-aquatic ecosystems and international collaborations. For example, total 24 articles were found referring to all the six aquatic ecosystems when searched in “subject” part, and most of them focused on eutrophication (Grelowski et al. 2000, Smith 2003, Davis & Koop 2006) and phytoplankton dynamics (Costa et al. 2009, Sin et al. 2013, Zhu et al. 2013) of different aquatic ecosystems. And the number of countries which authors belonging to of an article “Deep carbon export from a

Southern Ocean iron-fertilized diatom bloom" published in *Nature* reached 14 countries, since the above study was funded internationally and carried out during RV *Polarstern* cruise ANT XXI/3 (Smetacek et al. 2012). Moreover, some collaborative publications are associated with geographic locations. For example, the researches about Laurentian Great Lakes basin, which boarder the USA and Canada promoted the cooperation of the two countries (Lunetta et al. 2010; Biddanda et al. 2006). Other countries with strong correlations were also generally geographical neighbors. The linear increasing trend of dependent publications implied that collaborative research and publications would be the long term trend for studies on phytoplankton.

4.1.2 Research trend based on keywords

Research regions

The vast ocean area occupies about 71% of the Earth's surface, and publications in this largest aquatic ecosystem reach 50% of total phytoplankton articles. Consequently, the keywords "ocean" and "sea" could be found in the tenth and eleventh position respectively among the top 20 keywords (Fig. 8). Moreover, the keywords with either ascending or descending trends associated with research regions are mostly in the sea (or ocean) area, and these trends are mainly contributed by geographic adjacent countries. These countries collaborated and investigated in the mutual marine areas. Either three ascending keywords "baltic sea", "atlantic ocean", "gulf of mexico" or four descending keywords "north atlantic", "chesapeak bay", "sargasso sea", "north sea" are geographically adjacent. Furthermore, most of the adjacent countries could be found in the top 20. For example, the authors of a new article "Distinct responses of Gulf of Mexico phytoplankton communities to crude oil and the dispersant corexit(A (R)) Ec9500A under different nutrient regimes" in Gulf of Mexico (Ozhan & Bargu 2014) are from the United States. The authors of an article "Phytoplankton distribution patterns in the northwestern Sargasso Sea revealed by small subunit rRNA genes from plastids" in Sargasso Sea (Treusch et al. 2012) are also from the United States. Moreover, the two ascending keywords "east China sea" and "south China sea" represent the important sea area of China, which is located the

sixth position in top 20 countries for phytoplankton publications. With the fast development of economy, environmental pollution has currently become a key problem for Chinese government to deal with, thus more and more research projects are funded to study the aquatic ecosystems, especially in the important sea area during recent years.

Research methods

Modeling is a useful way to analyze and explore a large and complex dataset. Ecological models have now been widely applied in studies of phytoplankton ecology (Elliott et al., 2000, 2007; Mieleitner & Reichert, 2008) and algal dynamics (Serizawa et al., 2009; Zhang et al., 2013). Although the keyword "model" shows a descending trend, it is still located at the eighteenth in top 20 keywords, and "ecosystem model" is found in ascending trend. The two keywords "remote sensing" and "seawif" in ascending trend are effective methods for large scale studies, especially in ocean area (Macias et al. 2007, Alkawri & Gamoyo 2014, Ben Mustapha et al. 2014), and some could also be found in lake (Odermatt et al. 2012, Bolpagni et al. 2014, Perkins et al. 2014) and bay (Zhao et al. 2014). Other methods also exhibit ascending trend, for example, "stable isotope" and "stoichiometric" are associated with trace element studies in phytoplankton (Sugimoto et al. 2014, Van de Waal et al. 2014); "classification" and "algorithm" indicate the importance of analysis in phytoplankton studies (Barron et al. 2014, Mihaljevic et al. 2014).

Research contents

An ecosystem is a community of living organisms (plants, animals and microbes) in conjunction with the nonliving components of their environment (things like air, water and mineral soil), interacting as a system. The stability of an ecosystem, especially the interactions among organisms, and between organisms and their environment, always attracts the ecologists' attention. An aquatic ecosystem is an ecosystem in a body of water. In the present study, the two keywords "marine ecosystem" and "aquatic ecosystem" are in ascending trend, which implies that ecosystem studies have been closely related to phytoplankton research.

An ecosystem-scale experiment in the equatorial Pacific Ocean showed that a

massive phytoplankton bloom was triggered by iron fertilization (Coale et al. 1996). Bloom, an uncommon extreme growth of phytoplankton, becomes more and more frequent under the global climate change and territorial aggravating pollution, and it can also cause great financial losses. Although the keyword “spring bloom” exhibits a descending trend, all the other four keywords (“phytoplankton bloom”, “harmful algal bloom”, “algal bloom” and “cyanobacteria bloom”) associated with bloom indicate ascending trend. The number of articles is more than 2000 in the way of searching “bloom” in title and “phytoplankton” in subject. However, traditional keywords in phytoplankton publications, including “alga”, “plankton”, “diatom”, “chlorophyll”, “bacterioplankton” and “microalga” exhibit descending trend. But “picophytoplankton” is in ascending trend. Moreover, the keywords, associated with growth, community (or population) and production (carbon), also indicate descending trend.

Biodiversity affects ecosystem function, as do the processes of disturbance and succession. The global biodiversity patterns of plants and animals have always attracted researchers’ attention (Gaston 2000, Willig et al. 2003). But similar patterns of microorganisms are still less understood. The global biodiversity patterns of marine phytoplankton reported by Irigoien et al. (2004) indicate that marine phytoplankton diversity is a unimodal function of phytoplankton biomass, with maximum diversity at intermediate levels of phytoplankton biomass and minimum diversity during massive blooms. However, in recent years, global phytoplankton biomass decline has been observed (Boyce et al. 2010), with a global rate of decline of ~1% of the global median per year. Therefore, how does phytoplankton diversity respond to the decline trend of phytoplankton biomass will be more attractive. Accordingly, the three keywords “diversity”, “biodiversity” and “species richness” are in ascending trend.

Climate change is a significant time variation in weather patterns occurring over periods ranging from decades to millions of years, it is also the peripheral environment of any ecosystems. Many serious ecosystem consequences of climate change will take decades or even centuries to emerge (Luo et al. 2010). Long-term ecological responses to global change are strongly regulated by slow processes.

Therefore, keywords associated with time variation (“interannual variable”, “time series”, “long term change” and “seasonal dynamics”) are in ascending trend.

Environmental factors

Environmental factors can directly impact phytoplankton growth and community composition. Among all the environmental factors, nutrients are regarded as the most important. Although traditional keywords associated with nutrient limitation (“iron”, “nutrient trend”, “nutrient”, “phosphorus” and “nitrogen”) are in descending trend, “phosphorus limit” and “iron fertilization” actually indicate ascending trend, which may imply that nitrogen eutrophication has become the global background for aquatic ecosystems and it results in the unbalance of N : P ratio, thus P-limit is in ascending trend. Moreover, several other keywords (“climate change”, “atmospheric corode” and “sea surface temperature”) in ascending trend indicate that large scale environmental variations attract researchers more attention now.

4.1.3 Conclusion

Although phytoplankton publications showed a linear increasing trend during the last 20 years, its contributions to total scientific articles remained a steady level. Under the background of fast scientific research development, dependent publications (reflected in multi-aquatic ecosystems and international collaborations) indicate a linear increasing trend. The variations of keywords associated with research regions are mostly contributed by the geographic adjacent countries, and these countries are generally the top contributors. Variation trends of all the keywords relating to research methods, research contents and environmental factors indicate that phytoplankton studies carried out in large scale are in a significant ascending trend, while traditional and local scale studies are in a descending trend.

4.2 Patterning and predicting phytoplankton assemblages in the main stream

4.2.1 Environmental conditions

The environmental conditions of the sampled section were not only indirectly influenced by the upstream conditions through continual flow transportations (e.g. inoculums from upstream and branched tributaries), but also directly influenced by regional disturbance events (e.g. inputs of urban pollution). The annual patterns of environmental factors showed that physical and hydrological factors varied regularly with obvious seasonal characteristics (alternating between warm and cold seasons), while chemical factors did not. Warm seasons were accompanied by frequent rainfall and high discharge (floods), and the latter two factors were always found closely correlated (Wu et al. 2011, Townsend et al. 2012). Frequent rainfall could result in high discharge, thus floods formed. However, the relatively low daily values of precipitation during floods seemed to conflict with the high daily values in drought seasons. We assumed that the flood peaks resulted from the simultaneous raining in the whole river basin, while the single high daily values in drought seasons were just regional scale events. This assumption was supported by Lu et al. (2014), who reported that summer was the most important raining season in the Pearl River basin based on 50 years data. But the typhoon events of 2009 might enhance the regional precipitation in drought seasons. Researchers often reported that the water flow and rainfall brought external nutrients from the terrestrial ecosystem (Karadžić et al. 2013, Zhu et al. 2013). However in this study, all nutrients were uncorrelated with hydrological rhythms and varied without regular seasonal characteristics. Anthropogenic eutrophication of rivers is now a worldwide problem, particularly in catchments with dense human populations, well-developed industry, or intense agricultural land use (Kiss 1985, Smith et al. 2006). Some scientists have even used downstream increases in nitrate as useful indicators of eutrophication in large rivers (Turner et al. 2003, Almasri & Kaluarachchi 2004), which is a common human impact caused by agriculture. The median values of nutrients in the studied area

($P–PO_4$: 0.18 mg L^{-1}, $Si–SiO_4$: 3.84 mg L^{-1}, TN: 1.70 mg L^{-1}, $N–NO_3$: 0.64 mg L^{-1}, $N–NH_4$: 0.67 mg L^{-1}) were markedly higher than the threshold for half-saturation for most algal species according to Reynolds (2006). This situation is similar with that of the River Danube (Kiss 1994). Some studies had reported that nutrients played a subordinate role in determining algal biomass relative to the flow regime in rivers (Kiss 1997, Biggs & Smith 2002, Mitrovic et al. 2008). Above all, nutrient conditions in the investigated section seemed to be in excess and not limiting or controlling the phytoplankton behavior. Such eutrophic status was assumed to be mainly attributed to regional anthropogenic nutrient inputs along the river bank, since seasonal hydrology had little impact on them. This was contrary to conditions of the River Danube in which seasonal hydrology played a very important role in the actual trophic level (Kiss 1997).

4.2.2 Phytoplankton community structure

Wehr & Descy (1998) believed that the most successful algal groups in large rivers were Bacillariophyceae and Chlorophyceae. Our results indicated similar results, and these two groups contributed more than 75% of the total species richness. Kiss & Schmidt (1998) stated the same results for a few decades in the River Danube. Garnier et al. (1995) also reported similar patterns in the River Seine that contained a mixed group comprising approximately 200 taxa of which 90 were diatoms and 60 were Chlorophyceae. In the present study, only several taxa (four of six are diatoms) had a common occurrence rate (> 50%), and the phytoplankton biomass was even dominated by a single filamentous diatom species (*A. granulata*). Researchers have proved that the presence of a few dominant species accompanied by a large number of sporadic species is the main feature of phytoplankton community structures in large river ecosystems (Descy 1993, Devercelli 2006), and similar results have also been reported in many European rivers (Kiss & Schmidt 1998, Ržaničanin et al. 2005, Hindák et al. 2006, Desortová & Punčochář 2011, Tavernini et al. 2011) and other rivers (Wehr & Descy 1998, Hamilton 2011) in the world. In conclusion, our results illustrated a diatom-dominated community, which might benefit from good adaptive abilities of this group in lotic and turbid river ecosystems (Dokulil 1994, 2006,

Dokulil & Donabaum, 2014). Generally, diatoms developed well under turbid riverine conditions compared with other taxa (Wetzel 2001, Allan & Castillo 2007), and their efficiency under low light conditions was also well described (Litchman & Klausmeier 2008, Schwaderer et al. 2011, Beaver et al. 2013). In addition, dominance by single *A. granulata* (functional group P) in phytoplankton assemblages has been reported in many other large rivers (Lewis et al. 1995, O'Farrell et al. 1996, Zalocar de Domitrovic et al. 2007), preferable due to the eutrophication status and turbulent conditions. Dokulil & Teubner (2005) found that eutrophications of freshwater ecosystems ultimately led to the dominance of one or a few dominant species. Townsend et al. (2012) also believed that a single diatom species could not dominate under low nutrient conditions.

4.2.3 Patterning and predicting of phytoplankton assemblages

Based on species similarities, all samples were classified into four clusters through the self-organizing map (SOM). And their correlations with environments were also predicted using LDA. Cluster IIb1 covered warm seasons, and mainly composed of June and July. Cluster I also covered warm dates within only half a month. This similar point of these two clusters might imply that phytoplankton assemblages in warm seasons were so changeable that similarities and steady successions were only limited in short periods. Moreover, these two clusters could clearly be differentiated by discharge (precipitation), and temporal succession also reflected that cluster I was actually an after-flood (IIb1) period. Contrary to the above two clusters, IIb2 was characterized by cold and drought periods. The maximum sample numbers and the widest temporal distribution of this cluster illustrated that the phytoplankton composition was similar most of the time during the year. Cluster IIa was characterized by P-linkage. The wide time span but discontinuous samples of this cluster indicated that phosphate limitation happened occasionally.

Plankton selection and dynamics relate conspicuously to flow at higher discharges but other environmental features are important at low flow rates (Reynolds 2000). River discharge and the variables directly linked to water fluxes had a significant impact on the development of phytoplankton biomass, particularly during

the periods more favorable for algal growth (Salmaso & Zignin 2010). Although warm conditions of cluster IIb1 was suitable for algal growth, high discharge could prevent the accumulation of phytoplankton biomass through a dilution and advection process, and the associated rapid speed was also detrimental for phytoplankton to utilize resources efficiently (Salmaso & Braioni 2008). The low biomass was the direct response to a negative dilution effect and short residence time resulting from high discharge. The lower occurrence probability of species in this cluster also reflected the negative impact of floods. However, relatively high species richness seemed to be benefiting from the high flow conditions, which triggered the inoculations from both outer channels (mainly green algae) and benthic environments (mainly diatoms). Moreover, composition indicators of this cluster: euplanktonic *Monoraphidium komarkovae* (Chlorophyceae) and *Trachelomonas sp.* (Euglenophyceae) indicated the inoculations from outer sources; tychoplanktonic diatoms (*Amphora sp.*, *Fragilaria hinganensis* var. *longissima* and *Ulnaria delicatissima* var. *angustissima*) and indicated the resuspension from the benthos under violent turbulent conditions. Most of these species were found to have survival advantages under high flow conditions for their larger surface-volume ratio.

The largest peaks of algal biomass in the lowland rivers were determined by a combination of higher temperatures, low discharge and more favorable light (Rossetti et al. 2009, Descy et al. 2012). The maximum biomass of cluster I benefited from these favorable conditions. Kiss (1996) also reported that phytoplankton of River Danube could divide very quickly and double the abundance during one to two days in the low water period. Although light intensity was not measured during our investigation, the long photoperiod with intense light was always typical in warm seasons of such subtropical regions. Moreover, the concentration effect during decreasing discharge was also thought to be positive for both high diversity and biomass achieved in this cluster. This could be supported by the most diverse indicators and high occurrence probability of species in cluster I, since the other warm but flood cluster IIb1 showed contrasting low biomass. The considerable composition of euplanktonic (mainly green algae) and tychoplanktonic indicators (mainly diatoms)

also suggested that cluster I was an after-flood period. Romanov & Kirillov (2012) believed that the most significant changes in phytoplankton structure tended to occur in the period between flood decline and the beginning of low water. Thus, cluster I corresponded in this respect. Moreover, zooplankton most likely had weak predating pressure on phytoplankton in the studied area, since its abundance mostly kept low (unpublished data).

Low water temperature was thought to be key factor resulting in the low biomass and species richness of cluster IIb2, since it interrupted the physiological and biochemical processes of algal cell growth (Mata et al. 2010), and thus limited the phytoplankton abundance development. Meanwhile, the sinking loss increased during this drought period. However, the concomitant low water levels permitted benthic algae to easily resuspend in the water column. In this respect, benthic diatom *M. varians* benefited and gained the second rank in both occurrence rate and biomass. During the low water period, the light climate was also favourable for benthic algae and therefore developed more and could wash out to the plankton (Ács et al. 2003, 2006). Moreover, some samples distributed between flood peaks, and they were assumed to be an important link between clusters IIb2 and IIa, because of their high composition of green algae.

The linkage of cluster IIa to phosphate indicated that phytoplankton assemblages were occasionally P-limited. As phosphorus is often considered to be the biomass-limiting constraint in pelagic ecosystems, P enrichment can provide a significant stimulus to the sustainable biomass of phytoplankton (Reynolds 2006). However, the impact of this nutrient mainly happened in drought periods having concomitant suitable temperature. Both species richness and biomass of this cluster were at intermediate levels, but apparently higher than corresponding cold drought periods (IIb2).

In conclusion, annual patterns of phytoplankton assemblages at the downstream of West River could be easily differentiated by physical factors (water temperature, discharge and precipitation) during most times of the year. However, there was occasional P-limitation, especially in drought periods with suitable water temperature.

4.3 Patterning and predicting phytoplankton assemblages in the river delta system

4.3.1 Environmental conditions

The river water of the PRD is well known as low quality and in a reductive circumstance. The observed eutrophication deterioration in this region has been related to the long-term trends of nutrient delivery by the Pearl River (Duan & Bianchi 2006; Qu & Kroeze 2010). Nitrogen, phosphorus, and organic compounds are the most predominant pollutants (Ouyang et al. 2005). Our results showed that the nutrient concentrations in the investigated river delta were markedly higher than the threshold for half-saturation for most algal species according to Reynolds (2006). The P concentration of all sites exceeded 0.1 mg/l, which was the recommended concentration in flowing water to encourage excessive growth of aquatic plants (Cheung et al. 2003). The concentrations of nitrogen were under the maximum contaminant level in public drinking water supplies (10 mg/l). Urbanization is thought to be a great threat to such river water qualities. Within the same river, the water quality of sample from rural area was much better than that from urban zone (Ouyang et al. 2006). ZJQ and LHS, the two sites closer to Guangzhou city, are apparently different from other sites for their extremely pollution (high nutrient concentrations, low transparency and DO). And their corresponding low standard deviation values of transparency, DO and TN also reflected the weak seasonal fluctuations of water quality in urban sites. Spatial distributions in water qualities implied that local drainage was a main factor impacting pollution status at different sites (Lu et al. 2009). Municipal wastewater is thought to be the greatest pollution source for the two urban sites. Ouyang et al. (2006) had reported the positive correlation between the rapidity of urbanization and the pollution levels of urban river water in the PRD. Moreover, these two sites were also impacted by sea tide, which could be reflected by their relatively higher salinity. Through this way, high tide would result in the flow backward of pollutants discharge along the tidal backwater and enhance the circulation of sewage in such tidal region. As for other rural sites, chemical fertilizers

and pesticides used in agriculture and rural living sewage all contributed to the water pollution. Above all, the high nutrient concentrations of the studied area have exceeded the growth threshold of algal species significantly, which implied that physical and hydrological variables would play a more important role in patterning phytoplankton assemblages.

4.3.2 Phytoplankton community structure

The existence of various upstream river channels and floodplain habitats, along with various recruitment processes, might explain the high taxonomic diversity recorded in the PRD. As expected, Bacillariophyceae and Chlorophyceae were the dominant classes in phytoplankton diversity and Bacillariophyceae in biomass in the present study, which agreed well with the phytoplankton structures of the upper and lower adjacent water areas: downstream of the West River (Wang et al. 2013) and the Pearl River Estuary (Wang et al. 2010). Bortolini & Bueno (2013) also reported the similar phytoplankton community structure in São João River of Brazil. Wehr & Descy (1998) believed that the most successful algal groups in large rivers were Bacillariophyceae and Chlorophyceae, which were more abundant in the lower reaches. Generally, higher flow rates and shorter water residence time tend to favor faster-growing diatom taxa (Mihaljević et al. 2014). Besides this, diatoms are heavier and better adapted to low light availability than other algal groups, thus can benefit from intense water mixing (Trevisan et al. 2010). Moreover, conditions of high water flow could cause drifting of tychoplanktonic and meroplanktonic algae into the water column (Centis et al. 2010), thus several diatom genuses (*Navicula*, *Gomphonema*, *Aulacoseira* (*Melosira*), *Nitzschia* and *Cymbella*) exhibited high richness in our studies. In addition, the present high diversity also benefitted from the continual inoculations from upsteam main stream and river tributaries, and this could be reflected from the apparently high richness of *Euglena* (29 taxa) and *Scenedesmus* (24 taxa), which belonged to limnetic species and generally flushed to river channels during floods.

The presence of a few dominant species accompanied by a large number of sporadic species is the main feature of phytoplankton community structures in large

river ecosystems (Devercelli 2006, Hindák et al. 2006, Desortová & Punčochář 2011, Tavernini et al. 2011). In the present study, the centric diatom *A. granulata* contributed more than 50% of the total biomass during the whole investigation. And this result was in accordance with its dominance in the two adjacent water areas: the downstream of the West River (Wang et al., 2012) and the lower Pearl River Estuary (Wang et al., 2009), located upper and lower of the PRD respectively. The dominance of *A. granulata* and its bioforms was reported as typical of large rivers of the world (Rojo et al., 1994; Lewis et al., 1995; O'Farrell et al., 1996; Zalocar de Domitrovic et al., 2007). According to Reynolds (1994), the dominance of filamentous diatoms was associated with their capacity to form inoculants, which were deposited in the sediment and are re-suspended into the water column through the turbulence. Therefore, the predominance of *A. granulata* in the PRD was mainly dependent on inoculations from both upper flowing waters and lower tidal backwaters, and resuspension of benthic colonies. In addition, small-celled and fast growing diatom species *C. meneghiniana* also showed dominant and ranked second to *A. granulata*. It was thought to have advantages to survive under turbulent conditions (Reynolds et al., 2002) and was more competitive for nutrients and light utilization based on its larger surface-volume ratio (Litchman & Klausmeier, 2008). Moreover, *C. meneghiniana* had low sedimentation rates due to their dimension and persisted in the water column at slow flow rates. Several other algal species exhibited either high biomass contributions or high occurrence rate, which might be due to their seasonal preference or ecological properties reflection, e.g. *Dictyosphaeria cavernosa* was dominant in floods periods, *Entomoneis alata* was typical of brackish species, and *Desmodesmus armatus* was mainly dependent on outer channel inoculations.

4.3.3 Patterning and predicting of phytoplankton assemblages

Based on species biomass similarities, all samples were ordinate and classified into five groups through the NMDS and hclust respectively. And the contribution of significant environmental variables in differentiating the phytoplankton pattern groups were also predicted using LDA. G2 was composed of samples from all seasons of the two urban sites, and it was clearly differentiated from other groups through its high

eutrophication (bad water quality). G4 was composed of samples from August and December of five inner sites (XT, CC, BJ, LH and SQ), but it was uncorrelated with the present environmental variables. The similar point of these two groups was that their samples did not show distinct seasonal trait, thus mainly representing the spatial patterns. Moreover, both of them had apparently higher species richness and biomass than other three groups (G1, 3, 5), even though the differences between these two groups were also significant. The seasonally driven ecological gradient was expressed in the other three groups (G1-March, G3-May and August, G5-December), which assembled and overlapped with each other to some extent. But their distinct differences exhibited only in species richness. G1 and G3 had maximum samples, and they represented drought and flood seasons respectively. Generally, high level of connectivity in flood seasons would lead to high similar species composition, but both drought (G1) and flood season (G3) showed high similarities in the present study, which reflected the well connectivity between river channels of rural area. Bortolini & Bueno (2013) thought that the similarity of the distribution of communities in lotic environments was due to the unidirectional flow. These two groups showed equal total species richness and biomass, and the only difference between them was the alternating dominance of diatom and green algae in species richness. G5 also represented the drought period, but it had apparently lower species richness than G1 and G3, and the equal contribution of diatom and green algae in species richness indicated that the hydrological conditions of G5 were different from G1 to some extent. Above all, differences in the phytoplankton diversity and biomass between the patterning groups were significant in spatial dimension.

G2 had significant higher species diversity and biomass, especially for its biomass beyond at least 5 folds of other groups, even though the concomitant extremely low transparency and DO seemed detrimental for phytoplankton development. Of course, the nutrient conditions of the two urban sites could satisfy the requirements for most species growth, and this was regarded as an important precondition for high species diversity. Moreover, the two urban sites were located along the river channel of the Humen outlet, which had both the maximum volume of

runoff (18.5% of total the Pearl River discharge into China South Sea) and the maximum tidal throughput among the eight outlets of the Pearl River Estuary (Lu, 1990). Thus, the consequent intense and frequent water exchanges in this area could also guarantee the continual inoculations from both water flows and benthic recruitments. The high proportion of green algae and considerable contribution of diatom and Euglenophyta in total species richness of this group was a good example for the above conclusion. Although salinity was thought to be a negative effect on growth of freshwater phytoplankton, a concentration between 0.5 and 10 psu was not strong enough to lead to the disappearance of freshwater and brackish water phytoplankton (Lionard et al., 2005). Indicator species composition of G2 was most diverse, and most of them had low occurrence rate, preferred high temperature and high nutrients. Only five indicator species (Wbos, Qchi, Stsp, Mogr and Sbog) tended to occur in cold season.

The reason for the extremely high biomass of G2 was that both chemical and hydrological factors favored the predominance of *A. granulata*, since its maximum contribution to total phytoplankton biomass could reach 85% in the urban sites. First, high silicate concentrations of urban sites could not only satisfy the growth need in cell wall but also help reducing sinking velocity. Since studies by Gibson (1984) on another *Aulacoseira* species, *A. subarctica*, found that depletion of silicate would increase sinking velocity, thus density decreased exponentially. Second, both the upper river discharge and the lower tidal backwaters would provide continual supplements in density, since it also dominated in both the upper (Wang et al., 2012) and lower adjacent water areas (Wang et al., 2009). Third, its chain-forming colonies would increase the surface-area ratio and therefore the frictional resistance, resulting in lower sinking velocities (Young et al., 2012). In addition, the strong turbulence (e.g. low transparency) could also reduce the sinking velocity and enhance the recruitment from sediments through resuspension process. Fourth, this species was able to tolerate the high turbidity (Kilham et al., 1986) and low light intensity for its high chloroplast content in each cell (Stoermer et al., 1981). Moreover, its dominance in the Pearl River Estuary (Wang et al., 2009) also reflected its distinct adaptation to salinity

fluctuations. Therefore, the single dominance of *A. granulata* limited the species diversity of diatom, especially in warm seasons when suitable for its growth.

G4 showed higher values than other three groups in both species richness and biomass, but it seemed uncorrelated with the present environmental variables. Studies by Descy et al. (2012) in River Loire (France) found that the variation of water level in the river channel largely controlled growth and losses of potamoplankton. Since this group was composed of five inner sites, the relatively weak water exchanges and low water levels might be beneficial for phytoplankton development.

The other three groups were different from each other not in biomass but in species richness. G1 was characterized by low water temperature, and the concomitant low water levels, turbid kinetic and low light conditions favored diatoms (Reynolds, 1994). Therefore, both species diversity and biomass of this group was dominated by diatoms. Almost all indicator species of G1 were composed of diatoms, most of them were benthic disturbance indicators, and their water temperature tolerance results indicated that they occurred more in cold season. Although G3 was equal with G1 in both total species richness and biomass, the relative contribution between diatom and green algae was contrary. The higher proportion of green algae in species richness and low biomass values reflected the high discharge impact in summer. Jung et al. (2014) reported that phytoplankton abundance during the dry season was approximately two times higher than that during the flood season in the lower Han River of South Korea. The reason for high similarity between G1 and G3 might be that the negative effect of low temperature of G1 was counteracted by well mixed water columns thus lower sinking velocity for diatoms and high inoculations of benthic diatoms; while the positive effect of high temperature of G3 was counteracted by high dilution and short residence time. G5 was also characterized by low temperature, and it had the minimum species richness. Its apparently high transparency (78 ± 13 cm) must be negative for the suspension of benthic algae into the water column, which could be reflected from the equal contribution of diatom and green algae in diversity during drought season.

4.4 Morphological variability of *A. granulata* in response to environmental variables

4.4.1 Coherence between morphological parameters

Size variation is not only related to the life cycle but also associated with natural size selectivity (Jewson, 1992). Especially for diatoms with filamentous colonies, such as *A. granulata*, both cell size and filament dimensions should be considered when referring to morphological variability and explaining by its correlations with the environment. In this respect, cell and filament dimensions were considered linked to the life cycle and size selectivity respectively. In the present results, all the three different methodological approaches (linear regression, wavelet analysis and RDA) illustrated that the coherence and correlations between cell and filament dimensions appeared weaker than that between cell parameters. This implied that cell and filament size showed different response to environmental variations, thus resulted in a conflict between the life cycle and size selectivity. The wider range of morphological parameters of *A. granulata* in river ecosystems than that in other aquatic ecosystems (Table 7) also indicated the significant role of lotic conditions in size regulation. Moreover, phase angles (pointing right) during full coherence periods illustrated that cell diameter varied in before-phase corresponding to other size parameters, and this might be the link between cell and filament dimensions. O'Farrell et al. (2001) reported that an inverse relationship was confirmed between cell diameter and cell length in the Lower Paraná River, and it was explained as a tendency to maintain cell volume. Similar reports could also be found for another filamentous diatom species *Aulacoseira subarctica* (O. Müller) Haworth in Kurilskoye Lake (Lepskaya et al. 2010). Davey (1986) referred to the above phase as a period of relative stability, following the regrowth of filaments from auxospores. However, the positive relationship between cell diameter and cell length was observed in the present study, which might imply that the inverse relationship was defined in the regrowth period.

Table 7. Comparison of *Aulacoseira granulata* morphological parameters in the West River with other aquatic systems.

Type of water area	Sampling site	Sampling time	Cell diameter (μm, average and range)	Cell length (μm, average and range)	Filament length (μm)	Filament length (number of cells)	References
Lake	Lake Huron (North America)	1977.08	17.3 (15~20)	21.7 (19~23)			Stoermer et al., 1981
	8 lakes of Finland (Finland)	1986.07	10.4~16.8	19.8~33.2			Turkia and Lepistö, 1999
	Shear Water (England)	1982.08~1984.07	8~11.3		120~720	4~25	Davey, 1987
	24 Michigan lakes (America)		3~11.5	10~17			Manoylov et al., 2009
Reservoir	Embalse Rapel (Chile)	1984.03	7.8~10.4	28.6~37.7		2~16	Reynolds et al., 1986
	28 reservoirs scattered throughout Spain (Spain)	Winter of 1987~1988, summer of 1988	5.33 (3.88~6.78)	14.38 (12.39~16.33)		6.68 (1.95~9.69)	Gómez et al., 1995
River	Lower Paraná River (Argentina)	1993.04~1994.02	6.8 (2.0~28.0)	24.8 (7.0~59.5)		3.7 (1.0~26.0)	O'Farrell et al., 2001
	The Murray River (Australia)	1980.05~1992.06			90 (30.0~420.0)	Commonly around 6 cells	Hötzel and Croome, 1996
	Xijiang River (China)	2009.01~2009.12	9.25 (5.0~20.0)	14.03 (7.0~27.0)	192.46 (6.50~2652.00)	12.64 (1~156)	The present paper

4.4.2 Comparison of wavelet analysis and RDA

Wavelet analysis was applied as a direct measure to quantify statistical relationships between two non-stationary time series (Chatfield 1989, Daubechies 1992), for example the coherence between cell diameter and water temperature with time series dataset in the present study. As a complementary method of constrained ordination: RDA (Rao 1964) could analyze multivariate data, since all morphological and environmental variables were projected on a two-dimensional way in the present study. Thus, results from wavelet analysis exhibited correlations between two variables, while results from RDA projected all variables to a two-dimensional plane and exhibited the multi-correlations.

However, the decomposition function of wavelet analysis could make a better understanding on correlations of different periods with different scales (Daubechies 1990), since the correlation between the two analyzed variables varied with time series. Moreover, phase angles could help understanding the phase difference between the two variables deeply. Except for a qualitative result for the whole dataset, RDA referred little to correlations in time series and phase difference between variables. In a word, these two methods could complement and test each other's conclusions, which benefited our understanding on the temporal trend of morphological variability of *A. granulata* in correlations with environmental factors.

4.4.3 Correlations between morphological parameters and environmental factors

Although high coherence with nutrients was found in winter, cell diameter kept low values but with relatively higher cell length/cell diameter ratios (average 2.1 and maximum 3.0) during the entire cold season, and this made cell size closer to the narrow variant form, var. *angustissima*. Our studies in the Pearl River Estuary found that the dominance of the nominated form could be replaced by a narrow form in winter, which was explained as the narrow form could tolerate low temperatures (Wang et al. 2009). O'Farrell et al. (2001) also reported that a decrease in cell diameter and a slight increase in length occurred at the end of winter in the Lower Paraná River. However, Gómez et al. (1995) found no correlation between water

temperature and cell size in Spanish reservoirs. Our present results seemed to support this, since phase angles (pointing right) illustrated that both cell and filament dimensions varied before temperature change. Similarly, water temperature was eliminated from the significant impact factors by RDA. Therefore, we assumed that water temperature was an essential factor for algal growth and thus for size variations. Tsukada et al. (2006) reported that *A. granulata* could not grow at 8 ℃ but grew well at 32 ℃ in culture. Davey (1987) also observed the increase in filament length of *A. granulata* after cold winter. However, cell diameter did not increase immediately until it past a transitional period from March to April, characterized by frequent absences from water column and slight ascending fluctuations. This was thought to be the early stage of the life cycle. Davey (1987) considered that the spring absences were in a close relationship with the largely senescent process of over-wintering, and therefore responses to changing environmental conditions were delayed. The coherence analysis with environments and phase angles indicated that phosphate might contribute to the slight ascending fluctuations during the transitional period, and precipitation might explain the low occurrence rate since rainfall-triggered turbulence could cause the inconsecutive recruitment from sediments.

Two consecutive ascending-descending cycles in cell size occurred between early May and early June, with similar trends in both cell length and volume, but an inconsistent trend in filament length. The coherence between cell and filament dimensions disappeared during this period. Another explanation might be that cells started a new growth cycle under improved conditions, but filament growth was limited by water turbulence corresponding to ascending discharge. Evidence could be found from the coherence with water temperature and nitrite nitrogen for cell diameter, and coherence with discharge for filament length. RDA also reflected the negative relationship between morphology and discharge during this period. Previous studies had reported that fast flowing water and short residence time in conjunction with high river discharge prevented phytoplankton from efficiently utilizing resources and adequately developing population size (Salmaso & Braioni 2008, Salmaso & Zignin 2010, Waylett et al. 2013). Moreover, cell diameter was also found in anti-phase with

discharge, which might be the flushing impact that resulted in the shortened life cycle. Devercelli (2010) also reported that *A. granulata* could increase growth rate during flood periods. After this period, high coherence between cell and filament reappeared, but lasted for only one month, during which cell diameter decreased continuously, with a contrary ascending filament length. We regarded this short period as an important vegetative production period, since a corresponding rise in cell abundance was also confirmed (Wang et al. 2012). Total nitrogen was responsible for both cell and filament changes. Jewson (1992) gained similar conclusions from another filamentous centric diatom (*A. subarctica*) with similar morphology to *A. granulata*.

The other two consecutive cycles of cell diameter occurred between early July and early October, and its coherence with both cell and filament length disappeared during this period. Increasing water temperature and decreasing discharge in this period could provide better conditions for the algal growth (Zhu et al. 2013). And an increase in *A. granulata* abundance developing into the first peak was also found (Wang et al. 2012). However, the weak turbulent conditions could undermine to silicify colonial diatoms that typically occurred in large-sized natural water bodies (Mitrovic et al. 2011, Tavernini et al. 2011). Therefore, we assumed that the gradual decrease in filament length was a strategy to adapt to the adverse situations, since short filaments assisted with greater dispersal of cells within the water bodies. Moreover, the continual ascending trend in cell length could also increase the surface-area ratio and thereby the frictional resistance, especially with shortening filament length, finally resulting in lower sinking velocities (Young et al. 2012). In a word, when discharge impacted the life cycle length, both cell and filament length variations could counteract the change in conditions.

Extremely high values of both cell and filament dimensions were observed at the end of the year, which was regarded as an uncommon event, most probably the re-suspension from benthos. Results from benthic samples illustrated the dominance of *A. granulata* on surface sediment, and most cells were living (unpublished data). As for the uncommon large size of the algae, it might be explained in following ways. First, corresponding high density was also determined during this period, especially as

it occurred after a six week's low density period (Wang et al. 2012). Hötzel & Croome (1996) proposed that a rapid increase in abundance after prolonged periods of absence was attributed to the inoculums of cells from sediments. Second, a high filament length was generally unsuitable for *A. granulata* to maintain a distribution in the water column (Davey & Walsby 1985), especially with a discharge below 1500 $m^3 s^{-1}$ in drought seasons. Karim & Saeed (1978) reported that *A. granulata* sank and disappeared at over 6m-depth water column when turbulence became too low in the White Nile, and similar results were also reported in the Murray River (Hötzel & Croome 1996). Third, surface sediments could provide nutrient-rich conditions for *A. granulata* growth and the benthic algae were assumed to be saturated with nutrients and thus developed larger dimensions. The dramatic increase in nutrients (e.g. phosphate and silicate, unpublished data) was also related to nutrient regeneration from the sediment bed. Cross wavelet analysis illustrated that both cell and filament dimensions were in high coherence with almost all nutrients during this period. RDA also indicated that high coherence between morphology and nutrients mainly appeared at the end of the year. Other chain-forming diatoms had also shown a similar pattern of increase in filament length in response to greater nutrient abundance (Takabayashi et al. 2006, Poister et al. 2012). Fourth, the relatively calm conditions on surface sediments would limit the formation of separation valves, which was regarded as the key step for natural separation of the filaments (Davey & Crawford 1986), since necessary micro-turbulence on internal cells of a filament was lacking. Thus, long filament chains were easily formed under benthic calm conditions. Gómez et al. (1995) also reported that filaments were longer in the stratification period than the turnover period in Spanish reservoirs.

4.4.4 Conclusion

In conclusion, high coherence between morphological parameters, especially for cells, had been confirmed and demonstrated with both one-dimensional and two-dimensional analysis methods in the present study, and cell diameter was more sensitive than other parameters to environmental variables. However, the high coherence between morphological parameters could be disturbed by water turbulence

associated with discharge. Water temperatures had negative impacts on the occurrence rates and size values only during the spring-winter period. While discharge not only impacted the life cycle in terms of growth rate, but also impacted filament length by allowing for selection of chains with optimum buoyancy. The responses of algae size to nutrients, especially silicate, total nitrogen and phosphate, were associated with a life cycle. The above correlations were supported by both wavelet analysis and RDA. Moreover, the extremely high values at the end of the year could result from algal recruitment from benthos.

5. General conclusions and perspective

Generally, the present study focused on patterning and predicting the phytoplankton assemblages at the downstream of a large subtropical river, the Pearl River, China. Our results have first summarized the global research trends of phytoplankton through bibliometric analysis, highlighted that phytoplankton studies carried out in the large scale and long-term ways are in significant ascending trend, while that in traditional and local scale ways are in descending trend. We also modeled the temporal variation pattern of phytoplankton assemblages in the main stream, and the spatial pattern in the river delta system. The results indicated that physical and chemical variables impacted the temporal and spatial patterns, respectively. Finally, the morphological variability of the dominant diatom in response to environments implied that more sensitive and precise indicating role could be determined.

However, further investigations are encouraged to go deeply on the long-term mechanism of how phytoplankton diversity and distribution patterns response to environments and human activities, more research also need to be carried out in the upstream and sub-tributary to test the conclusions in the main stream. Further study of advanced statistical methods should be encouraged to advance our understanding of the profound correlations between the micro-organisms and environments under the global climate change background.

References

1. Ács É, Szabó K, Kiss K T, Hindák F, 2003. Benthic algal investigations in the Danube River and some of its main tributaries from Germany to Hungary. Biologia, Bratislava 58: 545-554.
2. Ács É, Szabó K, Kiss Á K, Tóth B, Záray G, Kiss K T, 2006. Investigation of epilithic algae on the River Danube from Germany to Hungary and the effect of a very dry year on the algae of the River Danube. Arch. Hydrobiol. Suppl. Large Rivers 16: 389-417.
3. Alexander R B, Böhlke J K, Boyer E W et al., 2009. Dynamic modeling of nitrogen losses in river networks unravels the coupled effects of hydrological and biogeochemical processes. Biogeochemistry, 93: 91-116.
4. Alhoniemi E, Himberg J, Parhankangas J, Vesanto J, 2000. SOM Toolbox [online] http://www.cis.hut.fi/projects/somtoolbox.
5. Alkawri A & Gamoyo M, 2014. Remote sensing of phytoplankton distribution in the Red Sea and Gulf of Aden. Acta Oceanologica Sinica, 33(9): 93-99.
6. Allan J D & Castillo M M, 2007. Stream ecology, 2nd edn. Springer, Berlin.
7. Almasri M N & Kaluarachchi J J, 2004. Assessment and management of long-term nitrate pollution of ground water in agriculture-dominated watersheds. Journal of Hydrology 295: 225-245.
8. Aymerich I F, Piera J, Mohr J, Soria-Frisch A, Obermayer K, 2009. Fast phytoplankton classification from fluorescence spectra: comparison between PSVM and SOM. Oceans 2009 – Europe: 1-4.
9. Babanazarova O V, Likhoshway Y V, Sherbakov D Y, 1996. On the morphological variability of *Aulacoseira baicalensis* and *Aulacoseira islandica* (Bacillariophyta) of Lake Baikal, Russia. Phycologia, 35(2): 113-123.
10. Barron R K, Siegel D A, Guillocheau N, 2014. Evaluating the importance of phytoplankton community structure to the optical properties of the Santa Barbara Channel, California. Limnology and Oceanography, 59(3): 927-946.

11. Battauz Y S, de Paggi S B J, Paggi J C, 2014. Passive zooplankton community in dry littoral sediment: Reservoir of diversity and potential source of dispersal in a subtropical floodplain lake of the Middle Parana River (Santa Fe, Argentina). International Review of Hydrobiology, 99(3): 277-286.
12. Bayer A E & Folger J, 1966. Some correlates of a citation measure of productivity in science. Sociology of Education, 39 (4): 381-390.
13. Beaver J R, Casamatta D A, East T L, Havens K E, Rodusky A J, James R T, Tausz C E, Buccier K M, 2013. Extreme weather events influence the phytoplankton community structure in a large lowland subtropical lake (Lake Okeechobee, Florida, USA). Hydrobiologia 709: 213-226.
14. Ben Mustapha Z, Alvain S, Jamet C, Loisel H, Dessailly D, 2014. Automatic classification of water-leaving radiance anomalies from global SeaWiFS imagery: Application to the detection of phytoplankton groups in open ocean waters. Remote Sensing Environment, 146: 97-112.
15. Biggs B J F & Smith R A, 2002. Taxonomic richness of stream benthic algae: effects of flood disturbance and nutrients. Limnology and Oceanography 47: 1175-1186.
16. Billen G, Gamier J, Hanset P, 1994. Modelling phytoplankton development in whole drainage networks: the RIVERSTRAHLER Model applied to the Seine river system. Hydrobiologia 289: 119-137.
17. Blauw A N, Beninc à E, Laane RWPM, Greenwood N, Huisman J, 2012. Dancing with the tides: fluctuations of coastal phytoplankton orchestrated by different oscillatory modes of the tidal cycle. Plos One, 7(11): e49319. doi:10.1371/journal.pone.0049319.
18. Bliss C I, 1970. Statistics in Biology. New York: McGraw-Hill Book Company.
19. Bolpagni R, Bresciani M, Laini A, Pinardi M, 2014. Remote sensing of phytoplankton-macrophyte coexistence in shallow hypereutrophic fluvial lakes. Hydrobiologia, 737(1): 67-76.
20. Bonada N, Rieradevall M, Prat N, 2007. Macroinvertebrate community structure and biological traits related to flow permanence in a Mediterranean

river network. Hydrobiologia, 589: 91-106.

21. Bortolini J C & Bueno N C, 2013. Seasonal variation of the phytoplankton community structure in the São João River, Iguaçu National Park, Brazil. Brazilian Journal of Biology, 73(1): 1-14.
22. Boyce D G, Lewis M R & Worm B, 2010. Global phytoplankton decline over the past century. Nature, 466: 591-596.
23. Callon M, Courtial J P, Laville F, 1991. Co-word analysis as a tool for describing the network of interactions between basic and technological research – the case of polymer chemistry. Scientometrics, 22(1): 155-205.
24. Cao H L, Hong Y G, Li M, Gu J D, 2012. Community shift of ammonia-oxidizing bacteria along an anthropogenic pollution gradient from the Pearl River Delta to the South China Sea. Applied Microbiology and Biotechnology, 94: 247-259.
25. Carneiro F M, Nabout J C, Bini L M, 2008. Trends in the scientific literature on phytoplankton. Limnology, 9: 153-158.
26. Centis B, Tolotti M, Salmaso N, 2010. Structure of the diatom community of the River Adige (North-Eastern Italy) along a hydrological gradient. Hydrobiologia, 639: 37-42.
27. Chatfield J, 1989. The Analysis of Time Series: An Introduction. Chapman & Hall, London.
28. Chau K W, 2005. Characterization of transboundary POP contamination in aquatic exosystems of Pearl River Delta. Marine Pollution Bulletin, 51: 960-965.
29. Cheng B, Wang M H, Morch A I, Chen N S et al, 2014. Research on e-learning in the workplace 2000-2012: A bibliometric analysis of the literature. Educational Research Review, 11: 56-72.
30. Cheung K C, Poon B H T, Lan C Y, Wong M H, 2003. Assessment of metal and nutrient concentrations in river water and sediment collected from the cities in the Pearl River Delta, South China. Chemosphere, 52: 1431−1440.
31. Coale K H, Johnson K S, Fitzwater S E et al, 1996. A massive phytoplankton

bloom induced by an ecosystem-scale iron fertilization experiment in the equatorial Pacific Ocean. Nature, 383: 495-501.

32. Cressie N, Frey J, Harch B, Smith M, 2006. Spatial prediction on a river network. Journal of Agricultural, Biological and Environmental Statistics, 11(2): 127-150.
33. Daubechie I, 1990. The wavelet transform, time–frequency localization and signal analysis. IEEE Transactions on Information Theory, 36(5): 961-1005.
34. Daubechies I, 1992. Ten Lectures on Wavelets, Society for Industrial and Applied Mathematics, Philadelphia.
35. Davey M C, 1986. The relationship between size, density and sinking velocity through the life cycle of *Melosira granulata* (Bacillariophyta). Diatom Research, 1(1): 1-18.
36. Davey M C & Crawford R M, 1986. Filament formation in the diatom *Melosira granulata*. Journal of Phycology, 22: 144-150.
37. Davey M C, 1987. Seasonal variation in the filament morphology of the freshwater diatom *Melosira granulata* (Ehr.) Ralfs. Freshwater Biology, 18: 5-16.
38. Davey M C & Walsby A E, 1985. The form resistance of sinking chains. British Phycological Journal, 20: 243-248.
39. Davies D L & Bouldin D W, 1979. A cluster separation measure. IEEE Transactions on Pattern Analysis and Machine Intelligence 1: 224-227.
40. Descy J P, 1993. Ecology of the phytoplankton of the River Moselle: effects of disturbances on community structure and diversity. Hydrobiologia 249: 111-116.
41. Descy J P, Leitao M, Everbecq E, Smitz J S, Deliège J F, 2012. Phytoplankton of the River Loire, France: a biodiversity and modeling study. Journal of Plankton Research 34(2): 120-135.
42. Desortová B & Punčochář P, 2011. Variability of phytoplankton biomass in a lowland river: response to climate conditions. Limnologica 41: 160-166.
43. Devercelli M, 2006. Phytoplankton of the Middle Paraná River during an

anomalous hydrological period: a morphological and functional approach. Hydrobiologia 563: 465-478.

44. Devercelli M, 2010. Changes in phytoplankton morpho-functional groups induced by extreme hydroclimatic events in the Middle Paraná River (Argentina). Hydrobiologia 639: 5-19.
45. Dmitrieva V A, 2011. Change in the river network and water resources in the upper and middle reaches of the Don River due to current climatic and economic conditions. Arid Ecosystems, 1(3): 193-199.
46. Dodds W K, 2006. Eutrophication and trophic state in rivers and streams. Limnology and Oceanography 51: 671-680.
47. Dokulil M T, 1994. Environmental control of phytoplankton productivity in turbulent turbid systems. Hydrobiologia 289: 65-72.
48. Dokulil M T, 2006. Short and long term dynamics of nutrients, potamoplankton and primary productivity in an alpine river (Danube, Austria). Arch. Hydrobiol. Suppl. 158/4 (Large Rivers 16): 473-493.
49. Dokulil M T & Donabaum U, 2014. Phytoplankton of the Danube River: Composition and Long-Term Dynamics. Acta Zoologica Bulgarica, Suppl. 7: 147-152.
50. Dokulil M T & Teubner K, 2005. Do phytoplankton communities correctly track trophic changes? An assessment using directly measured and palaeolimnological data. Freshwater Biology 50: 1594-1604.
51. Domingues R B, Barbosa A B, Sommer U, Galvão H M, 2012. Phytoplankton composition, growth and production in the Guadiana estuary (SW Iberia): unraveling changes induced after dam construction. Science of the Total Environment 416: 300-313.
52. Duan S W & Bianchi T S, 2006. Seasonal changes in the abundance and composition of plant pigments in particulate organic carbon in the lower Mississippi and Pearl Rivers. Estuaries and Coasts, 29: 427-442.
53. Dufrêne M & Legendre P, 1997. Species assemblages and indicator species: the need for a more flexible asymmetrical approach. Ecological Monographs, 67:

345-366.

54. Elliott J A, 2012. Predicting the impact of changing nutrient load and temperature on the phytoplankton of England's largest lake, Windermere. Freshwater Biology 57: 400-413.
55. Elliott J A, Irish A E, Reynolds C S, Tett P, 2000. Modelling freshwater phytoplankton communities: an exercise in validation. Ecological Modelling, 128(1): 19-26.
56. Elliott J A, Persson I, Thackeray S J, Blenckner T, 2007. Phytoplankton modeling of Lake Erken, Sweden by linking the models PROBE and PROTECH. Ecological Modelling, 202(3-4): 421-426.
57. Feng L, Wang D G, Chen B, 2011. Water quality modeling for a tidal river network: A case study of the Suzhou River. Frontiers of Earth Science, 5(4): 428-431.
58. Fornarelli R, Antenucci J P, Marti C L, 2013. Disturbance, diversity and phytoplankton production in a reservoir affected by inter-basin water transfers. Hydrobiologia 705: 9-26.
59. Garnier J, Billen G, Coste M, 1995. Seasonal succession of diatoms and Chlorophyceae in the drainage network of the Seine River: observations and modelling. Limnology and Oceanography 40: 750-765.
60. Gamier J, Billen G, Hannon E, Fonbonne S, Videnina Y, Soulie M, 2002. Modelling the transfer and retention of nutrients in the drainage network of the Danube River. Estuarine, Coastal and Shelf Science, 54: 285-308.
61. Gaston K J, 2000. Global patterns in biodiversity. Nature, 405: 220-227.
62. Gibson C E, 1984. Sinking rates of planktonic diatoms in an unstratified lake: a comparison of field and laboratory observations. Freshwater Biology, 14(6): 631-638.
63. Giraudoux P, 2006. Pgirmess: data analysis in ecology. R package version 1.3.8 http://perso.orange.fr/giraudoux/.
64. Gómez N, Riera J L, Sabater S, 1995. Ecology and morphological variability of *Aulacoseira granulata* (Bacillariophyceae) in Spanish reservoirs. Journal of

Plankton Research, 17(1): 1-16.

65. Grinsted A, Moore J C, Jevrejeva S, 2004. Application of the cross wavelet transform and wavelet coherence to geophysical time series. Nonlinear Processes in Geophysics, 11: 561-566.
66. Ha K, Jang M H, Joo G J, 2002. Spatial and temporal dynamics of phytoplankton communities along a regulated river system, the Nakdong River, Korea. Hydrobiologia, 470: 235-245.
67. Hamilton P B, Lavoie I, Ley L M, Poulin, M, 2011. Factors contributing to the spatial and temporal variability of phytoplankton communities in the Rideau River (Ontario, Canada). River Systems 19: 189-205.
68. Hamilton P B, Lavoie I, Poulin M, 2012. Spatial, seasonal and inter-annual variability in environmental characteristics and phytoplankton standing stock of the temperate, lowland Rideau River, Ontario, Canada. River Research and Applications 28: 1551-1566.
69. He Y F, Wang J W, Lek S, Cao W X, Lek-Ang S, 2011. Structure of endemic fish assemblages in the upper Yangtze River basin. River Research and Applications 27: 59-75.
70. Hillebrand H, Dûrselen C D, Kirschtel D, Pollingher U, Zohary T, 1999. Biovolume calculation for pelagic and benthic microalgae. Journal of Phycology 35: 403-424.
71. Hindâk F, Hindâková A, Marvan P, Heteša J, Hašler P, 2006. Diversity, abundance and volume biomass of the phytoplankton of the Morava River (Czech Republic, Slovakia) and the Dyje River (Czech Republic) in November 2005. Czech Phycology Olomouc 6: 77-97.
72. Ho Y S, 2014. Classic articles on social work field in Social Science Citation Index: a bibliometric analysis. Scientometrics, 98: 137-155.
73. Horn H, Paul L, Horn W, Petzoldt T, 2011. Long-term trends in the diatom composition of the spring bloom of a German reservoir: is *Aulacoseira* subarctica favoured by warm winters? Freshwater Biology, 56: 2483-2499.
74. Hornberger G & Wiberg P, 2006. Numerical methods in the hydrological

sciences, American Geophysical Union, Washington, DC.

75. Hötzel G & Croome R, 1996. Population dynamics of *Aulacoseira granulata* (Ehr.) SIMONSON (Bacillariophyceae, Centrales), the dominant alga in the Murray River, Australia. Archiv für Hydrobiologie, 136(2): 191-215.

76. Huang L M, Jian W J, Song X Y, Huang X P et al, 2004. Species diversity and distribution for phytoplankton of the Pearl River estuary during rainy and dry seasons. Marine Pollution Bulletin, 49: 588-596.

77. Ihaka R & Gentleman R, 1996. R: a language for data analysis and graphics. Journal of Computational and Graphical Statistics 5: 299-314.

78. Irigoien X, Huisman J, Harris R P, 2004. Global biodiversity patterns of marine phytoplankton and zooplankton. Nature, 429: 863-867.

79. Istvánovics V, Honti M, Vörös L, Kozma Z, 2010. Phytoplankton dynamics in relation to connectivity, flow dynamics and resource availability—the case of a large, lowland river, the Hungarian Tisza. Hydrobiologia, 637: 121-141.

80. Istvánovics V, Honti M, Kovács Á, Kocsis G, Stier I, 2014. Phytoplankton growth in relation to network topology: time-averaged catchment-scale modeling in a large lowland river. Freshwater Biology, 59(9): 1856-1871.

81. Jeong K S, Kim D K, Joo G J, 2006. River phytoplankton prediction model by Artificial Neural Network: Model performance and selection of input variables to predict time-series phytoplankton proliferations in a regulated river system. Ecological Informatics 1: 235-245.

82. Jewson D H, 1992. Size reduction, reproductive strategy and the life cycle of a centric diatom. Philosophical Transactions of the Royal Society London B, 336: 191-213.

83. Jewson D H, Granin N G, Zhdarnov A A, Gorbunova L A, Gnatovsky R Y, 2010. Vertical mixing, size change and resting stage formation of the planktonic diatom *Aulacoseira baicalensis*. European Journal of Phycology, 45: 354-364.

84. Jung S W, Kwon O Y, Yun S M, Joo H M, Kang J H, Lee J H, 2014. Impacts of dam discharge on river environments and phytoplankton communities in a

regulated river system, the lower Han River of South Korea. Journal of Ecology and Environment, 37(1): 1-11.

85. Justić D, Rabalais N N, Turner R E, 2002. Modeling the impacts of decadal changes in riverine nutrient fluxes on coastal eutrophication near the Mississippi River Delta. Ecological Modelling, 152(1): 33-46.
86. Kamenir Y, Dubinsky Z, Zohary T, 2004. Phytoplankton size structure stability in a meso-eutrophic subtropical lake. Hydrobiologia 520, 89-104.
87. Karadžić V, Simić G S, Natić D, Ržaničanin A, Ćirić M, Gačić Z, 2013. Changes in the phytoplankton community and dominance of *Cylindrospermopsis raciborskii* (Wolosz.) Subba Raju in a temperate lowland river (Ponjavica, Serbia). Hydrobiologia 711: 43-60.
88. Karim-Abdel A G & Saeed O M, 1978. Studies on the freshwater algae of the Sudan Ⅲ, vertical distribution of *Melosira granulata* (Ehr.) Ralfs in the White Nile, with reference to certain environmental variables. Hydrobiologia, 57: 73-79.
89. Keiser J & Utzinger J, 2005. Trends in the core literature on tropical medicine: A bibliometric analysis from 1952–2002. Scientometrics, 62 (3): 351-365.
90. Kilham P, Kilham S S, Hecky R E, 1986. Hypothesized resource relationships among African planktonic diatoms. Limnology and Oceanography, 31(6): 1169-1181.
91. Kilroy C, Larned S T, Biggs B J F, 2009. The non-indigenous diatom *Didymosphenia geminata* alters benthic communities in New Zealand rivers. Freshwater Biology, 54: 1990-2002.
92. King R S & Richardson C J, 2003. Integrating bioassessment and ecological risk assessment: an approach to developing numerical water-quality criteria. Environmental Management, 31: 795-809.
93. Kiss K T, l985. Changes of trophity conditions in the River Danube at Göd. Danubialia Hungarica XCIV. Annal. Univ. Sci. Budapest Sect. Biol., 24-26: 47-59.

94. Kiss K T, l987. Phytoplankton studies in the Szigetköz section of the Danube during 1981-1982. Archiv für Hydrobiologie, 78(2), Algological Studies 47: 247-273.

95. Kiss K T, 1994. Trophic level and eutrophication of the River Danube in Hungary. Verh.Internat.Verein.Limnol., 25: 1688-1691.

96. Kiss K T, 1996. Diurnal change of planktonic diatoms in the River Danube near Budapest (Hungary). Arch. Hydrobiol. Algol. Studies, 80: 113-122.

97. Kiss K T, 1997. The main results of phytoplankton studies on the River Danube and its side arm system at the Szigetköz area during the nineties (Hungary). In. Dokulil (Red.) Limnologische Berichte Donau 1997. Band. I: 153-158.

98. Kiss K T & Schmidt A, 1998. Changes of the Chlorophyta species in the phytoplankton of the Hungarian Section of the Danube river during the last decades (1961-1997). Biologia, Bratislava., 53: 509-518.

99. Kruskal J B & Wish M, 1978. Multidimensional Scaling. Sage Publications, Beverly Hills.

100. Larroudé S, Massei N, Reyes-Marchant P, Delattre C, Humbert J F, 2013. Dramatic changes in a phytoplankton community in response to local and global pressures: a 24-year survey of the river Loire (France). Global Change Biology, 19: 1620-1631.

101. Lei G Y, Yang Y F, Wang Q, Hu R, Wang Z H, 2007. Characteristics of water quality and phytoplankton community in the Guangzhou segment of the Pearl River. Journal of Jinan University (Natural Science), 28(3): 302-307. (in Chinese with English abstract)

102. Lepskaya E V, Jewson D H, Usoltseva M V, 2010. *Aulacoseira subarctica* in Kurilskoye Lake, Kamchatka: a deep, oligotrophic lake and important pacific salmon nursery. Diatom Research, 25(2): 323-335.

103. Leppistö L, Kauppila P, et al, 2006. Estimation of reference conditions for phytoplankton in a naturally eutrophic shallow lake. Hydrobiologia 568, 55-66.

104. Lewis W M Jr, Hamilton S K, Saunders J F, 1995. Rivers of northern South America. In: Cushing, C. E., Cummins, K. W., Minshall, G. W. (Eds), River

and stream ecosystems. Elsevier, Amsterdam.

105. Li L L, Ding G H, Feng N, Wang M H, Ho Y S, 2009. Global stem cell research trend: Bibliometric analysis as a tool for mapping of trends from 1991 to 2006. Scientometrics, 80(1): 39-58.

106. Li Q H, Chen L L, Chen F F, Gao T J et al, 2013. Maixi River estuary to the Baihua Reservoir in the Maotiao River catchment: phytoplankton community and environmental factors. Chinese Journal of Oceanology and Limnology, 31(2): 290-299.

107. Liao J Q & Huang Y, 2014. Global trend in aquatic ecosystem research from 1992 to 2011. Scientometrics, 98: 1203-1219.

108. Lionard M, Muylaert K, Van Gansbeke D, Vyverman W, 2005. Influence of changes in salinity and light intensity on growth of phytoplankton communities from the Schelde river and estuary (Belgium/The Netherlands). Hydrobiologia, 540: 105-115.

109. Litchman E & Klausmeier C A, 2008. Trait-based community ecology of phytoplankton. Annual Review of Ecology, Evolution and Systematics, 39: 615-639.

110. Lu F H, Ni H G, Liu F, Zeng E Y, 2009. Occurrence of nutrients in riverine runoff of the Pearl River Delta, South China. Journal of Hydrology, 376(1-2): 107-115.

111. Lu K X, 1990. Fishery Resources of the Pearl River System. Guangzhou: Guangdong Science and Technology Press, p27-39. (in Chinese)

112. Lu W X, Liu B J, Chen J F, Chen X H, 2014. Variation trend of precipitation in the Pearl River basin in recent 50 years. Journal of Natural Resources, 29(1): 80-90. (in Chinese with English abstract)

113. Luo Y Q, Melillo J, Niu S L et al, 2010. Coordinated approaches to quantify long-term ecosystem dynamics in response to global change. Global Change Biology, 17(2): 843-854.

114. Ma F C, Lyu P H, Yao Q, Yao L, Zhang S J, 2013. Publication trends and knowledge maps of global translational medicine research. Scientometrics,

98(1): 221-246.

115. Macias D, Navarro G, Echevarria F, Garcia C M, Cueto J L, 2007. Phytoplankton pigment distribution in the northwestern Alboran Sea and meteorological forcing: A remote sensing study. Journal of Marine Research, 65(4): 523-543.
116. Mallat S G, 1989. A theory for multi-resolution signal decomposition: the wavelet representation. IEEE Transactions on Pattern Analysis and Machine Intelligence, 11(7): 674-693.
117. Manoylov K M, Ognjanova-Rumenova N, Stevenson R J, 2009. Morphotype variations in subfossil diatom species of *Aulacoseira* in 24 Michigan Lakes, USA. Acta Botanica Croatica, 68(2): 401-419.
118. Maraun D & Kurths J, 2004. Cross wavelet analysis: significance testing and pitfalls. Nonlinear Processes in Geophysics, 11: 505-514.
119. Mata T M, Martins A A, Caetano N S, 2010. Microalgae for biodiesel production and other applications: a review. Renewable and Sustainable Energy Reviews, 14: 217-232.
120. Matthaei C D, Piggott J J, Townsend C R, 2010. Multiple stressors in agricultural streams: interactions among sediment addition, nutrient enrichment and water abstraction. Journal of Applied Ecology, 47: 639-649.
121. Mieleitner J & Reichert P, 2008. Modelling functional groups of phytoplankton in three lakes of different trophic state. Ecological Modelling, 211(3-4): 279-291.
122. Mihaljević M, Stević F, Špoljarić D, Žuna Pfeiffer T, 2014a. Application of morpho-functional classifications in the evaluation of phytoplankton changes in the Danube River. Acta Zoologica Bulgarica, suppl. 7: 153-158.
123. Mihaljević M, Stević F, Špoljarić D, Žuna Pfeiffer T, 2014b. Spatial pattern of phytoplankton based on the morphology-based functional approach along a river – floodplain gradient. River Research and Applications, DOI: 10.1002/rra.2739.
124. Mitrovic S M, Chessman B C, Davie A, Avery E L, Ryan N, 2008.

Development of blooms of *Cyclotella meneghiniana* and *Nitzschia spp.* (Bacillariophyceae) in a shallow river and estimation of effective suppression flows. Hydrobiologia 596: 173-185.

125. Mitrovic S M, Hardwick L, Dorani F, 2011. Use of flow management to mitigate cyanobacterial blooms in the Lower Darling River, Australia. Journal of Plankton Research, 33: 229-241.
126. Miyajima T, Nakanishi M, Nakano S I, Tezuka Y, 1994. An autumnal bloom of the diatom *Melosira granulata* in a shallow eutrophic lake: physical and chemical constraints on its population dynamics. Arch Hydrobiology, 130(2): 143-162.
127. Morlet J, Arens G, Fourgeau E, Giard D, 1982. Wave propagation and sampling theory—Part I: Complex signal and scattering in multilayered media. Geophysics, 47(2): 203-221.
128. Nakano S, Seike Y, Sekino T, Okumura M, Kawabata K, Fujinaga K, Nakanishi M, Mitamura O, Kumagai M, Hashitani H, 1996. A rapid growth of *Aulacoseira granulata* (Bacillariophyceae) during the typhoon season in the South Basin of Lake Biwa. Japanese Journal of Limnology, 57: 493-500.
129. Niu B B, Hong S, Yuan J F, Peng S, Wang Z, Zhang X, 2014. Global trends in sediment-related research in earth science during 1992-2011: a bibliometric analysis. Scientometrics, 98(1): 511-529.
130. Nogueira M G, 2000. Phytoplankton composition, dominance and abundance as indicators of environmental compartmentalization in Jurumirim Reservoir (Paranapanema River), São Paulo, Brazil. Hydrobiologia 431, 115-128.
131. Odermatt D, Pomati F, Pitarch J, Carpenter J et al, 2012. MERIS observations of phytoplankton blooms in a stratified eutrophic lake. Remote Sensing of Environment, 126: 232-239.
132. O'Farrell I, Izaguirre I, Vinocur A, 1996. Phytoplankton ecology of the Lower Paraná River (Argentina). Archiv für Hydrobiologie Supplement 115: 75-89.
133. O'Farrell I, Tell G, Podlejski A, 2001. Morphological variability of *Aulacoseira granulata* (Ehr.) Simonsen (Bacillariophyceae) in the Lower Paraná River

(Argentina). Limnology, 2: 65-71.

134. Ohniwa R L, Hibino A, Takeyasu K, 2010. Trends in research foci in life science fields over the last 30 years monitored by emerging topics. Scientometrics, 85(1): 111-127.
135. Ouyang T P, Zhu Z Y & Kuang Y Q, 2005. River water quality and pollution sources in the Pearl River Delta, China. Journal of Environmental Monitoring, 7: 664-669.
136. Ouyang T P, Zhu Z Y & Kuang Y Q, 2006. Assessing impact of urbanization on river water quality in the Pearl River Delta economic zone, China. Environmental Monitoring and Assessment, 120: 313-325.
137. Ozhan K & Bargu S, 2014. Distinct responses of Gulf of Mexico phytoplankton communities to crude oil and the dispersant corexit(A (R)) Ec9500A under different nutrient regimes. Ecotoxicology, 23(3): 370-384.
138. Patrick R & Reimer C W, 1966. The diatoms of the United States (exclusive of Alaska and Hawaii). Monogr Acad Nat Sci Philadelphia, 113:1-688
139. Peretyatko A, Teissier S, Symoens J J, Triest L, 2007. Phytoplankton biomass and environmental factors over a gradient of clear to turbid peri-urban ponds. Aquatic Conservation-Marine and Freshwater Ecosystems 17: 584-601.
140. Perkins M, Effler S W, Strait C M, 2014. Phytoplankton absorption and the chlorophyll a-specific absorption coefficient in dynamic Onondaga Lake. Inland Waters, 4(2): 133-146.
141. Piirsoo K, Pall P, Tuvikene A, Viik M, 2008. Temporal and spatial patterns of phytoplankton in a temperate lowland river (Emajõgi, Estonia). Journal of Plankton Research 30: 1285-1295.
142. Poister D, Kurth A, Farrell A, Gray S, 2012. Seasonality of *Aulacoseira ambigua* abundance and filament length: biogeochemical implications. Plankton Benthos Research, 7(2): 55-63.
143. PRWRC (Pearl River Water Resources Commission), 2006. Pearl River bulletins of 2000, 2001, 2002, 2003, 2004 and 2005. PRWRC, website: http://www.pearlwater.gov.cn. November 2006 (in Chinese).

144. Qiu D J, Huang L M, Zhang J L, Lin S J, 2010. Phytoplankton dynamics in and near the highly eutrophic Pearl River Estuary, South China Sea. Continental Shelf Research, 30(2): 177-186.

145. Qu H J & Kroeze C, 2010. Past and future trends in nutrients export by rivers to the coastal waters of China. Science of the Total Environment, 408: 2075-2086.

146. Rao C R, 1964. The use and interpretation of principal component analysis in applied research. Sankhya áA 26: 329-358.

147. Reavie E D, Jicha T M, Angradi T R, Bolgrien D W, Hill B H, 2010. Algal assemblages for large river monitoring: comparison among biovolume, absolute and relative abundance metrics. Ecological Indicators 10: 167-177.

148. Recknagel F, Ostrovsky I, Cao H Q, Zohary T, Zhang X Q, 2013. Ecological relationships, thresholds and time-lags determining phytoplankton community dynamics of Lake Kinneret, Israel elucidated by evolutionary computation and wavelets. Ecological Modelling, 255: 70-86.

149. Reynolds C S, 1984. The Ecology of Freshwater Phytoplankton. Cambridge University Press, Cambridge.

150. Reynolds C S, 1994. The long, the short and the stalled: on the attributes of phytoplankton selected by physical mixing in lakes and rivers. Hydrobiologia, 289: 9-21.

151. Reynolds C S, 2000. Hydroecology of river plankton: the role of variability in channel flow. Hydrological Processes 14: 3119-3132.

152. Reynolds C S, 2006. The Ecology of Phytoplankton. Cambridge University Press, Cambridge.

153. Reynolds C S, Huszar V, Kruk C, Naselli-Flores L, Melo S, 2002. Towards a functional classification of the freshwater phytoplankton. Journal of Plankton Research, 24: 417-428.

154. Reynolds C S, Montecino V, Graf M E, Cabrera S, 1986. Short-term dynamics of a *Melosira* population in the plankton of an impoundment in central Chile. Journal of Plankton Research, 8(4): 715-740.

155. Rojo C, Alvarez Cobelas M & Arauzo M, 1994. An elementary, structural

analysis of river phytoplankton. Hydrobiologia, 289: 43-55.

156. Romanov R E & Kirillov V V, 2012. Analysis of the seasonal dynamics of river phytoplankton based on succession rate indices for key event identification. Hydrobiologia 695: 293-304.
157. Rossetti G, Viaroli P, Ferrari I, 2009. Role of abiotic and biotic factors in structuring the metazoan plankton community in a lowland river. River Research and Applications 25: 814-835.
158. Ržaničanin A, Cvijan M, Krizmanić J, 2005. Phytoplankton of the Tisa River. Archives of Biological Sciences 57: 223-235.
159. Sabater S, Artigas J, Durán C, Pardos M, Romani A M, Tornés E, Ylla I, 2008. Longitudinal development of chlorophyll and phytoplankton assemblages in a regulated large river (the Ebro River). Science of the Total Environment 404: 196-206.
160. Salmaso N & Braioni M G, 2008. Factors controlling the seasonal development and distribution of the phytoplankton community in the lowland course of a large river in Northern Italy (River Adige). Aquatic Ecology 42: 533-545.
161. Salmaso N & Zignin A, 2010. At the extreme of physical gradients: phytoplankton in highly flushed, large rivers. Hydrobiologia 639: 21-36.
162. Schwaderer A S, Yoshiyama K, de Tezanos Pinto P, Swenson N G, Klausmeier C A, Litchman E, 2011. Ecoevolutionary differences in light utilization traits and distributions of freshwater phytoplankton. Limnology and Oceanography 56: 589-598.
163. Serizawa H, Amemiya T, Itoh K, 2009. Patchiness and bistability in the comprehensive cyanobacterial model (CCM). Ecological Modelling, 220(6): 764-773.
164. Shen P P, Li G, Huang L M, Zhang J L, Tan Y H, 2011. Spatio-temporal variability of phytoplankton assemblages in the Pearl River estuary, with special reference to the influence of turbidity and temperature. Continental Shelf Research, 31(16): 1672-1681.
165. Sipkay C, Kiss K T, Vadadi-Fölöp C, Homoródi R, Hufnagel L, 2012.

Simulation modeling of phytoplankton dynamics in a large eutrophic river, Hungary-Danubian Phytoplankton Growth Model (DPGM). Biologia 67(2): 323-337.

166. Smetacek V, Klaas C, Strass V H, Assmy P and others, 2012. Deep carbon export from a Southern Ocean iron-fertilized diatom bloom. Nature 487:313-319
167. Smith V, Joye S, Howarth R W, 2006. Eutrophication of freshwater and marine ecosystems. Limnology and Oceanography 51: 351-355.
168. Sneath P H A & Sokal R R, 1973. Numerical Taxonomy: The Principles and Practice of Numerical Classification. Freeman: San Francisco; 278.
169. Spatharis S, Tsirtsis G, Danielidis D B, Chi T D, Mouillot D, 2007. Effects of pulsed nutrient inputs on phytoplankton assemblage structure and blooms in an enclosed coastal area. Estuarine, Coastal and Shelf Science, 73: 807-815.
170. Stoermer E F, Kreis R G, Sicko-Goad L, 1981. A systematic, quantitative, and ecological comparison of *Melosira islandica* O. Müll. With *M. granulata* (Ehr.) Ralfs from the Laurentian Great Lakes. Journal of Great Lakes Research, 7(4): 345-356.
171. Sugimoto R, Sato T, Yoshida T, Tominaga O et al., 2014. Using stable nitrogen isotopes to evaluate the relative importance of external and internal nitrogen loadings on phytoplankton production in a shallow eutrophic lake (Lake Mikata, Japan). Limnology and Oceanography, 59(1): 37-47.
172. Takabayashi M, Lew K, Johnson A, Marchi A, Dugdale R, 2006. The effect of nutrient availability and temperature on chain length of the diatom, *Skeletonema costatum*. Journal of Plankton Research, 28: 831-840.
173. Talling J F & Prowse G A, 2010. Selective recruitment and resurgence of tropical river phytoplankton: evidence from the Nile system of lakes, rivers, reservoirs and ponds. Hydrobiologia, 637(1): 187-195.
174. Tavernini S, Pierobon E, Viaroli P, 2011. Physical factors and dissolved reactive silica affect phytoplankton community structure and dynamics in a lowland eutrophic river (Po River, Italy). Hydrobiologia 669: 213-225.

175. Thebault J M & Qotbi A, 1999. A model of phytoplankton development in the Lot River (France). Simulations of scenarios. Water Research 33(4): 1065-1079.

176. Torremorell A, Llames M E, Pérez G L, Escaray R, Bustingorry J, Zagarese H, 2009. Annual patterns of phytoplankton density and primary production in a large, shallow lake: the central role of light. Freshwater Biology 54: 437-449.

177. Townsend S A, Przybylska M, Miloshis M, 2012. Phytoplankton composition and constraints to biomass in the middle reaches of an Australian tropical river during base flow. Marine and Freshwater Research 63: 48-59.

178. Tremarin P I., Ludwig T A V, Torgan L C, 2012. Ultrastructure of *Aulacoseira brasiliensis* sp. nov. (Coscinodiscophyceae) and comparison with related species. Fottea, Olomouc, 12: 171-188.

179. Treusch A H, Demir-Hilton E, Vergin K L, Worden A Z, 2012. Phytoplankton distribution patterns in the northwestern Sargasso Sea revealed by small subunit rRNA genes from plastids. The ISME journal, 6: 481-492.

180. Trevisan R, Poggi C, Squartini A, 2010. Factors affecting diatom dynamics in the alpine lakes of Colbricon (Northern Italy): a 10-year survey. Journal of Limnology 69: 199-208.

181. Tsukada H, Tsujimura S, Nakahara H, 2006. Seasonal succession of phytoplankton in Lake Yogo over 2 years: effect of artificial manipulation. Limnology, 7: 3-14.

182. Turkia J & Lepistö L, 1999. Size variations of planktonic *Aulacoseira* Thwaites (Diatomae) in water and in sediment from Finnish lakes of varying trophic state. Journal of Plankton Research, 21(4): 757-770.

183. Turner R E, Rabalais N N, Justic D, Dortch Q, 2003. Global patterns of dissolved N, P and Si in large rivers. Biogeochemistry, 64: 297-317.

184. Ultsch A, 1993. Self-organizing neural networks for visualization and classification. In Information and classification, Opitz O, Lausen B, Klar R (eds). Springer-Verlag: Berlin, p307-313.

185. Usoltseva M V & Tsoy I B, 2010. Elliptical species of the freshwater genus

Aulacoseira in Miocene sediments from Yamato Rise (Sea of Japan). Diatom Research, 25(2): 397-415.

186. Van de Waal D B, Smith V H, Declerck S A J, Stam E C M, Elser J J, 2014. Stoichiometric regulation of phytoplankton toxins. Ecology Letters, 17(6): 736-742.
187. Van den Hoek C, Mann D G, Jahns H M, 1995. Algae: an Introduction to Phycology. Cambridge University Press, Cambridge, UK.
188. Van Raan A F J, 2005. For your citations only? Hot topics in bibliometric analysis Measurement. Interdisciplinary Research and Perspectives, 3: 50-62.
189. Várbíró G, Ács É, Borics G et al., 2007. Use of Self-Organizing Maps (SOM) for characterization of riverine phytoplankton associations in Hungary. Archiv für Hydrobiologie, 17: 383-394.
190. Vesanto J, 2000. Neural network tool for data mining: SOM Toolbox. Proceedings of Symposium on Tool Environments and Development Methods for Intelligent Systems (TOOLMET2000). Oulun yliopisto-paino, Oulu, Finland. p184-196.
191. Walters D M, Leigh D S, Freeman M C, Freeman, B J, Pringle C M, 2003. Geomorphology and fish assemblages in a Piedmont river basin, U.S.A.. Freshwater Biology, 48: 1950-1970.
192. Wang C, Li X H, Lai Z N, Tan X C, Pang S X, Yang W L, 2009. Seasonal variations of *Aulacoseira granulata* population abundance in the Pearl River Estuary. Estuarine, Coastal and Shelf Science, 85: 585-592.
193. Wang C, Li X H, Lai Z N, Fang Z, Wu Q, Hu X Y, Pang S X, 2010. Studying on phytoplankton community structure at the late stage of a *Phaeocystis globosa* bloom in the Pearl River Delta. Ecological Science, 29(2): 140-146. (in Chinese with English abstract)
194. Wang C, Lai Z N, Li Y F, Li X H, Lek S, Hong Y, Tan X C, Li J, 2012. Population ecology of *Aulacoseira granulata* in Xijiang River. Acta Ecologica Sinica, 32(15): 4793-4802. (in Chinese with English abstract)
195. Wang C, Lai Z N, Li X H, Gao Y, Li Y F, Yu Y M, 2013a. Annual variation

pattern of phytoplankton community at the downstream of Xijiang River. Acta Ecologica Sinica, 33(14): 4398-4408. (in Chinese with English abstract)

196. Wang C, Li X H, Lai Z N, Zeng Y Y, Gao Y, Liu Q F, Yang W L, 2013b. Temporal and spatial pattern of the phytoplankton biomass in the Pearl River Delta. Acta Ecologica Sinica, 33(18): 5835-5847. (in Chinese with English abstract)
197. Waylett A J, Hutchins M G, Johnson A C, Bowes M J, Loewenthal M, 2013. Physico-chemical factors alone cannot simulate phytoplankton behaviour in a lowland river. Journal of Hydrology, 497: 223-233.
198. Wehr J D & Descy J P, 1998. Use of phytoplankton in large river management. Journal of Phycology, 34: 741-749.
199. Wen H & Huang Y, 2012. Trends and performance of oxidative stress research from 1991 to 2010. Scientometrics, 91(1): 51-63.
200. Wetzel R G, 2001. Limnology: lake and river ecosystems, 3rd edn. Academic Press, San Diego, California.
201. Willig M R, Kaufman D M, and Stevens R D. 2003. Latitudinal gradients of biodiversity: pattern, process, scale, and synthesis. Annual Review of Ecology, Evolution, and Systematics, 34: 273-309.
202. Wu N C, Schmalz B, Fohrer N, 2011. Distribution of phytoplankton in a German lowland river in relation to environmental factors. Journal of Plankton Research, 33: 807-820.
203. Yan Y, Yang Z F, Liu Q, 2013. Nonlinear trend in streamflow and its response to climate change under complex ecohydrological patterns in the Yellow River Basin, China. Ecological Modelling, 252: 220-227.
204. Yang T, Xu C Y, Shao Q X, Chen X, 2010. Regional flood frequency and spatial patterns analysis in the Pearl River Delta region using L-moments approach. Stochastic Environmental Research and Risk Assessment, 24: 165-182.
205. Yang W, 2011. A multi-objective optimization approach to allocate environmental flows to the artificially restored wetlands of China's Yellow

River Delta. Ecological Modelling, 222(2): 261-267.

206. Young A M, Karp-Boss L, Jumars P A, Landis E N, 2012. Quantifying diatom aspirations: mechanical properties of chain-forming species. Limnology and Oceanography, 57: 1789-1801.

207. Yu S P, Yang J S, Liu G M, 2014. Impact assessment of Three Gorges Dam's impoundment on river dynamics in the north branch of Yangtze River estuary, China. Environmental Earth Sciences, 72(2): 499-509.

208. Yue T X, Liu J Y, Jørgensen S E, Ye Q H, 2003. Landscape change detection of the newly created wetland in Yellow River Delta. Ecological Modelling, 164(1): 21-31.

209. Zalocar de Domitrovic Y, Devercelli M, García de Emiliani M O, 2007. Phytoplankton. In: Iriondo, M. H., Paggi, J. C., Parma, M. J. (eds), The Middle Paraná River. Limnology of a Subtropical Wetland. Springer, Berlin, 175-203.

210. Zhang J Y, Jiang J L, Liu Q, Gong Y X, Wang Q, Yang Y F, 2011. The characteristics of microbial and phytoplankton community and water quality in the Guangzhou segment of Pearl River. Journal of Hydroecology, 32(2): 38-46. (in Chinese with English abstract)

211. Zhang X Q, Chen Q W, Recknagel F, Li R N, 2014. Wavelet analysis of time-lags in the response of cyanobacteria growth to water quality conditions in Lake Taihu, China. Ecological Informatics, 22: 52-57.

212. Zhang Y H, Liu X J, Nguyen T, He Q Q, Hong S, 2013. Global remote sensing research trends during 1991-2010: a bibliometric analysis. Scientometrics, 96: 203-219.

213. Zhao J, Cao W X, Yang Y Z, Wang G F et al, 2008. Measuring natural phytoplankton fluorescence and biomass: A case study of algal bloom in the Pearl River estuary. Marine Pollution Bulletin, 56(10): 1795-1801.

214. Zhao J, Peter H U, Zhang H S, Han Z B et al, 2014. Short- and long-term response of phytoplankton to ENSO in Prydz Bay, Antarctica: Evidences from field measurements, remote sensing data and stratigraphic biomarker records. Journal of Ocean University of China, 13(3): 437-444.

215. Zhu K X, Bi Y H, Hu Z Y, 2013. Responses of phytoplankton functional groups to the hydrologic regime in the Daning River, a tributary of Three Gorges Reservoir, China. Science of the Total Environment 450-451: 169-177.

Part Ⅱ: Publications

Fundam. Appl. Limnol. Vol. 185/3–4 (2014), 263–279
published online 11 November 2014, published in print December 2014

Article

Patterning and predicting phytoplankton assemblages in a large subtropical river

Chao Wang[1, 2, 4], **Xinhui Li**[1, 4, *], **Zini Lai**[1, 4], **Yuefei Li**[1, 4], **Alain Dauta**[3] and **Sovan Lek**[2]

With 7 figures and 2 tables

Abstract: Through time-series sampling during the whole of 2009, phytoplankton patterns and prediction models were built up with a self-organizing map (SOM) and Linear Discriminant Analysis (LDA) within the downstream region of a large subtropical river, the Pearl River (China). The excessive nutrient conditions resulted in a diatom dominant phytoplankton community. While green algae contributed more only in species diversity, as they were mainly dependent on inoculations from external resources, and their abundance remained low under fast and turbid flow conditions. The time periods of phytoplankton samples were classified into four clusters using a self-organizing map (SOM) based on species similarities. These clusters were clearly different with respect to species richness, biomass and indicators. The LDA predicting model indicated that these clusters of species assemblages could easily be differentiated by physical factors such as water temperature, discharge and precipitation. As for nutrients, only phosphate could have an occasional impact on phytoplankton assemblages. By using the environmental variables, the global score for predicting the assemblages was 64.2 %, with the predicting performance rates for clusters I, IIa, IIb1 and IIb2 at 50, 48, 62 and 74 %, respectively. Cluster I benefited from a combination of higher temperatures and low discharge, and had the highest species richness and biomass. Cluster IIb1 benefited from high discharge and diverse species inoculations, but interruptions in increases of biomass. Cluster IIb2 showed that low temperatures resulted in both low species richness and biomass. Cluster IIa, characterized by phosphate, indicated that phytoplankton assemblages were occasionally P-limited in the studied section. In conclusion, the annual patterns of the downstream phytoplankton assemblages in the Pearl River were mainly regulated by physical factors but occasionally limited by nutrients.

Key words: phytoplankton, river, self-organizing map (SOM), Linear Discriminant Analysis (LDA), environments.

Introduction

Freshwater ecosystems throughout the world are experiencing increasing pressures from both climate changes and anthropogenic activities. Such pressures generally lead to variations in temperature, light availability, hydrologic conditions and nutrient contents of the water bodies (Devercelli 2010, Hamilton et al. 2012, Larroudé et al. 2013). Rivers, the typical lotic freshwater ecosystems, are also regarded as important pathways for the flow of energy, matter, and organisms through the landscape (Karadžić et al. 2013).

Authors' addresses:

[1] Pearl River Fisheries Research Institute, Chinese Academy of Fishery Science, Guangzhou 510380, China

[2] Université Toulouse, Lab Evolution & Diversité Biologique, UMR 5174, CNRS – Université Paul Sabatier, 118, route de Narbonne, 31062 Toulouse, Cedex4, France

[3] Université Toulouse, Laboratoire d'Ecologie fonctionnelle et environnement, UMR 5245, CNRS—Université Paul Sabatier, 118, route de Narbonne, 31062 Toulouse, Cedex4, France

[4] Experimental Station for Scientific Observation on Fishery Resources and Environment in the Middle and Lower Reaches of Pearl River, 526100, Ministry of Agriculture the People's Republic of China

* Corresponding author; lxhui01@aliyun.com

DOI: 10.1127/fal/2014/0684

www.schweizerbart.de
1863-9135/14/0684 $ 4.25

Phytoplankton constitute the base level of the aquatic food web, and species composition and variation can efficiently respond to environmental factors that regulate biological activity and water quality (Reavie et al. 2010, Hamilton et al. 2011, Hamilton et al. 2012). Studies on phytoplankton have been extensive in lentic fresh-waters such as lakes and reservoirs, where long residence times and low flow velocities allow sufficient time for growth and reproduction (Sabater et al. 2008, Torremorell et al. 2009, Elliott 2012, Fornarelli et al. 2013). However, relevant studies in lotic ecosystems (such as streams and rivers) are still less (Kiss 1987, Piirsoo et al. 2008, Wu et al. 2011, Sipkay et al. 2012) compared with lentic systems. Spatial and temporal patterns of phytoplankton communities in large rivers are driven by a mixture of physical, chemical and biological factors, which vary seasonally and their relative weight depends on river typologies (Rossetti et al. 2009, Tavernini et al. 2011). The response of phytoplankton to environmental factors has become a central topic of current research (Wu et al. 2011). The identification of key factors that control phytoplankton in a particular water body is essential for choosing an appropriate management strategy for the maintenance of a desired ecosystem (Peretyatko et al. 2007). However, as environmental drivers co-act simultaneously, it is not easy to identify which has the most important impact on the river community. Fortunately, more and more ecological models have been applied to phytoplankton studies in such lotic aquatic systems for this purpose (Billen et al. 1994, Thebault & Qotbi 1999, Jeong et al. 2006, Sipkay et al. 2012). Self Organizing Maps (SOMs) are capable of evaluating large and dense datasets, and have been applied successfully to phytoplankton studies for the classification and rapid discrimination function (Várbíró et al. 2007, Aymerich et al. 2009). To date, the discussion is still open: what are the main controlling factors of river phytoplankton? Are the factors physical (Devercelli 2010, Salmaso & Zignin 2010, Domingues et al. 2012) or chemical (Dodds 2006, Torremorell et al. 2009), or a combination of both? Therefore, further studies are still required, notably those reporting on classic large rivers in the world, and advanced ecological models may provide new approaches to answer the above questions.

The Pearl River Delta, characterized by a prosperous economy and dense human population, has always been an important center of southern China for politics, economics and culture. The Pearl River, the original river of this region, is the largest lowland river of South China. The oldest data for phytoplankton in the river basin are from the beginning of 1980s, when a general survey on aquatic organisms and water environments was carried out through the cooperation between several regional research organizations (Lu 1990). However, only a simple primary dataset was collected during the investigations, and the minimal identification unit of phytoplankton composition was only specific to genus; temporal and spatial distributing patterns were also unclear. After this basic investigation, relevant studies on the phytoplankton ecology of the main stream were interrupted for the following thirty years. The authors have focused on relevant studies in recent years, and the results in the main stream have been reported (Wang et al. 2012, Wang et al. 2013). Further understanding on phytoplankton patterns and predictions is in progress, introducing more advanced statistical methods with the goal of finally providing more effective management guidelines for government.

This paper describes and evaluates the annual pattern of phytoplankton assemblages at a fixed downstream sampling site of the Pearl River via yearly time-series sampling. The classification pattern model of phytoplankton assemblages was built up using a self-organizing map (SOM) and analysis of the correlations between temporal patterns and environmental factors was done using Linear Discriminent Analysis (LDA) as a way to identify the main driving factors and to assess the prediction capacity. Moreover, the dataset allowed us to formulate a hypothesis that the annual patterns of phytoplankton were fully constrained by physical drivers, i.e., water temperature, discharge and rainfall, in such a eutrophic downstream region where nutrients were supposed to be superfluous.

Methods and data treatment

Study site

The Pearl River, with a length of 2,320 km, a catchment area of 450,000 km^2, and an annual discharge of 3.3×10^{11} m^3, is the third longest river in China. The river consists of three major tributaries: West River, North River and East River, merging at the Pearl River Delta and ultimately flowing into the South China Sea. The West River (2129 km), running through Guangdong province and Guangxi province, is the largest tributary of the Pearl River (catchment area 345,700 km^2). The Changzhou Dam was built upstream in the West River in 2007, but it did not completely cut the river flow for shipping reasons. A seasonal flow regime of West River corresponds to high flows during spring and summer, and low flows during autumn and winter.

The Zhaoqing section of the West River, with an average width of 1,100 m and a peak flow of 30,000 m^3 s^{-1}, is the passage for the river flow entering into the downstream river web of the Pearl River Delta. Our fixed long-term sampling site

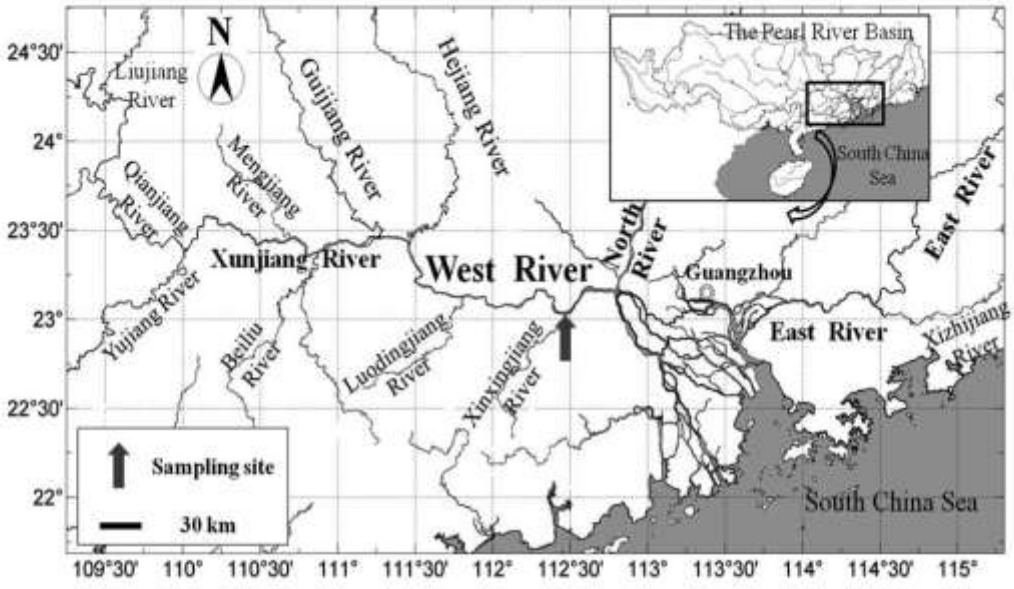

Fig. 1. The downstream river network of the Pearl River, including its location in the Pearl River Basin, river tributaries and sampling site. The West River is the main tributary of the Pearl River. The sampling site in the Zhaoqing section is a fixed long-term sampling station established in 2005.

(23°2′40″N, 112°27′5″E) is located in the Zhaoqing section near the wharf of the Zhaoqing Fishery Administration, which is about 160 km upstream from the Pearl River Estuary (Fig. 1). The depth of the sampling site is between the lowest and highest water levels and ranges from 3 to 5 meters.

Sampling work and collected data

In order to understand the temporal variations of primary production and their correlation with environmental factors, phytoplankton samples and environmental data have been collected since 2009. Phytoplankton samples were collected at 8:00 am every 5 days each month. For each phytoplankton sample, 1 L of water was collected from 0.5 m below the surface using a 5 L HQM-1 sampler. The sample was put into a polyethylene bottle and fixed immediately with formaldehyde solution (5 %). A phytoplankton sample was fixed and concentrated by sedimentation to 100 ml. All the algae were counted using a 1-ml Sedgewick-Rafte counting frame (inverted microscope Nikon Eclipse TS100). A second phytoplankton sample was assigned for diatom identification and enumeration. This sample was concentrated and treated with dilute HCl and H_2O_2, and at least 400 valves were counted. The systematic grouping of phytoplankton was done following the manual of Van den Hoek et al. (1995).

An additional water sample of 250 ml was filtered *in situ*, and taken back to the laboratory for nutrient analysis (phosphate, silicate, total nitrogen, nitrate, nitrite and ammonia) using a water flow injection analyzer (Skalar-SA1100) and spectrophotometer (Shimadzu UV-2501PC). Water temperatures were recorded using an automatic water temperature recorder at a frequency of once per hour at the sampling site. Water discharge data were downloaded from the website: http://xxfb.hydroinfo.gov.cn. Precipitation was obtained from the website: http://weatheronline.co.uk.

Data treatment

Phytoplankton biomass was calculated from the biovolume of each species, assuming unit specific gravity, by geometrical approximation according to Hillebrand et al. (1999). Median values of both species richness and biomass were used to represent the population dynamics of each group or cluster.

Phytoplankton species assemblages were classified using a self-organizing map (SOM), which is one of the most well-known neural networks with unsupervised learning rules. In this study, the temporal variation pattern of phytoplankton species was described by the SOM model: a total of 69 species with more than 10 % occurrence rate was analyzed. Sampling dates with similar species composition and structure were classified into the same neuron or into neighboring neurons, according to the degree of dissimilarity. A total of 90 neurons (virtual units) was the output of the SOM, which was arranged into a 10 × 9 hexagonal lattice to provide better visualization. The map size was set according to $5 \times (\text{number of samples})^{1/2}$ (Vesanto 2000), and then based on the minimum best values of quantization and topographic errors. The cells of the map were then subdivided into different groups according to the similarity of the weight vectors of the neurons using Ward's linkage method. The group numbers were mainly based on the degree of dissimilarity of each SOM cell in the hierarchical clustering. The unified distance matrix (U-matrix; Ultsch 1993) and Davies-Bouldin index (Davies & Bouldin 1979) were also applied to reinforce the group definition. All these analyses were carried out with Matlab software (Mathworks Inc 2001) using the SOM toolbox (Alhoniemi et al. 2000).

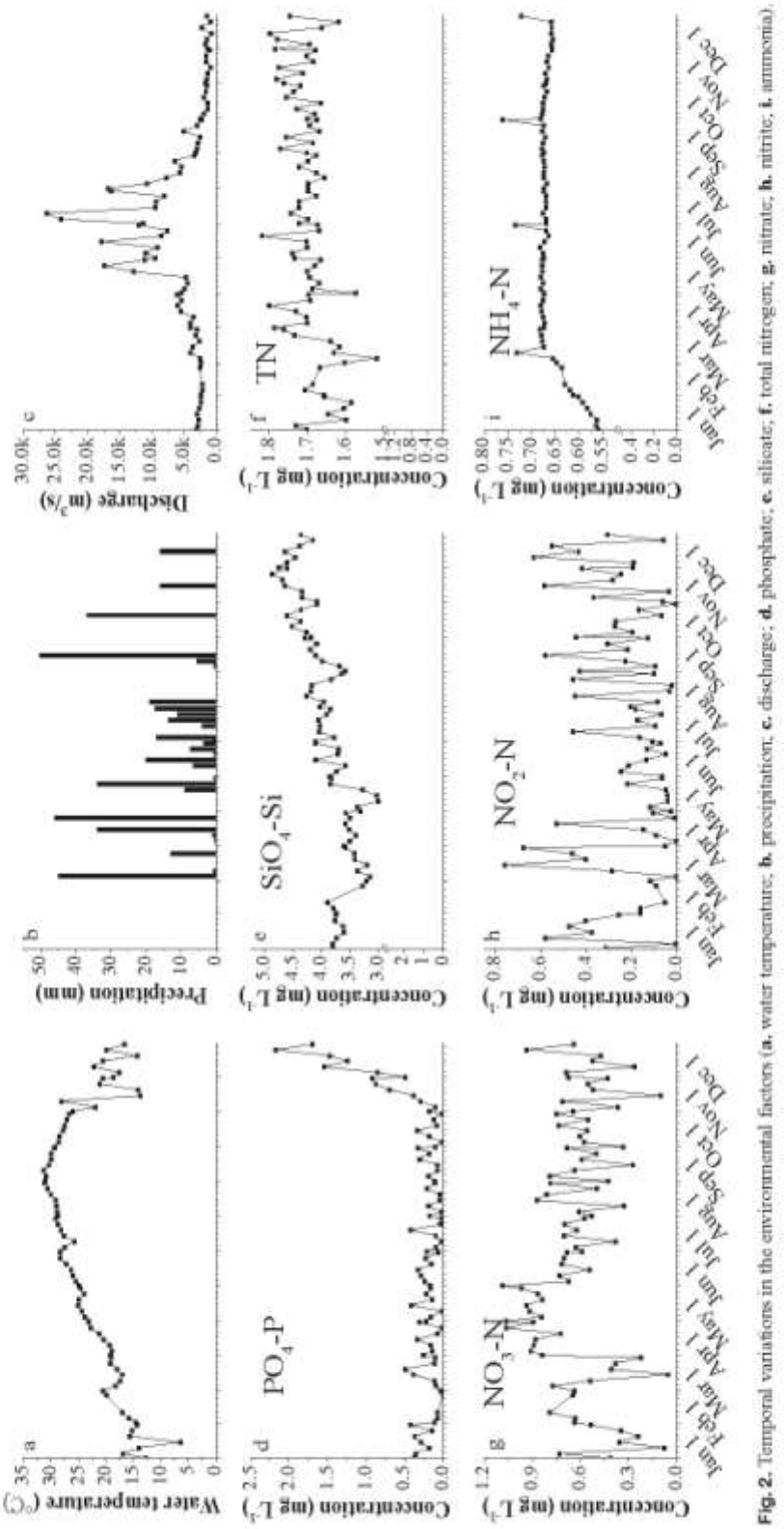

Fig. 2. Temporal variations in the environmental factors (**a.** water temperature; **b.** precipitation; **c.** discharge; **d.** phosphate; **e.** silicate; **f.** total nitrogen; **g.** nitrate; **h.** nitrite; **i.** ammonia).

To assess the effectiveness of the hierarchical clustering on the SOM units, the cophenetic correlation coefficient (Sneath & Sokal 1973) was calculated using R software (Ihaka & Gentleman 1996). The contributions of each input component with respect to cluster structures were obtained from weight vectors of the SOM and then visualized by boxplot (He et al. 2011). We used the Kruskall-Wallis test to compare differences of species richness among clusters in the R software. After the Kruskall-Wallis test, multiple comparison tests were also carried out in the R software using the 'pgirmess' package (Giraudoux 2006).

The IndVal method was used to identify indicator species, which were defined as the most characteristic species of each group (He et al. 2011). Based on the fidelity and the specificity of species for each cluster, INDVAL 2.0 was used to identify indicator species of different phytoplankton assemblages at the downstream of the West River. The formula is as following: $IndVal_{ij} = A_{ij} \times B_{ij} \times 100$, where $A_{ij} = Nbiomass_{ij} / Nbiomass_{+j}$, $B_{ij} = Nsample_{ij} / Nsample_{+j}$, and i means species i, j means cluster j. Only significant and greater than 25 IndVal have been taken into account. In this way, it implies that a characteristic species occurs in at least 50 % of one site's group, and that its relative abundance in that group reaches at least 50 %.

Linear Discriminant Analysis (LDA) was carried out to determine which environmental variables discriminate between the clusters previously defined by the SOM procedure. Standardized coefficients for each variable in each discriminated function represent the contribution of the respective variable to the discrimination between clusters. A random Monte Carlo test with 1000 permutations was used to reveal the significance of environmental variables among clusters. The Kruskall-Wallis test was then carried out to reveal the difference of environmental variables among clusters, and then multiple comparison tests were also conducted in the R software using the 'pgirmess' package.

Results

Environmental factors

Temporal variations of nine environmental factors are shown in Fig. 2. Water temperature increased continually from the beginning of the year and peaked on September 10th, and then decreased continually to the end of the year (Fig. 2a). The values ranged from 6.4 to 31.4 °C, with a median value of 24.4 °C. There was rain in all seasons except for winter (January and February). Precipitation was relatively low but frequent in summer (flood season) compared with other seasons, while heavy rain could occur occasionally in drought winters (Fig. 2b). In winter, discharge was very low, with values under 3000 $m^3 \cdot s^{-1}$. It increased gradually to floods (June to August) with values no less than 5000 $m^3 \cdot s^{-1}$ (Fig. 2c). The concentration of phosphate fluctuated under 0.5 mg L^{-1} before November, but it increased dramatically after that and peaked on December 25th (Fig. 2d). The concentration of silicate fluctuated around 3.5 mg L^{-1} before May, and then increased continuously to the end of the year (Fig. 2e). The concentration of total nitrogen showed large fluctuations before May, but remained steadily around 1.70 mg L^{-1} after that period (Fig. 2f). The concentration of nitrate had a similar trend as total nitrogen before May, and then it showed a weak decreasing trend to the end of the year (Fig. 2g). The concentration of nitrite fluctuated dramatically during most times of the year except in May and June (Fig. 2h). The concentration of ammonia increased gradually from the beginning of the year and remained around 0.67 mg L^{-1} from mid March, with only four high values appearing on March 10th, June 30th, September 30th and December 30th, respectively (Fig. 2i).

Phytoplankton composition

A total of 245 algal taxa (including varieties and forms) were identified. Seven phytoplankton phylum groups – Bacillariophyceae, Chlorophyceae, Euglenophyceae, Cyanobacteria, Dinophyceae, Chrysophyceae and Xanthophyceae – were represented. The highest richness was 104 taxa for Bacillariophyceae, contributing 42.4 % of the total species numbers; the second was Chlorophyceae (85 taxa, 34.7 %); third was 31 taxa for Euglenophyceae (12.7 %), and the fourth was 18 taxa for Cyanobacteria (7.3 %). Of the Bacillariophyceae, *Navicula* had the highest richness of 14 species, and the following were *Aulacoseira* (*Melosira*) (10 taxa), *Nitzschia* (9 taxa), *Cymbella* (8 taxa), *Synedra* (8 taxa). Of the Chlorophyceae, *Scenedesmus* had the highest richness with 17 species, and *Pediastrum* had 8 species. *Euglena* of the Euglenophyceae had 17 species.

Latin names and abbreviations of the 107 taxa whose occurrence rate was greater than 5 % are listed in Table 1. We can see from Fig. 3 that a single species shows an apparently high proportion of the biomass (> 80 %), and even the second rank species is lower than 5 %, which means almost a 20-fold difference (Fig. 3a). The two species are *Aulacoseira granulata* var. *granulata* and *Melosira varians* respectively. According to occurrence frequency rank (Fig. 3b), four species are very common (occurrence rate > 70 %), and one even beyond 80 %. The sequence of the four species is *A. granulata* var. *granulata* > *M. varians* > *Closterium acutum* var. *variabile* > *Cyclotella meneghiniana*. Two other species were also common (occurrence rate between 50 % and 70 %): *Cyclotella comta* and *Desmodesmus armatus*. The other 13 species were moderately common (occurrence rate between 25 % and 50 %). Eighty-eight species were scarce (occurrence rate < 25 %), and among them,

Table 1. List of 107 taxa with an occurrence rate over 5% in all samples.

Group	Species name	Abbreviation	Occurrence rate (%)
Bacillariophyceae	*Amphora ovalis*	Amov	9.9
	Amphora sp.	Amsp	22.2
	Aulacoseira ambigua	Auam	19.8
	Aulacoseira distans	Audi	27.2
	Aulacoseira granulata var. *curvata*	Augc	12.3
	Aulacoseira granulata var. *granulata*	Augg	82.7
	Aulacoseira granulata var. *angustissima*	Auga	35.8
	Aulacoseira granulata var. *angustissima* f. *spiralis*	Augas	6.2
	Aulacoseira italica	Auit	13.6
	Bacillaria paxillifera	Bapa	23.5
	Belonastrum berolinensis	Bebe	30.9
	Caloneis sp.	Casp	23.5
	Carinastigma rectum	Care	14.8
	Cocconeis sp.	Cosp	18.5
	Craticula cuspidata	Crcu	8.6
	Cyclotella bodanica	Cybo	16
	Cyclotella comta	Cyco	63
	Cyclotella meneghiniana	Cyme	74.1
	Cymbella affinis	Cyaf	22.2
	Cymbella cistula	Cyci	9.9
	Cymbella sp.	Cysp	17.3
	Cymbella tumida	Cytu	12.3
	Fragilaria crotonensis	Frcr	7.4
	Fragilaria hinganensis	Frhi	11.1
	Fragilaria hinganensis var. *longissima*	Frhl	19.8
	Fragilaria sp.	Frsp	12.3
	Gomphonema sp.	Gosp	8.6
	Gyrosigma sp.	Gysp	14.8
	Halamphora coffeaeformis	Haco	8.6
	Hantzschia sp.	Hasp	7.4
	Licmophora abbreviata	Liab	46.9
	Melosira varians	Meva	75.3
	Navicula dicephala	Nadi	17.3
	Navicula lanceolata	Nala	11.1
	Navicula sp.	Nasp	44.4
	Navicula subminuscula	Nasu	21
	Navicula transitans	Natr	9.9
	Nitzschia acicularis	Niac	17.3
	Nitzschia lorenziana var. *subtilis*	Nils	9.9
	Nitzschia palea	Nipa	33.3
	Nitzschia pandurifformis	Nipan	24.7
	Nitzschia sigmoidea	Nisi	6.2
	Pinnularia microstauron	Pimi	6.2
	Pleurosigma sp.	Plspl	18.5
	Pseudostaurosira brevistriata	Psbr	6.2
	Surirella minuta	Sumi	16
	Surirella robusta	Suro	8.6
	Synedra sp.	Sysp	22.2
	Synedra ulna	Syul	30.9
	Tabellaria sp.	Tasp	7.4
	Tabularia fasciculata	Tufa	14.8
	Thalassiosira sp.	Thsp	24.7
	Ulnaria acus	Ulac	7.4

Table 1. Continued.

Group	Species name	Abbreviation	Occurrence rate (%)
Bacillariophyceae	*Ulnaria contracta*	Ulco	6.2
	Ulnaria delicatissima var. *angustissima*	Ulaa	12.3
Chlorophyceae	*Actinastrum hantzschii*	Acha	14.8
	Acutodesmus acuminatus	Acac	9.9
	Acutodesmus dimorphus	Acdi	25.9
	Ankyra ancora	Anan	14.8
	Chlamydocapsa planctonica	Chpl	7.4
	Closterium acutum var. *variabile*	Clav	75.3
	Closterium praelongum	Clpr	11.1
	Cosmarium sp.	Cospl	6.2
	Crucigenia fenestrata	Crfe	18.5
	Crucigenia lauterbornei	Crla	9.9
	Desmodesmus armatus	Dear	71.6
	Desmodesmus denticulatus	Dede	12.3
	Desmodesmus perforatus	Depe	9.9
	Dictyosphaeria cavernosa	Dica	28.4
	Micractinium pusillum	Mipu	14.8
	Monactinus simplex	Mosi	11.1
	Monoraphidium arcuatum	Moar	12.3
	Monoraphidium griffithii	Megr	18.5
	Monoraphidium komarkovae	Moko	12.3
	Monoraphidium mirabile	Momi	42
	Palmella mucosa	Pamu	9.9
	Pediastrum simplex var. *duodenarium*	Pesd	16
	Pediastrum tetras var. *tetraodon*	Pett	6.2
	Planktosphaeria sp.	Plsp	12.3
	Quadrigula chodatii	Quch	11.1
	Radiococcus planktonicus	Rapl	14.8
	Scenedesmus armatus var. *boglariensis* f. *bicaudatus*	Scabb	25.9
	Scenedesmus biguga	Scbi	11.1
	Scenedesmus communis	Scco	18.5
	Schroederia nitzschioides	Scni	19.8
	Sphaerocystis schroeteri	Spsc	9.9
	Staurastrum gracile	Stgr	6.2
	Westella botryoides	Webo	8.6
Cyanobacteria	*Aphanocapsa* sp.	Apsp	6.2
	Arthrospira platensis	Arpl	9.9
	Merismopedia glauca	Megl	6.2
	Merismopedia tenuissima	Mete	12.3
	Microcystis sp.	Misp	8.6
	Oscillatoria fraca	Osfr	29.6
	Oscillatoria limosa	Osli	9.9
	Oscillatoria subbrevis	Ossu	30.9
	Phormidium chlorinum	Phch	16
	Raphidiopsis curvata	Racu	8.6
Euglenophyceae	*Euglena cylindrica*	Eucy	11.1
	Euglena gracilis	Eugr	6.2
	Euglena mutabilis	Eumu	8.6
	Euglena sp.	Eusp	11.1
	Lepocinclis acus	Leac	6.2
	Phacus circulatus	Phci	6.2
	Trachelomonas sp.	Trsp	22.2
Dinophyceae	*Peridinium umbonatum*	Peum	6.2
	Peridinium sp.	Pesp	14.8

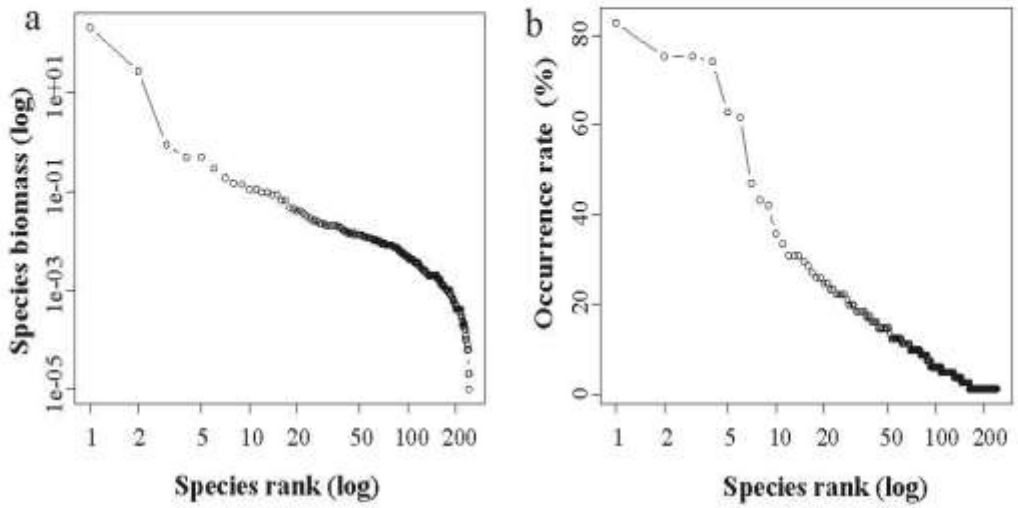

Fig. 3. The rank of biomass and occurrence rate for all phytoplankton species (**a.** biomass; **b.** occurrence rate).

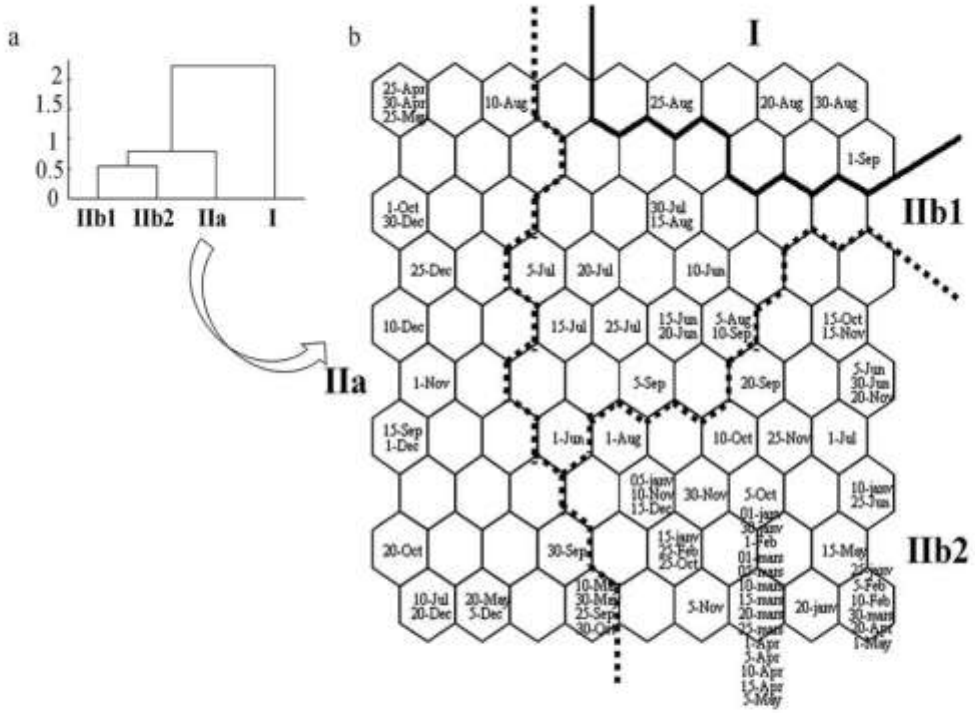

Fig. 4. Relationship between each cluster and distribution of the sampling days on the SOM (The similarity of neighboring cells can be grouped in clusters (bold line) and sub-clusters (dashed line) using a U-matrix algorithm).

thirty-eight species were very scarce (occurrence rate <10%). Above all, *A. granulata* var. *granulata* is the single predominant species of the phytoplankton assemblages.

The species assemblage analysis

The samples in terms of 81 sampling days were projected onto the 10 × 9 SOM map cells according to the similarity of their species composition (Fig. 4b). Based

on the phytoplankton composition and similarity of different cells, two clusters of communities, I and II, were primarily identified. The cluster II was then subdivided into two smaller sub-clusters, IIa and IIb (IIb was further subdivided into two sub-clusters IIb1 and IIb2) (Fig. 4a). In all, four clusters were defined on the SOM. No further subdivisions were considered in the present study. The cophenetic correlation coefficient ($r = 0.81$) indicated that the hierarchical clustering of different cells was stable. Cluster IIb2 had the highest with 43 samples, which covered all the 12 months of the year, and most samples of this cluster belonged to the cold season. For example, all the samples from January to March could be found there. Cluster IIa had the second highest with 21 samples, which covered all the months from April to December but June. The last four months contributed more than half of the total. Cluster IIb1 had 13 samples, which covered all the months from June to September, and most samples of June and July contributed to this cluster. Cluster I was the lowest with 4 samples, with continual time series from August 20th to September 1st.

Box-plots of phytoplankton species richness and biomass with the percentage of different groups of each cluster are shown in Fig. 5: the values varied and differed significantly among clusters (the Kruskall-Wallis test, $p < 0.001$). Cluster I showed the maximum median values among all clusters in both species richness and biomass. The other three clusters had very close median values in biomass, but they had obvious different median values in species richness. Cluster IIb2 showed the minimum median values in both species richness and biomass (Fig. 5a1, 5b1).

The most significant feature for the percentage of different groups in each cluster was that diatoms contributed the most in terms of both species richness and biomass. However, green algae, the second contributor, showed an obvious difference in species richness

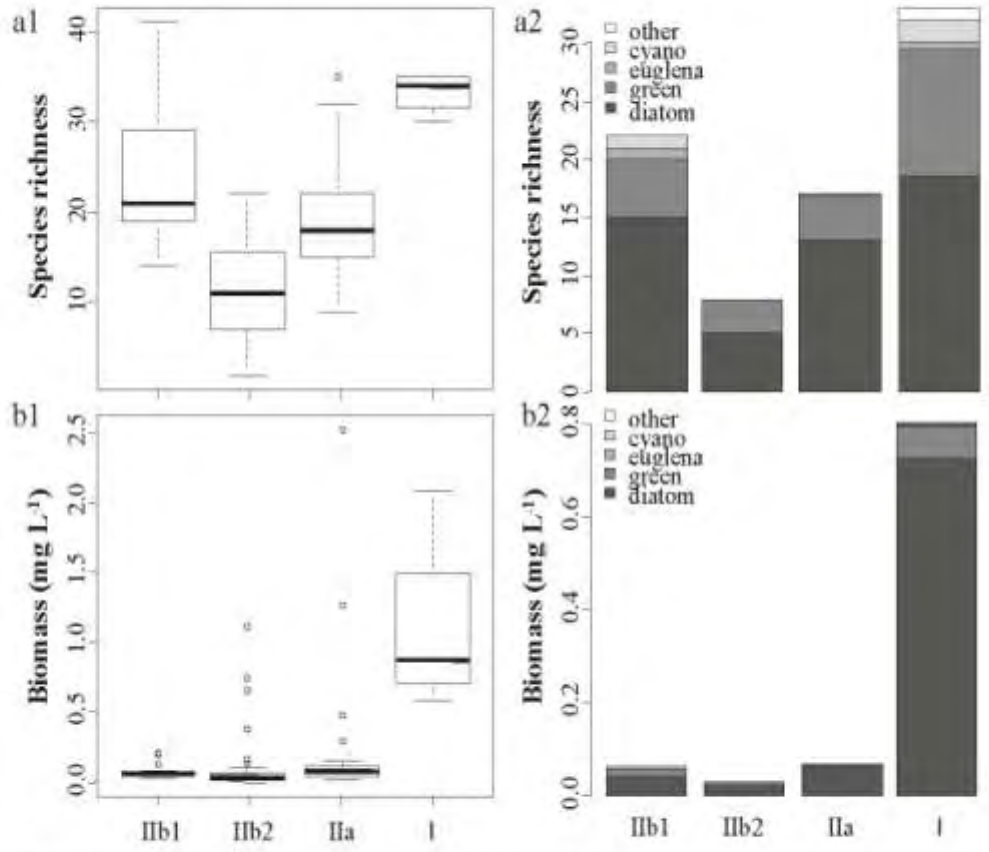

Fig. 5. Box plot of phytoplankton species richness and biomass of each cluster (**a1.** species richness; **a2.** percentage of different groups to species richness in terms of median values; **b1.** biomass; **b2.** percentage of different groups to biomass in terms of median values)

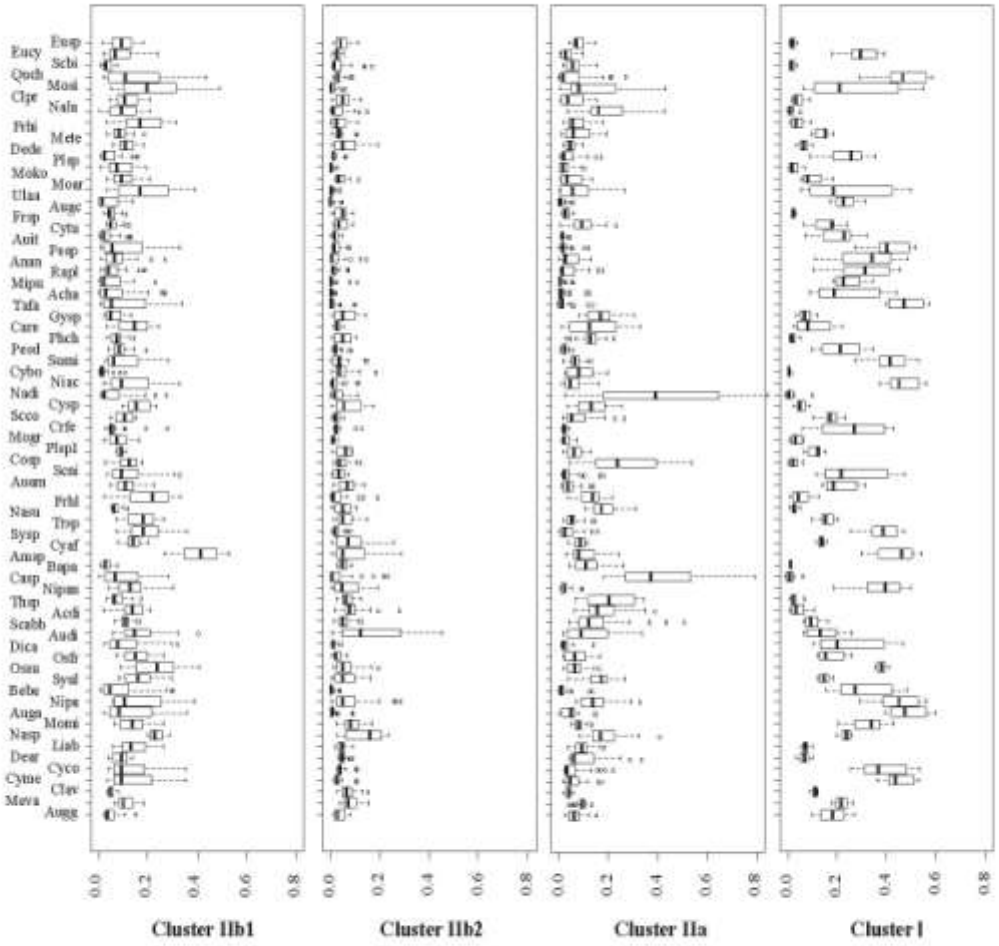

Fig. 6. Box-plots showing the occurrence probability (%) of each species (see full-names in Table 1) in each of four clusters. Values were obtained from the weight of virtual vectors of the trained SOM.

and biomass composition. They contributed more in species richness, and the percentages in cluster I and IIb1 were obviously higher than that in the other two clusters (Fig. 5a2, 5b2).

Fig. 6 showed the occurrence probability of individual species in each cluster, and the results show apparent differences among clusters. Cluster I was most diverse in contributing species with relatively higher occurrence probabilities in terms of median values. The occurrence probabilities of most taxa in this cluster were below 20 %. The median values of nine taxa, of which seven were diatoms (including four tychoplankton and three euplankton), varied in the range of 40–60 %. Another group of nineteen taxa, mainly composed of diatoms (including five tychoplankton and three euplankton) and green algae (all nine taxa were euplankton), were in the range of 20–40 %. The other three clusters had apparently low occurrence probabilities in contributing species, and the median values of most species were below 20 %. The three highest probable occurrence diatoms (*Navicula dicephala*, *Caloneis* sp. and *Cocconeis* sp.) of cluster IIa were in the range of 20–40 %, and they all belonged to tychoplankton. In cluster IIb1, the median value of *Amphora sp.* was greater than 40 %, while the other three species: *F. hinganensis* var. *longissima*, *Navicula* sp. and *Oscillatoria subbrevis*, were in the range of 20–40 % with all these taxa belonging to tychoplankton. In cluster IIb2, the median values of all species were below 20 %, and only *Aulacoseira distans* and *Navicula* sp. were a little higher than the others.

Based on both IndVal (indicator value > 25) and SOM code book values, i.e. the high occurrence prob-

Table 2. Indicators of each cluster based on IndVal (indicator value) and SOM (occurrence probability in each cluster, see Fig. 6). Only species that are significant in both criteria should be accepted. X means significant, Y means accepted.

Cluster	Indicator species	Indicator value (%)	IndVal	SOM	Indicator
I	Auge	99	X	X	Y
	Mipu	98	X	X	Y
	Acha	97	X		
	Tafa	96	X	X	Y
	Bebe	94	X	X	Y
	Auga	89	X	X	Y
	Niac	85	X	X	Y
	Sumi	83	X	X	Y
	Cyme	82	X	X	Y
	Cyco	78	X	X	Y
	Nipan	74	X	X	Y
	Augg	70	X		
	Pesp	68	X	X	Y
	Sose	65	X	X	Y
	Crfe	63	X	X	Y
	Pesd	59	X	X	Y
	Quch	58	X	X	Y
	Dica	58	X		
	Ossu	57	X	X	Y
	Mcmi	56	X	X	Y
	Sysp	54	X	X	Y
	Meva	54	X	X	Y
	Nipa	48	X	X	Y
	Rapl	43	X	X	Y
	Plsp	42	X	X	Y
	Eucy	41	X	X	Y
	Anan	36	X	X	Y
	Osfr	33	X		
IIa	Casp	62	X	X	Y
	Nadi	54	X	X	Y
	Cosp	32	X	X	Y
IIb1	Frhl	51	X	X	Y
	Meko	45	X		
	Amsp	42	X	X	Y
	Trsp	34	X		
	Frhi	29	X		

ability in each SOM cluster, a total of 29 indicator species were determined in different hierarchical levels (Table 2). The number of indicator species composition varied significantly among clusters, and increased along the sequence IIb2, IIb1, IIa and I (0, 2, 3 and 24, respectively). The indicator species of cluster I had significantly higher IndVal and occurrence probabilities than those of cluster IIa and IIb1, which suggested that the second dichotomy (cluster I) had a strong ecological significance. Indicator species were found with a low occurrence frequency, especially those that had extremely high indicator values.

Cluster I contained the most diverse indicator species, including twelve diatoms, of which five were euplankton and seven were tychoplankton; nine green algae, of which eight were euplankton and one was tychoplankton, one tychoplanktonic cyanobacteria, one euplanktonic *Euglena* and one euplanktonic dinoflagellate. Three diatoms (*M. varians*, *C. meneghiniana* and *C. comta*), which had an apparently high occurrence frequency (>60 %) in the whole year, were also good indicator species of this cluster. The indicator species cluster IIa was composed of three diatoms, and the indicator sequence in importance was *Caloneis* sp., *Navicula dicephala* and *Cocconeis* sp., and all of them were tychoplankton. The indicator species of cluster IIb1 included two tychoplanktonic diatoms: *Amphora sp.* and *Fragilaria hinganensis* var. *longissima*, and both were pennate diatoms. The cluster IIb2 had no indicator species.

The prediction of phytoplankton assemblages from environmental factors

The most influential factors predicting the four clusters I, IIa, IIb1 and IIb2 (Fig. 7) were identified by discriminant function analysis and principal component analysis. Three discriminant functions were generated and the random Monte Carlo permutation test showed that they were highly significant ($p < 0.001$). These axes (F1, F2 and F3) accounted for 59, 22 and 18% of the between-cluster variability, respectively. All the four community clusters overlapped each other to some extent, and cluster IIa overlapped more with three other clusters. Since F2 and F3 contributed approximately equal proportions to the results, two dimensional figures based on F1 × F2 and F1 × F3, were shown respectively, with a corresponding distribution of water quality parameters. In this respect, the correlations could be exhibited adequately.

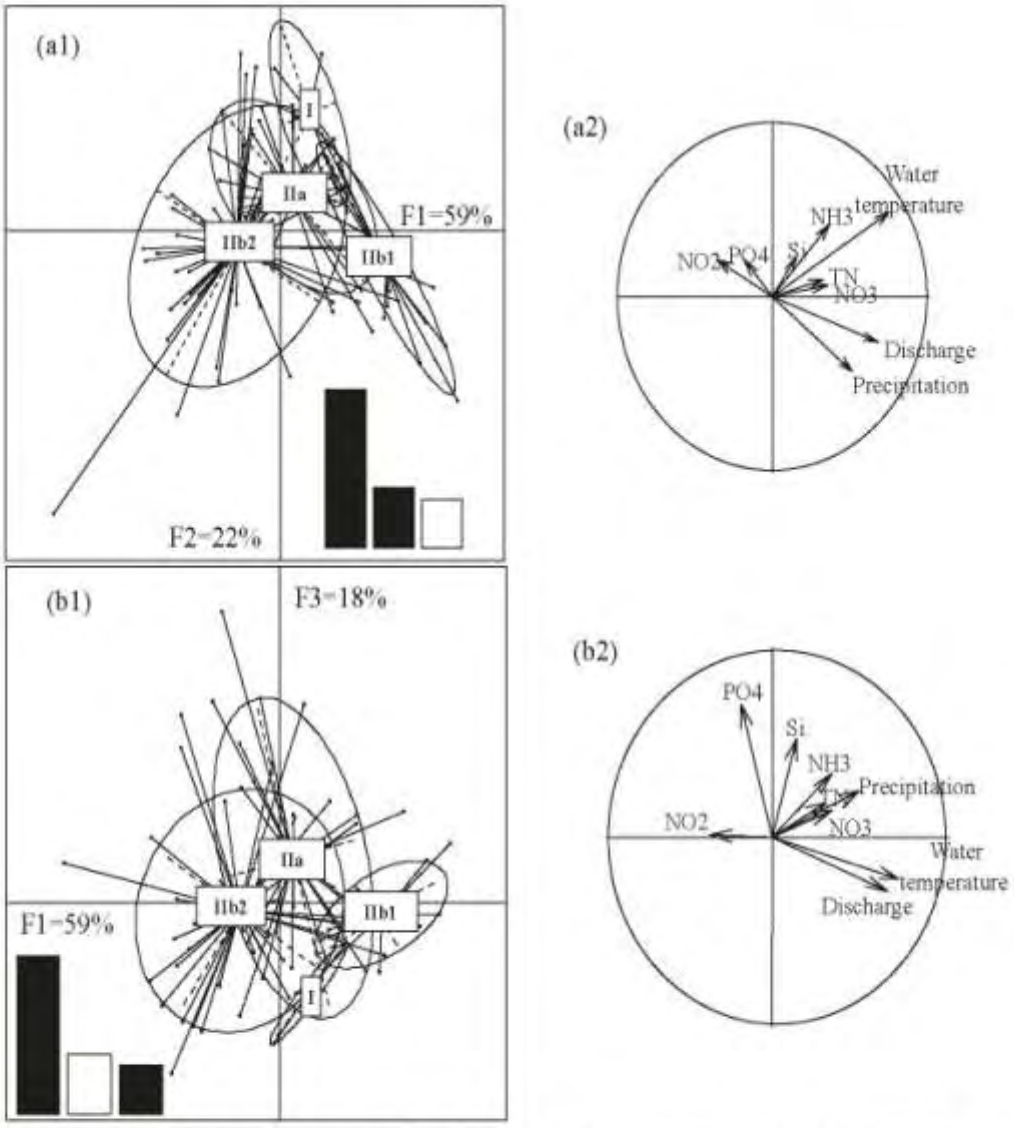

Fig. 7. Results from the LDA analysis showing: (**a1**) the distribution and overlap of clusters in F1 and F2 dimensions; (**a2**) the distribution of water quality parameters corresponding to F1 and F2; (**b1**) the distribution and overlap of clusters in F1 and F3 dimensions; (**b2**) the distribution of water quality parameters corresponding to F1 and F3. The three bar plots in a1 represent F1, F2 and F3 in sequence.

The nine environmental factors used were able to predict the community clusters and types of phytoplankton species assemblage patterns (i.e. global score of prediction) at 64.2 % accuracy, and the prediction success rate for clusters I, IIa, IIb1 and IIb2 were 50, 48, 62 and 74 %, respectively.

Cluster IIb1 and IIb2 were ordered along the first axis F1 (i.e. horizontal axis) of the analysis based on both F1 × F2 (Fig. 7a1, 7a2) and F1 × F3 (Fig. 7b1, 7b2) figures, and the gradients of water temperature, discharge and precipitation were loaded along this axis and were important controlling variables. Meanwhile, phosphate was along the second axis F2 (i.e. vertical axis) and was an important controlling variable to cluster IIa, based on the F1 × F3 figure. Cluster I was ordered between the horizontal and vertical axes (Fig. 7a1, 7b1) and its linkage with environmental variables was unclear (Fig. 7a2, 7b2).

Discussion

Environmental conditions

The environmental conditions of the sampled section were not only indirectly influenced by the upstream conditions through continual flow transportations (e.g. inoculums from upstream and branched tributaries), but also directly influenced by regional disturbance events (e.g. inputs of urban pollution). The annual patterns of environmental factors showed that physical and hydrological factors varied regularly with obvious seasonal characteristics (alternating between warm and cold seasons), while chemical factors did not. Warm seasons were accompanied by frequent rainfall and high discharge (floods), and the latter two factors were always found closely correlated (Wu et al. 2011, Townsend et al. 2012). Frequent rainfall could result in high discharge, thus floods formed. However, the relatively low daily values of precipitation during floods seemed to conflict with the high daily values in drought seasons. We assumed that the flood peaks resulted from the simultaneous raining in the whole river basin, while the single high daily values in drought seasons were just regional scale events. This assumption was supported by Lu et al. (2014), who reported that summer was the most important raining season in the Pearl River basin based on 50 years data. But the typhoon events of 2009 might enhance the regional precipitation in drought seasons. Researchers often reported that the water flow and rainfall brought external nutrients from the terrestrial ecosystem (Karadžić et al. 2013, Zhu et al. 2013). However in this study, all nutrients were uncorrelated with hydrological rhythms and varied without regular seasonal characteristics. Anthropogenic eutrophication of rivers is now a worldwide problem, particularly in catchments with dense human populations, well-developed industry, or intense agricultural land use (Kiss 1985, Smith et al. 2006). Some scientists have even used downstream increases in nitrate as useful indicators of eutrophication in large rivers (Turner et al. 2003, Almasri & Kaluarachchi 2004), which is a common human impact caused by agriculture. The median values of nutrients in the studied area ($P–PO_4$: 0.18 mg L^{-1}, $Si–SiO_4$: 3.84 mg L^{-1}, TN: 1.70 mg L^{-1}, $N–NO_3$: 0.64 mg L^{-1}, $N–NH_4$: 0.67 mg L^{-1}) were markedly higher than the threshold for half-saturation for most algal species according to Reynolds (2006). This situation is similar with that of the River Danube (Kiss 1994). Some studies had reported that nutrients played a subordinate role in determining algal biomass relative to the flow regime in rivers (Kiss 1997, Biggs & Smith 2002, Mitrovic et al. 2008). Above all, nutrient conditions in the investigated section seemed to be in excess and not limiting or controlling the phytoplankton behavior. Such eutrophic status was assumed to be mainly attributed to regional anthropogenic nutrient inputs along the river bank, since seasonal hydrology had little impact on them. This was contrary to conditions of the River Danube in which seasonal hydrology played a very important role in the actual trophic level (Kiss 1997).

Phytoplankton community structure

Wehr & Descy (1998) believed that the most successful algal groups in large rivers were Bacillariophyceae and Chlorophyceae. Our results indicated similar results, and these two groups contributed more than 75 % of the total species richness. Kiss & Schmidt (1998) stated the same results for a few decades in the River Danube. Garnier et al. (1995) also reported similar patterns in the River Seine that contained a mixed group comprising approximately 200 taxa of which 90 were diatoms and 60 were Chlorophyceae. In the present study, only several taxa (four of six are diatoms) had a common occurrence rate (> 50 %), and the phytoplankton biomass was even dominated by a single filamentous diatom species (*A. granulata*). Researchers have proved that the presence of a few dominant species accompanied by a large number of sporadic species is the main feature of phytoplankton community structures in large river ecosystems (Descy 1993, Devercelli 2006), and similar results have also been reported in many European rivers (Kiss & Schmidt 1998,

Ržaničanin et al. 2005, Hindák et al. 2006, Desortová & Punčochář 2011, Tavernini et al. 2011) and other rivers (Wehr & Descy 1998, Hamilton 2011) in the world. In conclusion, our results illustrated a diatom-dominated community, which might benefit from good adaptive abilities of this group in lotic and turbid river ecosystems (Dokulil 1994, Dokulil 2006, Dokulil & Donabaum 2014). Generally, diatoms developed well under turbid riverine conditions compared with other taxa (Wetzel 2001, Allan & Castillo 2007), and their efficiency under low light conditions was also well described (Litchman & Klausmeier 2008, Schwaderer et al. 2011, Beaver et al. 2013). In addition, dominance by single *A. granulata* (functional group P) in phytoplankton assemblages has been reported in many other large rivers (Lewis et al. 1995, O'Farrell et al. 1996, Zalocar de Domitrovic et al. 2007), preferable due to the eutrophication status and turbulent conditions. Dokulil & Teubner (2005) found that eutrophications of freshwater ecosystems ultimately led to the dominance of one or a few dominant species. Townsend et al. (2012) also believed that a single diatom species could not dominate under low nutrient conditions.

Patterning and predicting of phytoplankton assemblages

Based on species similarities, all samples were classified into four clusters through the self-organizing map (SOM). And their correlations with environments were also predicted using LDA. Cluster IIb1 covered warm seasons, and mainly composed of June and July. Cluster I also covered warm dates within only half a month. This similar point of these two clusters might imply that phytoplankton assemblages in warm seasons were so changeable that similarities and steady successions were only limited in short periods. Moreover, these two clusters could clearly be differentiated by discharge (precipitation), and temporal succession also reflected that cluster I was actually an after-flood (IIb1) period. Contrary to the above two clusters, IIb2 was characterized by cold and drought periods. The maximum sample numbers and the widest temporal distribution of this cluster illustrated that the phytoplankton composition was similar most of the time during the year. Cluster IIa was characterized by P-linkage. The wide time span but discontinuous samples of this cluster indicated that phosphate limitation happened occasionally.

Plankton selection and dynamics relate conspicuously to flow at higher discharges but other environmental features are important at low flow rates (Reynolds 2000). River discharge and the variables directly linked to water fluxes had a significant impact on the development of phytoplankton biomass, particularly during the periods more favorable for algal growth (Salmaso & Zignin 2010). Although warm conditions of cluster IIb1 was suitable for algal growth, high discharge could prevent the accumulation of phytoplankton biomass through a dilution and advection process, and the associated rapid speed was also detrimental for phytoplankton to utilize resources efficiently (Salmaso & Braioni 2008). The low biomass was the direct response to a negative dilution effect and short residence time resulting from high discharge. The lower occurrence probability of species in this cluster also reflected the negative impact of floods. However, relatively high species richness seemed to be benefiting from the high flow conditions, which triggered the inoculations from both outer channels (mainly green algae) and benthic environments (mainly diatoms). Moreover, composition indicators of this cluster: euplanktonic *Monoraphidium komarkovae* (Chlorophyceae) and *Trachelomonas* sp. (Euglenophyceae) indicated the inoculations from outer sources; tychoplanktonic diatoms (*Amphora* sp., *Fragilaria hinganensis* var. *longissima* and *Ulnaria delicatissima* var. *angustissima*) indicated the resuspension from the benthos under violent turbulent conditions. Most of these species were found to have survival advantages under high flow conditions for their larger surface-volume ratio.

The largest peaks of algal biomass in the lowland rivers were determined by a combination of higher temperatures, low discharge and more favorable light (Rossetti et al. 2009, Descy et al. 2012). The maximum biomass of cluster I benefited from these favorable conditions. Kiss (1996) also reported that phytoplankton of River Danube could divide very quickly and double the abundance during one to two days in the low water period. Although light intensity was not measured during our investigation, the long photoperiod with intense light was always typical in warm seasons of such subtropical regions. Moreover, the concentration effect during decreasing discharge was also thought to be positive for both high diversity and biomass achieved in this cluster. This could be supported by the most diverse indicators and high occurrence probability of species in cluster I, since the other warm but flood cluster IIb1 showed contrasting low biomass. The considerable composition of euplanktonic (mainly green algae) and tychoplanktonic indicators (mainly diatoms) also suggested that cluster I was an after-flood period. Romanov & Kirillov (2012) believed that the most significant changes in

phytoplankton structure tended to occur in the period between flood decline and the beginning of low water. Thus, cluster I corresponded in this respect. Moreover, zooplankton most likely had weak predating pressure on phytoplankton in the studied area, since its abundance mostly kept low (unpublished data).

Low water temperature was thought to be key factor resulting in the low biomass and species richness of cluster IIb2, since it interrupted the physiological and biochemical processes of algal cell growth (Mata et al. 2010), and thus limited the phytoplankton abundance development. Meanwhile, the sinking loss increased during this drought period. However, the concomitant low water levels permitted benthic algae to easily resuspend in the water column. In this respect, benthic diatom *M. varians* benefited and gained the second rank in both occurrence rate and biomass. During the low water period, the light climate was also favourable for benthic algae and therefore developed more and could wash out to the plankton (Ács et al. 2003, Ács et al. 2006). Moreover, some samples distributed between flood peaks, and they were assumed to be an important link between clusters IIb2 and IIa, because of their high composition of green algae.

The linkage of cluster IIa to phosphate indicated that phytoplankton assemblages were occasionally P-limited. As phosphorus is often considered to be the biomass-limiting constraint in pelagic ecosystems, P enrichment can provide a significant stimulus to the sustainable biomass of phytoplankton (Reynolds 2006). However, the impact of this nutrient mainly happened in drought periods having concomitant suitable temperature. Both species richness and biomass of this cluster were at intermediate levels, but apparently higher than corresponding cold drought periods (IIb2).

In conclusion, annual patterns of phytoplankton assemblages at the downstream of West River could be easily differentiated by physical factors (water temperature, discharge and precipitation) during most times of the year. However, there was occasional P-limitation, especially in drought periods and without water temperature limitation.

Acknowledgements

We wish to thank the Zhaoqing Fishery Team of Guangdong Province Fishery Team for their assistance in sampling work, and John Woodley for language improvements. This work was financially supported by The Guangxi Province Natural Science Foundation of Key Projects (2013GXNSFEA053003) and The Public Sector (agriculture) Special Scientific Research Projects (201303056-5).

References

Ács, É., Szabó, K., Kiss, K. T. & Hindák, F., 2003: Benthic algal investigations in the Danube River and some of its main tributaries from Germany to Hungary. – Biologia, Bratislava **58**: 545–554.

Ács, É., Szabó, K., Kiss, Á. K., Tóth, B., Záray, G. & Kiss, K. T., 2006: Investigation of epilithic algae on the River Danube from Germany to Hungary and the effect of a very dry year on the algae of the River Danube. – Archiv für Hydrobiologie, Supplement Large Rivers **16**: 389–417.

Alhoniemi, E., Himberg, J., Parhankangas, J. & Vesanto, J., 2000: SOM Toolbox [online] – http://www.cis.hut.fi/projects/somtoolbox.

Allan, J. D. & Castillo, M. M., 2007: Stream ecology, 2nd ed. – Springer, Berlin.

Almasri, M. N. & Kaluarachchi, J. J., 2004: Assessment and management of long-term nitrate pollution of ground water in agriculture-dominated watersheds. – Journal of Hydrology **295**: 225–245.

Aymerich, I. F., Piera, J., Mohr, J., Soria-Frisch, A. & Obermayer, K., 2009: Fast phytoplankton classification from fluorescence spectra: comparison between PSVM and SOM. – Oceans 2009 Europe, pp. 1–4.

Beaver, J. R., Casamatta, D. A., East, T. L., Havens, K. E., Rodusky, A. J., James, R. T., Tausz, C. E. & Buccier, K. M., 2013: Extreme weather events influence the phytoplankton community structure in a large lowland subtropical lake (Lake Okeechobee, Florida, USA). – Hydrobiologia **709**: 213–226.

Biggs, B. J. F. & Smith, R. A., 2002: Taxonomic richness of stream benthic algae: effects of flood disturbance and nutrients. – Limnology and Oceanography **47**: 1175–1186.

Billen, G., Garnier, J. & Hanset, P., 1994: Modelling phytoplankton development in whole drainage networks: the RIVERSTRAHLER Model applied to the Seine river system. – Hydrobiologia **289**: 119–137.

Davies, D. L. & Bouldin, D. W., 1979: A cluster separation measure. – IEEE Transactions on Pattern Analysis and Machine Intelligence **1**: 224–227.

Descy, J. P., 1993: Ecology of the phytoplankton of the River Moselle: effects of disturbances on community structure and diversity. – Hydrobiologia **249**: 111–116.

Descy, J. P., Leitao, M., Everbecq, E., Smitz, J. S. & Deliège, J. F., 2012: Phytoplankton of the River Loire, France: a biodiversity and modeling study. – Journal of Plankton Research **34** (2): 120–135.

Desortová, B. & Punčochář, P., 2011: Variability of phytoplankton biomass in a lowland river: response to climate conditions. – Limnologica **41**: 160–166.

Devercelli, M., 2006: Phytoplankton of the Middle Paraná River during an anomalous hydrological period: a morphological and functional approach. – Hydrobiologia **563**: 465–478.

Devercelli, M., 2010: Changes in phytoplankton morpho-functional groups induced by extreme hydroclimatic events in the Middle Paraná River (Argentina). – Hydrobiologia **639**: 5–19.

Dodds, W. K., 2006: Eutrophication and trophic state in rivers and streams. – Limnology and Oceanography **51**: 671–680.

Dokulil, M. T., 1994: Environmental control of phytoplankton productivity in turbulent turbid systems. – Hydrobiologia **289**: 65–72.

Dokulil, M. T., 2006: Short and long term dynamics of nutrients, potamoplankton and primary productivity in an alpine river (Danube, Austria). – Archiv für Hydrobiologie, Supplement **158** (4), Large Rivers **16**: 473–493.

Dokulil, M. T. & Donabaum, U., 2014: Phytoplankton of the Danube River: Composition and Long-Term Dynamics. – Acta Zoologica Bulgarica, Supplement **7**: 147–152.

Dokulil, M. T. & Teubner, K., 2005: Do phytoplankton communities correctly track trophic changes? An assessment using directly measured and palaeolimnological data. – Freshwater Biology **50**: 1594–1604.

Domingues, R. B., Barbosa, A. B., Sommer, U. & Galvão, H. M., 2012: Phytoplankton composition, growth and production in the Guadiana estuary (SW Iberia): unraveling changes induced after dam construction. – Science of the Total Environment **416**: 300–313.

Elliott, J. A., 2012: Predicting the impact of changing nutrient load and temperature on the phytoplankton of England's largest lake, Windermere. – Freshwater Biology **57**: 400–413.

Fornarelli, R., Antenucci, J. P. & Marti, C. L., 2013: Disturbance, diversity and phytoplankton production in a reservoir affected by inter-basin water transfers. – Hydrobiologia **705**: 9–26.

Garnier, J., Billen, G. & Coste, M., 1995: Seasonal succession of diatoms and Chlorophyceae in the drainage network of the Seine River: observations and modelling. – Limnology and Oceanography **40**: 750–765.

Giraudoux, P., 2006: Pgirmess: data analysis in ecology. – R package version 1.3.8 http://perso.orange.fr/giraudoux/.

Hamilton, P. B., Lavoie, I., Ley, L. M. & Poulin, M., 2011: Factors contributing to the spatial and temporal variability of phytoplankton communities in the Rideau River (Ontario, Canada). – River Systems **19**: 189–205.

Hamilton, P. B., Lavoie, I. & Poulin, M., 2012: Spatial, seasonal and inter-annual variability in environmental characteristics and phytoplankton standing stock of the temperate, lowland Rideau River, Ontario, Canada. – River Research and Applications **28**: 1551–1566.

He, Y. F., Wang, J. W., Lek, S., Cao, W. X. & Lek-Ang, S., 2011: Structure of endemic fish assemblages in the upper Yangtze River basin. – River Research and Applications **27**: 59–75.

Hillebrand, H., Dürselen, C. D., Kirschtel, D., Pollingher, U. & Zohary, T., 1999: Biovolume calculation for pelagic and benthic microalgae. – Journal of Phycology **35**: 403–424.

Hindák, F., Hindáková, A., Marvan, P., Heteša, J. & Hašler, P., 2006: Diversity, abundance and volume biomass of the phytoplankton of the Morava River (Czech Republic, Slovakia) and the Dyje River (Czech Republic) in November 2005. – Czech Phycology Olomouc **6**: 77–97.

Ihaka, R. & Gentleman, R., 1996: R: a language for data analysis and graphics. – Journal of Computational and Graphical Statistics **5**: 299–314.

Jeong, K. S., Kim, D. K. & Joo, G. J., 2006: River phytoplankton prediction model by Artificial Neural Network: Model performance and selection of input variables to predict time-series phytoplankton proliferations in a regulated river system. – Ecological Informatics **1**: 235–245.

Karadžić, V., Simić, G. S., Natić, D., Ržaničanin, A., Ćirić, M. & Gačić, Z., 2013: Changes in the phytoplankton community and dominance of *Cylindrospermopsis raciborskii* (Wolosz.) Subba Raju in a temperate lowland river (Ponjavica, Serbia). – Hydrobiologia **711**: 43–60.

Kiss, K. T. L., 1985: Changes of trophity conditions in the River Danube at Göd. Danubialia Hungarica XCIV. – Annal. Univ. Sci. Budapest Sect. Biol. **24–26**: 47–59.

Kiss, K. T., 1987: Phytoplankton studies in the Szigetköz section of the Danube during 1981–1982. – Archiv für Hydrobiologie **78** (2), Algological Studies **47**: 247–273.

Kiss, K. T., 1994: Trophic level and eutrophication of the River Danube in Hungary. – Verhandlungen Internationale Vereinigung der theoretischen und angewandten Limnologie **25**: 1688–1691.

Kiss, K. T., 1996: Diurnal change of planktonic diatoms in the River Danube near Budapest (Hungary). – Archiv für Hydrobiologie, Algological Studies **80**: 113–122.

Kiss, K. T., 1997: The main results of phytoplankton studies on the River Danube and its side arm system at the Szigetköz area during the nineties (Hungary). – In: Dokulil, M. T. (ed.): Limnologische Berichte Donau 1997. Band. I., pp. 153–158.

Kiss, K. T. & Schmidt, A., 1998: Changes of the Chlorophyta species in the phytoplankton of the Hungarian Section of the Danube river during the last decades (1961–1997). – Biologia, Bratislava **53**: 509–518.

Larroudé, S., Massei, N., Reyes-Marchant, P., Delattre, C. & Humbert, J. F., 2013: Dramatic changes in a phytoplankton community in response to local and global pressures: a 24-year survey of the river Loire (France). – Global Change Biology **19**: 1620–1631.

Lewis, W. M. Jr., Hamilton, S. K. & Saunders, J. F., 1995: Rivers of northern South America. – In: Cushing, C. E., Cummins, K. W. & Minshall, G. W. (eds): River and stream ecosystems. – Elsevier, Amsterdam.

Litchman, E. & Klausmeier, C. A., 2008: Trait-based community ecology of phytoplankton. – Annual Review of Ecology, Evolution and Systematics **39**: 615–639.

Lu, K. X., 1990: Fishery Resources of the Pearl River System. – Guangzhou: Guangdong Science and Technology Press, pp. 27–39. (in Chinese)

Lu, W. X., Liu, B. J., Chen, J. F. & Chen, X. H., 2014: Variation trend of precipitation in the Pearl River basin in recent 50 years. – Journal of Natural Resources, **29** (1): 80–90. (in Chinese with English abstract)

Mata, T. M., Martins, A. A. & Caetano, N. S., 2010: Microalgae for biodiesel production and other applications: a review. – Renewable and Sustainable Energy Reviews **14**: 217–232.

Mitrovic, S. M., Chessman, B. C., Davie, A., Avery, E. L. & Ryan, N., 2008: Development of blooms of *Cyclotella meneghiniana* and *Nitzschia* spp. (Bacillariophyceae) in a shallow river and estimation of effective suppression flows. – Hydrobiologia **596**: 173–185.

O'Farrell, I., Izaguirre, I. & Vinocur, A., 1996: Phytoplankton ecology of the Lower Paraná River (Argentina). – Archiv für Hydrobiologie, Supplement **115**: 75–89.

Peretyatko, A., Teissier, S., Symoens, J. J. & Triest, L., 2007: Phytoplankton biomass and environmental factors over a gradient of clear to turbid peri-urban ponds. – Aquatic Conservation-Marine and Freshwater Ecosystems **17**: 584–601.

Piirsoo, K., Pall, P., Tuvikene, A. & Viik, M., 2008: Temporal and spatial patterns of phytoplankton in a temperate lowland river (Emajõgi, Estonia). – Journal of Plankton Research **30**: 1285–1295.

Reavie, E. D., Jicha, T. M., Angradi, T. R., Bolgrien, D. W. & Hill, B. H., 2010: Algal assemblages for large river monitoring: comparison among biovolume, absolute and relative abundance metrics. – Ecological Indicators **10**: 167–177.

Reynolds, C. S., 2000: Hydroecology of river plankton: the role of variability in channel flow. – Hydrological Processes **14**: 3119–3132.

Reynolds, C. S., 2006: The Ecology of Phytoplankton. – Cambridge University Press, Cambridge.

Romanov, R. E. & Kirillov, V. V., 2012: Analysis of the seasonal dynamics of river phytoplankton based on succession rate indices for key event identification. – Hydrobiologia **695**: 293–304.

Rossetti, G., Viaroli, P. & Ferrari, I., 2009: Role of abiotic and biotic factors in structuring the metazoan plankton community in a lowland river. – River Research and Applications **25**: 814–835.

Ržaničanin, A., Cvijan, M. & Krizmanić, J., 2005: Phytoplankton of the Tisa River. – Archives of Biological Sciences **57**: 223–235.

Sabater, S., Artigas, J., Durán, C., Pardos, M., Romaní, A. M., Tornés, E. & Ylla, I., 2008: Longitudinal development of chlorophyll and phytoplankton assemblages in a regulated large river (the Ebro River). – Science of the Total Environment **404**: 196–206.

Salmaso, N. & Braioni, M. G., 2008: Factors controlling the seasonal development and distribution of the phytoplankton community in the lowland course of a large river in Northern Italy (River Adige). – Aquatic Ecology **42**: 533–545.

Salmaso, N. & Zignin, A., 2010: At the extreme of physical gradients: phytoplankton in highly flushed, large rivers. – Hydrobiologia **639**: 21–36.

Schwaderer, A. S., Yoshiyama, K., de Tezanos Pinto, P., Swenson, N. G., Klausmeier, C. A. & Litchman, E., 2011: Eco-evolutionary differences in light utilization traits and distributions of freshwater phytoplankton. – Limnology and Oceanography **56**: 589–598.

Sipkay, C., Kiss, K. T., Vadadi-Fölöp, C., Homoródi, R. & Hufnagel, L., 2012: Simulation modeling of phytoplankton dynamics in a large eutrophic river, Hungary-Danubian Phytoplankton Growth Model (DPGM). – Biologia **67** (2): 323–337.

Smith, V., Joye, S. & Howarth, R. W., 2006: Eutrophication of freshwater and marine ecosystems. – Limnology and Oceanography **51**: 351–355.

Sneath, P. H. A. & Sokal, R. R., 1973: Numerical Taxonomy: The Principles and Practice of Numerical Classification. – Freeman, San Francisco, pp. 1–278.

Tavernini, S., Pierobon, E. & Viaroli, P., 2011: Physical factors and dissolved reactive silica affect phytoplankton community structure and dynamics in a lowland eutrophic river (Po River, Italy). – Hydrobiologia **669**: 213–225.

Thebault, J. M. & Qotbi, A., 1999: A model of phytoplankton development in the Lot River (France). Simulations of scenarios. – Water Research **33** (4): 1065–1079.

Torremorell, A., Llames, M. E., Pérez, G. L., Escaray, R., Bustingorry, J. & Zagarese, H., 2009: Annual patterns of phytoplankton density and primary production in a large, shallow lake: the central role of light. – Freshwater Biology **54**: 437–449.

Townsend, S. A., Przybylska, M. & Miloshis, M., 2012: Phytoplankton composition and constraints to biomass in the middle reaches of an Australian tropical river during base flow. – Marine and Freshwater Research **63**: 48–59.

Turner, R. E., Rabalais, N. N., Justic, D. & Dortch, Q., 2003: Global patterns of dissolved N., P and Si in large rivers. – Biogeochemistry **64**: 297–317.

Ultsch, A., 1993: Self-organizing neural networks for visualization and classification. – In: Opitz, O., Lausen, B. & Klar, R. (eds): Information and classification. – Springer-Verlag, Berlin, pp. 307–313.

Van den Hoek, C., Mann, D. G. & Jahns, H. M., 1995: Algae: an Introduction to Phycology. – Cambridge University Press, Cambridge, UK.

Várbíró, G., Ács, É., Borics, G. et al., 2007: Use of Self-Organizing Maps (SOM) for characterization of riverine phytoplankton associations in Hungary. – Archiv für Hydrobiologie, Supplement Large Rivers **17**: 383–394.

Vesanto, J., 2000: Neural network tool for data mining: SOM Toolbox. – Proceedings of Symposium on Tool Environments and Development Methods for Intelligent Systems (TOOLMET2000). Oulun yliopisto-paino, Oulu, Finland, pp. 184–196.

Wang, C., Lai, Z. N., Li, Y. F., Li, X. H., Lek, S., Hong, Y., Tan, X. C. & Li, J., 2012: Population ecology of *Aulacoseira granulata* in Xijiang River. – Acta Ecologica Sinica **32** (15): 4793–4802. (in Chinese with English abstract)

Wang, C., Lai, Z. N., Li, X. H., Gao, Y., Li, Y. F. & Yu, Y. M., 2013: Annual variation pattern of phytoplankton community at the downstream of Xijiang River. – Acta Ecologica Sinica **33** (14): 4398–4408. (in Chinese with English abstract)

Wehr, J. D. & Descy, J. P., 1998: Use of phytoplankton in large river management. – Journal of Phycology **34**: 741–749.

Wetzel, R. G., 2001: Limnology: lake and river ecosystems, 3rd ed. – Academic Press, San Diego, California.

Wu, N. C., Schmalz, B. & Fohrer, N., 2011: Distribution of phytoplankton in a German lowland river in relation to environmental factors. – Journal of Plankton Research **33**: 807–820.

Zalocar de Domitrovic, Y., Devercelli, M. & Garcia de Emiliani, M. O., 2007: Phytoplankton. – In: Iriondo, M. H., Paggi, J. C. & Parma, M. J. (eds): The Middle Paraná River. Limnology of a Subtropical Wetland. – Springer, Berlin, pp. 175–203.

Zhu, K. X., Bi, Y. H. & Hu, Z. Y., 2013: Responses of phytoplankton functional groups to the hydrologic regime in the Daning River, a tributary of Three Gorges Reservoir, China. – Science of the Total Environment **450–451**: 169–177.

Submitted: 20 June 2014; accepted: 14 October 2014.

ARTICLE IN PRESS

ECOINF-00536; No of Pages 11

Ecological Informatics xxx (2014) xxx–xxx

Contents lists available at ScienceDirect

Ecological Informatics

journal homepage: www.elsevier.com/locate/ecolinf

Exploring temporal trend of morphological variability of a dominant diatom in response to environmental factors in a large subtropical river

Chao Wang [a,b,c], Christophe Baehr [b,d], Zini Lai [a,c], Yuan Gao [a,c], Sovan Lek [b], Xinhui Li [a,c,*]

[a] Pearl River Fisheries Research Institute, Chinese Academy of Fishery Science, Guangzhou 510380, China
[b] Université Toulouse, Lab Evolution and Diversité Biologique, UMR 5174, CNRS–Université Paul Sabatier, 118, route de Narbonne, 31062 Toulouse Cedex 4, France
[c] Experimental Station for Scientific Observation on Fishery Resources and Environment in the Middle and Lower Reaches of Pearl River, Ministry of Agriculture the People's Republic of China, 526100, People's Republic of China
[d] French National Centre for Meteorological Research, 42 Avenue de Coriolis, 31057 Toulouse Cedex, France

ARTICLE INFO

Article history:
Received 24 July 2014
Received in revised form 23 October 2014
Accepted 5 November 2014
Available online xxxx

Keywords:
Aulacoseira granulata
Morphological variability
Wavelet analysis
Redundancy analysis
River

ABSTRACT

The temporal trend of morphological variability of *Aulacoseira granulata* (Ehrenberg) Simonsen and its response to environments was studied within the downstream region of a large subtropical river, the Pearl River (China), through time-series sampling during 2009. Both wavelet analysis and redundancy analysis (RDA) were used to demonstrate not only the correlations between morphological parameters but also the correlations between morphology and environments. High coherence between morphological parameters, especially cell size, was confirmed; but the coherence, especially that between cell and filament, could easily be impacted by water turbulence which was associated with discharge, this might reflect the interaction between life cycle and size selectivity. Moreover, phase angles in wavelet figures illustrated that cell diameter was the most sensitive parameter to environmental variations, and changes in cell diameter triggered the size change in both cell and filament; thus through this way cell and filament size variations could be related.

Based on the annual variation pattern of morphological parameters, the morphology of *A. granulata* exhibited an integrated cycle; during which morphological parameters might have different responses to physicochemical factors. Water temperature was closely associated with algal occurrence rates and size values during the spring–winter period. Algal life cycle could be affected by discharge, as well as filament length by allowing for selection of chains with optimum buoyancy. The responses of algal sizes to nutrients, especially silicate, phosphate, and total nitrogen, were associated with the start and end of a life cycle. These correlations between size and nutrients were supported by both wavelet analysis and RDA. Moreover, the extremely high values at the end of the year were explained as algal recruitment from benthos.

1. Introduction

Diatoms are known as the most important group of phytoplankton assemblages in lotic river ecosystems (Reynolds, 2006). The genus *Aulacoseira* contains a group of centric diatoms with chain colonies composed of cylindrical frustules united by shortened linking spines (Tremarin et al., 2012). Population dynamics and new species records of this genus were often reported in various aquatic ecosystems (Horn et al., 2011; Hörtzel and Croome, 1996; Poister et al., 2012; Usoltseva and Tsoy, 2010; Wang et al., 2009) due to its high taxonomic compositions and obvious high density. Moreover, morphological studies of this genus always generated interests because changes in cell size and hence in filament dimension were often observed and reported in natural waters (Babanazarova et al., 1996; Davey, 1987; Manoylov et al., 2009; O'Farrell et al., 2001; Poister et al., 2012; Turkia and Lepistö, 1999), and these morphological features could potentially be used as indicators when their correlations with environments were built up, as the response of morphological changes was more rapid than possible observations of changes in population dynamics (Gibson et al., 2003). In addition, the rigid silica cell wall of members of this genus permits only two main possibilities for adaptation: varying either length or diameter; thus the process of morphological changes could be observed (Jewson et al., 2010).

Aulacoseira granulata, a cosmopolitan species of this genus, has an international distribution due to its adaptive capacity and tolerance of a wide range of environmental conditions. Generally, *A. granulata* is regarded as a good indicator species to eutrophic water conditions (Kamenir et al., 2004; Lepistö et al., 2006; Nogueira, 2000), since it can easily form predominant populations and even become blooms (Miyajima et al., 1994; Nakano et al., 1996) in eutrophic waters under suitable conditions (e.g. high temperature). The author has also reported that *A. granulata* is predominant in the downstream of the Pearl River (Wang et al., 2009, 2012, 2013), which is known as a hyper-eutrophic

* Corresponding author at: Pearl River Fisheries Research Institute, Chinese Academy of Fishery Science, Guangzhou 510380, China.

http://dx.doi.org/10.1016/j.ecoinf.2014.11.002
1574-9541/

Please cite this article as: Wang, C., et al., Exploring temporal trend of morphological variability of a dominant diatom in response to environmental factors in a large subtrop..., Ecological Informatics (2014), http://dx.doi.org/10.1016/j.ecoinf.2014.11.002

river system. Except for population abundance, morphological variability of *A. granulata* was also found closely related to environmental variations, especially sensitive to nutrient concentrations (Davey, 1987; Gómez et al., 1995; Stoermer et al., 1981; Turkia and Lepistö, 1999). Relevant studies on the correlations between its morphology and environments have been carried out more in lentic water bodies such as lakes (Davey, 1987; Manoylov et al., 2009; Stoermer et al., 1981; Turkia and Lepistö, 1999) and reservoirs (Gómez et al., 1995; Reynolds et al., 1986), in which strong stratification occurred. Generally, the eutrophic status and specific nutrient availability of the studied water system explained a significant proportion of the observed morphological results (Gómez et al., 1995; O'Farrell et al., 2001; Turkia and Lepistö, 1999). In rivers, conditions are different: the lotic flows and oligotrophic status may enhance the importance of physical and hydrological factors in impacting morphological changes, especially in filament size selectivity. In such lotic systems, exploring temporal trend of morphological variability of *A. granulata*, based on frequent sampling, might help finding more elaborate and accurate correlations between this diatom species and environments.

Modern statistical methods provide different ways to analyze and explore a large and complex data set. Wavelet analysis is a multi-resolution analytical approach by which to analyze signal timescales (Yan et al., 2013). Wavelet coherency reveals dependencies between two signals and accounts for non-stationarity within ecological time series (Zhang et al., 2014). This method has now been well applied to examine time-scale specific correlations between two variables in phytoplankton (Blauw et al., 2012; Recknagel et al., 2013) and algal dynamics (Zhang et al., 2014). Redundancy analysis (RDA) is similar to canonical correlation analysis but allows users to derive a specified number of synthetic variables from one set of (independent) variables that explain as much variance as possible in another (independent) set. This innovative multivariate canonical analysis can detect the above wavelet analysis and improve the rigor for linking morphology to environmental conditions through comparing one of our quantitative response variables (morphometrics), with one or more categorical explanatory variables (environmental conditions).

The purpose of this study was to explore the temporal trend of morphological variability of *A. granulata* within the downstream region of the Pearl River based on consecutive and frequent sampling throughout a whole year. Wavelet analysis was used to demonstrate the possible coherence between the selected two variables, and RDA was used to test the validation of the one dimensional cross wavelet analysis. To this end, we aimed to demonstrate the basic annual variations of morphological size and their response to environmental factors. We also postulate that cell size, closely associated with life cycle, correlated more with nutritional factors, i.e. nitrogen and phosphate; while filament morphology, generally representing results of size selectivity, correlated more with physical factors, i.e. water temperature and discharge (Poister et al., 2012).

2. Materials and methods

2.1. Study area

The Pearl River, with a length of 2,320 km, a catchment area of 450,000 km^2, and annual discharge of 10,000 m^3 s^{-1}, is the third longest river in China. The river consists of three major tributaries: the West River, the North River and the East River, merging at the Pearl River Delta and ultimately flowing into the South China Sea. The West River, running through Guangdong and Guangxi province, is the largest tributary of the Pearl River. A seasonal flow regime is evident, with high flows during spring and summer, and low flows during autumn and winter.

The Zhaoqing section of the West River, with an average width of 1100 m and a peak flow of 30,000 m^3 s^{-1}, is the primary passage for river flow entering into the downstream river web of the Pearl River Delta. Our long term sampling site (23° 2′ 40″ N, 112° 27′ 5″ E) is located in this section, near the wharf of the Zhaoqing Fishery Administration, which is about 160 km upper from the Pearl River Estuary (Fig. 1). The largest difference between the minimum and maximum water level at the site does not exceed 15 m, and the depth of sampling site ranges from 3 to 5 m. In order to understand the temporal variations of primary production and their correlation with environmental factors, we collected phytoplankton samples and undertaken environmental measurements at this fixed site in 2009.

2.2. Sampling and data collection

Qualitative subsurface phytoplankton samples were collected at 8:00 am every 5 days each month. For each qualitative sample, 9–10 L of water was collected from subsurface and passed through a 20 μm nylon mesh. The retained particles were then washed into a preweighed glass bottle using 100–200 mL of water. Aliquots of the qualitative samples were cleaned by conventional methods (Patrick and Reimer, 1966) and subsequently used to prepare permanent slides. The valve diameter and mantle height were measured for a minimum of 100 cells per sample, and the results represented cell diameter and cell length respectively. Moreover, the cell volume was calculated from diameter and mantle height by applying geometric formulae. In each sample, the number of cells per colony was recorded for a

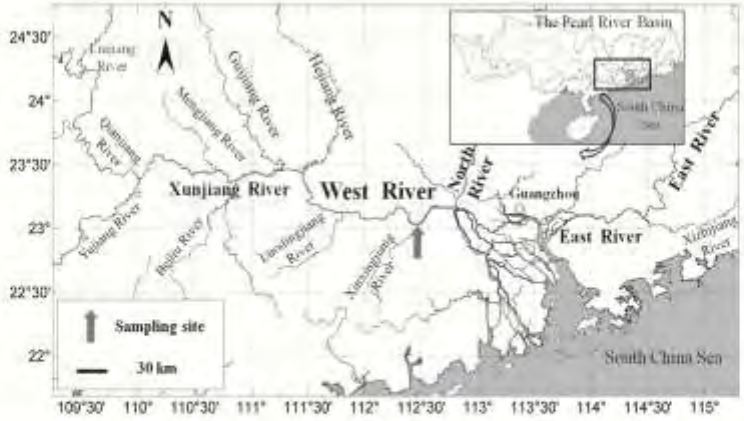

Fig. 1. The downstream river network of the Pearl River, including its location in the Pearl River Basin, river tributaries and sampling site.

Please cite this article as: Wang, C., et al., Exploring temporal trend of morphological variability of a dominant diatom in response to environmental factors in a large subtrop..., Ecological Informatics (2014), http://dx.doi.org/10.1016/j.ecoinf.2014.11.002

minimum of 100 colonies to determine the average filament length of *A. granulata*.

An additional water sample of 250 mL was filtered in situ, and taken back to the laboratory for nutrient analysis (including phosphate, silicate, total nitrogen, nitrate nitrogen, nitrite nitrogen and ammonia nitrogen) using an injection water quality analyzer (Skalar-SA1100) or a spectrophotometer (Shimadzu UV-2501PC). Water temperature was recorded using an automatic water temperature recorder (HOBO water temp Pro V2) at a frequency of once per hour at the sampling site. Water discharge data was collected from the website: http://xxfb.hydroinfo.gov.cn, and precipitation data was collected from the website: http://weatheronline.co.uk/weather.

2.3. Wavelet analysis

The signals contained in data set often reflect the results of the superimposition of different natural mechanisms. These mechanisms may have different time characteristics and different patterns (Bliss, 1970). Most of them are periodic and correspond to cyclic phenomena. The Fourier transform is a mathematical tool used to analyze the different cycles or frequencies embedded in a time series (Hornberger and Wiberg, 2006). However, calculating processes of some natural mechanisms are irrelevant with a Fourier analysis. Therefore we have to use more powerful techniques taking into account the time series characteristics. For instance we may use methods considering the possibility of patterns different from the harmonics. Moreover, we may also use methods reflecting the shape, the time characteristics of the embedded phenomena and their time localization. The wavelet analysis has been designed during the 80s in order to analyze local signals or non-cyclic patterns (Mallat, 1989; Morlet et al., 1982). The wavelets can also be used to extract information from many different types of time-series data such as audio signals and images.

In order to introduce the wavelet analysis method, we have to explain the concept of scale for data series and the concept of localization (see Fig. 2). We assume that the signal may be not only composed of periodic harmonics, but also composed of a sequence of structures (a structure is a specific pattern, like steps or transitory signals for instance) with different characteristic time lengths. The scale structure refers to the time length of the phenomenon (see Fig. 2). Then the whole time series may be seen as the superimposition of all the structures existing at the different scales (Daubechies, 1990). To proceed to the wavelet analysis, a dilatation/contraction of a specific pattern (called mother wavelet) is performed (see Fig. 2); meanwhile a comparison with a part of the series is also performed. These local comparisons are equivalent with local correlations using a special inner product. This method is able to analyze any type of time series, regular or not, continuous or not, periodic or not. The more adaptive to the time series the wavelet is, the better the analysis will be. Thus this tool is very suitable for analyzing natural and geophysical data series.

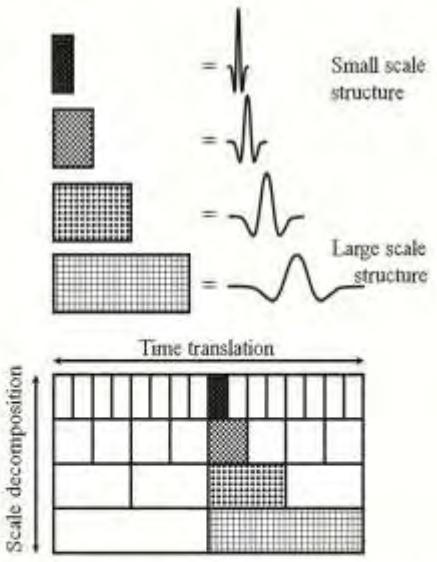

Fig. 2. The different parts of the time series are compared with a wavelet. The wavelet pattern is dilated or contracted according to the scale of analyze and translated in time.

From the mathematical point of view, considering the time $t \in [1, T]$, where $T > 0$ and a mother wavelet $\Psi(t)$ satisfying the admissibility conditions (Daubechies, 1992), we define the wavelet $\Psi_{m,n}$ for the m-th scale and the n-th time by the equation: $\Psi_{m,n}(t) = \frac{1}{\sqrt{m}}\Psi\left(\frac{t-n}{m}\right)$, $m \in \mathbb{R}^+$, $n \in]1, T]$. Considering now a time series or a signal $f(t)$, the wavelet coefficient for the m-th scale and the n-th time is given by the equation: $W_{m,n}(f) = \int_1^T f(t)\Psi_{m,n}^*(t)dt$, where * denotes the complex conjugate. The scale factor m may be seen as a dilation of the function f while the number n is the time translation. As said previously, the wavelet coefficients provide local (in time) correlations between the data and the wavelet with respect to analyzed scale.

Using the wavelet concept, it is possible to define the analog of a cross-correlation with a time series and a scale point. This is the purpose of the coherency estimation using the cross-wavelet analysis. The cross-wavelet has an equivalent in frequency domain with the Fourier cross-spectrum and reflects the Wiener–Khintchine theorem. If two series present some common structures, the high values of the cross-wavelet coefficients are locally highlighting these structures. To the contrary when the two series have no relation the cross-wavelet analysis gives back weak coefficients.

Mathematically, let be a first time series $f(t)$ and a second $g(t)$ both defined in the interval $[1, T]$. One may define the cross-wavelet $W_{m,n}(f, g)$ by the wavelet coefficients inner product: $W_{m,n}(f, g) = < W_{m,n}(f), W_{m,n}^*(g) >$ (Grinsted et al., 2004; Maraun and Kurths, 2004). Thus a cross-wavelet coefficient is a complex number with an absolute value and an argument (or phase angle). By definition, the cross-wavelet coefficients are un-normalized coefficients. To be relied to the cross-correlation, the cross-wavelet coefficients have to be normalized. These new figures are called coherency (Maraun and Kurths, 2004). The coherency is the ratio of the energy of $W_{m,n}(f, g)$ by the product of the energy of $W_{m,n}(f)$ and $W_{m,n}(g)$. More precisely using a normalized smoothing operator $< >$ in scale and in time, the wavelet coherency is given by the equation: $R_{m,n}(f, g) = \frac{|<W_{m,n}(f,g)>|}{\left(|<W_{m,n}(f)>|<W_{m,n}(g)>|\right)^{1/2}}$. The coherency is 1 if the two series f and g are linearly dependant around the time n and on a scale m. A zero value means no local cross-correlation. The coherency is therefore an excellent tool to qualify the relationship between two parameters. In the sequel we perform analyses between biological characteristic of algae and environmental parameters in order to highlight their possible links. The wavelet coherency phase angle $\phi_{m,n}(f, g)$ is the argument of the coefficient: $W_{m,n}(f, g)$, which could be computed using the following equation: $\phi_{m,n}(f, g) = \text{atan}\left(\frac{\Im(<W_{m,n}(f,g)>)}{\Re(<W_{m,n}(f,g)>)}\right)$, where for a complex number $z \in \mathbb{C}$, $\Re(z)$ is its real part, and $\Im(z)$ is its imaginary part.

The phase angle is a common way to illustrate the difference between two waves, for instance when they reach their maximum. A null phase angle means that the two waves are in phase ($\uparrow$), i.e. they reach their maximum at the same time. The phase angle is $-\pi$ when the waves are anti-phased ($\downarrow$), i.e. the first is reaching its maximum while the second is at its minimum. The phase angle is $\pi/2$ when the first series leads the second ($\rightarrow$) and is $-\pi/2$ when the second series leads the first ($\leftarrow$). The phase angle may be also seen as the phase difference between the two series (the shape of the time lag between the series). Therefore the wavelet analysis is a well-adapted tool to

Please cite this article as: Wang, C., et al., Exploring temporal trend of morphological variability of a dominant diatom in response to environmental factors in a large subtrop..., Ecological Informatics (2014), http://dx.doi.org/10.1016/j.ecoinf.2014.11.002

study data series with local structures or with sparse occurrence like hydrological quantities or physiological parameters. In our work instead of use the direct coefficient, we choose to examine the wavelet power spectrum (WPS). WPS is defined as $2^j|W_{n,k}(f)|^2$, where j is the scale level. This technical choice provides easier graphical examination among hydrologic changes and physiological parameters. In the sequel the Morlet wavelet transform will be used (with the mother wavelet for the parameter k given by $\Psi_k(t) = \pi^{-\frac{1}{4}} e^{-ikt} e^{-\frac{|t|}{2}}$) and we selected the 95% confidence interval for wavelet power as significance criteria. The coherency and phase angle are evaluated to bear out the first analyses and complete the diagnoses.

2.4. Redundancy analysis (RDA)

Morphological parameters responding to environmental factors were also identified by redundancy analysis (RDA) using the software package R 3.0.2 (http://www.r-project.org). To analyze the influence of these environmental factors on morphological parameters of *A. granulata*, RDA was performed using the R add-on package "vegan." A forward selection of environmental factors was applied to avoid using collinear environmental factors in the same constrained ordination model. Only those parameters contributing significantly ($p < 0.05$ via 1000 times permutation tests) to morphological variations were added to the model.

3. Results

3.1. Annual variation pattern of morphological parameters of A. granulata

The annual variations of cell size parameters and filament length (in terms of number of cells per filament) are shown in Fig. 3. The mean cell diameter ranged from 5 ± 0 to 17.25 ± 2.22 μm, with an average of 9.25 ± 1.45 μm. The highest value appeared on November 15th, and the lowest value appeared on January 30th. The annual variation pattern of cell diameter showed four distinct periods. The first period lasted from January to April, characterized by low values and light fluctuations, with values mainly ranging from 6 to 9 μm. The second period was from early May to early July, which started with two narrow consecutive ascending–descending cycles and then decreased continually until early July. The third period lasted from mid July to mid October, which was characterized by two wider consecutive ascending–descending cycles; with the small cycle lasting 1 month and the big cycle lasting 2 months. The fourth period was from October 15th to December 20th, characterized by extremely high values mainly in the range of 10 to 16 μm, and the maximum value of this period was 17.25 ± 2.22 μm on November 15th (Fig. 3a).

The mean cell length ranged from 11.25 ± 3.75 to 17.75 ± 6.5 μm, with an average of 14.03 ± 1.12 μm. The highest value appeared on December 1st, and the lowest value appeared on May 25th. The annual variation pattern showed two distinct periods. The first period was from January 1st to August 10th, characterized by fluctuations under 15 μm, mainly in the range of 11 to 15 μm. The second period was from August 15th to December 20th, characterized by an apparent ascending trend which peaked and then dropped, and the mean values ranged primarily from 13 to 17 μm (Fig. 3b).

The mean cell volume ranged from 235.50 ± 0 to 4131.77 ± 1820.86 μm^3, with an average of 1145.37 ± 424.40 μm^3. The highest value appeared on November 30th, and the lowest value appeared on January 30th. The annual variation pattern was almost the same as that of cell diameter, but only one big cycle was significant during the corresponding two mid periods (Fig. 3c).

The mean filament length (number of cells per filament) ranged from 1.16 ± 0.37 to 67.80 ± 48.80 cells, with an average of 12.64 ± 9.28 cells. The highest value appeared on November 10th, and the lowest value appeared on September 5th. The annual variation pattern showed two distinct periods. The first period was from the beginning of the year to mid October, with low filament length, mainly fluctuating under 10 cells. The second period was from October 20th to December 20th, with high filament length, and mean values mainly ranging from 20 to 70 cells (Fig. 3d).

3.2. Relationship between morphological parameters

Relationships between morphological parameters were analyzed; a significant positive correlation ($r^2 = 0.6402$, $p < 0.0001$) was found between cell diameter and cell length (Fig. 4a), and a significant correlation was also found between cell diameter and cell volume ($r^2 = 0.9803$, $p < 0.0001$) with polynomial function (Fig. 4b). No significant

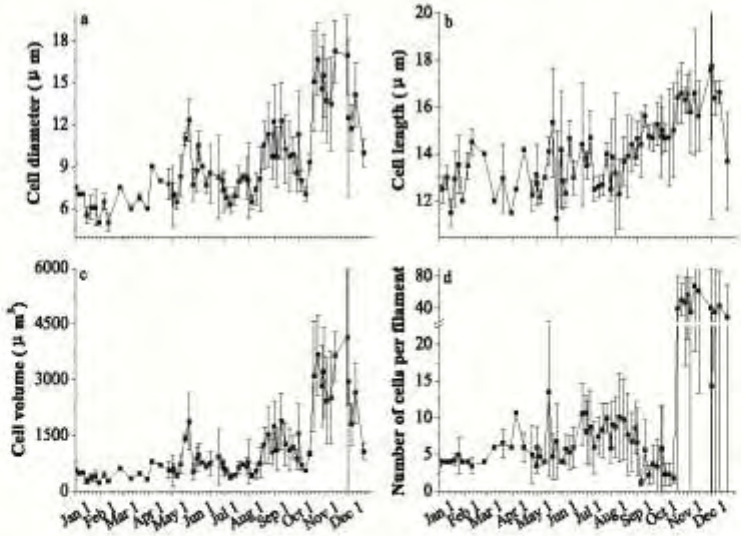

Fig. 3. Annual variation pattern of cell and filament dimensions (means ± SD). a. Cell diameter; b. cell length; c. cell volume; d. filament length. Only values of the 67 samples that *A. granulata* positioned are shown in the figure.

Please cite this article as: Wang, C., et al., Exploring temporal trend of morphological variability of a dominant diatom in response to environmental factors in a large subtrop..., Ecological Informatics (2014), http://dx.doi.org/10.1016/j.ecoinf.2014.11.002

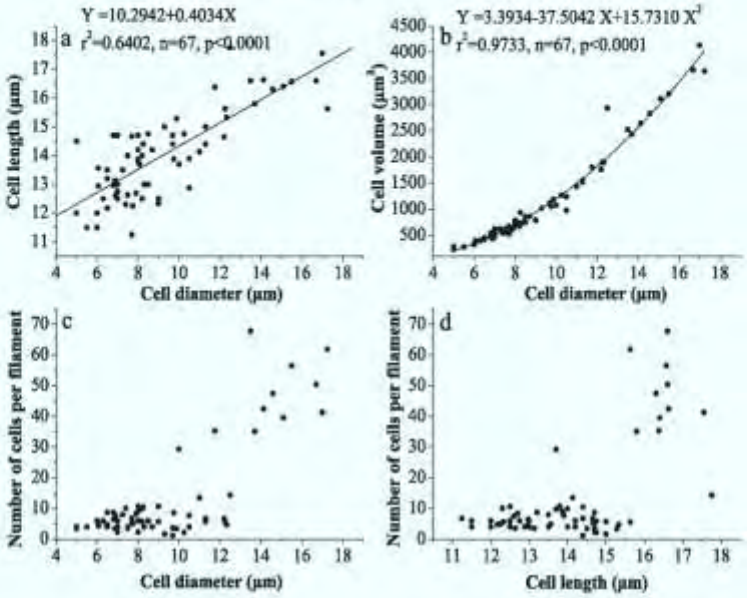

Fig. 4. Regression analysis on morphological parameters (a. cell diameter and cell length; b. cell diameter and cell volume; c. cell diameter and filament length (number of cells per filament); d. cell length and filament length (number of cells per filament)).

correlation was found between cell diameter and filament length (Fig. 4c), cell length and filament length (Fig. 4d).

3.3. Cross wavelet analysis on morphological parameters

The relationship between cell diameter and cell length with cross wavelet analysis is shown in Fig. 5. The horizontal axis indicates the study period, and the vertical axis is the scale number for the wavelet analysis. The areas blocked by the black lines indicate the 95% confidence interval.

Fig. 5a showed that full coherence existed between cell diameter and cell length with the scale number of 0 to 8, except for a period from April to May around scale 3, and a period from mid July to late October with the scale number of 0 to 6, but light coherence was also found between late August and late September nearing scale 0. Arrows pinpoint left-to-right directions in the highest coherence area, which meant that cell diameter varied before cell length during this period. Fig. 5b represents the cross wavelet coefficients and confirms the reading of the coherence in Fig. 5a.

Full coherence between the cell diameter and filament length was shown in Fig. 6a with the scale number of 0 to 6, except for a period from late April to early June in scale range of 0 to 4, and a period from early July to early October in scale range of 0 to 6. Most arrows of high coherence area were in direction of left to right, meaning that cell diameter varied before filament length during this period (Fig. 6a). Fig. 6b confirms the reading of the coherence in Fig. 6a.

3.4. Cross wavelet analysis of correlations between morphological parameters and environmental factors

3.4.1. Relationship between cell diameter and environmental factors

In Fig. 7a to 7i, a full coherence was highlighted by wavelet analysis between the variable cell diameter and environmental factors. Table 1 gave the details including period, analyzing scale and the possible link between the variables. Full coherence with water temperature occurred in three periods with different scales, and phase angles indicated the moderate before-in-phase in spring, in-phase for one period of autumn, and before-phase for the rest of autumn (Fig. 7a, Table 1). The full coherence period with discharge occurred in flood season through

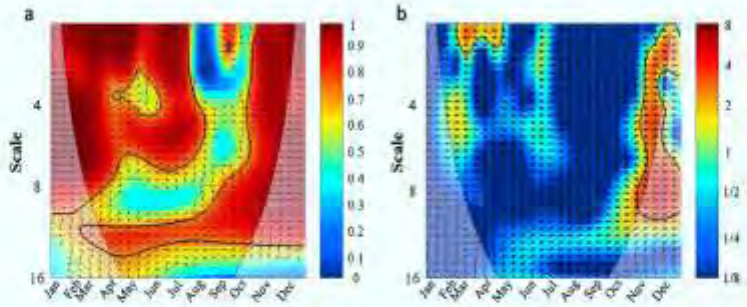

Fig. 5. Cross wavelet analysis of relationships between cell diameter and cell length (a. coherence; b. cross wavelet coefficients). The 5% significance level against red noise is shown as a thick contour. The relative phase relationship is shown as arrows (before-phase pointing right, after-phase pointing left, in-phase pointing up, and anti-phase pointing down). The horizontal axis represents the 81 sampling days, and the vertical axis represents scale number. Color bar with coefficients represents coherence level (from red to blue means coherence is from high to low). (For interpretation of the references to color in this figure legend, the reader is referred to the web version of the article.)

Please cite this article as: Wang, C., et al., Exploring temporal trend of morphological variability of a dominant diatom in response to environmental factors in a large subtrop..., Ecological Informatics (2014), http://dx.doi.org/10.1016/j.ecoinf.2014.11.002

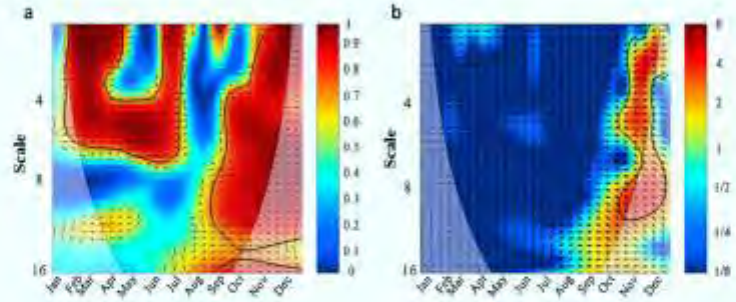

Fig. 6. Cross wavelet analysis of relationships between cell diameter and filament length (a. coherence; b. cross wavelet coefficients). The 5% significance level against red noise is shown as a thick contour. The relative phase relationship is shown as arrows (before-phase pointing right, after-phase pointing left, in-phase pointing up, and anti-phase pointing down). The horizontal axis represents the 81 sampling days, and the vertical axis represents scale number. Color bar with coefficients represents coherence level (from red to blue means coherence is from high to low). (For interpretation of the references to color in this figure legend, the reader is referred to the web version of the article.)

spring and summer, and phase angles indicated the anti-phase (Fig. 7b, Table 1). While the full coherence period with precipitation occurred in spring and the coherence was in-phase (Fig. 7c, Table 1). Full coherence with phosphate was confirmed in four periods, two of which appeared at the beginning and the end of the year, and the other two appeared in spring and autumn respectively. Phase angles of the fourth period exhibited definite after-phase coherence, while the first and third period exhibited moderate after-in-phase, and the second period exhibited moderate before-anti-phase (Fig. 7d, Table 1). Full coherence with silicate appeared in winter, summer and autumn, and corresponding relationship was before-in-phase, before-anti-phase and after-phase respectively (Fig. 7e, Table 1). Four full coherence periods with total nitrogen occurred in all seasons except spring, and phase angles indicated the relationship was before-phase in winter, after-phase in summer, moderate after-anti-phase for the first autumn period, and before-anti phase for the second autumn period (Fig. 7f, Table 1). All four full coherence periods with nitrate nitrogen occurred in summer and autumn, and the relationship was moderate before-in-phase in summer, after-phase for both the first and fourth autumn period, and in-phase for the second autumn period (Fig. 7g, Table 1). Full coherence with nitrite nitrogen was confirmed in four periods covering all seasons except winter, and the relationship was after-anti-phase in spring, before-in-phase in the first autumn period, before-phase in the second autumn period, and anti-phase in the last period (Fig. 7h, Table 1). Only two

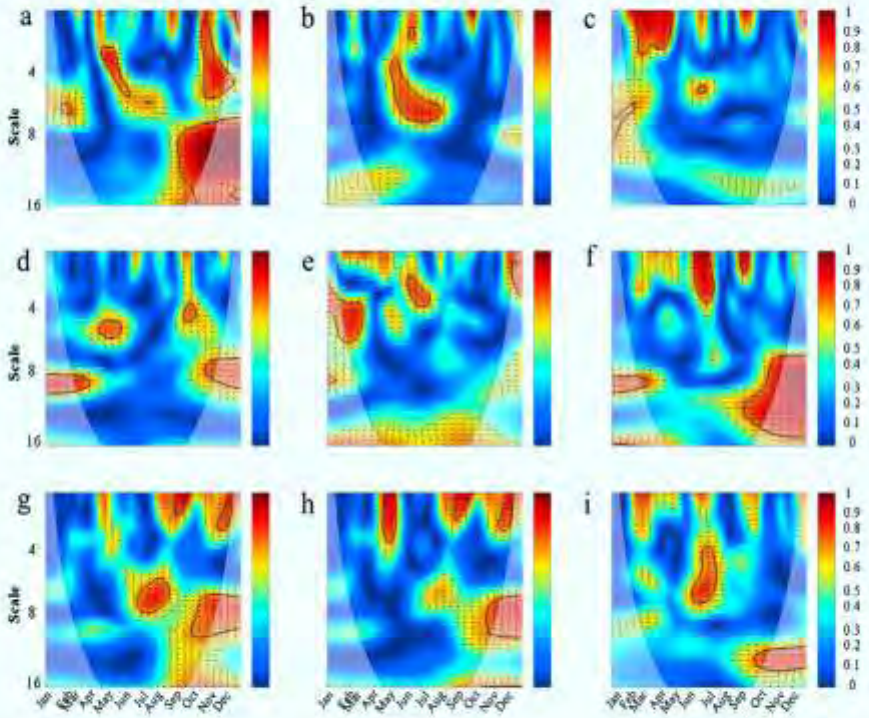

Fig. 7. Cross wavelet analysis of relationships between cell diameter and environmental factors (a. water temperature; b. discharge; c. precipitation; d. phosphate; e. silicate; f. total nitrogen; g. nitrate nitrogen; h. nitrite nitrogen; i. ammonia nitrogen). The 5% significance level against red noise is shown as a thick contour. The relative phase relationship is shown as arrows (before-phase pointing right, after-phase pointing left, in-phase pointing up, and anti-phase pointing down). The horizontal axis represents the 81 sampling days, and the vertical axis represents scale number. Color bar with coefficients represents coherence level (from red to blue means coherence is from high to low). (For interpretation of the references to color in this figure legend, the reader is referred to the web version of the article.)

Please cite this article as: Wang, C., et al., Exploring temporal trend of morphological variability of a dominant diatom in response to environmental factors in a large subtrop..., Ecological Informatics (2014), http://dx.doi.org/10.1016/j.ecoinf.2014.11.002

Table 1
Summary of information (including period, analyzing scale and phase angle) on full coherence between morphological parameters (cell diameter and filament length) and environmental factors based on Figs. 6 and 7. All the periods in significant correlations with each environmental factor are shown in the table.

Environmental factors	Cell diameter			Filament length		
	Period	Analyzing scale	Phase angle	Period	Analyzing scale	Phase angle
Water temperature	15/04–10/06	3–5		01/01–15/01	Around 8	
	15/10–15/12	1–5		10/10–20/11	2–5	
	05/09–30/12	7–16		15/08–30/12	7–16	
Discharge	05/05–10/06	3–7		10/05–30/06	Around 6	
Precipitation	10/02–25/04	0–3		25/02–10/04	0–2	
Phosphate	01/01–01/04	Around 8		30/03–20/05	Around 5	
	15/04–30/05	Around 5		20/05–01/06	Around 1	
	20/09–05/10	Around 4				
	25/10–30/12	Around 8				
Silicate	01/01–15/03	2–6		01/01–05/03	2–5	
	01/06–15/07	Around 3		15/06–05/07	Around 3	
	10/12–30/12	1–3		05/12–30/12	Around 2	
				05/09–30/12	13–16	
Total nitrogen	01/01–25/03	Around 8		01/06–15/07	0–5	
	01/06–10/07	0–3		25/08–01/09	0–2	
	30/08–15/09	0–1		10/10–30/12	7–14	
	05/09–30/12	7–15				
Nitrate nitrogen	25/06–20/08	6–8		20/11–30/12	Around 7	
	05/09–30/09	Around 1		30/08–30/12	13–16	
	01/10–30/12	7–9				
	20/11–15/12	Around 2				
Nitrite nitrogen	20/04–15/05	0–3		20/11–30/12	7–9	
	30/08–30/09	Around 1		15/09–30/12	Around 16	
	20/11–10/12	Around 2				
	30/10–30/12	7–11				
Ammonia nitrogen	30/05–15/07	3–6		01/01–10/01	0–2	
	30/09–30/12	Around 13		05/06–15/07	Around 6	

full coherence periods between cell diameter and ammonia nitrogen were confirmed, which occurred in summer and autumn, and the opposite phase angles indicated the before-phase in summer and after-phase in autumn (Fig. 7i, Table 1).

3.4.2. Relationships between filament length and environmental factors

From Fig. 8a to 8i, a full coherence was highlighted by the wavelet analysis between the variable filament length and environmental factors. Table 1 also gave details including the temporal distribution and the possible link between the variables. Full coherence with water temperature occurred in three periods covering all seasons except spring, and phase angles indicated the before-phase in winter, in-phase for the first autumn period, and moderate before-in-phase for the second autumn period (Fig. 8a, Table 1). The full coherence period with discharge covered spring and summer, and phase angles indicated the moderate after-anti-phase (Fig. 8b, Table 1), while the full coherence with precipitation occurred in spring, and phase angles indicated in-phase (Fig. 8c, Table 1). Both the two full coherence periods with phosphate appeared in spring, with different scales, and phase angles indicated the moderate before-anti-phase and before-phase respectively (Fig. 8d, Table 1). Full coherence with silicate appeared in four periods covering all seasons except spring, and the relationships were moderate before-in-phase in winter, anti-phase in summer, and after-phase in both the two autumn periods (Fig. 8e, Table 1). Full coherence with total nitrogen occurred in three periods covering summer and autumn, and phase angles indicated after-phase in both the summer periods, and before-phase in the autumn period (Fig. 8f, Table 1). Both the full coherence periods with nitrate nitrogen appeared in autumn and the relationships were moderate after-in-phase and before-in-phase (Fig. 8g, Table 1). Full coherence with nitrite nitrogen was also confirmed in two autumn periods, and the relationships were moderate before-anti-phase and after-anti-phase (Fig. 8h, Table 1). Two full coherence periods with ammonia nitrogen occurred in winter and summer, and with the same correlation: before-phase (Fig. 8i, Table 1).

3.5. Canonical correlations between morphological parameters and environmental factors

Constrained RDA with environmental factors resulted in five significant variables, which explained 53.4% of the variation in morphological parameters of *A. granulata* (Fig. 9). The ANOVA test on the RDA model indicated that the reduced model could reflect the correlations between morphology and selected variables well ($p = 0.001$), and test on all canonical axes indicated that axis RDA1 ($p = 0.001$) had a significant influence on the correlations. The eigenvalue of the axis RDA1 was 0.659, and it explained 97.48% of the total variance in morphology variation. Silicate ($p = 0.001$), total nitrogen ($p = 0.001$), discharge ($p = 0.002$), phosphate ($p = 0.002$) and ammonia nitrogen ($p = 0.01$) were the main factors that jointly influenced the morphological parameters, and their coordinates on RDA1 were 0.82, 0.55, −0.54, 0.48 and 0.37 respectively. All nutrients exhibited a positive effect on morphological parameters especially cell diameter, cell volume and filament length, while discharge exhibited a negative effect. Correlation between cell diameter and cell length was greater than with any other two parameters (Fig. 9).

Using the *K*-means classification method, sample dates were divided into four clusters based on the weighted orthonormal site scores of the RDA model. The sum of squares within errors of cluster 1 to 4 was 0.06, 0.22, 0.21 and 0.08 respectively, indicating that differences between samples within cluster 2 and 3 were bigger than any other two clusters. Four clusters along the dotted line corresponded to the succession in

Please cite this article as: Wang, C., et al., Exploring temporal trend of morphological variability of a dominant diatom in response to environmental factors in a large subtrop..., Ecological Informatics (2014), http://dx.doi.org/10.1016/j.ecoinf.2014.11.002

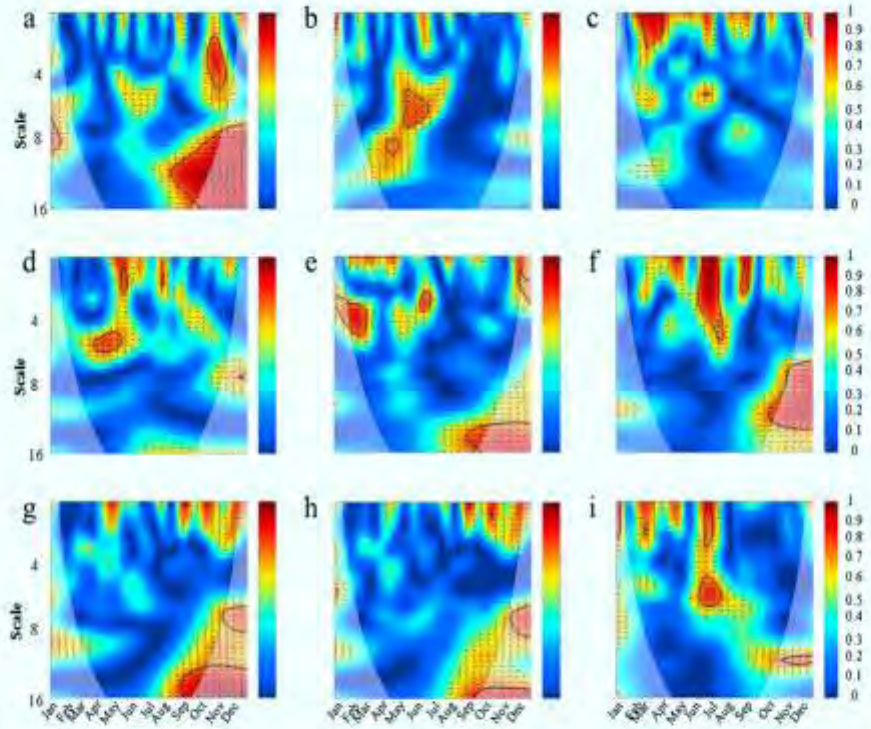

Fig. 8. Cross wavelet analysis of relationships between filament length and environmental factors (a. water temperature; b. discharge; c. precipitation; d. phosphate; e. silicate; f. total nitrogen; g. nitrate nitrogen; h. nitrite nitrogen; i. ammonia nitrogen). The 5% significance level against red noise is shown as a thick contour. The relative phase relationship is shown as arrows (before-phase pointing right, after-phase pointing left, in-phase pointing up, and anti-phase pointing down). The horizontal axis represents the 81 sampling days, and the vertical axis represents scale number. Color bar with coefficients represents coherence level (from red to blue means coherence is from high to low). (For interpretation of the references to color in this figure legend, the reader is referred to the web version of the article.)

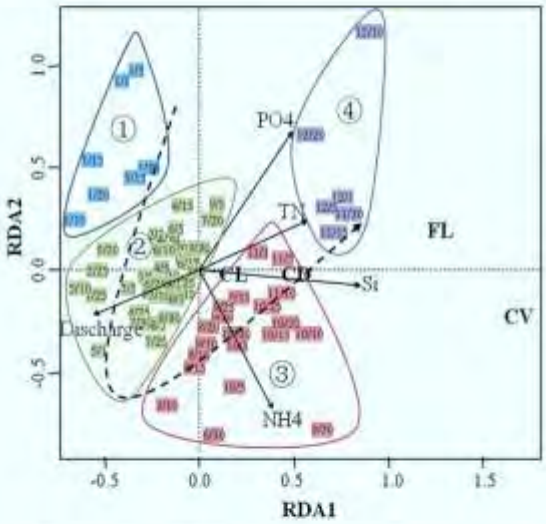

Fig. 9. Redundancy analysis (RDA) of the effect of environmental factors on morphological parameters, with date sample clusters positioned on the ordination diagram. Only those environmental factors which significantly ($p < 0.05$ by 1000 times permutation tests) explain the variation in morphological parameters is shown. Regular lines with arrows represent environmental factors, bold characters represent morphological parameters. Four clusters (from *K*-means classification) along the dashed arrow line show the time-series gradient among dates and clusters. Abbreviations: CD: cell diameter; CL: cell length; CV: cell volume; FL: filament length; PO4—phosphate; Si—silicate; TN—total nitrogen; NH4—ammonia nitrogen.

time series; when they were combined with the correlations between morphology and environments, we could find that the positive relationship between morphological parameters and nutrients mainly occurred from middle August to the end of the year, while the negative relationship between morphological parameters and discharge mainly appeared in flood period (Fig. 9).

4. Discussion

4.1. Coherence between morphological parameters

Size variation is not only related to the life cycle but also associated with natural size selectivity (Jewson, 1992). Especially for diatoms with filamentous colonies, such as *A. granulata*, both cell size and filament dimensions should be considered when referring to morphological variability and explaining by its correlations with the environment. In this respect, cell and filament dimensions were considered linked to the life cycle and size selectivity respectively. In the present results, all the three different methodological approaches (linear regression, wavelet analysis and RDA) illustrated that the coherence and correlations between cell and filament dimensions appeared weaker than that between cell parameters. This implied that cell and filament size showed different response to environmental variations, thus resulted in a conflict between the life cycle and size selectivity. The wider range of morphological parameters of *A. granulata* in river ecosystems than that in other aquatic ecosystems (Table 2) also indicated the significant role of lotic conditions in size regulation. Moreover, phase angles (pointing right) during full coherence periods illustrated that cell diameter varied in before-phase corresponding to other size parameters, and this might be the link between cell and filament dimensions.

Table 2
Comparison of *Aulacoseira granulata* morphological parameters in the West River with other aquatic systems.

Type of water area	Sampling site	Sampling time	Cell diameter (μm, average and range)	Cell length (μm, average and range)	Filament length (μm)	Filament length (number of cells)	References
Lake	Lake Huron (North America)	1977.08	17.3 (15–20)	21.7 (19–23)			Stoermer et al., 1981
	8 lakes of Finland (Finland)	1986.07	10.4–16.8	19.8–33.2			Turkia and Lepistö, 1999
	Shear Water (England)	1982.08–1984.07	8–11.3		120–720	4–25	Davey, 1987
	24 Michigan lakes (America)		3–11.5	10–17			Marsoylov et al., 2009
Reservoir	Embalse Rapel (Chile)	1984.03	7.8–10.4	28.6–37.7		2–16	Reynolds et al., 1986
	28 reservoirs scattered throughout Spain (Spain)	Winter of 1987–1988, summer of 1988	5.33 (3.88–6.78)	14.38 (12.39–16.33)		6.68 (1.95–9.69)	Gómez et al., 1995
River	Lower Paraná River (Argentina)	1993.04–1994.02	6.8 (2.0–28.0)	24.8 (7.0–59.5)		3.7 (1.0–26.0)	O'Farrell et al., 2001
	The Murray River (Australia)	1980.05–1992.06			90 (30.0–420.0)	Commonly around 6 cells	Hillrel and Crome, 1986
	The West River (China)	2009.01–2009.12	9.25 (5.0–20.0)	14.03 (7.0–27.0)	192.46 (6.50–2652.60)	12.64 (1–156)	The present paper

O'Farrell et al. (2001) reported that an inverse relationship was confirmed between cell diameter and cell length in the Lower Paraná River, and it was explained as a tendency to maintain cell volume. Similar reports could also be found for another filamentous diatom species *Aulacoseira subarctica* (O. Müller) Haworth in Kurilskoye Lake (Lepskaya et al., 2010). Davey (1986) referred to the above phase as a period of relative stability, following the regrowth of filaments from auxospores. However, the positive relationship between cell diameter and cell length was observed in the present study, which might imply that the inverse relationship was defined in the regrowth period.

4.2. Comparison of wavelet analysis and RDA

Wavelet analysis was applied as a direct measure to quantify statistical relationships between two non-stationary time series (Chatfield, 1989; Daubechies, 1992), for example the coherence between cell diameter and water temperature with time series data set in the present study. As a complementary method of constrained ordination: RDA (Rao, 1964) could analyze multivariate data, since all morphological and environmental variables were projected on a two-dimensional way in the present study. Therefore, results from wavelet analysis exhibited correlations between two variables (Figs. 5–8), while results from RDA projected all variables to a two-dimensional plane and exhibited the multi-correlations (Fig. 9).

However, the decomposition function of wavelet analysis could make a better understanding on correlations of different periods with different scales (Daubechies, 1990), since the correlation between the two analyzed variables varied with time series. Moreover, phase angles could help in understanding the phase difference between the two variables deeply. Except for a qualitative result for the whole data set, RDA referred little to correlations in time series and phase difference between variables. In a word, these two methods could complement and test each other's conclusions, which benefited our understanding on the temporal trend of morphological variability of *A. granulata* in correlations with environmental factors.

4.3. Correlations between morphological parameters and environmental factors

Although high coherence with nutrients (Fig. 7d, e and f) was found in winter, cell diameter kept low values but with relatively higher cell length/cell diameter ratios (average 2.1 and maximum 3.0) during the entire cold season, and this made cell size closer to the narrow variant form, var. *angustissima*. Our studies in the Pearl River Estuary found that the dominance of the nominated form could be replaced by a narrow form in winter, which was explained as the narrow form could tolerate low temperatures (Wang et al., 2009). O'Farrell et al. (2001) also reported that a decrease in cell diameter and a slight increase in length occurred at the end of winter in the Lower Paraná River. However, Gómez et al. (1995) found no correlation between water temperature and cell size in Spanish reservoirs. Our present results seemed to support this, since phase angles (pointing right) (Figs. 7a and 8a, Table 1) illustrated that both cell and filament dimensions varied before temperature change. Similarly, water temperature was eliminated from the significant impact factors by RDA (Fig. 9). Therefore, we assumed that water temperature was an essential factor for algal growth and thus for size variations. Tsukada et al. (2006) reported that *A. granulata* could not grow at 8 °C but grew well at 32 °C in culture. Davey (1987) also observed the increase in filament length of *A. granulata* after cold winter. However, cell diameter did not increase immediately until it past a transitional period from March to April, characterized by frequent absences from water column and slight ascending fluctuations. This was thought to be the early stage of the life cycle. Davey (1987) considered that the spring absences were in a close relationship with the largely senescent process of over-wintering, and therefore responses to changing environmental conditions were

delayed. The coherence analysis with environments and phase angles indicated that phosphate (Fig. 7d) might contribute to the slight ascending fluctuations during the transitional period, and precipitation (Figs. 7c and 8c) might explain the low occurrence rate since rainfall-triggered turbulence could cause the inconsecutive recruitment from sediments.

Two consecutive ascending–descending cycles in cell size occurred between early May and early June, with similar trends in both cell length and volume, but an inconsistent trend in filament length (Fig. 3). The coherence between cell and filament dimensions disappeared during this period (Fig. 6). Another explanation might be that cells started a new growth cycle under improved conditions, but filament growth was limited by water turbulence corresponding to ascending discharge. Evidence could be found from the coherence with water temperature and nitrite nitrogen for cell diameter (Fig. 7a and h), and coherence with discharge for filament length (Fig. 8b). RDA also reflected the negative relationship between morphology and discharge during this period (Fig. 9). Previous studies had reported that fast flowing water and short residence time in conjunction with high river discharge prevented phytoplankton from efficiently utilizing resources and adequately developing population size (Salmaso and Braioni, 2008; Salmaso and Zignin, 2010; Waylett et al., 2013). Moreover, cell diameter was also found in anti-phase with discharge (Fig. 7b), which might be the flushing impact that resulted in the shortened life cycle. Devercelli (2010) also reported that *A. granulata* could increase growth rate during flood periods. After this period, high coherence between cell and filament reappeared, but lasted for only 1 month (Fig. 6), during which cell diameter decreased continuously, with a contrary ascending filament length. We regarded this short period as an important vegetative production period, since a corresponding rise in cell abundance was also confirmed (Wang et al., 2012). Total nitrogen was responsible for both cell and filament changes (Table 1). Jewson (1992) gained similar conclusions from another filamentous centric diatom (*A. subarctica*) with similar morphology to *A. granulata*.

The other two consecutive cycles of cell diameter occurred between early July and early October, and its coherence with both cell and filament length disappeared during this period (Figs. 5 and 6). Increasing water temperature and decreasing discharge in this period could provide better conditions for the algal growth (Zhu et al., 2013). Also, an increase in *A. granulata* abundance developing into the first peak was also found (Wang et al., 2012). However, the weak turbulent conditions could undermine to silicify colonial diatoms that typically occurred in large-sized natural water bodies (Mitrovic et al., 2011; Tavernini et al., 2011). Therefore, we assumed that the gradual decrease in filament length was a strategy to adapt to the adverse situations, since short filaments assisted with greater dispersal of cells within the water bodies. Moreover, the continual ascending trend in cell length could also increase the surface-area ratio and thereby the frictional resistance, especially with shortening filament length, finally resulting in lower sinking velocities (Young et al., 2012). In a word, when discharge impacted the life cycle length, both cell and filament length variations could counteract the change in conditions.

Extremely high values of both cell and filament dimensions were observed at the end of the year (Fig. 3), which was regarded as an uncommon event, most probably the re-suspension from benthos. Results from benthic samples illustrated the dominance of *A. granulata* on surface sediment, and most cells were living (unpublished data). As for the uncommon large size of the algae, it might be explained in following ways. First, corresponding high density was also determined during this period, especially as it occurred after a six week's low density period (Wang et al., 2012). Hötzel and Croome (1996) proposed that a rapid increase in abundance after prolonged periods of absence was attributed to the inoculums of cells from sediments. Second, a high filament length was generally unsuitable for *A. granulata* to maintain a distribution in the water column (Davey and Walsby, 1985), especially with a discharge below 1500 $m^3 s^{-1}$ in drought seasons. Karim-Abdel and Saeed (1978) reported that *A. granulata* sank and disappeared at over 6 m-depth water column when turbulence became too low in the White Nile, and similar results were also reported in the Murray River (Hötzel and Croome, 1996). Third, surface sediments could provide nutrient-rich conditions for *A. granulata* growth and the benthic algae were assumed to be saturated with nutrients and thus developed larger dimensions. The dramatic increase in nutrients (e.g. phosphate and silicate, unpublished data) was also related to nutrient regeneration from the sediment bed. Cross wavelet analysis illustrated that both cell and filament dimensions were in high coherence with almost all nutrients during this period (Figs. 7 and 8). RDA also indicated that high coherence between morphology and nutrients mainly appeared at the end of the year (Fig. 9). Other chain-forming diatoms had also shown a similar pattern of increase in filament length in response to greater nutrient abundance (Poister et al., 2012; Takabayashi et al., 2006). Fourth, the relatively calm conditions on surface sediments would limit the formation of separation valves, which was regarded as the key step for natural separation of the filaments (Davey and Crawford, 1986), since necessary micro-turbulence on internal cells of a filament was lacking. Thus, long filament chains were easily formed under benthic calm conditions. Gómez et al. (1995) also reported that filaments were longer in the stratification period than the turnover period in Spanish reservoirs.

5. Conclusion

In conclusion, high coherence between morphological parameters, especially for cells, had been confirmed and demonstrated with both one-dimensional and two-dimensional analysis methods in the present study, and cell diameter was more sensitive than other parameters to environmental variables. However, the high coherence between morphological parameters could be disturbed by water turbulence associated with discharge. Water temperatures had negative impacts on the occurrence rates and size values only during the spring–winter period, while discharge not only impacted the life cycle in terms of growth rate, but also impacted filament length by allowing for selection of chains with optimum buoyancy. The responses of algae size to nutrients, especially silicate, total nitrogen and phosphate, were associated with a life cycle. The above correlations were supported by both wavelet analysis and RDA. Moreover, the extremely high values at the end of the year could result from algal recruitment from benthos.

Acknowledgements

We wish to thank Zhaoqing Fishery Team of Guangdong Province Fishery Team for their assistance in sampling work, and Radika Michniewicz for language improvements. This work was financially supported by National Natural Science Foundation of China (41403071), Guangxi Province Natural Science Foundation of Key Projects (2013GXNSFEA053003) and Public Sector (agriculture) Special Scientific Research Projects (201303056-5).

References

Babanazarova, O.V., Likhoshway, Y.V., Sherbakov, D.Y., 1996. On the morphological variability of *Aulacoseira baicalensis* and *Aulacoseira islandica* (Bacillariophyta) of Lake Baikal, Russia. Phycologia 35 (2), 113–123.

Blauw, A.N., Benincà, E., Laane, R.W.P.M., Greenwood, N., Huisman, J., 2012. Dancing with the tides: fluctuations of coastal phytoplankton orchestrated by different oscillatory modes of the tidal cycle. PLoS ONE 7 (11), e48319. http://dx.doi.org/10.1371/journal.pone.0048319.

Bliss, C.I., 1970. Statistics in Biology. McGraw-Hill Book Company, New York.

Chatfield, J., 1989. The Analysis of Time Series: An Introduction. Chapman & Hall, London.

Daubechie, I., 1990. The wavelet transform, time-frequency localization and signal analysis. IEEE Trans Inf. Theory 36 (5), 961–1005.

Daubechies, I., 1992. Ten Lectures on Wavelets, Society for Industrial and Applied Mathematics. Philadelphia.

Please cite this article as: Wang, C., et al., Exploring temporal trend of morphological variability of a dominant diatom in response to environmental factors in a large subtrop..., Ecological Informatics (2014), http://dx.doi.org/10.1016/j.ecoinf.2014.11.002

Davey, M.C., 1986. The relationship between size, density and sinking velocity through the life cycle of Melosira granulata (Bacillariophyta). Diatom Res. 1 (1), 1–18.
Davey, M.C., 1987. Seasonal variation in the filament morphology of the freshwater diatom Melosira granulata (Ehr.) Ralfs. Freshw. Biol. 18, 5–16.
Davey, M.C., Crawford, R.M., 1986. Filament formation in the diatom Melosira granulata. J. Phycol. 22, 144–150.
Davey, M.C., Walsby, A.E., 1985. The form resistance of sinking chains. Br. Phycol. J. 20, 243–248.
Devercelli, M., 2010. Changes in phytoplankton morpho-functional groups induced by extreme hydrometric events in the Middle Paraná River (Argentina). Hydrobiologia 639, 5–19.
Gibson, C.E., Anderson, N.J., Haworth, E., 2003. Aulacoseira subarctica: taxonomy, physiology, ecology and palaeoecology. Eur. J. Phycol. 38, 83–101.
Gómez, N., Riera, J.L., Sabater, S., 1995. Ecology and morphological variability of Aulacoseira granulata (Bacillariophyceae) in Spanish reservoirs. J. Plankton Res. 17 (1), 1–16.
Grinsted, A., Moore, J.C., Jevrejeva, S., 2004. Application of the cross wavelet transform and wavelet coherence to geophysical time series. Nonlinear Process. Geophys. 11, 561–566.
Horn, H., Paul, L., Horn, W., Petzoldt, T., 2011. Long-term trends in the diatom composition of the spring bloom of a German reservoir: is Aulacoseira subarctica favoured by warm winters? Freshw. Biol. 56, 2483–2499.
Hornberger, G., Wiberg, P., 2006. Numerical Methods in the Hydrological Sciences. American Geophysical Union, Washington, DC.
Hötzel, G., Croome, R., 1996. Population dynamics of Aulacoseira granulata (Ehr.) SIMONSON (Bacillariophyceae, Centrales), the dominant alga in the Murray River, Australia. Arch. Hydrobiol. 136 (2), 191–215.
Jewson, D.H., 1992. Size reduction, reproductive strategy and the life cycle of a centric diatom. Philos. Trans. R. Soc. London. Ser. B 336, 191–213.
Jewson, D.H., Granin, N.G., Zhdanov, A.A., Gorbunova, L.A., Gnatovsky, R.Y., 2010. Vertical mixing, size change and resting stage formation of the planktonic diatom Aulacoseira baicalensis. Eur. J. Phycol. 45, 354–364.
Kamenir, Y., Dubinsky, Z., Zohary, T., 2004. Phytoplankton size structure stability in a meso-eutrophic subtropical lake. Hydrobiologia 520, 89–104.
Karim-Abdel, A.G., Saeed, O.M., 1978. Studies on the freshwater algae of the Sudan III. vertical distribution of Melosira granulata (Ehr.) Ralfs in the White Nile, with reference to certain environmental variables. Hydrobiologia 57, 73–79.
Lepistö, L., et al., 2006. Estimation of reference conditions for phytoplankton in a naturally eutrophic shallow lake. Hydrobiologia 568, 55–66.
Lepskaya, E.V., Jewson, D.H., Usoltseva, M.V., 2010. Aulacoseira subarctica in Kurilskoye Lake, Kamchatka: a deep, oligotrophic lake and important pacific salmon nursery. Diatom Res. 25 (2), 323–335.
Mallat, S.G., 1989. A theory for multi-resolution signal decomposition: the wavelet representation. IEEE Trans. Pattern Anal. Mach. Intell. 11 (7), 674–693.
Manoylov, K.M., Ognjanova-Rumenova, N., Stevenson, R.J., 2009. Morphotype variations in subfossil diatom species of Aulacoseira in 24 Michigan lakes, USA. Acta Bot. Croat. 68 (2), 401–419.
Maraun, D., Kurths, J., 2004. Cross wavelet analysis: significance testing and pitfalls. Nonlinear Process. Geophys. 11, 505–514.
Mitrovic, S.M., Hardwick, L., Dorani, F., 2011. Use of flow management to mitigate cyanobacterial blooms in the Lower Darling River, Australia. J. Plankton Res. 33, 229–241.
Miyajima, T., Nakanishi, M., Nakano, S.I., Tezuka, Y., 1994. An autumnal bloom of the diatom Melosira granulata in a shallow eutrophic lake: physical and chemical constraints on its population dynamics. Arch. Hydrobiol. 130 (2), 143–162.
Morlet, J., Arens, G., Fourgeau, E., Giard, D., 1982. Wave propagation and sampling theory – part I: complex signal and scattering in multilayered media. Geophysics 47 (2), 203–221.
Nakano, S., et al., 1996. A rapid growth of Aulacoseira granulata (Bacillariophyceae) during the typhoon season in the South Basin of Lake Biwa. Jpn. J. Limnol. 57, 493–500.
Nogueira, M.G., 2000. Phytoplankton composition, dominance and abundance as indicators of environmental compartmentalization in Jurumirim Reservoir (Paranapanema River), São Paulo, Brazil. Hydrobiologia 431, 115–128.
O'Farrell, I., Tell, G., Podlejski, A., 2001. Morphological variability of Aulacoseira granulata (Ehr.) Simonsen (Bacillariophyceae) in the Lower Paraná River (Argentina). Limnology 2, 65–71.
Patrick, R., Reimer, C.W., 1966. The diatoms of the United States (exclusive of Alaska and Hawaii). Monogr. Acad. Nat. Sci. Phila. 113, 1–688.
Poister, D., Kurth, A., Farrell, A., Gray, S., 2012. Seasonality of Aulacoseira ambigua abundance and filament length: biogeochemical implications. Plankton Benthos Res. 7 (2), 55–63.
Rao, C.R., 1964. The use and interpretation of principal component analysis in applied research. Sankhyaā A 26, 329–358.
Recknagel, F., Ostrovsky, I., Cao, H.Q., Zohary, T., Zhang, X.Q., 2013. Ecological relationships, thresholds and time-lags determining phytoplankton community dynamics of Lake Kinneret, Israel elucidated by evolutionary computation and wavelets. Ecol. Model. 255, 70–86.
Reynolds, C.S., 2006. The Ecology of Phytoplankton. Cambridge University Press, Cambridge.
Reynolds, C.S., Montecino, V., Graf, M.E., Cabrera, S., 1986. Short-term dynamics of a Melosira population in the plankton of an impoundment in central Chile. J. Plankton Res. 8 (4), 715–740.
Salmaso, N., Braioni, M.G., 2008. Factors controlling the seasonal development and distribution of the phytoplankton community in the lowland course of a large river in Northern Italy (River Adige). Aquat. Ecol. 42, 533–545.
Salmaso, N., Zignin, A., 2010. At the extreme of physical gradients: phytoplankton in highly flushed, large rivers. Hydrobiologia 639, 21–36.
Stoermer, E.F., Kreis, R.G., Sicko-Goad, L., 1981. A systematic, quantitative, and ecological comparison of Melosira islandica O. Müll. With M. granulata (Ehr.) Ralfs from the Laurentian Great Lakes. J. Great Lakes Res. 7 (4), 345–356.
Takabayashi, M., Lew, K., Johnson, A., Marchi, A., Dugdale, R., 2006. The effect of nutrient availability and temperature on chain length of the diatom, Skeletonema costatum. J. Plankton Res. 28, 831–840.
Tavernini, S., Pierobon, E., Viaroli, P., 2011. Physical factors and dissolved reactive silica affect phytoplankton community structure and dynamics in a lowland eutrophic river (Po river, Italy). Hydrobiologia 669, 213–225.
Tremarin, P.I., Ludwig, T.A.V., Torgan, L.C., 2012. Ultrastructure of Aulacoseira brasiliensis sp. nov. (Coscinodiscophyceae) and comparison with related species. 12. Fottea, Olomouc, pp. 171–188.
Tsukada, H., Tsujimura, S., Nakahara, H., 2006. Seasonal succession of phytoplankton in Lake Yogo over 2 years: effect of artificial manipulation. Limnology 7, 3–14.
Tuukia, J., Lepistö, L., 1999. Size variations of planktonic Aulacoseira Thwaites (Diatomeae) in water and in sediment from Finnish lakes of varying trophic state. J. Plankton Res. 21 (4), 757–770.
Usoltseva, M.V., Tsoy, I.B., 2010. Elliptical species of the freshwater genus Aulacoseira in Miocene sediments from Yamato Rise (Sea of Japan). Diatom Res. 25 (2), 397–415.
Wang, C., Li, X.H., Lai, Z.N., Tan, X.C., Pang, S.X., Yang, W.L., 2009. Seasonal variations of Aulacoseira granulata populatiae abundance in the Pearl River Estuary. Estuar. Coast. Shelf Sci. 85, 585–592.
Wang, C., et al., 2012. The study on population ecology of Aulacoseira granulata in Xijiang River. Acta Ecol. Sin. 32 (15), 4793–4802 (in Chinese with English abstract).
Wang, C., et al., 2013. Temporal and spatial pattern of the phytoplankton biomass in the Pearl River Delta. Acta Ecol. Sin. 33 (18), 5835–5847 (in Chinese with English abstract).
Waylett, A.J., Hutchins, M.G., Johnson, A.C., Bowes, M.J., Loewenthal, M., 2013. Physico-chemical factors alone cannot simulate phytoplankton behaviour in a lowland river. J. Hydrol. 497, 223–233.
Yan, Y., Yang, Z.F., Liu, Q., 2013. Nonlinear trend in streamflow and its response to climate change under complex ecohydrological patterns in the Yellow River Basin, China. Ecol. Model. 252, 220–227.
Young, A.M., Karp-Boss, L., Jumars, P.A., Landis, E.N., 2012. Quantifying diatom aspirations: mechanical properties of chain-forming species. Limnol. Oceanogr. 57, 1789–1801.
Zhang, X.Q., Chen, Q.W., Recknagel, F., Li, R.N., 2014. Wavelet analysis of time-lags in the response of cyanobacteria growth to water quality conditions in Lake Taihu, China. Ecol. Inform. 22, 52–57.
Zhu, K.X., Bi, Y.H., Hu, Z.Y., 2013. Responses of phytoplankton functional groups to the hydrologic regime in the Daning River, a tributary of Three Gorges Reservoir, China. Sci. Total Environ. 450–451, 169–177.

Please cite this article as: Wang, C., et al., Exploring temporal trend of morphological variability of a dominant diatom in response to environmental factors in a large subtrop..., Ecological Informatics (2014), http://dx.doi.org/10.1016/j.ecoinf.2014.11.002

Spatial-temporal pattern and prediction of phytoplankton assemblages in a subtropical river delta system

Chao Wang[1,2,3], Xinhui Li[1,3], Xiangxiu Wang[4], Zini Lai[1,3]✉, Qianfu Liu[1,3], Wanling Yang[1,3], Sovan Lek[2]

1. Pearl River Fisheries Research Institute, Chinese Academy of Fishery Science, Guangzhou 510380, China;
2. Université Toulouse, Lab Evolution & Diversité Biologique, UMR 5174, CNRS—Université Paul Sabatier, 118, route de Narbonne, 31062 Toulouse, Cedex4, France;
3. Experimental Station for Scientific Observation on Fishery Resources and Environment in the Middle and Lower Reaches of Pearl River, 526100, Ministry of Agriculture the People's Republic of China;
4. Tongji University, Shanghai 200092, China.

✉Correspondence: Zini Lai, Pearl River Fisheries Research Institute, Chinese Academy of Fishery Science, Guangzhou 510380, China.

Email: znlai01@163.com

[completed]

Abstract

Through spatial and seasonal sampling, phytoplankton patterns and prediction models were built up using a non-metric multidimensional scaling (NMDS) and Linear Discriminant Analysis (LDA) within a subtropical river delta system, the Pearl River Delta (China). The excessive nutrient conditions and well water exchanges resulted in a phytoplankton community that Bacillariophyceae and Chlorophyceae dominated in diversity and Bacillariophyceae dominated in biomass. Temporal and spatial distributions of phytoplankton assemblages were revealed by the ordination method using a NMDS and five groups were determined by using hierarchical clustering based on species biomass similarities. These five groups were clearly different, with respect to species richness, biomass and indicators, which implied the importance of spatial dimension. The LDA model indicated that the spatial patterns of phytoplankton community assemblages are mostly explained by variables (TP, Si, DO and transparency), associated with water quality. As for temporal patterns, only water temperature had a weak impact on diversity composition. By using the above environmental variables, the global score for predicting the assemblages was 75%, with the predicting performance rates for groups 1, 2, 3, 4 and 5 of 69, 88, 94, 0 and 100% respectively. G2, representing urban sites, benefited from a combination of high nutrients and well water exchanges, had the highest species richness. Moreover, the absolutely dominance of *A. granulata* resulted in extremely high biomass of this group. G4, representing inner sites, benefitted from relatively weak water exchanges and low water levels, ranked second to G2 in both species richness and biomass. G1 and G3 represented the drought and flood season respectively, but differences between them only existed in alternative dominance of diatom and green algae in species richness. And the combination of positive and negative environmental factors associated with phytoplankton development resulted in equal level of total species richness and biomass of these two groups. G5, also representing drought period, was impacted by sinking loss due to high transparency, showed both low species richness and biomass. In conclusion, the phytoplankton assemblages were mainly spatially different in the river delta system, and chemical factors plus hydrological conditions

played a more important role.

Key words: phytoplankton, Pearl River Delta, non-metric multidimensional scaling (NMDS), Linear Discriminant Analysis (LDA), environments.

Introduction

Large rivers, from headwaters to estuaries, represent a continuum of interdependent ecosystems, so studying each section of the river will be base to understand the whole aquatic ecosystem (Gamier et al., 1995). A river delta system is formed at the mouth of the river, where the river water flows into an ocean, sea, estuary, lake, or reservoir. Such a characteristic alluvial geographic system generally possesses crisscross river channels, which help branching water flows and extending retention time, and therefore it also acts as an important buffer area for pollutants and organisms that brought by the continuous flows. Ecological models have been proved to be effective in demonstrating complex aquatic ecosystems through simplified ways. In large scale river network systems which own similar complex river channels, different models have been applied to demonstrate the water quality and resources (Cressie et al., 2006; Dmitrieva, 2011; Feng et al., 2011), nutrients transportation (Gamier et al., 2002; Alexander et al., 2009), and population dynamics of organisms (Gamier et al., 1995; Bonada et al., 2007; Istvánovics et al., 2014) in previous studies, and prospective results have been gained. Therefore, advanced statistical methods are also anticipated to be applied in river delta systems, which have contractible river networks. Non-metric multidimensional scaling (NMDS) is an extremely flexible ordination method that can accommodate a variety of different kinds of data and is especially well suited to data that are discontinuous, non-normal, on arbitrary or otherwise questionable scales (Kruskal & Wish, 1978). This method has been well applied in different aquatic ecosystems for analyzing both environments (King & Richardson, 2003; Matthaei et al., 2010) and population dynamics of organisms (Walters et al., 2003; Spatharis et al., 2007; Kilroy et al., 2009). The present publications of ecological models applied in river delta systems mainly focus on aquatic environments (Justić et al. 2002, Yue et al. 2003, Yang 2011), still few refer to organisms.

The Pearl River Delta (PRD), characterized by a prosperous economy and dense human population, has always been an important center of southern China for politics,

economics and culture. The alluvial river delta owns criss-cross river channels and forms a complex regional river net structure, which offers a dramatic example of a river-estuary network whose ecological functioning has been strongly affected by both natural hydrological events and human activities during the last few decades (Chau, 2005; Qiu et al., 2010; Cao et al., 2012). Phytoplankton provides the base upon which the aquatic food chains culminating in the natural fish populations are founded (Reynolds, 1984), and it also exhibits quick responses to environmental variations. Most previously published studies of phytoplankton dynamics in rivers, however, mainly take into account the results from the main stream of the river (Ha et al., 2002; Devercelli, 2006; Salmaso & Braioni, 2008; Istvánovics et al., 2010; Waylett et al., 2013), still less referred to that in complex river delta systems. The oldest data for phytoplankton in the Pearl River basin are from the beginning of 1980s, when a general survey on aquatic organisms and water environments was carried out through the cooperation between several regional research organizations (Lu 1990). Moreover, only a simple primary dataset was collected during the investigations, and the minimal identification unit of phytoplankton composition was only specific to genus; temporal and spatial distributing patterns were still unclear. After this basic investigation, studies on phytoplankton ecology in the river basin were interrupted for the following thirty years. The author carries out relevant studies in recent years, and the results of the main stream have been reported (Wang et al. 2012, 2013). Further understanding on phytoplankton patterns and predictions is in progress, introducing more advanced statistical methods with the goal of finally providing more effective management guidelines for government.

This paper describes the temporal and spatial patterns of phytoplankton assemblages at a complex river delta system, the Pearl River Delta (China) via spatial and seasonal investigations. The classification pattern model of phytoplankton assemblages was built up using hierarchical clustering and non-metric multidimensional scaling (NMDS), and prediction analysis of how the above patterns were differentiated by environmental factors was done using Linear Discriminent Analysis (LDA), as a way to identify the main driving factors and to assess the

prediction capacity. Moreover, we postulated that the temporal patterns were fully constrained by physical drivers, i.e., water temperature and discharge, and the spatial patterns were fully constrained by chemical drivers, i.e., phosphate and nitrogen.

Methods and data treatment

Study site

The Pearl River, which consists of West, North and East Rivers, is the third largest river system in China after the Yangtze River and the Yellow River. Before entering to the South China Sea, the three rivers join together and form the Pearl River Delta (Yang et al., 2010). Figure 1 shows a general layout of the PRD basin: the basin location, the main river sources and tributaries, and the 13 spatial sampling sites. The area of PRD (21°40'–23°N, 112°–113°20'E) is about 9,750 km^2, wherein the West River delta and the North River delta account for about 93.7% of the total area of PRD, and the East River delta accounts for 6.3% (PRWRC 2006). The PRD is dominated by a sub-tropical monsoon climate with abundant precipitation. The annual mean precipitation is 1,470 mm and most rains occur in April–September. The topography of the PRD has mixed features of crisscross river-network, channels, shoals and river mouths (gates).

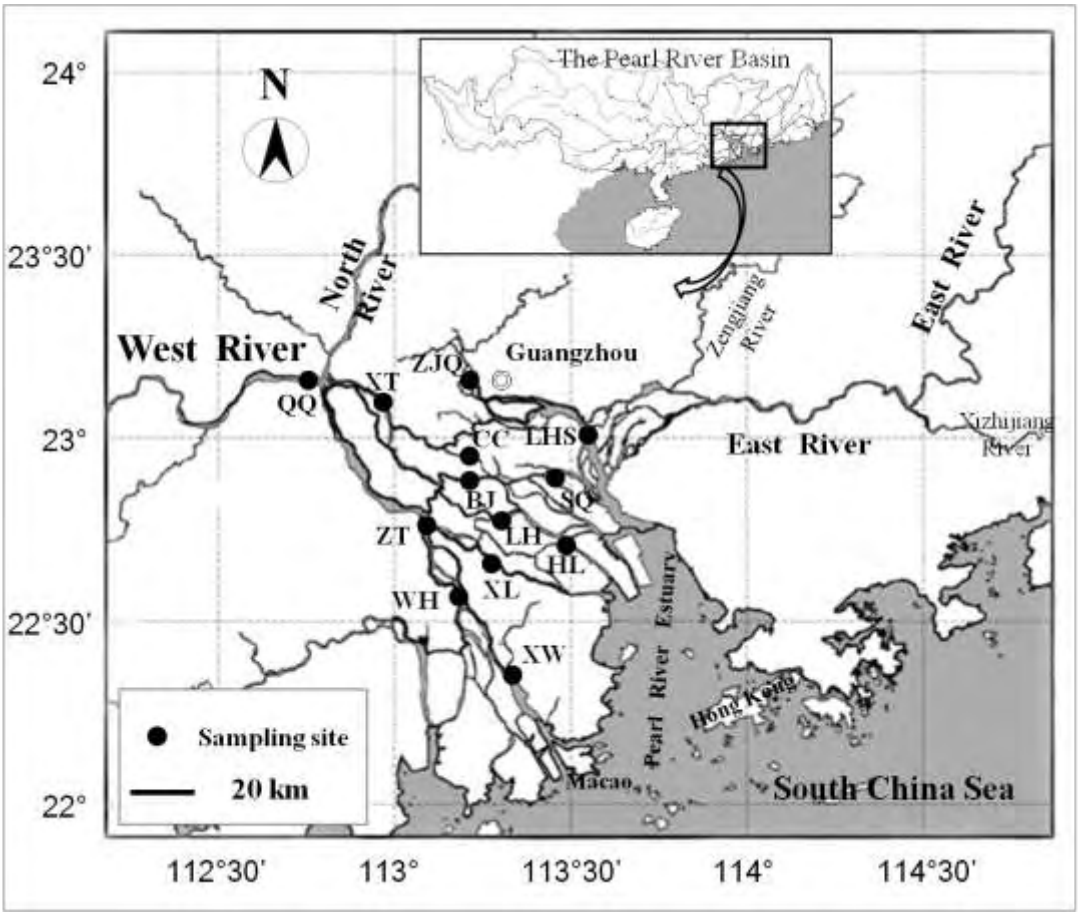

Figure 1 The river network system of the Pearl River Delta, including three main tributaries of the Pearl River and sampling sites. QQ—Qingqi, ZT—Zuotan, WH—Waihai, XW—Xinwei, XL—Xiaolan, XT—Xiaotang, BJ—Beijiao, LH—Lanhe, HL—Hengli, CC—Chencun, ZJQ—Zhujiangqiao, LHS—Lianhuashan.

A total of 13 sampling sites are set up, covering the important positions of the river network, including Qingqi (QQ), Zuotan (ZT), Waihai (WH), Xinwei (XW), Xiaolan (XL), Xiaotang (XT), Beijiao (BJ), Lanhe (LH), Hengli (HL), Chencun (CC), Zhujiangqiao (ZJQ), Lianhuashan (LHS) and Shiqiao (SQ). Among of them, QQ, ZT, WH and XW are located along the main channel of West River, finally flowing through Modao mouth and entering into the estuary. ZJQ and LHS are located along the other side of the delta, of which ZJQ is in Guangzhou channel and LHS is in East River side. Other sites are located in inner part of the delta. Coordinates of all sites are collected using GPS positioning system and listed in table 1.

Sampling work and data collected

Phytoplankton samples were collected seasonally (March, May, August and December) during 2012, and the investigation of each season was managed in

successive 2 to 3 days. For each phytoplankton sample, 1 L of water was collected from 0.5 m below the surface using a 5 L HQM-1 sampler. The sample was put into a polyethylene bottle and fixed immediately with formaldehyde solution (5%). A phytoplankton sample was fixed and concentrated by sedimentation to 100 ml. All algae were counted using a 1-ml Sedgewick-Rafte counting frame (inverted microscope Nikon Eclipse TS100). A second phytoplankton sample was assigned for diatom identification and enumeration. This sample was concentrated and treated with dilute HCl and H_2O_2, and at least 400 valves were counted. The systematic grouping of phytoplankton was done following the manual of Van den Hoek et al. (1995).

Water temperature, salinity, pH value and dissolved oxygen (DO) was determined in situ with a portable instrument (YSI6600-02). Transparency was determined using black and white transparent plate. An additional water sample of 250 ml was filtered *in situ*, and taken back to the laboratory for nutrient analysis (phosphate, silicate, total nitrogen, nitrate, nitrite and ammonia) using water flow injection analyzer (Skalar-SA1100) and spectrophotometer (Shimadzu UV-2501PC).

Data treatment

To describe the phytoplankton community, the species richness, algal biomass, species rank-biomass, occurrence rate and species indicator values were calculated. Phytoplankton biomass was calculated from biovolume of each species, assuming unit specific gravity, by geometrical approximation according to Hillebrand et al. (1999). Biomass data were $\lg(x + 1)$ transformed to reduce the effects of extreme values.

Non-metric multidimensional scaling (NMDS) was used to evaluate among-sites separation (Kruskal & Wish, 1978), which does not rely on (primarily Euclidean) distances like other ordination techniques but uses rank orders, and thus it is an extremely flexible ordination method that can accommodate a variety of different kinds of data and is especially well suited to data that are discontinuous, non-normal, on arbitrary or otherwise questionable scales. “Ordination stress” is a measure of departure from monotonicity in the relationship between the dissimilarity (distance) in the original *p*-dimensional space and distance in the reduced *k*-dimensional ordination space (Wu et al., 2011). In this analysis, we used Bray-Curtis similarity as the distance

measure. Then, hierarchical clustering, also called hierarchical cluster analysis was used to build a hierarchy of clusters based on the Ward agglomerative method.

To identify indicator species, the IndVal method (Dufrêne & Legendre 1997) was used to define the most characteristic species of each group. These indicator species were found mostly in a single group of the typology and present in the majority of the sites belonging to that group, for summarizing the assemblage patterns (He et al. 2011). Based on the fidelity and the specificity of species for each cluster, INDVAL 2.0 was used to identify indicator species. The formula is as following: $IndVal_{ij} = A_{ij} \times B_{ij} \times 100$, where $A_{ij} = Nbiomass_{ij} / Nbiomass_i$, $B_{ij} = Nsample_{ij} / Nsample_j$, and *i* means species *i*, *j* means cluster *j*. Only significant and greater than 25 IndVal have been taken into account. In this way, it implies that a characteristic species occurs in at least 50% of one site's group, and that its relative abundance in that group reaches at least 50%.

Linear Discriminant Analysis (LDA) is a method used in statistics, pattern recognition to find a linear combination of features which characterizes or separates two or more classes of objects or events. LDA explicitly attempts to model the difference between the classes of data. Here, LDA was conducted to determine which environment variables discriminate between the groups previously defined by the hierarchical cnustering. Standardized coefficients for each variable in each discriminated function represent the contribution of the respective variable to the discrimination between clusters. A random Monte Carlo test with 1000 permutations was used to reveal the significance of environmental variables among clusters.

Results

Environmental factors

Means (± SD) of main environmental factors at all sites were listed in table 1. Among all sampling sites, the two sites (ZJQ and LHS) nearing Guangzhou were apparently different from others. These two sites had apparently higher values of water temperature, salinity and nutrients, but apparently lower values of transparency and DO. Moreover, pH values of them were also lower than other sites.

Table 1 Means (±SD) of main environmental factors at all sites in the river network of PRD

Station	Longitude and latitude	Water temperature (℃)	Salinity	pH	Transparency (cm)	Dissolved oxygen (mg/L)	Total nitrogen (mg/L)	Total phosphate (mg/L)	Silicate (mg/L)
QQ	112°47'11.0"E 23°10'14.5"N	20.7 ±6.9	0.15 ±0.07	7.89 ±0.52	55 ±21	6.3 ±1.4	3.06 ±0.64	0.18 ±0.02	3.39 ±0.41
ZT	113°03'26.0"E 22°48'46.6"N	22.1 ±8.1	0.14 ±0.06	7.88 ±0.52	56 ±31	7.5 ±1.6	3.74 ±2.56	0.13 ±0.03	3.85 ±0.41
WH	113°09'20.3"E 22°36'14.5"N	22.2 ±8.5	0.14 ±0.07	7.92 ±0.35	44 ±20	8.0 ±1.4	2.43 ±0.14	0.15 ±0.05	3.91 ±0.33
XW	113°16'41.5"E 22°22'45.6"N	21.4 ±7.0	0.15 ±0.07	7.92 ±0.38	53 ±14	7.4 ±1.9	3.69 ±2.39	0.20 ±0.09	3.95 ±0.51
XL	113°17'17.9"E 22°38'13.8"N	21.6 ±7.7	0.14 ±0.06	7.83 ±0.23	54 ±21	7.3 ±2.0	2.54 ±0.51	0.12 ±0.03	3.78 ±0.36
XT	112°57'51.1"E 23°05'27.4"N	21.3 ±8.1	0.12 ±0.06	7.87 ±0.43	43 ±30	6.9 ±1.0	3.09 ±0.77	0.19 ±0.10	4.20 ±0.24
BJ	113°11'54.5"E 22°54'04.1"N	21.4 ±7.9	0.13 ±0.06	7.75 ±0.51	46 ±27	7.1 ±2.1	4.69 ±3.32	0.15 ±0.05	4.29 ±0.71
LH	113°19'53.4"E 22°49'15.2"N	21.5 ±7.5	0.13 ±0.07	7.88 ±0.40	46 ±25	6.8 ±1.4	2.82 ±0.46	0.15 ±0.06	4.67 ±0.55
HL	113°29'02.2"E 22°44'05.4"N	21.5 ±6.9	0.14 ±0.09	7.70 ±0.27	48 ±17	6.9 ±1.7	3.18 ±0.18	0.16 ±0.06	3.54 ±0.40
CC	113°14'55.7"E 22°58'15.1"N	21.4 ±8.6	0.13 ±0.07	7.84 ±0.47	48 ±30	6.0 ±1.1	2.76 ±0.45	0.16 ±0.05	5.02 ±1.57
ZJQ	113°13'16.5"E 23°08'12.6"N	22.8 ±8.6	0.31 ±0.20	7.49 ±0.44	28 ±6	1.0 ±0.4	7.06 ±0.49	0.56 ±0.17	5.63 ±1.21

LHS	113°30'37.0"E 23°00'58.0"N	24.3 ± 8.0	1.53 ± 2.55	7.51 ± 0.30	25 ± 4	4.2 ± 1.2	4.58 ± 1.04	0.28 ± 0.07	5.04 ± 0.86
SQ	113°24'49.0"E 22°55'24.2"N	22.3 ± 8.0	0.16 ± 0.12	7.95 ± 0.44	44 ± 8	5.6 ± 0.8	3.00 ± 0.70	0.21 ± 0.06	4.44 ± 0.38
All dates and sites		21.9 ± 6.9	0.26 ± 0.73	7.80 ± 0.39	45 ± 21	6.2 ± 2.2	3.59 ± 1.75	0.20 ± 0.13	4.29 ± 0.89

Phytoplankton composition

A total of 383 algal taxa (including varieties and forms) were identified, of them seven phyla – Bacillariophyceae, Chlorophyceae, Euglenophyceae, Cyanobacteria, Dinophyceae, Chrysophyceae and Cryptophyceae – were represented. The highest richness was 160 taxa for Bacillariophyceae, contributing 41.8% of the total species numbers; and the second was Chlorophyceae (112 taxa, 29.2%); third was 84 taxa for Euglenophyceae (21.9%); and the fourth was 20 taxa for Cyanobacteria (5.2%). Of the Bacillariophyceae, *Navicula* had the highest richness of 19 species, and the following were *Gomphonema* (15 taxa), *Aulacoseira* (*Melosira*) (14 taxa), *Nitzschia* (12 taxa), *Cymbella* (12 taxa), *Synedra* (8 taxa). Of the Chlorophyceae, *Scenedesmus* had the highest richness with 24 species, and *Pediastrum* and *Crucigenia* had 8 and 7 species respectively. *Euglena* of the Euglenophyceae had 29 species.

Scientific names and abbreviations of the 123 taxa whose occurrence rate is greater than 10% are listed in Table 2, with corresponding tolerance range (+ median value) of important factors for each species. The species rank of biomass and occurrence rate for all phytoplankton species is shown in Fig. 2. According to biomass rank (Fig. 2a), one species (*Aulacoseira granulata* var. *granulata*) shows an apparently high biomass, contributing 51.7% to total assemblages. The following secondary level contains three species, i.e. *Entomoneis alata*, *Cyclotella meneghiniana* and *Dictyosphaeria cavernosa*, which contributes 7.5%, 6.8% and 5.5% to total assemblages respectively. This means that the first and second ranking levels keep 7 to 10-fold difference. According to occurrence rate rank (Fig. 2b), three species are extremely common (occurrence rate > 90%), and the sequence of them is *A. granulata* var. *granulata* (98%) > *C. meneghiniana* (96%) > *Desmodesmus armatus* (94%). Five other species are very common (occurrence rate between 70% and 90%), and the sequence is *Acutodesmus dimorphus* (83%) > *S. armatus* var. *boglariensis f. bicaudatus* (79%) > *Nitzschia palea* (73%) = *Ulnaria acus* (73%) = *Belonastrum berolinensis* (73%). There are still other 14 species are common (occurrence rate between 50% and 70%), and 45 species are moderately common (occurrence rate between 25% and 50%). Most species are very scarce (occurrence

rate < 10%), with proportion of 67.9% in total species number. Based on biomass and occurrence rank, *A. granulata* and *C. meneghiniana* are the most important species of phytoplankton assemblages in the studied area.

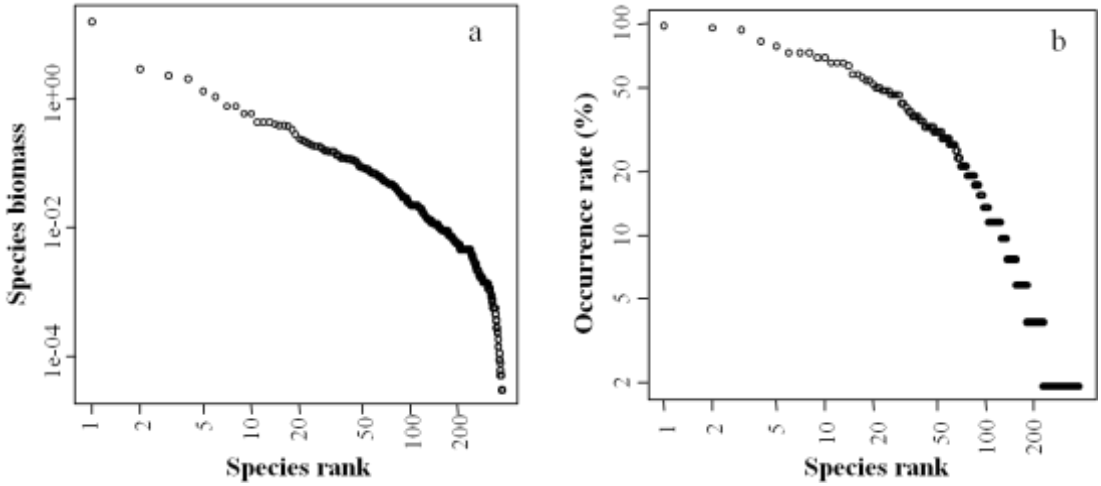

Figure 2 The rank of biomass and occurrence rate for phytoplankton species as function of the decreasing of the species rank, both horizontal and vertical axes are log-transformed (a. biomass; b. occurrence rate).

Table 2 List of 123 taxa whose occurrence rate over 10% in all samples, and corresponding tolerance range (+ median value) of environmental factors: WT (℃), TN (mg/L), TP (mg/L), Si (mg/L).

Group	Species name	Abbreviation	Occurrence rate (%)	WT	TN	TP	Si
Bacillariophyceae	*Acanthoceras zachariasii*	Acza	12	15.9 - 30.5 (29.6)	2.12 - 3.37 (2.78)	0.11 - 0.29 (0.24)	3.55 - 4.88 (4.54)
	Amphora ovalis	Aovs	21	13.3 - 29.9 (14.2)	2.31 - 6.42 (3.44)	0.12 - 0.47 (0.15)	2.92 - 5.32 (4.17)
	A. ovalis var. *gracilis*	Agrs	13	13.5 - 14.2 (14.0)	2.31 - 4.07 (2.99)	0.12 - 0.15 (0.12)	3.15 - 7.28 (3.54)
	Asterionella formosa	Afoa	13	13.5 - 28.1 (14.5)	2.21 - 7.58 (3.28)	0.10 - 0.23 (0.12)	3.15 - 5.66 (3.95)
	Aulacoseira distans	Adis	29	13.3 - 18.3 (14.2)	2.31 - 7.58 (3.44)	0.10 - 0.82 (0.15)	2.92 - 7.28 (4.42)
	A. distans var. *alpigena*	Aala	38	14.1 - 32.0 (17.0)	2.37 - 7.58 (2.96)	0.09 - 0.49 (0.19)	3.38 - 6.04 (4.53)
	A. granulata var. *angustissima*	Aana	69	13.5 - 32.0 (26.5)	2.12 - 9.64 (3.15)	0.10 - 0.82 (0.17)	3.38 - 7.28 (4.17)
	A. granulata var. *angustissima f. spiralis*	Asps	13	13.5 - 29.6 (15.8)	2.60 - 7.58 (3.37)	0.11 - 0.82 (0.24)	3.38 - 7.14 (4.24)
	A. granulata var. *curvata*	Acua	50	13.3 - 32.0 (27.4)	2.12 - 7.58 (3.37)	0.10 - 0.82 (0.22)	2.92 - 7.14 (4.42)
	A. granulata var. *granulata*	Agra	98	13.3 - 32.0 (23.4)	1.99 - 9.64 (2.96)	0.09 - 0.82 (0.16)	2.92 - 7.28 (4.15)
	A. islandica	Aisa	12	13.9 - 14.3 (14.1)	2.31 - 4.07 (2.59)	0.10 - 0.15 (0.12)	3.15 - 5.32 (3.54)

	A. italica f. curvata	Acur	23	13.5 - 29.8 (14.2)	2.31 - 7.27 (2.99)	0.10 - 0.82 (0.12)	3.15 - 7.28 (4.17)
	A. italica	Aita	35	13.9 - 29.7 (15.8)	2.21 - 9.64 (2.90)	0.10 - 0.82 (0.14)	3.15 - 7.28 (4.17)
	A. italica var. *tenuissima*	Aten	69	13.5 - 32.0 (17.0)	1.99 - 7.58 (2.90)	0.09 - 0.49 (0.15)	3.15 - 7.28 (4.17)
	Bacillaria paxillifera	Bapa	31	13.3 - 29.4 (14.3)	1.99 - 5.23 (2.83)	0.10 - 0.23 (0.13)	2.92 - 7.28 (4.28)
	Belonastrum berolinensis	Bebe	73	13.5 - 32.0 (18.3)	2.12 - 7.58 (2.99)	0.09 - 0.82 (0.17)	3.15 - 7.14 (4.28)
	Caloneis macedonica	Cmaa	12	13.3 - 29.8 (23.4)	2.23 - 4.02 (2.99)	0.12 - 0.35 (0.14)	2.92 - 5.32 (3.54)
	Carinasigma rectum	Care	12	14.1 - 32.0 (15.9)	2.12 - 3.49 (2.99)	0.09 - 0.38 (0.12)	3.65 - 5.32 (4.44)
	Cocconeis sp.	Cocs	33	13.5 - 29.4 (16.3)	1.99 - 9.64 (2.60)	0.10 - 0.19 (0.12)	3.15 - 5.32 (3.95)
	Craticula cuspidata	Crcu	19	13.5 - 29.9 (26.6)	2.21 - 7.58 (2.48)	0.10 - 0.35 (0.13)	3.40 - 4.53 (3.65)
	Cyclotella comta	Ccoa	65	13.3 - 32.0 (23.4)	1.99 - 7.58 (3.14)	0.09 - 0.82 (0.18)	2.92 - 7.28 (4.24)
	C. meneghiniana	Cmea	96	13.3 - 32.0 (23.4)	1.99 - 9.64 (2.94)	0.09 - 0.82 (0.16)	2.92 - 7.28 (4.21)
	Cylindrotheca closterium	Cycl	33	14.5 - 32.0 (29.0)	2.36 - 7.58 (3.15)	0.11 - 0.47 (0.23)	3.38 - 6.04 (4.42)
	Cymbella affinis	Cafs	27	13.5 - 29.9 (14.2)	2.31 - 7.27 (2.94)	0.10 - 0.82 (0.13)	3.15 - 7.28 (4.09)

	C. tumida	Ctua	29	13.9 - 29.9 (14.9)	2.21 - 4.07 (2.64)	0.10 - 0.18 (0.13)	3.15 - 7.28 (4.09)
	Fragilaria hinganensis var. *longissima*	Floa	12	13.9 - 29.8 (14.2)	2.59 - 4.07 (2.99)	0.12 - 0.35 (0.13)	3.53 - 5.32 (4.53)
	Gomphonema augur	Gaur	27	13.9 - 29.9 (26.5)	2.21 - 9.64 (2.59)	0.09 - 0.32 (0.16)	3.53 - 7.28 (4.06)
	G. subclavatum	Gsum	12	15.4 - 29.7 (28.6)	2.48 - 3.36 (2.96)	0.10 - 0.25 (0.22)	3.38 - 4.92 (4.28)
	Hantzschia amphioxys	Hams	12	13.5 - 16.6 (14.0)	2.90 - 5.23 (3.49)	0.12 - 0.23 (0.15)	3.15 - 7.28 (4.44)
	H. sp.	Hasp	12	14.9 - 29.0 (16.6)	2.36 - 7.26 (2.94)	0.10 - 0.23 (0.17)	3.56 - 4.92 (4.86)
	Licmophora abbreviata	Laba	27	13.3 - 29.7 (14.2)	2.31 - 4.07 (2.73)	0.10 - 0.22 (0.12)	2.92 - 7.28 (3.65)
	Melosira juergensii var. bothnica	Mboa	17	13.9 - 29.6 (14.9)	2.31 - 4.07 (2.81)	0.09 - 0.24 (0.13)	3.15 - 4.92 (4.15)
	M. varians	Mvas	56	13.3 - 32.0 (15.8)	2.21 - 7.58 (3.15)	0.09 - 0.82 (0.18)	2.92 - 7.28 (4.28)
	Navicula dicephala	Ndic	46	13.3 - 32.0 (16.6)	2.21 - 9.64 (2.90)	0.10 - 0.38 (0.15)	2.92 - 7.28 (4.08)
	N. lanceolata	Nlaa	27	14.0 - 29.9 (16.6)	2.21 - 7.26 (2.62)	0.10 - 0.47 (0.13)	3.15 - 4.92 (3.95)
	N. subminuscula	Nsua	37	13.5 - 30.3 (25.9)	2.23 - 9.64 (2.94)	0.11 - 0.47 (0.15)	3.38 - 4.57 (4.08)
	N. transitans	Ntrs	12	13.3 - 27.7 (14.3)	2.31 - 4.02 (2.59)	0.12 - 0.32 (0.18)	2.92 - 4.44 (3.93)

	Nitzschia acicularis	Nacs	12	15.1 - 29.9 (28.6)	2.50 - 7.58 (5.23)	0.18 - 0.47 (0.35)	3.38 - 6.04 (4.53)
	N. lorenziana	Nloa	25	13.9 - 30.2 (16.3)	2.12 - 4.07 (2.96)	0.09 - 0.35 (0.14)	3.15 - 7.28 (4.28)
	N. palea	Npaa	73	13.3 - 32.0 (17.0)	2.23 - 9.64 (3.06)	0.10 - 0.82 (0.16)	2.92 - 7.28 (4.35)
	Pinnularia sp.	Pisp	12	13.9 - 25.9 (14.3)	2.31 - 7.58 (3.49)	0.12 - 0.47 (0.15)	3.54 - 7.28 (4.44)
	Psammodictyon panduriforme	Pspa	21	15.9 - 32.0 (27.4)	2.12 - 5.26 (3.10)	0.09 - 0.38 (0.22)	3.63 - 5.86 (4.35)
	Stephanodiscus sp.	Stsp	48	13.5 - 32.0 (15.9)	2.31 - 7.58 (2.96)	0.10 - 0.82 (0.13)	3.15 - 7.28 (4.21)
	Synedra ulna	Sula	19	13.9 - 30.5 (28.3)	1.99 - 7.26 (3.15)	0.10 - 0.47 (0.23)	3.56 - 5.66 (4.48)
	Tabellaria sp.	Tasp	15	15.4 - 29.9 (26.6)	2.21 - 7.26 (2.50)	0.12 - 0.23 (0.14)	3.56 - 5.86 (3.63)
	Tabularia fasciculata	Tafa	54	14.0 - 32.0 (26.5)	2.12 - 9.64 (3.10)	0.09 - 0.82 (0.18)	3.15 - 7.14 (4.32)
	Ulnaria acus	Ulac	73	13.5 - 32.0 (25.9)	2.12 - 9.64 (2.99)	0.10 - 0.82 (0.16)	3.38 - 7.14 (4.15)
	U. contracta	Ulco	15	13.5 - 29.8 (15.4)	2.52 - 7.58 (3.36)	0.10 - 0.35 (0.13)	3.15 - 5.32 (4.17)
	Urosolenia sp.	Ursp	13	14.9 - 32.0 (29.8)	2.12 - 6.97 (3.15)	0.12 - 0.49 (0.24)	3.65 - 4.85 (4.53)
Chlorophyceae	*Actinastrum hantzschii*	Ahai	48	14.0 - 32.0 (28.1)	2.12 - 9.64 (3.18)	0.10 - 0.82 (0.19)	3.15 - 7.14 (4.24)

	Acutodesmus acuminatus	Acac	42	14.3 - 32.0 (25.7)	2.12 - 7.58 (2.94)	0.09 - 0.49 (0.19)	3.47 - 6.04 (4.24)
	A. dimorphus	Acdi	83	13.3 - 32.0 (23.4)	1.99 - 9.64 (2.96)	0.09 - 0.82 (0.17)	2.92 - 7.14 (4.15)
	A. obliquus	Acob	58	13.5 - 32.0 (26.5)	2.21 - 9.64 (2.96)	0.09 - 0.82 (0.16)	3.22 - 7.14 (4.08)
	Ankistrodesmus falcatus	Afas	31	14.1 - 30.5 (17.0)	2.12 - 6.42 (2.62)	0.09 - 0.47 (0.14)	3.38 - 5.32 (4.35)
	Ankistrodesmus gracilis	Angr	15	15.1 - 32.0 (27.7)	1.99 - 9.64 (3.10)	0.10 - 0.49 (0.16)	3.61 - 6.04 (3.93)
	Closterium acutum var. *variabile*	Cvae	37	14.0 - 32.0 (25.9)	2.37 - 9.64 (3.49)	0.10 - 0.82 (0.18)	3.15 - 7.14 (4.35)
	C. parvulum	Cpam	21	14.1 - 32.0 (26.5)	2.36 - 9.64 (6.42)	0.12 - 0.82 (0.23)	3.56 - 7.14 (4.57)
	Cosmarium tinctum	Ctim	12	13.3 - 16.6 (14.3)	2.99 - 7.27 (4.02)	0.12 - 0.82 (0.21)	2.92 - 7.14 (5.32)
	Crucigenia fenestrata	Cfea	44	13.3 - 32.0 (26.2)	2.12 - 9.64 (3.44)	0.10 - 0.82 (0.19)	2.92 - 7.14 (4.48)
	C. lauterbornei	Clai	29	14.1 - 32.0 (26.5)	1.99 - 9.64 (4.77)	0.10 - 0.82 (0.23)	3.54 - 7.14 (4.57)
	C. quadrata	Crqu	33	14.1 - 32.0 (27.7)	2.21 - 7.58 (2.96)	0.10 - 0.82 (0.22)	3.47 - 7.14 (4.48)
	C. tetrapedia	Ctea	65	13.3 - 32.0 (25.9)	1.99 - 9.64 (2.94)	0.09 - 0.82 (0.17)	2.92 - 7.14 (4.15)
	Crucigeniella apiculata	Crap	33	25.7 - 32.0 (29.1)	1.99 - 9.64 (3.14)	0.12 - 0.49 (0.18)	3.47 - 4.85 (3.93)

	C. rectangularis	Crre	40	14.9 - 32.0 (27.4)	2.12 - 7.58 (2.96)	0.09 - 0.49 (0.18)	3.22 - 6.04 (4.32)
	Desmodesmus armatus	Dear	94	13.3 - 32.0 (25.7)	1.99 - 9.64 (2.96)	0.09 - 0.82 (0.16)	2.92 - 7.14 (4.09)
	D. communis	Deco	23	15.8 - 32.0 (28.1)	2.23 - 9.64 (4.77)	0.10 - 0.82 (0.22)	3.47 - 7.14 (4.53)
	D. denticulatus	Dede	19	14.9 - 32.0 (29.0)	2.38 - 9.64 (3.15)	0.12 - 0.49 (0.23)	3.47 - 4.85 (4.28)
	D. granulatus	Degr	25	13.5 - 29.4 (26.5)	2.23 - 9.64 (3.20)	0.10 - 0.47 (0.15)	3.40 - 6.04 (4.06)
	D. opoliensis	Deop	54	14.5 - 32.0 (27.4)	1.99 - 9.64 (3.14)	0.10 - 0.82 (0.18)	3.22 - 7.14 (4.21)
	D. opoliensis var. carinatus	Deoc	13	16.6 - 29.6 (27.3)	1.99 - 9.64 (3.37)	0.13 - 0.24 (0.16)	3.47 - 4.86 (3.66)
	Dictyosphaeria cavernosa	Dcaa	42	14.9 - 32.0 (27.3)	1.99 - 9.64 (3.14)	0.11 - 0.49 (0.17)	3.22 - 6.04 (4.06)
	Enallax acutiformis	Enac	21	14.9 - 30.5 (28.9)	1.99 - 3.36 (2.48)	0.09 - 0.29 (0.16)	3.38 - 4.56 (3.65)
	Hyaloraphidium rectum	Hrem	63	14.1 - 32.0 (25.9)	1.99 - 9.64 (2.96)	0.09 - 0.82 (0.17)	3.22 - 7.14 (4.44)
	Lacunastrum gracillimum	Lagr	17	14.3 - 30.2 (27.4)	2.12 - 7.26 (3.18)	0.12 - 0.47 (0.16)	3.56 - 4.56 (4.21)
	Micractinium pusillum	Mpum	46	13.5 - 32.0 (26.5)	2.12 - 9.64 (3.15)	0.10 - 0.82 (0.18)	3.22 - 7.14 (4.24)
	Monactinus simplex	Mosi	12	16.3 - 32.0 (29.0)	2.62 - 7.26 (3.36)	0.10 - 0.49 (0.23)	3.38 - 4.92 (3.63)

	Monoraphidium arcuatum	Marm	35	13.3 - 32.0 (25.7)	2.21 - 9.64 (3.49)	0.10 - 0.82 (0.19)	2.92 - 7.14 (4.44)
	M. griffithii	Mogr	29	13.5 - 32.0 (16.3)	2.36 - 7.58 (3.06)	0.10 - 0.82 (0.18)	3.15 - 7.28 (4.85)
	M. komarkovae	Mkoe	58	13.3 - 32.0 (27.4)	2.12 - 9.64 (3.18)	0.10 - 0.82 (0.19)	2.92 - 7.14 (4.21)
	M. mirabile	Momi	31	13.5 - 30.5 (26.2)	2.12 - 7.58 (2.96)	0.10 - 0.82 (0.14)	3.40 - 7.14 (4.17)
	Oocystis lacustis	Olas	12	13.3 - 29.8 (28.3)	3.10 - 7.58 (6.42)	0.21 - 0.82 (0.47)	2.92 - 7.14 (4.84)
	Palmella miniata	Pmia	12	25.9 - 29.9 (29.0)	2.50 - 7.26 (3.14)	0.14 - 0.35 (0.18)	3.54 - 4.53 (3.56)
	P. mucosa	Pmua	65	14.0 - 32.0 (27.4)	1.99 - 9.64 (3.06)	0.10 - 0.49 (0.18)	3.15 - 6.04 (4.08)
	Pediastrum duplex	Pdux	23	14.9 - 29.4 (26.5)	2.21 - 9.64 (5.23)	0.10 - 0.82 (0.16)	3.55 - 7.14 (4.48)
	P. duplex var. *duodenarium*	Pdum	27	14.9 - 32.0 (26.2)	2.31 - 9.64 (3.72)	0.10 - 0.49 (0.16)	3.63 - 6.04 (4.48)
	Quadrigula chodatii	Qchi	29	13.5 - 32.0 (18.3)	2.44 - 9.64 (3.72)	0.11 - 0.82 (0.23)	3.40 - 7.14 (4.54)
	Radiococcus planktonicus	Rpls	35	13.5 - 32.0 (17.5)	2.38 - 9.64 (3.10)	0.11 - 0.82 (0.16)	3.40 - 7.14 (4.44)
	Scenedesmus arcuatus	Sars	33	14.1 - 32.0 (28.1)	2.23 - 9.64 (3.06)	0.10 - 0.49 (0.16)	3.47 - 6.04 (4.06)
	S. armatus var. boglariensis	Sbog	17	13.5 - 32.0 (16.3)	2.23 - 7.58 (3.06)	0.10 - 0.82 (0.29)	3.40 - 7.14 (4.54)

	S. armatus var. boglariensis f. bicaudatus	Sbis	79	14.1 - 32.0 (26.6)	1.99 - 9.64 (2.96)	0.09 - 0.82 (0.17)	3.22 - 7.14 (4.21)
	S. biguga	Sbia	33	13.3 - 32.0 (25.7)	1.99 - 7.58 (2.99)	0.10 - 0.49 (0.21)	2.92 - 5.66 (4.15)
	S. javaensis	Sjas	17	14.1 - 32.0 (27.4)	2.12 - 6.97 (3.18)	0.10 - 0.49 (0.19)	3.55 - 5.66 (4.57)
	Schroederia nitzschioides	Snis	12	14.3 - 29.8 (23.4)	2.64 - 7.58 (3.10)	0.10 - 0.35 (0.18)	3.22 - 4.84 (4.15)
	S. setigera	Ssea	12	14.1 - 30.5 (28.1)	2.23 - 7.58 (2.99)	0.10 - 0.29 (0.14)	3.56 - 5.32 (3.82)
	Spondylosium pygmaeum	Spym	31	14.9 - 32.0 (26.5)	2.12 - 9.64 (3.18)	0.10 - 0.49 (0.19)	3.38 - 6.04 (4.56)
	Stauridium tetras	Stte	27	14.3 - 32.0 (28.1)	2.44 - 9.64 (4.77)	0.10 - 0.49 (0.23)	3.65 - 6.04 (4.54)
	Tetraedron bifurcatum	Tbim	12	15.1 - 30.5 (28.3)	2.44 - 9.64 (4.77)	0.16 - 0.47 (0.29)	4.06 - 6.04 (4.48)
	T. minimum	Tmim	15	14.0 - 32.0 (23.4)	2.12 - 6.97 (2.90)	0.12 - 0.49 (0.16)	3.22 - 7.28 (4.15)
	T. trigonum	Ttrm	31	14.1 - 32.0 (28.3)	2.12 - 9.64 (3.10)	0.12 - 0.49 (0.24)	3.54 - 6.04 (4.48)
	Tetrastrum elegans	Tels	48	14.1 - 32.0 (26.5)	2.12 - 9.64 (2.94)	0.09 - 0.49 (0.16)	3.47 - 6.04 (4.44)
	T. punctatum	Tpum	15	13.5 - 29.4 (16.5)	2.23 - 9.64 (3.49)	0.09 - 0.82 (0.18)	3.40 - 7.14 (4.35)
	Westella botryoides	Wbos	17	15.1 - 32.0 (18.3)	2.52 - 7.58 (5.26)	0.12 - 0.82 (0.38)	4.08 - 7.14 (4.85)

Euglenophyceae	*Euglena cylindrica*	Ecya	37	16.6 - 32.0 (28.3)	2.21 - 9.64 (3.15)	0.10 - 0.49 (0.22)	3.22 - 5.86 (4.21)
	E. ehrenbergii	Eehi	13	15.1 - 32.0 (29.0)	3.06 - 7.58 (6.42)	0.22 - 0.49 (0.38)	3.56 - 6.04 (4.84)
	E. gracilis	Egrs	38	14.0 - 32.0 (27.4)	2.12 - 7.27 (2.83)	0.09 - 0.82 (0.18)	3.15 - 7.14 (4.09)
	E. mutabilis	Emus	13	16.6 - 32.0 (29.6)	2.44 - 6.97 (3.10)	0.16 - 0.49 (0.24)	3.86 - 4.86 (4.57)
	E. pisciformis	Epis	21	14.1 - 32.0 (28.9)	2.23 - 7.58 (3.10)	0.10 - 0.49 (0.18)	3.38 - 4.86 (3.82)
	Lepocinclis acus	Leac	37	13.5 - 32.0 (28.3)	2.21 - 7.58 (3.15)	0.12 - 0.82 (0.23)	3.22 - 7.14 (4.08)
	L. oxyuris	Leox	29	13.5 - 32.0 (27.7)	2.21 - 6.97 (2.78)	0.11 - 0.49 (0.17)	3.22 - 4.88 (4.15)
	Phacus triquetra	Ptrr	19	14.1 - 32.0 (29.0)	2.44 - 9.64 (4.77)	0.12 - 0.49 (0.29)	3.22 - 5.32 (4.53)
	Trachelomonas scabra	Tsca	17	13.5 - 30.2 (27.4)	2.12 - 9.64 (3.44)	0.10 - 0.47 (0.16)	3.22 - 4.56 (3.82)
Cyanophyceae	*Anabaenopsis sp.*	Ansp	12	15.1 - 30.5 (28.3)	2.44 - 7.58 (4.77)	0.10 - 0.47 (0.29)	3.82 - 6.04 (4.48)
	Arthrospira platensis	Apls	19	14.1 - 32.0 (29.6)	2.31 - 7.58 (2.62)	0.10 - 0.49 (0.18)	3.54 - 4.92 (4.24)
	Merismopedia cantonensis	Mcas	19	13.3 - 32.0 (26.5)	2.31 - 9.64 (3.10)	0.13 - 0.49 (0.23)	2.92 - 4.85 (4.35)
	M. tenuissima	Mtea	52	14.9 - 32.0 (28.6)	1.99 - 9.64 (3.06)	0.10 - 0.49 (0.18)	3.22 - 6.04 (3.86)

	Oscillatoria fraca	Ofra	31	14.3 - 32.0 (29.1)	2.44 - 9.64 (3.20)	0.10 - 0.49 (0.22)	3.54 - 5.66 (4.42)
	O. limosa	Olia	12	14.0 - 14.3 (14.2)	2.31 - 3.49 (2.99)	0.12 - 0.18 (0.13)	3.15 - 7.28 (4.44)
	O. subbrevis	Osus	21	14.0 - 32.0 (18.3)	2.23 - 5.26 (2.94)	0.12 - 0.38 (0.22)	3.15 - 7.28 (4.35)
	Phormidium chlorinum	Phch	50	14.1 - 32.0 (27.4)	1.99 - 9.64 (2.96)	0.11 - 0.49 (0.16)	3.38 - 6.04 (4.15)
	Raphidiopsis sinensia	Rsia	21	14.9 - 32.0 (29.0)	2.50 - 9.64 (3.20)	0.10 - 0.38 (0.18)	3.54 - 4.86 (4.06)
Dinophyceae	*Gonyaulax sp.*	Gosp	15	13.5 - 30.3 (28.1)	2.36 - 7.58 (3.44)	0.10 - 0.47 (0.17)	3.40 - 4.84 (3.82)
	Prorocentrum cordatum	Prco	19	16.1 - 32.0 (28.1)	1.99 - 7.58 (2.44)	0.10 - 0.49 (0.14)	3.47 - 4.85 (3.82)
Chrysophyceae	*Dinobryon sertularia*	Dsea	19	15.1 - 32.0 (27.4)	1.99 - 9.64 (3.72)	0.12 - 0.49 (0.24)	3.65 - 6.04 (4.54)

Phytoplankton species assemblage analysis

The ordination of the phytoplankton samples of PRD was obtained by mean of NMDS, and results indicated that most of the samples distributed in the same direction and only a small group in opposite direction. Similarities between samples were analyzed using the cluster analysis method, and similar samples were connected together with lines and groups were identified by distinct symbols and different colors (Fig. 3). Five groups (G1 to G5) were finally identified. G2, composed of all samples of the two urban sites ZJQ and LHS, was clearly differentiated from other groups with high values of water temperature, salinity and nutrients, but apparently lower values of transparency, pH and DO. G4, located between G2 and other three groups, was composed of samples of five inner sites. This group could also be differentiated from others. The other three groups (G1, 3, 5) distributed closely, and they could be differentiated mainly through seasonal differences. G3 was mainly composed of samples of summer (May and August), and its samples covered all rural sites. G1 was mainly composed of samples of winter (March), and its samples covered most of the rural sites. G5 was mainly composed of samples of December, and its samples covered most of the rural sites.

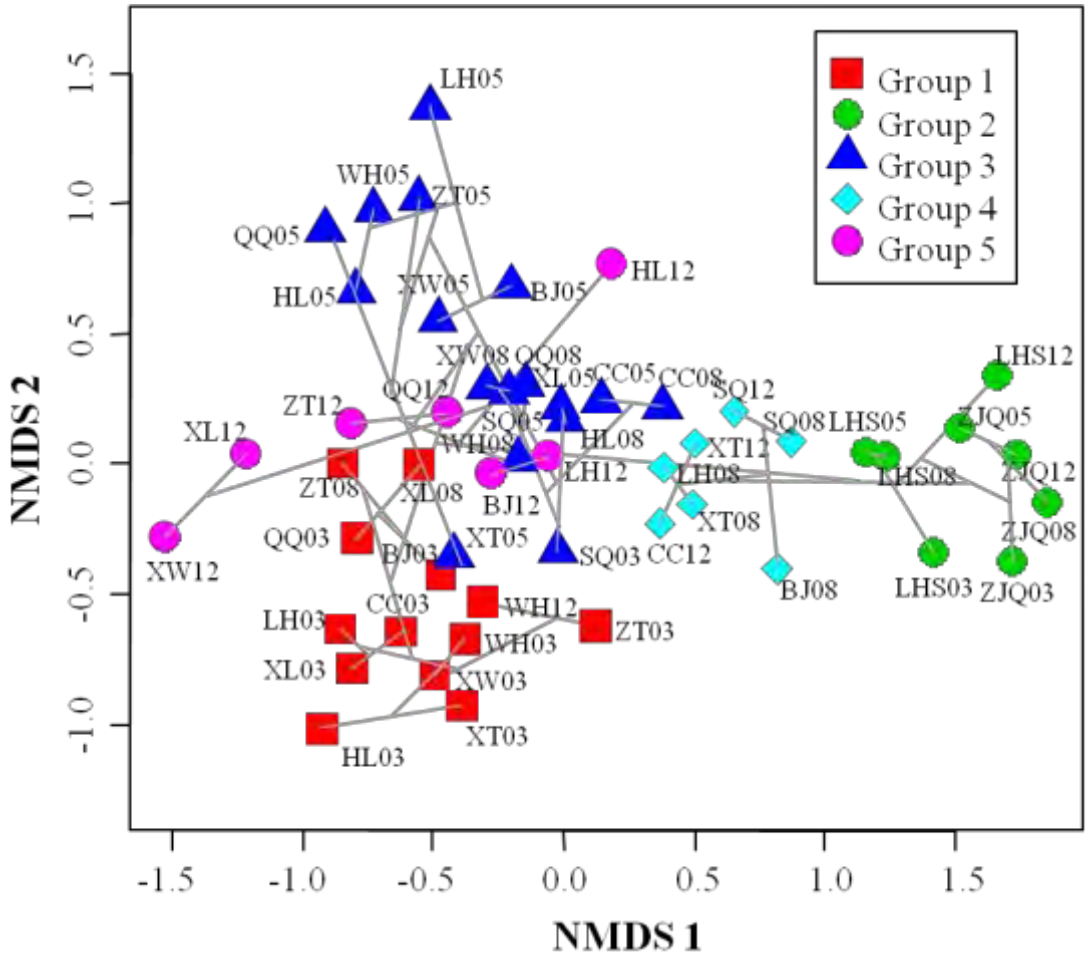

Figure 3 Ordination of phytoplankton samples in the two-dimensional non-metric multidimensional scaling (NMDS) configurations. Based on log (n + 1) transformed biomass values of taxa, five groups are extracted through ward clustering of Bray-Curtis dissimilarity matrix. And then, the NMDS result is combined and the dendrogram is added. Sample locations are coded with symbols denoting the groups they represent.

Phytoplankton species richness and biomass with the percentage of different phyla of each group are shown in Fig. 4: the values varied and differed significantly among groups (the Kruskall-Wallis test, $p < 0.001$). G2 shows the maximum median values and G4 ranks the second among all five groups in both biomass and species richness. The other three groups have very close median values in biomass, but they are also obviously different in species richness. G1 has the minimum median values in biomass and G5 shows the minimum median values in species richness (Fig. 4a1, b1).

The percentage of different phyla in each group indicated that diatom and green algae dominated in species richness and diatom in biomass (Fig. 4a2, b2). Compared to biomass proportion of different phyla in five groups that absolutely dominated by

diatom, the species richness proportion of them was more apparently different between each group. G1 was diatom dominated in species richness, and its proportion was higher than 70%, and green algae contributed less than 20%. G5 showed considerable equal proportion of diatom and green algae in species richness, and sum value reached around 90%. While all the other three groups showed that green algae dominated in species richness, although diatom contributed around 30% and other phyla also contributed more than 10%. Although diatom absolutely dominated in biomass of each group, the considerable proportion (> 10%) of green algae could also be found in G2, 3, 4.

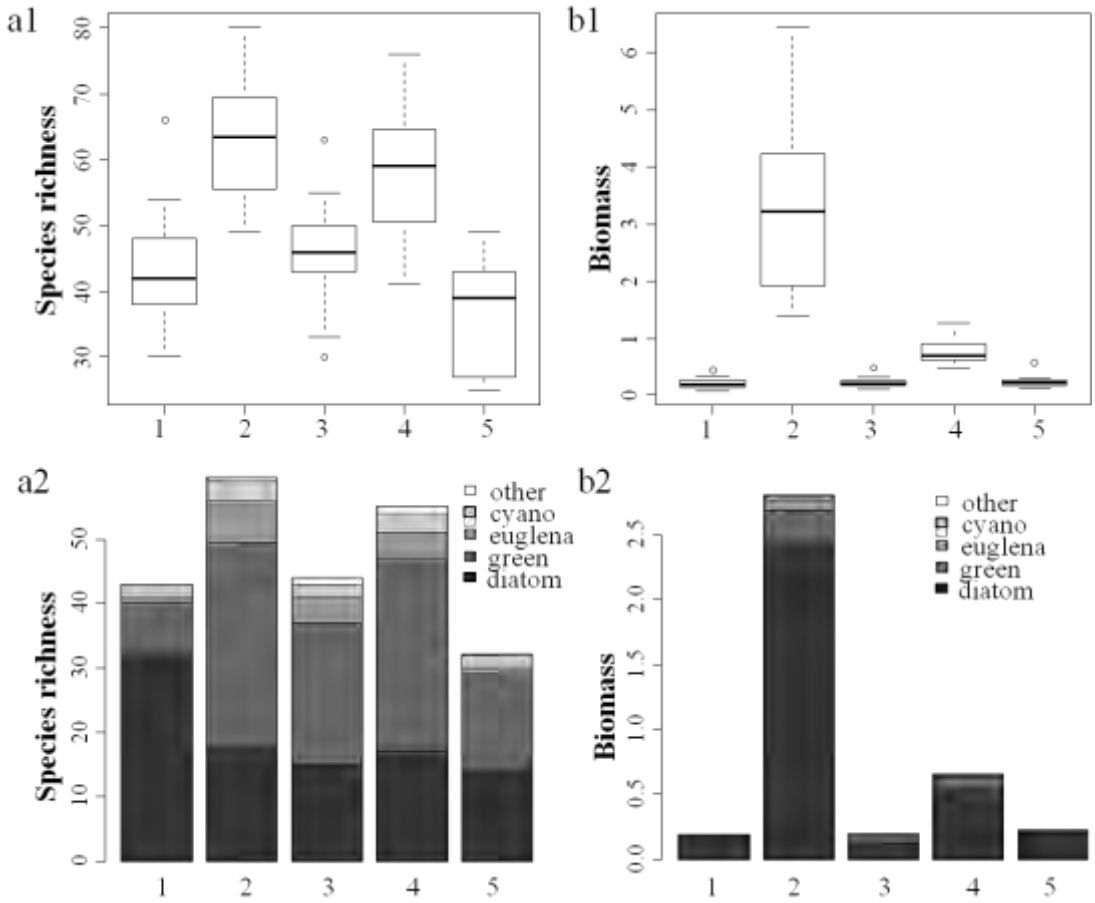

Figure 4 Variation of species richness and biomass of phytoplankton in each group of community (a1. species richness; a2. percentage of different groups to species richness in terms of median values; b1. biomass; b2. percentage of different groups to biomass in terms of median values).

Indicator species

Based on IndVal (indicator value > 25), a total of 56 indicator species were determined in different groups (Table 3). The number of indicator species varied significantly among groups, and increased along the sequence G3, G5, G4, G1, G2 (0, 3, 6, 12 and 35 indicator species, respectively). Indicator species were found with low occurrence frequency especially those that had extremely high indicator values.

G2, representing urban sites, contains the most diverse indicator species. Most of them are true plankton, including 7 diatoms, 24 green algae, 2 true *Euglena* and 2 cyanobacteria. Three species (Agra, Cmea and Dear), with extremely high occurrence frequency (> 90%), are also good indicator species of this group. G1, representing a period of cold winter in most rural sites, whose indicator species are composed of 11 diatoms and 1 blue alga, and most of them are tychoplankton. G4, representing some inner sites, whose indicator species include 3 tychoplanktonic diatoms, 1 planktonic and 1 tychoplanktonic green alga, and 1 true planktonic *Euglena*. G5, representing a period of winter in some rural sites, whose indicator species included 2 diatoms and 1 *Euglena*, and all of them are true plankton.

Table 3 Indicator species of each group based on IndVal (indicator value), with *p* values. The species, not included in table 2, were given the full name.

Group	Indicator species	Indicator value (%)	*P* value
1	Laba	75	0.001
1	Mvas	59	0.002
1	Cafs	57	0.001
1	Agrs	54	0.001
1	Aisa	46	0.005
1	Acur	43	0.011
1	Aovs	43	0.008
1	Bapa	42	0.026
1	Adis	40	0.01
1	*Fragilaria capucina*	31	0.017
1	*Fragilaria crotonensis*	31	0.01
1	Olia	29	0.042
2	Wbos	99	0.001
2	Acua	90	0.001
2	Cmea	84	0.002
2	Cvae	76	0.002
2	Qchi	76	0.001
2	Aana	74	0.001
2	Agra	73	0.001
2	Acdi	73	0.003
2	Cfea	71	0.003
2	Hrem	70	0.001
2	Cpam	70	0.001
2	Stsp	69	0.002
2	Leac	69	0.001
2	Mogr	69	0.001
2	Sbis	68	0.002
2	Ahai	63	0.019
2	Dear	59	0.007
2	Deop	58	0.001
2	Acac	57	0.002
2	Ccoa	54	0.004
2	Ttrm	52	0.019
2	Crqu	52	0.004
2	Mkoe	51	0.046
2	Sbia	51	0.022
2	Crre	50	0.046
2	Stte	48	0.008
2	Eehi	48	0.003
2	Sbog	38	0.008

2	Pdux	38	0.01
2	*Closterium intermedium*	37	0.014
2	Mcas	35	0.028
2	*Mesotaenium macrococcum*	34	0.013
2	Olas	34	0.045
2	*Anabaena flos-aquae*	29	0.016
2	Nacs	29	0.042
4	Tafa	50	0.034
4	Ursp	42	0.004
4	Egrs	35	0.033
4	Snis	35	0.005
4	*Staurastrum gracile*	32	0.011
4	*Cymatopleura solea* var. *subconstricta*	29	0.035
5	Aten	58	0.003
5	Aala	48	0.002
5	*Phacus tortifolius*	43	0.005

The prediction of phytoplankton assemblages from environmental factors

Five significant environmental variables were selected from 16 variables through constrained redundancy analysis (RDA), i.e. water temperature, dissolved oxygen, transparency, silicate and total phosphorus. The prediction analysis of how these five phytoplankton groups could be differentiated by the significant environmental variables was determined by discriminant function analysis (Fig. 5). Three discriminant functions were generated, and the random Monte Carlo permutation test showed that they were highly significant ($p < 0.001$). These axes (F1, F2 and F3) accounted for 47, 29 and 24% of the between-cluster variability, respectively. Since F2 and F3 contributed approximately equal proportions to the results, two dimensional figures based on F1 × F2 and F1 × F3, were shown respectively, with corresponding distribution of water quality parameters. In this respect, the correlations could be exhibited adequately.

The five environmental factors used were able to predict the phytoplankton assemblage groups and types of phytoplankton species assemblage patterns (i.e. global score of prediction) at 75% accuracy, and the prediction success rate for G1, G2, G3, G4 and G5 were 69, 88, 94, 0 and 100% respectively.

G2 was clearly separated from the other four groups which assembled and

overlapped with each other to some extent. G1 and G2 were ordered along the first axis F1 (i.e. horizontal axis) in opposite directions based on both F1 × F2 (Fig. 5a1, a2) and F1 × F3 (Fig. 5b1, b2) figures. And the gradients of total phosphate, silicate, dissolved oxygen and transparency were loaded along this axis and were important controlling variables to G1 and G2 (Fig. 5a1, a2). Meanwhile water temperature was along the second axis F2 (i.e. vertical axis) and was an important controlling variable to G3 and G5, based on F1 × F2 figure. Moreover, silicate, DO and transparency were also factors influencing G3 and G5 based on F1 × F3 figure. G4 was ordered around the center, and its linkage with environmental variables was unclear.

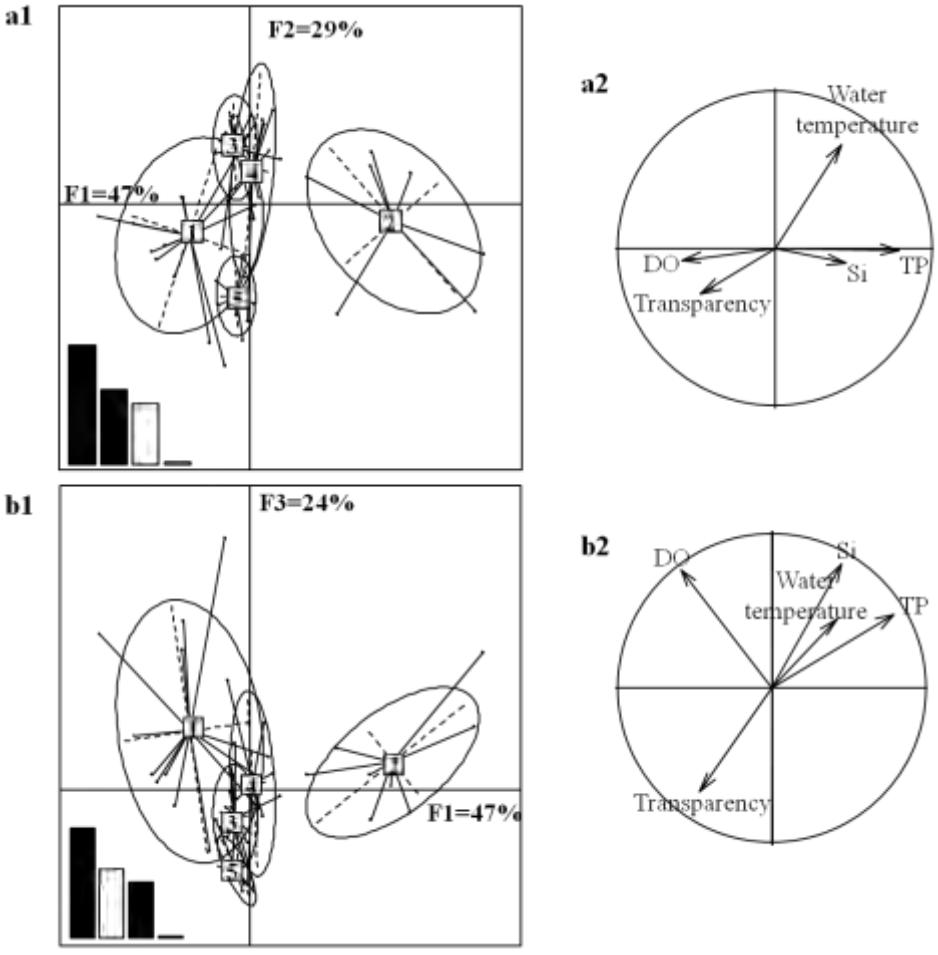

Figure 5 Results from the Linear Discriminent Analysis (LDA) and Principal Component Analysis (PCA) showing: (a1) the distribution and overlap of groups of community in F1 and F2 dimensions; (a2) the correlation circle of water quality parameters corresponding to F1 and F2; (b1) the distribution and overlap of groups in F1 and F3 dimensions; (b2) the correlation circle of water quality parameters corresponding to F1 and F3. The three bar plots in a1 and b1 represent Eigen values of the contributed axes.

Discussion

Environmental conditions

The river water of the PRD is well known as low quality and in a reductive circumstance. The observed eutrophication deterioration in this region has been related to the long-term trends of nutrient delivery by the Pearl River (Duan & Bianchi 2006; Qu & Kroeze 2010). Nitrogen, phosphorus, and organic compounds are the most predominant pollutants (Ouyang et al. 2005). Our results showed that the nutrient concentrations (Table 1) in the investigated river delta were markedly higher than the threshold for half-saturation for most algal species according to Reynolds (2006). The P concentration of all sites exceeded 0.1 mg/l, which was the recommended concentration in flowing water to encourage excessive growth of aquatic plants (Cheung et al. 2003). The concentrations of nitrogen were under the maximum contaminant level in public drinking water supplies (10 mg/l). Urbanization is thought to be a great threat to such river water qualities. Within the same river, the water quality of sample from rural area was much better than that from urban zone (Ouyang et al. 2006). ZJQ and LHS, the two sites closer to Guangzhou city, are apparently different from other sites for their extremely pollution (high nutrient concentrations, low transparency and DO). And their corresponding low standard deviation values of transparency, DO and TN (Table 1) also reflected the weak seasonal fluctuations of water quality in urban sites. Spatial distributions in water qualities implied that local drainage was a main factor impacting pollution status at different sites (Lu et al. 2009). Municipal wastewater is thought to be the greatest pollution source for the two urban sites. Ouyang et al. (2006) had reported the positive correlation between the rapidity of urbanization and the pollution levels of urban river water in the PRD. Moreover, these two sites were also impacted by sea tide, which could be reflected by their relatively higher salinity (Table 1). Through this way, high tide would result in the flow backward of pollutants discharge along the tidal backwater and enhance the circulation of sewage in such tidal region. As for other rural sites, chemical fertilizers and pesticides used in agriculture and rural living

sewage all contributed to the water pollution. Above all, the high nutrient concentrations of the studied area have exceeded the growth threshold of algal species significantly, which implied that physical and hydrological variables would play a more important role in patterning phytoplankton assemblages.

Phytoplankton community structure

The existence of various upstream river channels and floodplain habitats, along with various recruitment processes, might explain the high taxonomic diversity recorded in the PRD. As expected, Bacillariophyceae and Chlorophyceae were the dominant classes in phytoplankton diversity and Bacillariophyceae in biomass in the present study, which agreed well with the phytoplankton structures of the upper and lower adjacent water areas: downstream of the West River (Wang et al. 2013) and the Pearl River Estuary (Wang et al. 2010). Bortolini & Bueno (2013) also reported the similar phytoplankton community structure in São João River of Brazil. Wehr & Descy (1998) believed that the most successful algal groups in large rivers were Bacillariophyceae and Chlorophyceae, which were more abundant in the lower reaches. Generally, higher flow rates and shorter water residence time tend to favor faster-growing diatom taxa (Mihaljević et al. 2014). Besides this, diatoms are heavier and better adapted to low light availability than other algal groups, thus can benefit from intense water mixing (Trevisan et al. 2010). Moreover, conditions of high water flow could cause drifting of tychoplanktonic and meroplanktonic algae into the water column (Centis et al. 2010), thus several diatom genuses (*Navicula*, *Gomphonema*, *Aulacoseira* (*Melosira*), *Nitzschia* and *Cymbella*) exhibited high richness in our studies. In addition, the present high diversity also benefitted from the continual inoculations from upsteam main stream and river tributaries, and this could be reflected from the apparently high richness of *Euglena* (29 taxa) and *Scenedesmus* (24 taxa), which belonged to limnetic species and generally flushed to river channels during floods.

The presence of a few dominant species accompanied by a large number of sporadic species is the main feature of phytoplankton community structures in large river ecosystems (Devercelli 2006, Hindák et al. 2006, Desortová & Punčochář 2011,

Tavernini et al. 2011). In the present study, the centric diatom *A. granulata* contributed more than 50% of the total biomass during the whole investigation. And this result was in accordance with its dominance in the two adjacent water areas: the downstream of the West River (Wang et al., 2012) and the lower Pearl River Estuary (Wang et al., 2009), located upper and lower of the PRD respectively. The dominance of *A. granulata* and its bioforms was reported as typical of large rivers of the world (Rojo et al., 1994; Lewis et al., 1995; O'Farrell et al., 1996; Zalocar de Domitrovic et al., 2007). According to Reynolds (1994), the dominance of filamentous diatoms was associated with their capacity to form inoculants, which were deposited in the sediment and are re-suspended into the water column through the turbulence. Therefore, the predominance of *A. granulata* in the PRD was mainly dependent on inoculations from both upper flowing waters and lower tidal backwaters, and resuspension of benthic colonies. In addition, small-celled and fast growing diatom species *C. meneghiniana* also showed dominant and ranked second to *A. granulata*. It was thought to have advantages to survive under turbulent conditions (Reynolds et al., 2002) and was more competitive for nutrients and light utilization based on its larger surface-volume ratio (Litchman & Klausmeier, 2008). Moreover, *C. meneghiniana* had low sedimentation rates due to their dimension and persisted in the water column at slow flow rates. Several other algal species exhibited either high biomass contributions or high occurrence rate, which might be due to their seasonal preference or ecological properties reflection, e.g. *Dictyosphaeria cavernosa* was dominant in floods periods, *Entomoneis alata* was typical of brackish species, and *Desmodesmus armatus* was mainly dependent on outer channel inoculations.

Patterning and predicting of phytoplankton assemblages

Based on species biomass similarities, all samples were ordinate and classified into five groups through the NMDS and hclust respectively. And the contribution of significant environmental variables in differentiating the phytoplankton pattern groups were also predicted using LDA. G2 was composed of samples from all seasons of the two urban sites, and it was clearly differentiated from other groups through its high eutrophication (bad water quality). G4 was composed of samples from August and

December of five inner sites (XT, CC, BJ, LH and SQ), but it was uncorrelated with the present environmental variables. The similar point of these two groups was that their samples did not show distinct seasonal trait, thus mainly representing the spatial patterns. Moreover, both of them had apparently higher species richness and biomass than other three groups (G1, 3, 5), even though the differences between these two groups were also significant. The seasonally driven ecological gradient was expressed in the other three groups (G1-March, G3-May and August, G5-December), which assembled and overlapped with each other to some extent. But their distinct differences exhibited only in species richness. G1 and G3 had maximum samples, and they represented drought and flood seasons respectively. Generally, high level of connectivity in flood seasons would lead to high similar species composition, but both drought (G1) and flood season (G3) showed high similarities in the present study, which reflected the well connectivity between river channels of rural area. Bortolini & Bueno (2013) thought that the similarity of the distribution of communities in lotic environments was due to the unidirectional flow. These two groups showed equal total species richness and biomass, and the only difference between them was the alternating dominance of diatom and green algae in species richness. G5 also represented the drought period, but it had apparently lower species richness than G1 and G3, and the equal contribution of diatom and green algae in species richness indicated that the hydrological conditions of G5 were different from G1 to some extent. Above all, differences in the phytoplankton diversity and biomass between the patterning groups were significant in spatial dimension.

G2 had significant higher species diversity and biomass, especially for its biomass beyond at least 5 folds of other groups, even though the concomitant extremely low transparency and DO seemed detrimental for phytoplankton development. Of course, the nutrient conditions of the two urban sites could satisfy the requirements for most species growth, and this was regarded as an important precondition for high species diversity. Moreover, the two urban sites were located along the river channel of the Humen outlet, which had both the maximum volume of runoff (18.5% of total the Pearl River discharge into China South Sea) and the

maximum tidal throughput among the eight outlets of the Pearl River Estuary (Lu, 1990). Thus, the consequent intense and frequent water exchanges in this area could also guarantee the continual inoculations from both water flows and benthic recruitments. The high proportion of green algae and considerable contribution of diatom and Euglenophyta in total species richness of this group was a good example for the above conclusion. Although salinity was thought to be a negative effect on growth of freshwater phytoplankton, a concentration between 0.5 and 10 psu was not strong enough to lead to the disappearance of freshwater and brackish water phytoplankton (Lionard et al., 2005). Indicator species composition of G2 was most diverse, and most of them had low occurrence rate, preferred high temperature and high nutrients (Table 2, 3). Only five indicator species (Wbos, Qchi, Stsp, Mogr and Sbog) tended to occur in cold season.

The reason for the extremely high biomass of G2 was that both chemical and hydrological factors favored the predominance of *A. granulata*, since its maximum contribution to total phytoplankton biomass could reach 85% in the urban sites. First, high silicate concentrations of urban sites (Table 1) could not only satisfy the growth need in cell wall but also help reducing sinking velocity. Since studies by Gibson (1984) on another *Aulacoseira* species, *A. subarctica*, found that depletion of silicate would increase sinking velocity, thus density decreased exponentially. Second, both the upper river discharge and the lower tidal backwaters would provide continual supplements in density, since it also dominated in both the upper (Wang et al., 2012) and lower adjacent water areas (Wang et al., 2009). Third, its chain-forming colonies would increase the surface-area ratio and therefore the frictional resistance, resulting in lower sinking velocities (Young et al., 2012). In addition, the strong turbulence (e.g. low transparency) could also reduce the sinking velocity and enhance the recruitment from sediments through resuspension process. Fourth, this species was able to tolerate the high turbidity (Kilham et al., 1986) and low light intensity for its high chloroplast content in each cell (Stoermer et al., 1981). Moreover, its dominance in the Pearl River Estuary (Wang et al., 2009) also reflected its distinct adaptation to salinity fluctuations. Therefore, the single dominance of *A. granulata* limited the species

diversity of diatom (Fig. 4a2), especially in warm seasons when suitable for its growth.

G4 showed higher values than other three groups in both species richness and biomass, but it seemed uncorrelated with the present environmental variables. Studies by Descy et al. (2012) in River Loire (France) found that the variation of water level in the river channel largely controlled growth and losses of potamoplankton. Since this group was composed of five inner sites, the relatively weak water exchanges and low water levels might be beneficial for phytoplankton development.

The other three groups were different from each other not in biomass (Fig. 4b1, b2) but in species richness (Fig. 4a1, a2). G1 was characterized by low water temperature, and the concomitant low water levels, turbid kinetic and low light conditions favored diatoms (Reynolds, 1994). Therefore, both species diversity and biomass of this group was dominated by diatoms. Almost all indicator species of G1 were composed of diatoms (Table 3), most of them were benthic disturbance indicators, and their water temperature tolerance results (Table 2) indicated that they occurred more in cold season. Although G3 was equal with G1 in both total species richness and biomass, the relative contribution between diatom and green algae was contrary. The higher proportion of green algae in species richness and low biomass values reflected the high discharge impact in summer. Jung et al. (2014) reported that phytoplankton abundance during the dry season was approximately two times higher than that during the flood season in the lower Han River of South Korea. The reason for high similarity between G1 and G3 might be that the negative effect of low temperature of G1 was counteracted by well mixed water columns thus lower sinking velocity for diatoms and high inoculations of benthic diatoms; while the positive effect of high temperature of G3 was counteracted by high dilution and short residence time. G5 was also characterized by low temperature, and it had the minimum species richness. Its apparently high transparency (78 ± 13 cm) must be negative for the suspension of benthic algae into the water column, which could be reflected from the equal contribution of diatom and green algae in diversity during drought season.

Acknowledgements

We wish to thank Pang Shixun, Zeng Yanyi, Gao Yuan and Zhang Weizhen for their assistance in sampling work, and John Woodley for language improvements. This work was financially supported by Guangxi Province Natural Science Foundation of Key Projects (2013GXNSFEA053003) and Public Sector (agriculture) Special Scientific Research Projects (201303056-5).

References

Alexander, R. B., Böhlke, J. K., Boyer, E. W. et al., 2009. Dynamic modeling of nitrogen losses in river networks unravels the coupled effects of hydrological and biogeochemical processes. Biogeochemistry, 93: 91-116.

Bonada, N., Rieradevall, M., Prat, N., 2007. Macroinvertebrate community structure and biological traits related to flow permanence in a Mediterranean river network. Hydrobiologia, 589: 91-106.

Bortolini, J.C. & Bueno, N.C., 2013. Seasonal variation of the phytoplankton community structure in the São João River, Iguaçu National Park, Brazil. Brazilian Journal of Biology, 73(1): 1-14.

Cao, H. L., Hong, Y. G., Li, M., Gu, J. D., 2012. Community shift of ammonia-oxidizing bacteria along an anthropogenic pollution gradient from the Pearl River Delta to the South China Sea. Applied Microbiology and Biotechnology, 94: 247-259.

Centis B, Tolotti M, Salmaso N, 2010. Structure of the diatom community of the River Adige (North-Eastern Italy) along a hydrological gradient. Hydrobiologia, 639: 37–42.

Chau, K. W., 2005. Characterization of transboundary POP contamination in aquatic exosystems of Pearl River Delta. Marine Pollution Bulletin, 51: 960-965.

Cheung K. C., Poon B. H. T., Lan C. Y., Wong M. H. (2003). Assessment of metal and nutrient concentrations in river water and sediment collected from the cities in the Pearl River Delta, South China. Chemosphere, 52: 1431－1440.

Cressie, N., Frey, J., Harch, B., Smith, M., 2006. Spatial prediction on a river network. Journal of Agricultural, Biological and Environmental Statistics, 11(2): 127-150.

Descy, J-P, Lettao, M., Everbecq, E., Smitz, J.S., Deliège, J-F, 2012. Phytoplankton of the River Loire, France: a biodiversity and modeling study. Journal of Plankton Research, 34(2): 120-135.

Desortová, B. & Punčochář, P., 2011. Variability of phytoplankton biomass in a lowland river: response to climate conditions. Limnologica 41: 160–166.

Devercelli, M., 2006. Phytoplankton of the Middle Paraná River during an anomalous hydrological period: a morphological and functional approach. Hydrobiologia, 563: 465-478.

Dmitrieva, V. A., 2011. Change in the river network and water resources in the upper and middle reaches of the Don River due to current climatic and economic conditions. Arid Ecosystems, 1(3): 193-199.

Duan, S. W. & Bianchi, T. S., 2006. Seasonal changes in the abundance and composition of plant pigments in particulate organic carbon in the lower Mississippi and Pearl Rivers. Estuaries and Coasts, 29: 427-442.

Dufrêne, M. & Legendre, P., 1997. Species assemblages and indicator species: the need for a more flexible asymmetrical approach. Ecological Monographs, 67: 345–366.

Feng, L., Wang, D. G., Chen, B., 2011. Water quality modeling for a tidal river network: A case study of the Suzhou River. Frontiers of Earth Science, 5(4): 428-431.

Gamier, J., Billen, G., Coste, M., 1995. Seasonal succession of diatoms and Chlorophyceae in the drainage network of the Seine River: Observations and modeling. Limnology and Oceanography, 40(4): 750-765.

Gamier, J., Billen, G., Hannon, E., Fonbonne, S., Videnina, Y., Soulie, M., 2002. Modelling the transfer and retention of nutrients in the drainage network of the Danube River. Estuarine, Coastal and Shelf Science, 54: 285-308.

Gibson, C. E., 1984. Sinking rates of planktonic diatoms in an unstratified lake: a comparison of field and laboratory observations. Freshwater Biology, 14(6): 631-638.

Ha, K., Jang, M. H., Joo, G. J., 2002. Spatial and temporal dynamics of phytoplankton communities along a regulated river system, the Nakdong River, Korea. Hydrobiologia, 470: 235-245.

He, Y.F., Wang, J.W., Lek, S., Cao, W.X., Lek-Ang, S., 2011. Structure of endemic fish assemblages in the upper Yangtze River basin. River Research and Applications, 27: 59-75.

Hillebrand, H., Dûrselen, C. D., Kirschtel, D., Pollingher, U., Zohary, T., 1999. Biovolume calculation for pelagic and benthic microalgae. Journal of Phycology, 35, 403–424.

Hindák, F., Hindáková, A., Marvan, P., Heteša, J., Hašler, P., 2006. Diversity, abundance and volume biomass of the phytoplankton of the Morava River (Czech Republic, Slovakia) and the Dyje River (Czech Republic) in November 2005. Czech Phycology Olomouc 6: 77–97.

Istvánovics, V., Honti, M., Vörös, L., Kozma, Z., 2010. Phytoplankton dynamics in relation to connectivity, flow dynamics and resource availability—the case of a large, lowland river, the Hungarian Tisza. Hydrobiologia, 637: 121-141.

Istvánovics, V., Honti, M., Kovács, Á., Kocsis, G., Stier, I., 2014. Phytoplankton growth in relation to network topology: time-averaged catchment-scale modeling in a large lowland river. Freshwater Biology, 59(9): 1856-1871.

Jung, S.W., Kwon, O.Y., Yun, S.M., Joo, H.M., Kang, J-H, Lee, J.H., 2014. Impacts of dam discharge on river environments and phytoplankton communities in a regulated river system, the lower Han River of South Korea. Journal of Ecology and Environment, 37(1): 1-11.

Justić, D., Rabalais, N.N., Turner, R.E., 2002. Modeling the impacts of decadal changes in riverine nutrient fluxes on coastal eutrophication near the Mississippi River Delta. Ecological Modelling, 152(1): 33-46.

Kilham, P., Kilham, S.S, Hecky, R.E., 1986. Hypothesized resource relationships among African planktonic diatoms. Limnology and Oceanography, 31(6): 1169-1181.

Kilroy, C., Larned, S. T., Biggs, B. J. F., 2009. The non-indigenous diatom *Didymosphenia geminata* alters benthic communities in New Zealand rivers. Freshwater Biology, 54: 1990-2002.

King, R. S. & Richardson, C. J., 2003. Integrating bioassessment and ecological risk assessment: an approach to developing numerical water-quality criteria. Environmental Management, 31: 795-809.

Kruskal, J.B. & Wish, M., 1978. Multidimensional Scaling. Sage Publications, Beverly Hills.

Lewis, W. M. Jr., S. K. Hamilton & J. F. Saunders, 1995. Rivers of Northern South America. In Cushing, C. E., K. W. Cummins & G. W. Minshall (eds), River and Stream Ecosystems. Elsevier, Amsterdam: 219–256.

Lionard, M., Muylaert, K., Van Gansbeke, D., Vyverman, W., 2005. Influence of changes in salinity and light intensity on growth of phytoplankton communities from the Schelde river and estuary (Belgium/The Netherlands). Hydrobiologia, 540: 105-115.

Litchman, E. & Klausmeier, C. A., 2008. Trait-based community ecology of phytoplankton. Annual Review of Ecology Evolution and Systematics, 39: 615–639.

Lu, F.H., Ni, H.G., Liu, F., Zeng, E.Y., 2009. Occurrence of nutrients in riverine runoff of the Pearl River Delta, South China. Journal of Hydrology, 376(1-2): 107-115.

Lu, K. X., 1990. Fishery Resources of the Pearl River System. Guangzhou: Guangdong Science and Technology Press, p27–39. (in Chinese)

Matthaei, C. D., Piggott, J. J., Townsend, C. R., 2010. Multiple stressors in agricultural streams: interactions among sediment addition, nutrient enrichment and water abstraction. Journal of Applied Ecology, 47: 639-649.

Mihaljević, M., Stević, F, Špoljarić, D., Žuna Pfeiffer, T., 2014. Spatial pattern of phytoplankton based on the morphology-based functional approach along a river — floodplain gradient. River Research and Applications, DOI: 10.1002/rra.2739.

O'Farrell, I., I. Izaguirre & A. Vinocur, 1996. Phytoplankton ecology of the Lower Paraná River (Argentina). Large Rivers, Archiv für Hydrobiologie Supplement, 115(1): 75–89.

PRWRC (Pearl River Water Resources Commission), 2006. Pearl River bulletins of 2000, 2001, 2002, 2003, 2004 and 2005. PRWRC, website: http://www.pearlwater.gov.cn. November 2006 (in Chinese).

Qiu, D. J., Huang, L. M., Zhang, J. L., Lin, S. J., 2010. Phytoplankton dynamics in and near the highly eutrophic Pearl River Estuary, South China Sea. Continental Shelf Research, 30(2): 177-186.

Qu, H. J. & Kroeze, C., 2010. Past and future trends in nutrients export by rivers to the coastal waters of China. Science of the Total Environment, 408: 2075-2086.

Ouyang T P, Zhu Z Y & Kuang Y Q (2005). River water quality and pollution sources in the Pearl River Delta, China. Journal of Environmental Monitoring, 7: 664–669.

Ouyang T P, Zhu Z Y & Kuang Y Q (2006). Assessing impact of urbanization on river water quality in the Pearl River Delta economic zone, China. Environmental Monitoring and Assessment, 120: 313–325.

Reynolds, C. S., 1984. The Ecology of Freshwater Phytoplankton. Cambridge University Press, Cambridge.

Reynolds, C. S., 1994. The long, the short and the stalled: on the attributes of phytoplankton selected by physical mixing in lakes and rivers. Hydrobiologia, 289: 9-21.

Reynolds, C. S., Huszar, V., Kruk, C., Naselli-Flores, L., Melo, S., 2002. Towards a functional classification of the freshwater phytoplankton. Journal of Plankton Research, 24: 417–428.

Reynolds, C. S., 2006. The Ecology of Phytoplankton. Cambridge University Press, Cambridge.

Rojo, C., Alvarez Cobelas, M. & Arauzo, M., 1994. An elementary, structural analysis of river phytoplankton. Hydrobiologia, 289: 43–55.

Salmaso, N. & Braioni, M. G., 2008. Factors controlling the seasonal development and distribution of the phytoplankton community in the lowland course of a large river in Northern Italy (River Adige). Aquatic Ecology, 42: 533-545.

Spatharis, S., Tsirtsis, G., Danielidis, D. B., Chi, T. D., Mouillot, D., 2007. Effects of pulsed nutrient inputs on phytoplankton assemblage structure and blooms in an enclosed coastal area. Estuarine, Coastal and Shelf Science, 73: 807-815.

Stoermer, E.F., Kreis, R.G.Jr., Sicko-Goad, L., 1981. A systematic, quantitative, and ecological comparison of *Melosira islandica* O. Müll. with *M. granulata* (Ehren.) Ralfs from the Laurentian Great Lakes. Journal of Great Lakes Research, 7(4): 345-356.

Tavernini, S., Pierobon, E., Viaroli, P., 2011. Physical factors and dissolved reactive silica affect phytoplankton community structure and dynamics in a lowland eutrophic river (Po River, Italy). Hydrobiologia 669: 213–225.

Trevisan R, Poggi C, Squartini A. 2010. Factors affecting diatom dynamics in the alpine lakes of Colbricon (Northern Italy): a 10-year survey. Journal of Limnology 69: 199–208.

Van den Hoek, C. D., G. Mann, H. M. Jahns, 1995. Algae: an Introduction to Phycology. Cambridge University Press, Cambridge, UK.

Walters, D. M., Leigh, D. S., Freeman, M. C., Freeman, B. J., Pringle, C. M., 2003. Geomorphology and fish assemblages in a Piedmont river basin, U.S.A.. Freshwater Biology, 48: 1950-1970.

Wang, C., Li, X. H., Lai, Z. N., Tan, X. C., Pang, S. X., Yang, W. L., 2009. Seasonal variations of *Aulacoseira granulata* population abundance in the Pearl River Estuary. Estuarine, Coastal and Shelf Science, 85(4): 585-592.

Wang, C., Li, X. H., Lai, Z. N., Fang, Z., Wu, Q., Hu, X. Y., Pang, S. X., 2010. Studying on phytoplankton community structure at the late stage of a

Phaeocystis globosa bloom in the Pearl River Delta. Ecological Science, 29(2): 140-146. (in Chinese with English abstract)

Wang, C., Lai, Z. N., Li, Y. F., Li, X. H., Lek, S., Hong, Y., Tan, X. C., Li, J., 2012. Population ecology of *Aulacoseira granulata* in Xijiang River. Acta Ecologica Sinica, 32(15): 4793–4802. (in Chinese with English abstract)

Wang, C., Lai, Z. N., Li, X. H., Gao, Y., Li, Y. F., Yu, Y. M., 2013. Annual variation pattern of phytoplankton community at the downstream of Xijiang River. Acta Ecologica Sinica, 33(14), 4398–4408. (in Chinese with English abstract)

Waylett, A. J., Hutchins, M. G., Johnson, A. C., Bowes, M. J., Loewenthal, M., 2013. Physico-chemical factors alone cannot simulate phytoplankton behaviour in a lowland river. Journal of Hydrology, 497: 223-233.

Wehr, J. D. & Descy, J. P., 1998. Use of phytoplankton in large river management. Journal of Phycology 34: 741–749.

Wu, N. C., Schmalz, B., Fohrer, N., 2011. Distribution of phytoplankton in a German lowland river in relation to environmental factors. Journal of Plankton Research, 33, 807–820.

Yang, T., Xu, C. Y., Shao, Q. X., Chen, X., 2010. Regional flood frequency and spatial patterns analysis in the Pearl River Delta region using L-moments approach. Stochastic Environmental Research and Risk Assessment, 24: 165-182.

Yang, W., 2011. A multi-objective optimization approach to allocate environmental flows to the artificially restored wetlands of China's Yellow River Delta. Ecological Modelling, 222(2): 261-267.

Young, A.M., Karp-Boss, L., Jumars, P.A., Landis, E.N., 2012. Quantifying diatom aspirations: mechanical properties of chain-forming species. Limnology and Oceanography, 57: 1789–1801.

Yue, T.X., Liu, J.Y., Jørgensen, S.E., Ye, Q.H., 2003. Landscape change detection of the newly created wetland in Yellow River Delta. Ecological Modelling, 164(1): 21-31.

Zalocar de Domitrovic, Y., M. Devercelli & M. O. García de Emiliani, 2007. Phytoplankton. In Iriondo, M. H., J. C. Paggi & M. J. Parma (eds), The Middle Paraná River. Limnology of a Subtropical Wetland. Springer, Berlin: 175–203.